The Dissertation Committee for Sunghye Chang certifies that

this is the approved version of the following dissertation:

Atmospheric Chlorine Chemistry in Southeast Texas: Impacts on Ozone and Particulate Matter Formation and Control

Committee

David T. Allen, Supervisor

Richard L. Corsi

Howard Liljestrand

Kerry Kinney

Gary Rochelle

Elena McDonald-Buller

Atmospheric Chlorine Chemistry in Southeast Texas:

Impacts on Ozone and Particulate Matter Formation and Control

by

Sunghye Chang, B.S.E; M.S.

Dissertation

Presented to the Faculty of the Graduate School of

the University of Texas at Austin

in Partial Fulfillment

of the Requirements

for the Degree of

Doctor of Philosophy

The University of Texas at Austin

August 2005

Dedication

To my Lord and my parents Bong-Ou Chang and Soon-Ok Choi-Chang

Acknowledgements

First of all, I would like to give my utmost praise to my Lord for having been with me all the time.

I would like to express my true gratitude to my supervisor Dr. David T. Allen for his invaluable guidance, support, concerns, and patience throughout all the period of this research. In addition, I would like to thank Dr. Yosuke Kimura for his assistance with air quality modeling.

It is my great joy to show my love, gratitude and respect to my family on the first page of my dissertation. They have always been my sincere and strong supporters who trust me and pray for me continuously. Their endless love and encouragement has been powerful energy to keep studying. It is not me but my parents that deserve the entire honor for my accomplishment. I will also never forget my sister and my brother's constant praying for their sister's physical and spiritual health.

August 12, 2005

Atmospheric Chlorine Chemistry in Southeast Texas:

Impacts on Ozone and Particulate Matter Formation and Control

Publication No. _____

Sunghye Chang, Ph.D.

The University of Texas at Austin, 2005

Supervisor: David T. Allen

Recent evidence has demonstrated that chlorine radical chemistry can enhance tropospheric hydrocarbon oxidation and has the potential to enhance ozone formation in urban atmospheres. In order to assess these effects quantitatively, an August-September, 2000 photochemical episode in southeast Texas was simulated using the Comprehensive Air Quality Model, with extensions (CAMx). During this episode, ambient measurements of a unique marker of atmospheric chlorine chemistry, 1-chloro-3-methyl-3-butene-2-one (CMBO) were made and model performance was assessed by comparing modeled and observed CMBO mixing ratios. The model predicted ambient CMBO mixing ratios within the uncertainty limits of the emissions inventory, so the model was used to assess the impacts of chlorine chemistry on ozone formation. Based on the current emissions inventory, chlorine chemistry has the potential to enhance 8-hour averaged ozone mixing ratios by more than 20 ppb, and 1-hour averaged mixing ratios by more than 70 ppb. These enhancements occur largely in morning hours, and the impacts of chlorine chemistry on daily peak ozone concentrations are typically under 10 ppb. Chlorine emissions also influenced changes in ozone concentrations due to hydrocarbon and NO_x emission controls, and contributed formation of particulate matter through the production of HCl.

Table of Contents

List of Figures

List of Tables

Chapter 1: Introduction

1.1 Problem Statement

CHLORINE EMISSIONS, AND GROUND-LEVEL OZONE AND PARTICULATE MATTER FORMATION

This thesis examines the impact of chlorine emissions to the atmosphere on photochemical smog formation. While acute exposure to chlorine releases can be a direct health hazard and this health hazard should not be ignored, this thesis examines the impact of chronic, relatively low magnitude emissions. These emissions are a concern, not because of their direct health impacts, but because of the role they can play as photochemical oxidants, resulting in the formation of ground-level ozone and particulate matter.

GROUND-LEVEL OZONE AND OZONE REGULATION

Ozone (O_3) is a pervasive pollutant in the lower atmosphere. It is not usually emitted directly into the air, but at ground level is created by chemical reactions, primarily between oxides of nitrogen (NO_x) and volatile organic compounds (VOCs) in the presence of heat and sunlight. Many urban areas tend to have high concentrations of ground-level ozone because of local NO_x and VOCs emissions. However, even rural areas are subject to elevated ozone concentrations, since ozone is a relatively long-lived atmospheric species and winds can transport ozone for hundreds of miles.

Breathing ozone can cause serious health problems. In 1997, the U.S. EPA (Environmental Protection Agency) revised the air quality standards for ozone to better reflect the latest understanding of the health impacts of ozone inhalation. These studies showed that longer-term exposures to moderate levels of ozone might cause irreversible changes in the lungs. Therefore, EPA decided to revise the national ambient air quality standards (NAAQS) for ozone. The standard prior to the action in 1997 regulated ozone

based on concentrations averaged over 1-hour. This standard was eventually replaced by a standard based on concentrations averaged over 8-hours. The new ozone standard, based on concentrations averaged over 8-hours, is set at a level of 0.08 parts per million (ppm) with a form based on the 3-year average of the annual fourth-highest daily maximum 8-hour average O_3 concentrations measured at each monitor within an area. (Environmental Protection Agency, 2004). EPA is continuing to collect air quality monitoring data to identify areas of the country that are routinely unable to meet the previous (1-hour average) and new ozone air quality standards.

Southeast Texas, especially the Houston-Galveston-Brazoria (HGB) region, is one of the areas where ozone levels exceed both the previous (1-hour averaged concentrations) and the current (8-hour averaged concentrations) ozone standard. Counties affected are Brazoria, Chambers, Fort Bend, Galveston, Harris, Liberty, Montgomery, and Waller. The HGB area is classified as 'severe' by the EPA and must attain the one-hour ozone standard by November 15, 2007. Attainment in the HGB area is especially challenging, due to the magnitude of reductions needed for attainment (TCEQ, 2004a). To address this situation, Texas has developed a State Implementation Plan (SIP), which is an enforceable plan that describes the regulations that the state will put in place to reduce ozone concentrations to a level that complies with air quality standards defined in the federal Clean Air Act. SIPs are developed based on monitoring data, emissions inventories, and photochemical modeling (TCEQ, 2004a). This thesis uses these tools to examine the impact that chlorine chemistry has on ozone formation, and what role controls on chlorine emissions might have on reducing the concentrations of ozone in the Houston-Galveston area.

PARTICULATE MATTER AND PM REGULATION

Particulate matter, or PM, is a mixture of microscopic solids and liquid droplets suspended in air. Particulate matter is made up of a number of components, including acids, organic chemicals, metals, soil or dust particles, and plant material such as pollen. There are both natural and anthropogenic sources of particulate matter. The largest natural sources are wind-blown dust, volcanoes, and forest fires. Sea spray is also a large source of particles though most of these deposit close to where they were emitted. The largest anthropogenic sources of particles are combustion sources, mainly the burning of fossil fuels in vehicles and power plants, and wind blown dust from construction sites. Some particles are emitted directly to the atmosphere (primary emissions) and some are emitted as gases and form particles in the atmosphere (secondary aerosols).

Particulate matter causes a wide variety of environmental and health impacts, including premature mortality, higher instances of respiratory illness, reduced visibility (haze), and perturbations of the Earth's radiation balance. Atmospheric particulate matter is characterized by size. Particles less than 10 micrometers in diameter (PM_{10}) pose a health concern because they can be inhaled into and accumulate in the respiratory system. Particles less than 2.5 micrometers in diameter ($PM_{2.5}$) are referred to as fine particles and pose the largest health risks because of their accumulation deep in the lung.

A new standard for fine particles was set by EPA in 1997, and it is this standard that would be most influenced by chlorine emissions. The standard for annual average concentration is set at 15 micrograms per cubic meter ($\mu g/m^3$) and a 24-hour standard is set at 65 $\mu g/m^3$. To determine if an area meets the annual standard, EPA collects data on the yearly average $PM_{2.5}$ levels for three consecutive years. If the average of those three yearly averages is below 15 $\mu g/m^3$, the area will meet the standard. An area will meet the 24-hour standard if the 98^{th} percentile of daily $PM_{2.5}$ concentrations for each of three

years averages less than 65 $\mu g/m^3$. Preliminary monitoring data indicates that the Houston/Galveston area may have difficulty meeting the new $PM_{2.5}$ standard.

Chlorine emissions can increase fine particulate matter concentrations because one of the atmospheric reaction products of chlorine emissions is HCl. HCl can react in the atmosphere with ammonia to produce NH_4Cl, which can accumulate in fine particles. This thesis will examine the impact that chlorine and hydrogen chloride chemistry have on particulate matter formation, and what role controls on chlorine emissions might have on reducing the concentrations of particulate matter in the Houston-Galveston area.

1.2 Hypotheses

The specific hypotheses that will be investigated in this thesis are:

1. Anthropogenic chlorine emissions play a major role in the oxidation of hydrocarbons and influence ozone formation in Houston/Galveston area.
2. Emissions of atomic chlorine precursors in southeast Texas total approximately 10 tons/day and industrial cooling towers are the most significant source of anthropogenic chlorine emissions.
3. Chlorine emissions influence the relative effectiveness of ozone control strategies in Houston/Galveston area.
4. Chlorine emission controls are more effective for ozone reduction than many VOC or NO_x controls (on a pound for pound basis) in the Houston-Galveston area
5. Anthropogenic chlorine and hydrogen chloride emissions in southeast Texas influence particulate matter formation.

1.3 Organization

This thesis is organized into 7 chapters. Chapter 2 (background) presents an overview of air quality management plans, especially the air quality management plans for the Houston area, along with a review of the atmospheric chemistry of chlorine. Chapter 3 describes an inventory of chlorine emissions for the Houston-Galveston area, and reconciliation of the inventory with observational data. Chapters 4 and 5 present model predictions of the impacts of chlorine emissions on ozone formation. Chapter 6 describes formation of particulate matter due to the anthropogenic chlorine emissions and hydrochloric acid, and Chapter 7 provides recommendations and conclusions.

Chapter 2: Background

2.1 Air Quality Regulations for Ozone Control

2.1.1 THE PRIMARY NAAQS FOR OZONE

The U.S Environmental Protection Agency (EPA) has established National Ambient Air Quality Standards (NAAQS) for six air pollutants: ozone, lead, carbon monoxide, sulfur dioxide, nitrogen dioxide, and respirable particular matter. The primary NAAQS is the average concentration of an air pollutant that, in EPA's judgment, must be attained in order to protect public health with an adequate margin of safety. The secondary NAAQS is average concentration of an air pollutant that, in EPA's judgment, must be attained in order to protect public welfare from any known or anticipated adverse effects. The primary and secondary NAAQS for ozone are identical.

1) The ozone standard based on 8-hour averaged concentrations

In July 1997, U.S. EPA revised the National Ambient Air Quality Standards (NAAQS) for ozone to protect public health against longer ozone exposure periods. The threshold value for both the primary and secondary standard, based on 8-hour averaged concentrations, is 0.08 parts per million (ppm). To attain the ozone NAAQS, the 3-year average of the annual 4th-highest daily maximum 8-hour ozone concentration in a region must be less than or equal to 0.08 ppm.

2) The ozone standard based on 1-hour averaged concentrations

The ozone threshold value for both the primary and secondary standard is 0.12 parts per million (ppm), measured as a 1-hour averaged concentration. An area meets the ozone NAAQS if there is no more one day per year when the highest hourly value exceeds the threshold. If monitoring did not take place every day because of equipment malfunction or other operational problems, actual measurements are prorated for the

missing days. The estimated total number of above-threshold days must be 1.0 per year or less. To be in attainment, an area must meet the ozone NAAQS for three consecutive years.

2.1.2 STATE IMPLEMENTATION PLAN (SIP)- CONTROL STRATEGY FOR THE HOUSTON/GALVESTON/BRAZORIA AREA

The State Implementation Plan (SIP) is the federally-enforceable plan for each State which identifies how that State will attain and/or maintain the primary and secondary National Ambient Air Quality Standards (NAAQS) set forth in the Clean Air Act (CAA) and Federal Regulations. Each State is required to have a SIP which contains the control measures and strategies, developed through a public process, formally adopted by the State, and submitted to EPA as revisions to their plan to attain and maintain the NAAQS. The contents of a typical SIP fall into three categories- 1) State-adopted control measures which consist of either rules/regulations or source-specific requirements such as orders and consent decrees; 2) State-submitted "non-regulatory" components such as attainment plans, rate of progress authority, monitoring networks, etc.; 3) additional requirements promulgated by EPA to satisfy CAA requirements. Section VI of the Texas SIP details the state's effort to meet NAAQS by describing the targets, plans, and control strategies for each area designated as nonattainment. Section VI is the only section that is constantly revised and updated. These revisions are known as "SIP revisions".

The following is a list of control strategies currently being used in the HGB area.

- Vehicle inspection/maintenance (I/M)
- Texas emissions reduction plan (TERP)
- Emissions bank and trade program
- Vehicle idling restrictions

- Clean diesel
- Clean gasoline
- Gas-fired water heaters, small boilers, and process heaters
- Small, spark-ignition engine operating restrictions
- California spark-ignition engines
- Voluntary mobile emissions reduction program
- Transportation control measures (TCM)
- Speed limit reduction
- Point source NOx reductions

The HGB Attainment Demonstration SIP was adopted on December 2000, and is currently under revision. On June 23, 2004, the Texas Commission on Environmental Quality (TCEQ) proposed revisions to the SIP for the HGB nonattainment area and the Texas Administrative Code (TAC). Among these proposed revisions, controls on Highly-Reactive Volatile Organic Compounds (HRVOCs, defined as ethylene, propylene, butylenes, and 1,3-butadiene) and a HRVOC Emissions Cap and Trade (HECT) Program have been adopted. The relationships of the modifications of the SIP to atmospheric chlorine chemistry will be described in more detail in later sections. Briefly, the proposed HRVOC Emissions Cap and Trade (HECT) program is an annual cap and trade program for HRVOC emissions from process vents and cooling tower heat exchangers. Sites subject to the proposed program would be required to possess an HRVOC allowance for each ton of HRVOC emissions. Sites also have the option of trading excess HRVOC allowances on the open market within specific trading zones (TCEQ, 2004b). Since cooling towers emit chlorine used in biofouling, chlorine emission reductions could be considered as a substitute for HRVOC reductions.

The proposed SIP revision contains results of photochemical modeling and technical documentation in support of the attainment demonstration. These same

photochemical modeling tools will be used in this work to assess the impact of urban atmospheric chlorine chemistry.

2.2 Atmospheric Chemistry of Ozone in the Troposphere

Photochemical oxidants are produced in the atmosphere as a result of chemical reactions involving sunlight, NO_x, O_2, and a variety of hydrocarbons. Photochemical oxidants produced from such reactions include O_3, NO_2, PAN (peroxyacetyl nitrate), odd hydrogen compounds (HO, HO_2, H_2O_2, etc), and RO_2 (peroxy radicals). Because of its significant environmental effects, elevated tropospheric O_3 has received major scientific and regulatory attention.

Ozone is formed in the atmosphere when molecular O_2 reacts with ground-state atomic oxygen, $O\cdot(^3P)$ (Seinfield, 1998):

$$O_2 + O\ (^3P) + M \rightarrow O_3 + M \qquad (2.1)$$

O represents a highly reactive oxygen atom that has an unpaired electron, and M represents any third body which is usually N_2, O_2 or another third molecule that absorbs excess vibrational energy and thereby stabilizes the O_3 molecule formed.

In the troposphere, photodissociation of NO_2 at wavelengths of 280 to 430 nm is the only significant source of atomic oxygen:

$$NO_2 + h\nu \rightarrow NO + O\ (^3P) \qquad (2.2)$$

The reaction of O (^3P) with O_2 produces O_3, which reacts with NO to regenerate NO_2.

$$O_3 + NO \rightarrow NO_2 + O_2 \qquad (2.3)$$

Equations (2.1) to (2.3) proceed rapidly, producing a steady-state ozone concentration of 20 ppbv under solar noon conditions in mid-latitudes at atmospheric NO_2/NO concentration ratios equal to 1.

In both urban and non-urban atmospheres, O_3 concentrations are often much higher than those that occur from NO_2 photolysis. The key to elevated tropospheric O_3 levels is chemical reactions that convert NO to NO_2 without consuming O_3. In very polluted and even lightly polluted atmospheres, such shifts in O_3 chemistry occur in the presence of alkylperoxy radicals ($RO_2\cdot$) produced by the oxidation of hydrocarbons (HCs):

$$RO_2\cdot + NO \rightarrow NO_2 + RO\cdot \qquad (2.4)$$

$$NO_2 + h\nu \rightarrow NO + O\ (^3P) \qquad (2.2)$$

$$O\ (^3P) + O_2 + M \rightarrow O_3 + M \qquad (2.1)$$

$$\text{Net: } RO_2\cdot + O_2 + h\nu \rightarrow RO\cdot + O_3 \qquad (2.5)$$

The rate of O_3 formation is closely related to the concentration of $RO_2\cdot$. Peroxy radicals allow ozone to accumulate by reducing the ozone sink (NO) and increasing ozone sources (NO_2). Peroxy radicals are produced when OH and HO_x (odd oxygen species) react with VOC (volatile organic compounds, RH). Reactions (2.6) and (2.7) show the formation of alkyl radical ($R\cdot$) and $RO_2\cdot$.

$$RH + OH\cdot \rightarrow R\cdot + H_2O \qquad (2.6)$$

$$R\cdot + O_2 \rightarrow RO_2\cdot \qquad (2.7)$$

Hydroxyl radicals are produced by reactions involving the photodissociation of ozone indicated in Equations (2.8) and (2.9).

$$O_3 + h\nu \rightarrow O\cdot\ (^1D) + O_2 \qquad (2.8)$$

$$O\cdot\ (^1D) + H_2O \rightarrow 2OH\cdot \qquad (2.9)$$

Where $O\cdot\ (^1D)$ is singlet (excited) atomic oxygen.

Also $OH\cdot$ is produced by reaction (2.10).

$$HO_2\cdot + NO \rightarrow NO_2 + OH\cdot \qquad (2.10)$$

2.3 Chlorine Chemistry

2.3.1 Chlorine Chemistry and Interactions with Ozone Chemistry

Molecular chlorine and other chlorine radical precursors are emitted to the troposphere from anthropogenic and natural sources. Molecular chlorine is a source of radicals that accelerate the ozone formation process and enhance tropospheric VOC oxidation.

Chlorine radical is produced by photodissociation of Cl_2 and HOCl by visible and ultraviolet light.

$$Cl_2 + h\nu \rightarrow Cl\cdot + Cl\cdot \quad (2.11)$$

$$HOCl + h\nu \rightarrow OH\cdot + Cl\cdot \quad (2.12)$$

Atomic chlorine formed in the troposphere can react with ozone and hydrocarbons (RH):

$$Cl\cdot + O_3 \rightarrow ClO\cdot + O_2 \quad (2.13)$$

$$Cl\cdot + RH \rightarrow R\cdot + HCl \quad (2.14)$$

$$R\cdot + O_2 \rightarrow RO_2\cdot \quad (2.15)$$

Under typical urban conditions, concentrations of hydrocarbons are sufficiently high so that the rate of reaction of atomic chlorine with RH is much faster than the rate of reaction with ozone (Oldfield, 2000). Typically, the chlorine radical abstracts hydrogen from the hydrocarbon, producing a alkylradical and hydrogen chloride. The hydrocarbon radical then produces alkylperoxy radicals, which promote ozone formation. The following reactions show how chlorine atoms may initiate organic oxidation in a mechanism similar to that of hydroxyl radicals, accelerating the formation of ozone.

$$RH + Cl\cdot \text{ (or } OH\cdot) \rightarrow R\cdot + HCl \text{ (or } H_2O) \quad (2.14)$$

$$R\cdot + O_2 \rightarrow RO_2\cdot \quad (2.16)$$

$ROO\cdot + NO \rightarrow NO_2 + RO\cdot$ (2.17)

$RO\cdot + O_2 \rightarrow HO_2\cdot + \text{carbonyl}$ (2.18)

$HO_2\cdot + NO \rightarrow NO_2 + OH\cdot$ (2.19)

NO_2 produced in reactions (2.17) and (2.19) photodissociates to NO as shown in reactions (2.1) and (2.2). Also, the reaction (2.19) produces OH·, conserving free radicals in the hydrocarbon oxidation cycle.

The relative rates of chlorine reaction with ozone and with hydrocarbons determine whether chlorine radicals are a source or sink for ozone. The following reactions represent ozone sink mechanisms, which are initiated by the reaction of atomic chlorine with ozone.

$Cl\cdot + O_3 \rightarrow ClO\cdot + O_2$ (2.13)

$ClO\cdot + HO_2\cdot \rightarrow HOCl + O_2$ (2.20)

$HOCl + h\nu \rightarrow OH\cdot + Cl\cdot$ (2.12)

Net: $Cl\cdot + O_3 + HO_2\cdot \rightarrow Cl\cdot + 2O_2 + OH\cdot$ (2.21)

Both ozone sinks (chlorine reaction with ozone) and ozone sources (chlorine reaction with hydrocarbons) will be examined in this work. The details of the chemical mechanism are described in Section 2.4.

2.3.2 Chlorine/Hydrogen Chloride Chemistry and Interactions with Atmospheric Particulate Matter

Chlorine atoms, which are produced by photodissociation of Cl_2 and HOCl, are highly reactive toward hydrocarbons, leading to the formation of hydrogen chloride through hydrogen abstraction.

$RH + Cl\cdot \rightarrow R\cdot + HCl$ (2.14)

Hydrogen chloride can also be created by the reactions of seasalt aerosol, including the reaction with nitric acid:

$$NaCl(s) + HNO_3(g) \leftrightarrow NaNO_3(s) + HCl(g) \qquad (2.22)$$

As a result of this reaction, nitrate is transferred to the aerosol phase and is associated with the seasalt particles. At the same time, hydrochloric acid is liberated and the aerosol particles appear to be chloride deficient. This deficiency may also be a result of the reaction with sulfuric acid (Seinfeld and Pandis, 1998).

$$2\ NaCl(s) + H_2SO_4(g) \leftrightarrow Na_2SO_4(s) + 2\ HCl(g) \qquad (2.23)$$

$$NaCl(s) + H_2SO_4(g) \leftrightarrow NaHSO_4(s) + HCl(g) \qquad (2.24)$$

HCl(g), resulting from chlorine atom reactions, chloride displacement, or other sources, reacts with $NH_3(g)$, and can produce particle $NH_4Cl(s)$. More details of the atmospheric chemistry of atmospheric ammonium chloride are provided in Chapter 6.

2.3.3 CHLORINE MARKER SPECIES

Occurrence of Cl· chemistry in the urban troposphere can be confirmed through the detection of unique marker species, which are only produced from the reaction between Cl· and isoprene. These marker species are 1-chloro-3-methyl-3-butene-2-one (CMBO), and chloromethylbutenal (CMBA) (Ragains and Finlayson-Pitts, 1977; Riemer, 2001). The major reaction pathways resulting from addition of Cl· to isoprene are shown in Figure 2.1 (Riemer, 2001). In order to document the presence of CMBO and CMBA in ambient air above Houston, Reimer (2001) made measurements at a monitoring site at La Porte Airport, which is east of Houston. As shown in Figure 2.2, CMBO concentrations showed sharp maxima in the morning hours in most days. Peak concentrations were roughly 100 ppt (part per trillion). These results will be compared, later in this thesis, to

predicted values of CMBO concentrations generated by a three dimensional, gridded photochemical model, described in the next section.

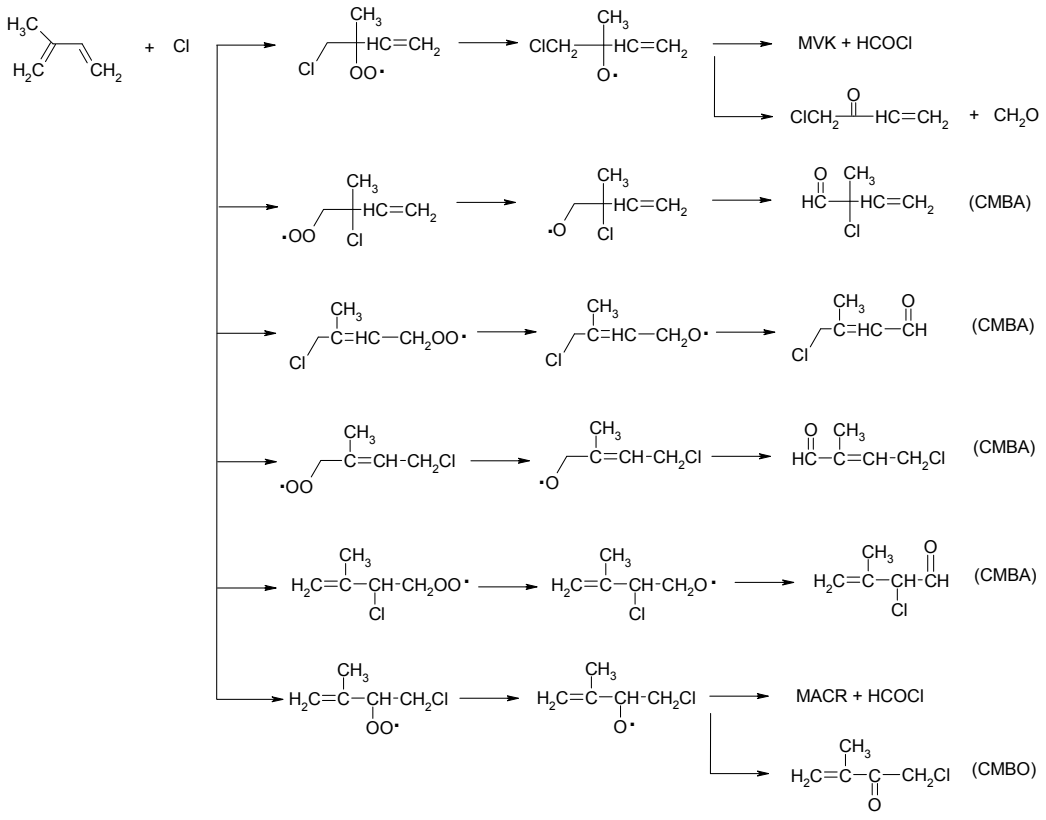

Figure 2.1 Major reaction pathways resulting from addition of Cl· to isoprene in NO_x free air

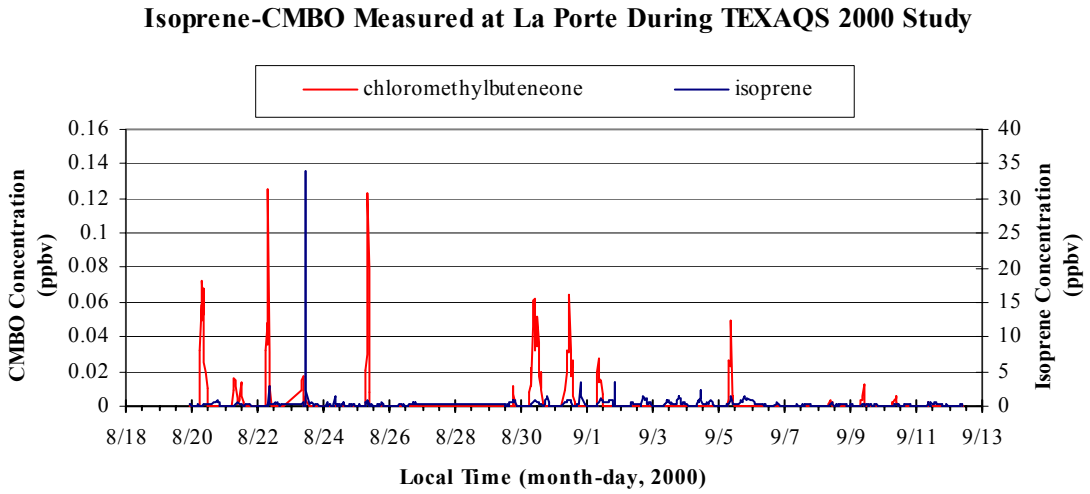

Figure 2.2 Isoprene-CMBO concentrations measured at La Porte Airport during TexAQS 2000 study

2.4 Comprehensive Air Quality Model with extensions (CAMx) and Carbon Bond IV Mechanism (CB-IV Mechanism)

Regional photochemical models, such as the comprehensive air quality model with extensions (CAMx) (ENVIRON, 2002) are used to simulate emission, chemical transformation, horizontal advection and diffusion, vertical transport and diffusion, dry deposition, and wet deposition of species in the atmosphere. Although any comparable photochemical grid model could be used, CAMx was selected for this study because it is currently being used by the State of Texas for attainment demonstrations in areas that have violated the National Ambient Air Quality Standards for ozone.

The State of Texas has developed an August 22 - September 6, 2000 photochemical modeling episode for evaluating its air quality management plans for southeast Texas. The horizontal modeling domain was a nested regional/urban scale 36-km/12-km/4-km grid shown in Figure 2.3. Meteorological inputs required by the model were based on results from the Mesoscale Meteorological Model, version 5, MM5.

Detailed descriptions of the meteorological modeling are available elsewhere (MM5 Community model, 2004).

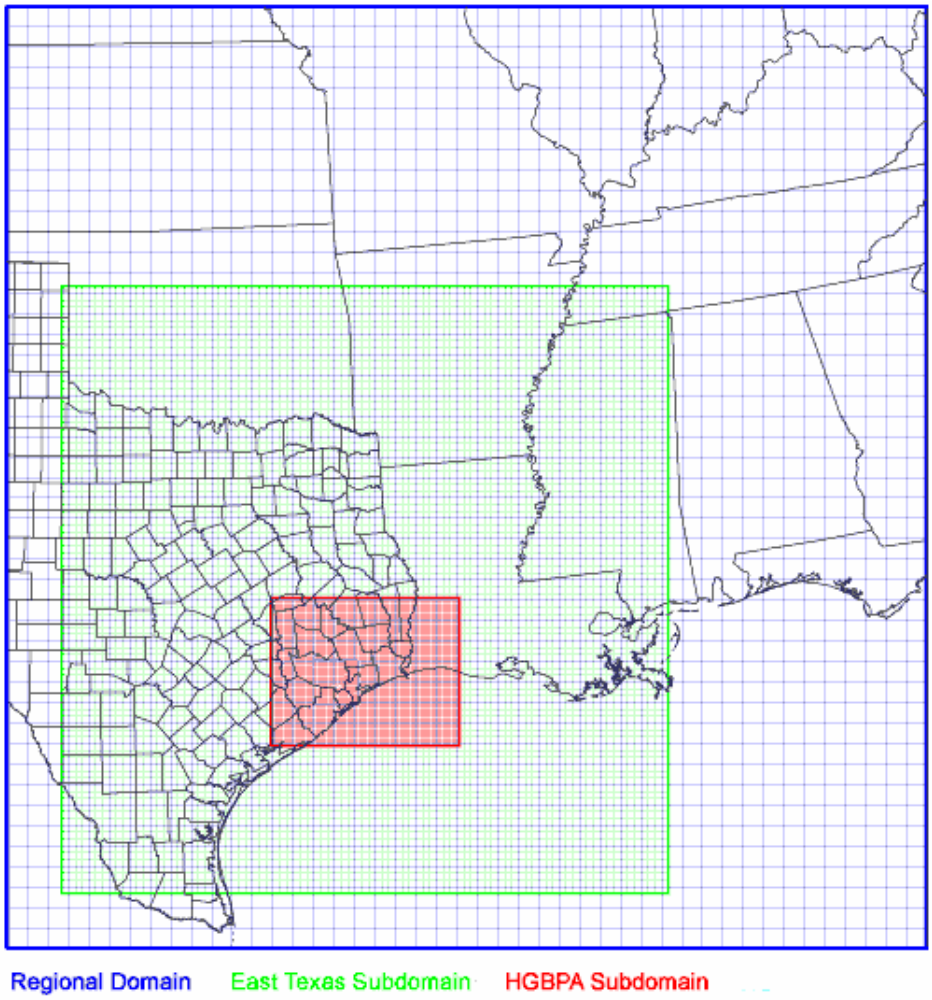

Figure 2.3 Modeling domain used in the study: The Regional, East Texas and Houston-Galveston-Beaumont-Port Arthur nested domains had 36, 12 and 4 km resolution, respectively.

The volatile organic compound (VOC) and NO_x emission inventories used as input for the modeling episode were prepared by the Texas Commission on Environmental Quality (TCEQ) in accordance with U.S. EPA guidance. A MOBILE6-based inventory was developed for on-road mobile source emissions; emissions for non-

road mobile and area sources were developed using emission factors and the U.S. EPA's NONROAD model, using local activity data when available. Biogenic emission inventories were estimated using the GLOBEIS emission model with locally developed land cover data (TCEQ, 2004b). Point source emissions were developed through a special inventory survey and were also estimated based on ambient data collected in the source region. Details of the VOC and NOx emission inventory development are available at (TCEQ, Houston /Galveston Air Quality Science Evaluation, 2004c).

CAMx can use either one of two simplified chemical mechanisms to describe ozone formation. Those are the Carbon Bond mechanism (developed by Atmospheric Research Associates and System Applications International (Gery et al., 1988)) and SAPRC (developed by the Statewide Air Pollution Research Center in California (Carter, 1996)) (Allen, 2002). Version IV of the Carbon Bond mechanism (CB-IV) has been used in most of the photochemical modeling performed in Texas and it was the original chemical mechanism used by CAMx (Gery et al., 1988)

The original CB-IV mechanism was modified by Tanaka and Allen (2001), who added reactive chlorine chemistry (Cl_2, Cl, and ClO reactions) to the mechanism; this revised mechanism has been available since CAMx version 3.01 (ENVIRON, 2002). The base chemical mechanism (the mechanism without chlorine chemistry) uses 96 reactions to describe ozone formation chemistry. Thirteen additional reactions, which were incorporated into the chemical mechanism, describe chlorine chemistry relevant to an urban atmosphere such as in Houston. Therefore, the chemistry employed during the CAMx simulations in this work included 109 reactions. The 13 reactions added to represent chlorine chemistry and corresponding rate constants are provided in Table 2.1. Table 2.2 contains a key to the species included in Table 2.1.

In order to run a CAMx simulation with chlorine chemistry mechanism, it was necessary to develop a chlorine emission inventory. Chang et al. (2001, 2002) has previously developed a chlorine emission inventory for a 1993 photochemical episode. Since observation data of chlorine marker species as well as the CAMx simulation are available for year 2000, however, a chlorine emission inventory for the 2000 photochemical episode was developed. The methods used in developing the inventory parallel those used by Chang et al. (2001) and are presented in Chapter 3 in this thesis.

Table 2.1 Chlorine Chemistry Incorporated into CAMx (cited from Tanaka, 2002)

Reactions	k ($cm^3 molecule^{-1} s^{-1}$)
1) Cl2 = 2Cl	(a)
2) HOCl = OH + Cl	(a)
3) Cl + PAR = HCl + 0.87XO2 + 0.13XO2N + 0.11HO2 + 0.11RCHO + 0.76ROR – 0.11PAR	$78*k_{OH,PAR}$
4) Cl + OLE = FMCL + RCHO + 2XO2 + HO2 – 1PAR	$20*k_{OH,OLE}$
5) Cl = HCl + XO2 + FORM + HO2	$6.6x10^{-12}exp(-1240/T)$
6) Cl + ETH = FORM + 2XO2 + FMCL + HO2	$12.6*k_{OH,ETH}$
7) Cl + ISOP = 0.15HCl + XO2 + HO2 + 0.28ICL1	$4.5*k_{OH,ISOP}$
8) OH + ICL1 = ICL2	$0.19*k_{OH,ISOP}$
9) Cl + BUTA = XO2 + HO2 + 0.70BCL1	$4.2*k_{OH,ISOP}$
10) OH + BCL1 = BCL2	$0.36*k_{OH,ISOP}$
11) Cl + O3 = ClO + O2	$2.9x10^{-11}exp(-260/T)$[(b)]
12) ClO + NO = Cl + NO2	$6.2x10^{-12}exp(295/T)$[(b)]
13) ClO + HO2 = HOCl + O2	$4.6x10^{-13}exp(710/T)$[(b)]

(a) The rate of these photolysis reactions is dependent on calculated sunlight intensity.

(b) Source: [*Atkinson et al.*, 2000]

Table 2.2 Key to Chemical Species Abbreviations (cited from Tanaka, 2002)

Name	Description
BUTA	1,3 Butadiene
BCL1	4-Chlorocrotonaldehyde (CCA)
BCL2	CCA + OH reaction products
ETH	Ethene
Cl	Chlorine atom
Cl2	Molecular chlorine
ClO	Chlorine oxide
CO	Carbon monoxide
FORM	Formaldehyde
FMCL	Formyl chloride
HCl	Hydrochloric acid
HOCl	Hypochlorous acid
HO2	Hydroperoxyl radical
ISOP	Isoprene
ICL1	1-Chloro-3-methyl-3-butene-2-one (CMBO)
ICL2	CMBO + OH reaction products
OH	Hydroxyl radical
OLE	Olefinic bond (Carbon double bond)
PAR	Paraffinic carbon
RCHO	Higher aldehyde
ROR	Organic nitrate forming peroxy radical
XO2	Universal peroxy radical operator
XO2N	Nitrate forming peroxy radical operator

CB-IV chemical mechanism and chemical parameters used in the modeling are presented in Table A-1 and A-2 in Appendix A.

Chapter 3: Chlorine Emission Estimation Methods and Reconciliation with Observational Data

The first hypothesis to be examined in this thesis (Chapter 1) is that anthropogenic chlorine emissions play a major role in the oxidation of hydrocarbons and influence ozone formation in Houston/Galveston area. Hypothesis 2 states that emissions of atomic chlorine precursors in southeast Texas total approximately 10 tons/day and industrial cooling towers are the most significant source of anthropogenic chlorine emissions. These two hypotheses will be addressed through a combination of emission inventory development and evaluation and tuning of the emission inventory using ambient measurements and the predictions of photochemical modeling. The emission inventory development is described in this Chapter; the evaluation of the inventory through comparison of model predictions and ambient measurements is described in Chapter 4.

3.1 Chlorine emission inventory Overview

Chlorine emissions were estimated for the HGBPA sub-domain shown in Figure 2.3. Chlorine emission estimates were made for the following source categories:

- point sources of Cl_2 emissions reported through the US Environmental Protection Agency's Toxic Release Inventory (TRI) and the State of Texas' Point Source Database (PSDB),
- atomic chlorine precursors from the use of biocides in cooling towers,
- atomic chlorine precursors from swimming pool disinfection,
- atomic chlorine precursors associated with reactions of chlorides in sea salt aerosol,

- other sources of atomic chlorine precursors associated with tap water use, water and wastewater treatment, chlorinated organics in the atmosphere, and indoor consumer products usage .

Cl_2 emissions were estimated using the methodologies summarized below, using activity data from 2000. Details of the emission estimation methodologies were reported in the M.S. thesis of the author (Chang, 2002), and are summarized in Appendix B.

3.2 Molecular Chlorine Emissions from Industrial Point Sources in Southeastern Texas

Point source emissions of molecular chlorine were estimated using the Point Source Data Base (PSDB), maintained by the State of Texas and by using the Toxic Release Inventory (TRI), maintained by the U.S. Environmental Protection Agency. Both inventories should provide the same information, but there are some discrepancies due to differences in reporting. A comparison of the TRI and PSDB data, also shown in Table B-1 in Appendix B, indicates that the two sources of point source emission data are in agreement in some areas, but some discrepancies arise. For this work, the larger of the PSDB and 2000 TRI emissions was selected for the photochemical modeling inventory based on conservative decision. Even though larger value of the PSDB and 2000 TRI emissions is used, the magnitude of emissions from point sources does not affect changes in total magnitude because 1 ton/day is smaller than total chlorine emissions of 10 tons/day from all sources.

Stack parameters and other model input data were drawn from the PSDB When these data were missing, they were assumed to be equal to default values recommended by the U.S. EPA for photochemical modeling. Some stack parameters were provided in the PSDB, otherwise default parameters for height (3m), diameter (0.2m), temperature

(294K), and stack gas velocity (0.5m/s) were used. Hourly emissions were assumed to be constant throughout the day as the PSDB from TCEQ is indicated. The spatial distribution of chlorine emission from industrial point sources in the revised inventory is shown in Figure 3.1. Total Cl_2 emissions from industrial point sources in the region were 0.65 tons day^{-1}.

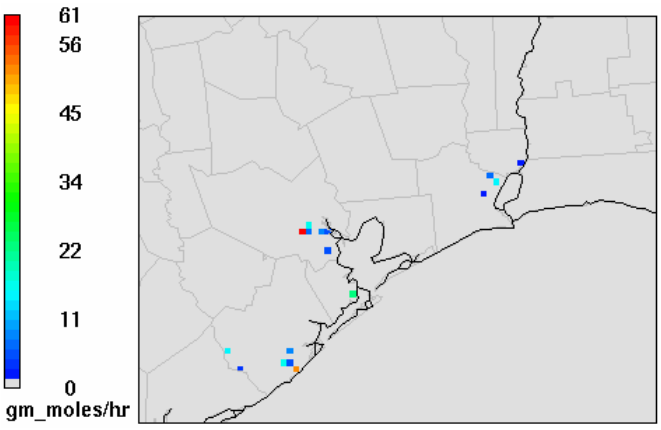

Figure 3.1 Spatial distribution of chlorine emissions from industrial point sources

3.3 Emissions of atomic chlorine precursors from cooling towers in Southeastern Texas

Cooling towers can be significant sources of atomic chlorine precursors. Chlorine is added, as molecular chlorine or as hypochlorite, to the recirculating water used in cooling towers in order to control biofouling. There are three possible sinks for the chlorine added to cooling towers (Holzwarth et al, 1984a, b).

1. The air flux through the cooling tower strips volatile constituents from the water, a process called flashoff ;
2. The blowdown stream carries off a portion of the HOCl and its products

3. A part of the HOCl is converted to other chemical species by reaction with contaminants in the water and the cooling system, a process called chlorine demand.

The extent of these chlorine emissions was estimated using the method developed by Chang et al. (2002). Briefly, this method is based on mass transfer considerations of flash-off and field measurements reported by Exxon (Holzwarth et al., 1984 a, b). Data were collected before, during and after a typical shock chlorination cycle of a 1.44 million gallon per day system. The shock consisted of 3 hours of chlorine addition at a rate of 28,000 g molecular chlorine gas/hr, followed by 1.5-hours at 17,000 g/hr, and 3,800 g/hr for the remainder of a 24-hour period. Assuming a flash-off fraction of 0.1 and that the emissions are in the form of molecular chlorine leads to an emission estimate for the 1.44 mgd cooling tower of:

*(28 kg/hr * 3hr + 17 kg/hr * 1.5hr + 3.8 kg/hr * 19.5hr) * 0.1*

=18.4 kg chlorine emission per 24 hours a day for a 1.44 mgd cooling tower

Field and laboratory data indicate that the fraction of chlorine that flashes is a strong function of pH and temperature, with higher pH and temperature leading to greater flash-off of atomic chlorine precursors. Reported flash-off fractions ranged from less than 0.1 to 1.0. To provide a preliminary estimate of the rate of atomic chlorine precursor release from cooling towers a flash-off fraction of 0.1 (10%) was used based on experimental value of Exxon cooling tower (Holzwarth et al., 1984 a, b).

This estimate is consistent with the estimates of chlorine used in cooling towers from surveys performed on refineries in the South Coast Air Basin (Rogozen, et al., 1988). Since data from South Coast Air Basin indicate that relatively few small capacity cooling towers used chlorine as a biocide, it is assumed that virtually all chlorine use in cooling towers is confined to the chemical manufacturing and refining sectors. In order to

arrive at an order of magnitude estimate of chlorine use in cooling towers, it was assumed that approximately 500 MGD of cooling water use (350 cooling towers in southeastern Texas with capacities of approximately 1.44 MGD including cooling towers of airport, hospitals, and schools as well as industrial cooling towers)

*18.4 kg/day/cooling tower * 350 cooling towers = 6,000 kg/day*

The estimate of cooling water use was based on an assumption of approximately 1 gal of cooling water used per pound of chemical produced (Schwatz et al., 2002), and that approximately 25% of the 300 million tons per year of commodity chemicals are produced in the region being modeled. Cooling towers were assumed by Chang et al (2002) to be co-located with the top 50-point sources of NO_x emissions in the area, excluding electricity-generating units (EGU), using a 1995 base-year inventory. The fraction of the total chlorine emissions assigned to each site was based on the fraction of the point source NO_x emissions located at each site.

The inventory used in this work differed from the original inventory developed by Chang et al. (2002) only in the spatial distribution of emissions. In this work, cooling towers, and their chlorine emissions, were assumed to be co-located with all the 596 point sources of NO_x emissions in the area, excluding electricity-generating units (EGUs). The NO_x source locations were based on a year 2000 inventory. The temporal distribution of chlorine emissions and the stack parameters used by Chang et al (2002) were used in this work. Shock chlorination was assumed to occur during 0700-1700 CDT shifts. The emission rate from 0700 hr to 1200 hr was assumed to be double the rate from 1200 hr to 1700 hr, based on shock chlorination profiles reported by Holzwarth et al. (1984a, b). Therefore, the fraction of emissions released each hour was 0.133 for each hour between 0700 and 1200 and 0.666 for each hour between 1200 and 1700. Stack parameters for a

typical cooling tower were assumed to be height as 20m, diameter as 5m, temperature as 294K, and stack gas velocity as 1m/s.

The spatial distribution of chlorine emission from cooling towers in the revised inventory is shown in Figure 3.2. Total chlorine emission rate from cooling towers in this region was 6 tons day^{-1} of molecular chlorine as Cl_2.

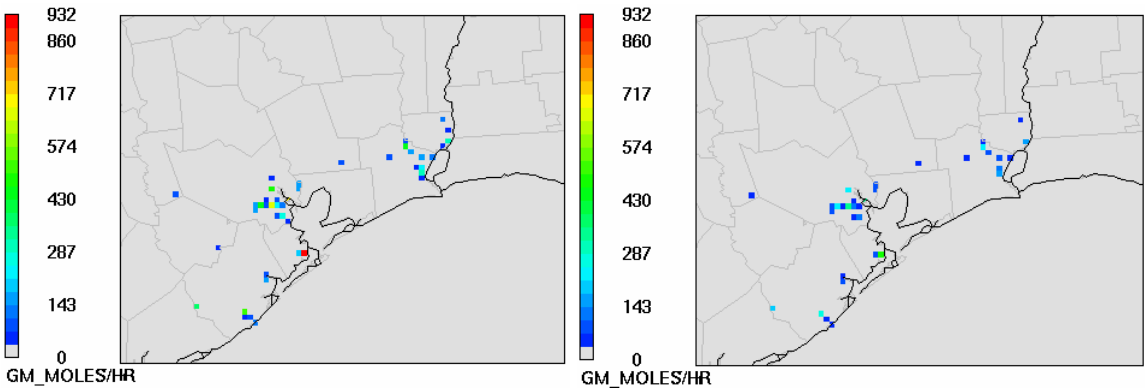

(a) 0700-1200 (b) 1200-1700

Figure 3.2 Spatial distributions of chlorine emissions from cooling towers during (a) 0700-1200 and (b) 1200-1700 CDT.

3.4 Emissions of atomic chlorine precursors from swimming pools

A variety of disinfectants are used for pool water treatment. The disinfectants used most frequently in large, heavily used pools are chlorine as gas, calcium/sodium hypochlorite, sodium dichloroisocyanurate, and electrolytic generation; Ozone/chlorine in combination; chlorine dioxide; chlorine dioxide/chlorine in combination are also frequently used. Disinfectants used less frequently are liquid bromine, bromochlorodimethylhydantoin (BCDMH), and combination of sodium bromide and hypochlorite (World Health Organization, 2005). Since bromine is less used than chlorine and less reactive than chlorine, in this thesis, chlorine is considered as a representative disinfecting agent added into swimming pools.

Estimates of the chlorine emissions from pools are generally based on an estimate of the number of pools and the emissions from each pool. Chang, et al. (2002) estimated the number of pools in Houston based on national and Los Angeles pool ownership data, and arrived at an estimate of 150,000 pools in the Houston area. The volatilization of chlorine from swimming pools was estimated using three different approaches. Rogozen et al. (1988) assumed that the average rate of chlorine addition during summer months was 2 gallons of NaOCl solution (10-12.5% by weight) per pool per week. This leads to an estimate for summertime hypochlorous acid use of:

$$0.1 NaOCl * 2\ gal\ week^{-1}\ (week / 7\ days) * 3.78\ kg\ gal^{-1} * 150{,}000\ pools$$

$$= 16{,}200\ kg\ NaOCl\ day^{-1}\ in\ 11\ counties\ in\ Southeast\ Texas$$

This suggests that approximately 16,200 kg day^{-1} of NaOCl is added to pools in 11 counties, some fraction of which will volatilize.

Another approach to estimating the rate of volatilization from pools is to apply an overall mass transfer coefficient coupled with estimates of pool surface area and free chlorine concentration. Rogozen et al. (1988) estimated an average pool surface area of 40 m^2 for southern California, and an average emission flux rate for chloroform of 22 μg m^{-2} min^{-1}, which is a weighted average of emission flux rates under agitated and non-agitated conditions. This overall emission flux rate is the product of an air phase mass transfer coefficient, a partitioning coefficient (Henry's law constant) and an aqueous phase concentration. Assuming that the air phase mass transfer coefficient is the same for chloroform and chlorine, the mass transfer coefficient for chlorine can be estimated by replacing the concentration and Henry's law constant for chloroform with the concentration and Henry's law constant for chlorine/hypochlorous acid. The data reported by Rogozen et al. (1988), suggest that free residual chlorine concentrations in the water are a factor of 5 greater than aqueous chloroform concentrations. Assuming that

the pH of the swimming pool water is maintained between 6.5 and 7.5, the Henry's law constant for chlorine (as HOCl in the aqueous phase) will be approximately a factor of 5 lower than the Henry's law constant for chloroform assumed by Rogozen et al. (1988). After adjusting for the difference in molecular weights, this analysis suggests that an overall mass transfer coefficient for hypochlorous acid is approximately 10-100 μg m^{-2} min^{-1}. The total surface area of swimming pools in the 11 counties is calculated based on the estimated number of swimming pools in Southeast Texas (Chang et al., 2002).

*$40m^2$ per pool * 150,000 pools in the 11 counties (5.18 million residents, US census Bureau) = 6.0 * 10^6 m^2*

Mass volatilized:

*10-100 μg m^{-2} min^{-1} * 6.0 * 10^6 m^2 * 1440 min day^{-1} * kg 10^9 μg $^{-1}$ = 90 - 900 kg day^{-1}*

The high end of the volatilization rate indicates that the chlorine evaporates at a rate of about 1000 kg day^{-1}, and this volatilization would occur during agitation when mass transfer coefficients are highest. Thus, the estimated emission rates based on a mass balance and on a mass transfer approach lead to very different estimates of emissions.

Yet another approach would be to assume that the volume of a typical pool is 50 m^3 (an average surface area of 40 m^2 and an average depth of 1.25 m). Further assuming that the required residual chlorine concentration in the swimming pool is 2ppm (Taylor Technology, 2001), the residual chlorine available in a pool is

*150,000 pools in 11 counties * 50,000 L/pool * 2ppm * 1 kg L^{-1} = 15,000 kg.*

This suggests that a large stock of chlorine residues in the pool volume.

Thus, three different estimation methods lead to estimates of 16,200 kg of NaOCl added per day to pools, a stock of 15,000 kg of free residual chlorine in the pools, and a volatilization rate of 100-1000 kg day^{-1}. Taking all of these divergent estimates into

account, it was assumed that total emissions in the 11-county area in the current study were 5 tons day^{-1} (4540kg day^{-1}) as Cl_2. This estimate is significantly larger than the rate suggested by limited mass transfer rate data, but only a small fraction of the available stock of free residual chlorine. Therefore, this estimate may be uncertain by an order of magnitude.

Chlorine emissions were spatially allocated based on population and income distributions. Chang, et al. (2002) used 1990 data on the spatial distribution of households with incomes above $50,000; this study used 2000 census data on the spatial distributions of households with incomes above $75,000 to spatially distribute swimming pool emissions. It was assumed that the chlorine emissions occur at a constant rate between 1200 hr and 2000 hr as the water was agitated by use. The spatial distribution of chlorine emissions from swimming pools is shown in Figure 3.3.

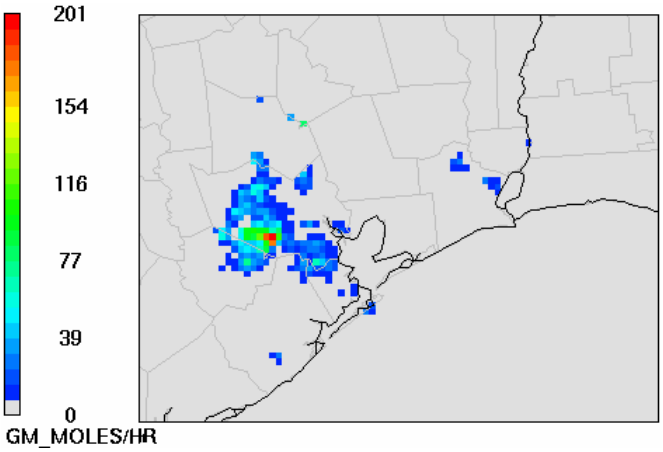

Figure 3.3 Spatial distributions of chlorine emissions from swimming pools during 1200 to 2000

3.5 Emissions of atomic chlorine precursors from the reactions of sea salt aerosol

Spicer et al (1998) has suggested that ozone and other components in photochemical smog react with chloride in sea salt to release Cl_2. Chang et al. (2002) estimated the chlorine emission rate from this source in the Houston-Galveston region based on the rates of molecular chlorine generation by sea salt observed on Long Island by Spicer et al. (1998). In this work, emissions were spatially allocated to grid cells that had both high sea salt concentrations and ozone (or other air pollutant) concentrations. This area was assumed to include the all grid cells in the photochemical model that were over water, but within 8 km of a coastline. The emission was modeled as an area source in each 4 km by 4 km grid cell with emissions of 1.6 kg day^{-1} per grid cell. Chlorine production was assumed to be evenly distributed over daylight hours, from 0600 hr to 1800 hr (Chang et al. 2002).

3.6 Emissions of atomic chlorine precursors associated with tap water use

On average, individuals use almost 100 gallons of drinking water per person per day. Traditionally, water use rates are described in units of gallons per capita per day (gpcd) (EPA, 2005). Water use amount per capita per day, by use type, is shown in the Table 3.1.

Table 3.1 Water Use per Capita

Water Use	Flow Rate
Bath	20 GPD
Toilet, flushing	24 GPD
Laundry	8.5 GPD
Dish washer	4 GPD
Garbage Disposal	1 GPD
Drinking and Cooking	2 GPD
Car washing	2.5 GPD
Lawn watering and pools	25 GPD

Among these water uses, car washing and lawn watering are potential outdoor sources of chlorine emissions. Water use for these sources is:

2.5 + 25 = 27.5 GPD

27.5 gpd * 1,953,631 Houston city population = 53,725,000 Gallons per day

Tap water residual chlorine concentration is calculated based on residual chlorine concentrations of 2.25 ppm for surface water (65% of supply in Houston) and 1ppm for ground water (35% of supply in Houston):

1.5 ppm * 0.65 surface water + 1ppm *0.35 ground water =1.325 ppm

1.325 ppm *53,725,000 gpd =1.325 ppm * 203 * 10^6 L/day = 269 kg/day

Since the emission estimate for this source was estimated to be more than an order of magnitude less than other potential sources, this emission will not be incorporated into the inventory used for modeling in this work.

3.7 Emissions of atomic chlorine precursors associated with water and wastewater treatment

Water and wastewater treatment accounts for approximately 5% of chlorine use in the United States (Ayres, 1997) and therefore should be considered as a potential source of chlorine or hypochlorous acid emissions. The subsections below separately estimate potential atomic chlorine precursor emissions for water and wastewater treatment.

3.7.1 CHLORINATION IN WATER TREATMENT

Houston obtains 65% of its municipal water supply from surface water sources and 35% from ground water sources, and chlorine dosages at Houston water treatment plants are adjusted according to the water source. Dosages for surface and ground water are 3 ppm (mass) chloramines and 2 ppm free chlorine, respectively. Residual chlorine concentrations are 1-1.5 ppm and 1 ppm, respectively. The difference between the chlorine dosage and the free chlorine residual has the potential to be emitted, where chlorine demand is defined as:

Chlorine demand = Chlorine dose – Chlorine residual

The chlorine demand is the sum of a variety of potential chlorine sinks including reactions promoted by sunlight, reactions with inorganic compounds, reactions with ammonia, reactions with organic compounds and volatilization. Based on interviews with water treatment experts (Lawler, 2001), it was assumed that 20% of the chlorine demand is due to volatilization.

If the chlorine volatilization per volume of water treated is known, then a preliminary estimate of chlorine releases requires only an estimate of the volume of water processed. The population of Houston is 1.95 million and the population of the county metropolitan statistical area is 4.5 million. The City of Houston supplies water to about 2.35 million people. The annual average water flow rate, for the City of Houston, is 315 million gallon per day (MGD) (Greenlee, 2001). However, summer time water flow rates are significantly larger (492.669MGD; water usage of summer 2000), and the summer water usage rates will be used in this analysis.

To estimate the quantity of atomic chlorine precursor emissions from water treatment plants, it was assumed 20% of the chlorine demand was due to volatilization and that the water demand was 492 MGD. Table 3.2 summarizes the data used in the

emission estimates. The estimated releases are small (a few hundred kg/day) compared to estimated releases from cooling towers. Since this estimate is based on a relatively conservative (high) flash-off fraction (0.2) these emissions are likely to be negligible.

0.2 * (2-1) ppm *492 MGD * 0.35 * 3.7854 (L/Gal) = 130 - 261 kg/day

(chlorine treatment of ground water)

0.2 *(3-1.5) ppm * 492MGD * 0.65 * 3.7854 (L/Gal) = 363 -726 kg/day

(chloramine treatment of surface water)

Table 3.2 Data on Chlorination Practices for Water Treatment in Houston

	Ground Water	Surface Water
Water Source Percentage	35%	65%
Free Chlorine Dosage	2ppm	3ppm
Residual Free Chlorine(Arithmetic Average)	1ppm	2.25ppm
Chlorine Reacted with Organic Matter	< 30ppb	<30ppb
Water Flow Rate during Summer Time	492MGD	

3.7.2 CHLORINATION IN WASTEWATER TREATMENT PLANT

Houston has 41 wastewater treatment plants (City of Houston, 2001) as shown in Table B-8 in Appendix B. The purpose of chlorinating during wastewater treatment prior to discharge of the final effluent is to kill pathogenic bacteria, viruses, and other microorganisms. Pathogenic microorganisms may enter the wastewater collection system from homes, hospitals, or other sources, and pose a threat to human health if the discharged effluent is later used for recreation or drinking water.

In order to estimate how much chlorine is released from wastewater treatment plants during chlorination, it was assumed that the quantity of chlorine used is similar to that used by water treatment plants since the City of Houston has no recorded chlorination data for wastewater treatment. The annual average quantity of wastewater that is treated in Houston is 234.588 MGD (Whitmey, 2001), which is two thirds of the

annual water treatment flow rate. Wastewater has a higher chlorine demand by assuming that wastewater contains more organic materials which make more chlorine consumption than water in water treatment plant. Therefore, in the absence of specific data, it was assumed that the chlorine emissions during chlorination of wastewater are similar to the emission rates due to water treatment, a few hundred kilograms per day.

In addition to volatilization during treatment, additional chlorine emissions may be associated with removal of residual chlorine. Following the chlorine contact basins, sulfur dioxide is added to the wastewater to remove residual chlorine to concentrations below 0.01 mg/L in order to protect fish and other aquatic life. The sulfur dioxide converts the free chlorine to chloride and it is reasonable to expect that the sulfur dioxide will scavenge a large fraction of the residual free chlorine. This dechlorination with sulfur dioxide is required if a wastewater treatment plant treats 1 MGD or more. However, if the plant treats less than 1 MGD, dechlorination is not required (Whitmey, 2001). Assuming that wastewater treatment plants handle more than 1 MGD, chlorine loss due to volatilization of residual chlorine is likely to be negligible.

Releases due to volatilization during wastewater treatment =

Two thirds of the value assigned to water treatment based on the lower volumes of wastewater treated

=300 kg/day

Since the emission estimates for these sources were estimated to be more than an order of magnitude less than other potential sources, these emissions will not be incorporated into the inventory used for modeling in this work.

3.8 Emissions of atomic chlorine precursors associated with chlorinated organics in the atmosphere

Another possible source for chlorine atoms in the troposphere is the photochemical decomposition of organochlorine compounds. Chlorine atoms are produced from the photochemical reactions of organochlorine compounds such as chlorinated solvents and pesticides (Carter, et al., 1997a, b).

An inventory of organochlorine compound emissions for Harris County (Houston and Ship channel area) was based on TRI data from 2000. The compounds with the highest releases to atmosphere are shown in Table 3.3. The five major chlorinated organic compounds (chloromethane, dichloromethane, chloroform, 1,2-dichlroethane, chlorodifluoromethane) account for 75% of the total chlorinated organic compounds. The total amount of chlorinated organic compounds released to the atmosphere is 3.5 times larger than atmospheric chlorine emissions.

For the chlorinated solvent, trichloroethene (TCE), the yield of chlorine atoms has been estimated at 60% of the moles of TCE initially present (Carter, et al, 1997b; Tuazon, et al., 1988). For the agricultural pesticide, chloropicrin, the yield is expected to be near unity because photolysis is the primary consumption pa /thway and this compound does not react with hydroxyl radical to a significant extent (x Carter, et al., 1997a). Applying the percentage for TCE to the other chlorinated organic compounds, it is assumed that 60% of the moles of chlorinated organic compounds yield chlorine atoms. An example calculation is shown as follows:

For Chloromethane,

(119929 lb/yr total emission) / (50.49 g/mol chloromethane) * 0.6 * (0.454 kg/lb) * (35.5 g/mol Cl) *(1yr /365days) = 62.9 kg/day as Cl = 31.5 kg/day as Cl_2

The total amount of molecular chlorine release from chlorinated organic compound reactions is 100 kg/day in Harris County. Since most point sources of chlorinated organic compounds are concentrated in the Harris County, it is expected that molecular chlorine release yielded from chlorinated organic compounds in 11 counties would be less than 200 kg/day.

Besides anthropogenic emissions, there are releases of chlorine-containing gases from natual sources including the oceans, soils, plants and fungi. Methyl chloride (CH_3Cl) has been measured in biomass burning plumes, and is the largest, natural contributor to organic chlorine in the atmosphere and is currently present at about 540 ppt (Lobert et al., 1999). For all the reactive chlorine gases such as CH_3Cl, $CHCl_3$, CH_2Cl_2, and C_2HCl_3, there are identified oceanic net emissions, but there is the shortage of relevant data as well as issues related to the measurements of these gases dissolved in seawater. Aside from the oceans, there is evidence for the production of chloroform in soils and the production of methyl chloride from the activity of certain white rot fungi (Khalil et al., 1999; Haselmann et al., 2000). Due to the lack of oceanic data and uncertainty of the flux, growth habitat of wood rotting fungi, and number of species of fungi capable of CH_3Cl release, the emissions of organochlorines from seawater, soil, and fungi are not considered in this thesis.

Table 3.3 Chlorinated organic compounds with the highest total air releases in the Harris County (2000 TRI)

Chemical	Fugitive Air (lb/yr)	Stack Air (lb/yr)	Total Air Emissions (lb/yr)	Percent of Total (%)	Molecu-lar weight (g/mol)	Molecular formula	Cl atom release (kg/day)
Chloromethane	77558	42371	119929	18.8	50.49	CH_3Cl	62.9
Dichloromethane	47792	62577	110369	17.3	84.93	CH_2Cl_2	34.4
Chloroform	21330	81919	103249	16.2	119.38	$CHCl_3$	22.9
1,2-Dichloroethane	73871	7898	81769	12.8	98.96	$C_2H_4Cl_2$	21.9
Chlorodifluoromethane	64326	0	64326	10.1	86.47	$CHClF_2$	19.7
Trichloroethylene	41884	864	42748	6.7	131.4	C_2HCl_3	8.6
Chlorobenzene	10537	32000	42537	6.7	112.56	C_6H_5Cl	10.0
1,1-Dichloro-1-fluoroethane	26000	0	26000	4.1	44.03	HCFC	15.7
Dichlorodifluoromethane	17244	.	17244	2.7	120.09	CCl_2F_2	3.8
1,2,3-Trichloropropane	14614	211	14825	2.3	147.43	$C_3H_5Cl_3$	2.7
Chloroethane	4838	4643	9481	1.5	64.52	C_2H_5Cl	3.9
1,1,1-Trichloroethane	4257	890	5147	0.8	133.42	CH_3CCl_3	1.0
Total			**637624**	**100**			**208**

3.9 Summary of emission inventory for atomic chlorine precursors

Figures 3.4a and 3.4b show the spatial distributions of total emissions of molecular chlorine from 0700 hr to 1200 hr and from 1200 hr to 1700 hr. Figures 3.4c and 3.4d show the spatial distribution of emissions of molecular chlorine from cooling towers from 0700 hr to 1200 hr, and the emission from swimming pools from 1200 hr to 2000 hr.

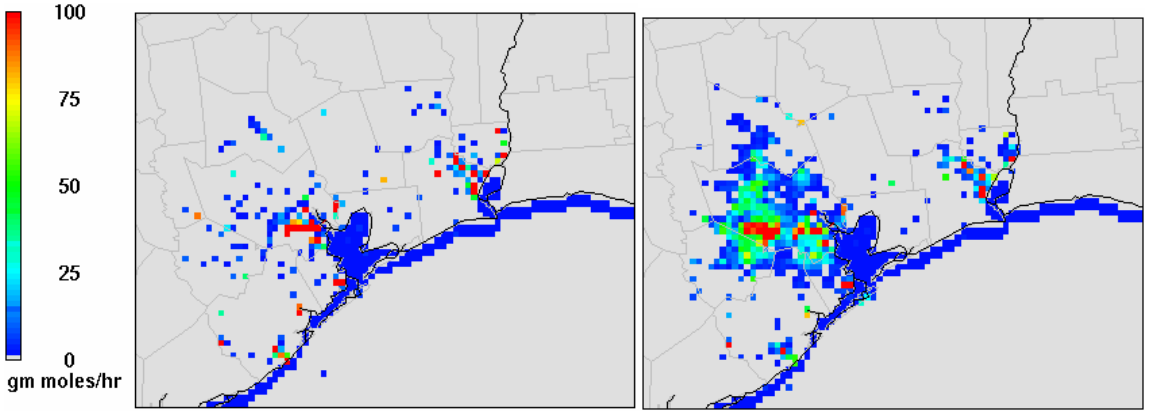

a) Total chlorine emissions 0700-1200

b) Total chlorine emissions 1200-1700

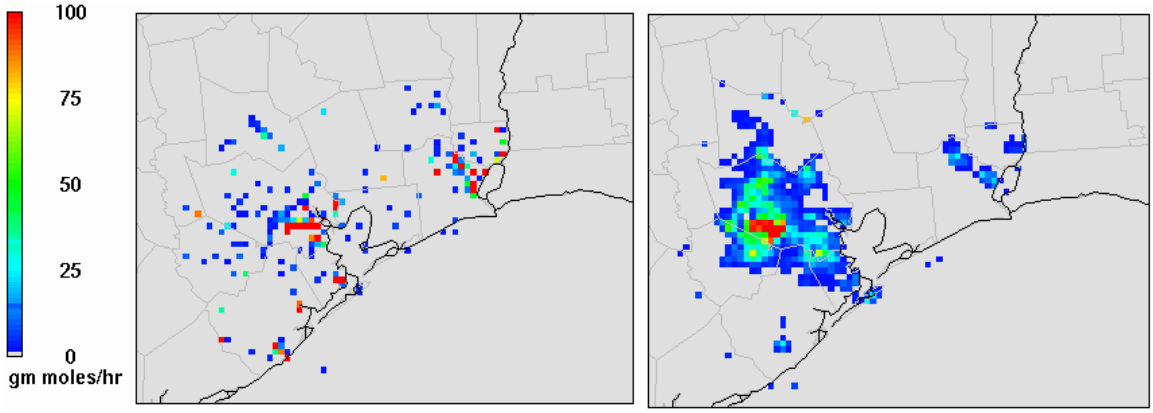

c) Cooling towers 0700-1200

d) Swimming pools 1200-2000

Figure 3.4 Estimated chlorine emissions in southeastern Texas nested CAMx modeling domain (4km HGBPA subdomain). a) Total emissions of molecular chlorine from cooling towers, swimming pools, point sources, and reactions of sea salt between 0700 and1200, b) total emissions of molecular chlorine between 1200 and 1700; c.) emissions of molecular chlorine from cooling towers between 0700 and 1200; this is the largest estimated source of emissions in the inventory; d.) emissions of molecular chlorine from swimming pools between 1200 and 2000; this is the second largest estimated source of emissions in the inventory

Chapter 4: Photochemical modeling of Chlorine Chemistry

The emission inventory described in Chapter 3 was used as input to the CAMx photochemical model, modified to include the urban atmospheric reactions of chlorine. The model was used to predict ozone and other air pollutant concentrations for the period August 22 – September 6 and these predictions were compared to ambient observations of ozone, isoprene, and the molecular marker of chlorine chemistry, CMBO concentrations. The sensitivity of the model predictions to changes in chlorine emissions, from a variety of source categories, was evaluated, and all of these analyses are presented in this chapter.

4.1 Comparison of predicted and observed ozone concentrations, without inclusion of chlorine chemistry

Measurements of ozone concentrations, which will be compared to model predictions in this work, were made using uv absorption at approximately two dozen sites located throughout the Houston area. These sites are the regulatory monitoring network for the Houston area. They are operated by the TCEQ; data and operating procedures are available at the TCEQ website (TCEQ, 2005a).

Comparisons between modeled and observed ozone concentrations, performed by TCEQ, without incorporation of chlorine chemistry into the photochemical modeling simulations, are summarized in Table 4.1. Table 4.1 reports model performance using standard EPA-recommended performance measures: relative bias, relative gross error, and unpaired peak accuracy (TCEQ, 2005b). The model generally underpredicts ozone concentrations on August 24, 25, and 30. Model performance meets the minimum EPA statistical requirements on August 25, 26, 29, and 31 and September 1, 3, 4, 5, and 6. The major performance issue is the model's inability to produce peak ozone

concentrations approaching the high monitored values on August 25 and 30 and September 1.

Table 4.1 Base case model performance in Houston Galveston area (4km grid) (TCEQ, 2005b)

Episode Date	Data Pair w/ Observation > 60.0ppb		Site Daily Maximum		Area-wide Maximum ozone				
	Normalized Bias	Normalized Gross Error	Normalized Bias	Normalized Gross Error	Accuracy	Modeled		Observed	
						ppb	Hour (CST)	ppb	Hour (CST)
08/24/2000	-38.5	38.5	-25.3	26.4	-34.8	78.4	1300	120.1	1100
08/25/2000	-9.9	20.9	-5.9	20.3	-19.3	156.5	1500	194.0	1300
08/26/2000	6.3	18.5	33.7	38.8	6.7	149.4	1500	140.0	1700
08/27/2000	25.2	25.2	25.7	25.7	29.0	112.3	1400	87.0	1700
08/28/2000	22.4	24.3	26.5	27.0	17.8	132.0	1500	112.0	1700
08/29/2000	8.1	15.8	16.9	21.1	3.1	151.2	1500	146.7	1500
08/30/2000	-11.0	20.4	-16.0	22.8	-31.6	137.2	1600	200.5	1600
08/31/2000	4.6	15.8	-5.1	13.6	-1.4	173.0	1500	175.5	1600
09/01/2000	8.1	13.7	16.0	20.6	-16.5	136.7	1500	163.7	1300
09/02/2000	-2.7	17.2	-0.8	12.4	21.7	152.7	1400	125.5	1400
09/03/2000	-3.7	19.4	6.7	11.1	9.5	139.3	1400	127.2	1600
09/04/2000	5.5	20.4	16.5	21.2	8.9	158.0	1300	145.0	1200
09/05/2000	6.9	26.6	39.2	50.0	13.3	209.7	1400	185.0	1400
09/06/2000	-5.1	18.9	3.2	18.0	-2.0	152.9	1400	156.0	1300

To assess model performance with the addition of chlorine chemistry, two sets of performance evaluations will be performed. First, model-predicted and observed CMBO concentrations will be compared, to assess whether the estimated magnitude, spatial distribution and temporal distribution of chlorine emissions is consistent with the data on molecular marker species. Then, predicted and observed ozone concentrations, with chlorine chemistry included, will be compared to observational data to determine if the addition of chlorine chemistry improves the performance of the model in predicting ozone concentrations.

4.2 Comparison of model predicted and observed concentrations of CMBO and isoprene at La Porte Airport

The concentration of the molecular marker of chlorine chemistry, 1-chloro-3-methyl-3-butene-2-one (CMBO), was measured at the La Porte Airport in the Houston area, during the episode period, by Riemer (2001). In order to determine if Cl chemistry is occurring in the Houston area, Riemer (2001) made measurements of isoprene and CMBO (as well as other species not directly relevant to this work) over the period August 12, 2000 to September 12, 2000 at the La Porte airport, east of Houston near an industrial source region. Ambient air samples were initially drawn from a continuously flushed glass manifold into fused-silica lined stainless steel traps and sample lines internal to a concentration system. Sample analysis was performed using gas chromatography with mass spectrometric detection. The spectrometer was used in single ion monitoring mode which allowed very low detection limits. The detection limit for isoprene was less than 1 ppt; for CMBO the detection limit was approximately 1-3 ppt.

Model-predicted and observed CMBO concentrations are compared in Figure 4.1. The model predicted CMBO mixing ratio that is reported in the Figure is the maximum concentration for the 44 km by 44 km (11 grid cells by 11 grid cells) region centered at the La Porte Airport. The comparison was done in this way because of the uncertainties in the spatial distribution of the chlorine emissions, as described later in this chapter.

The observed and predicted CMBO mixing ratios both exhibited sharp peaks in the mornings of August 25th, 30th, 31st, and September 1st. The model-predicted peak CMBO mixing ratios on August 25th 30th, and 31st are approximately a factor of 2 or more lower than the observed values. Predicted values appear to be more persistent than observations on most days.

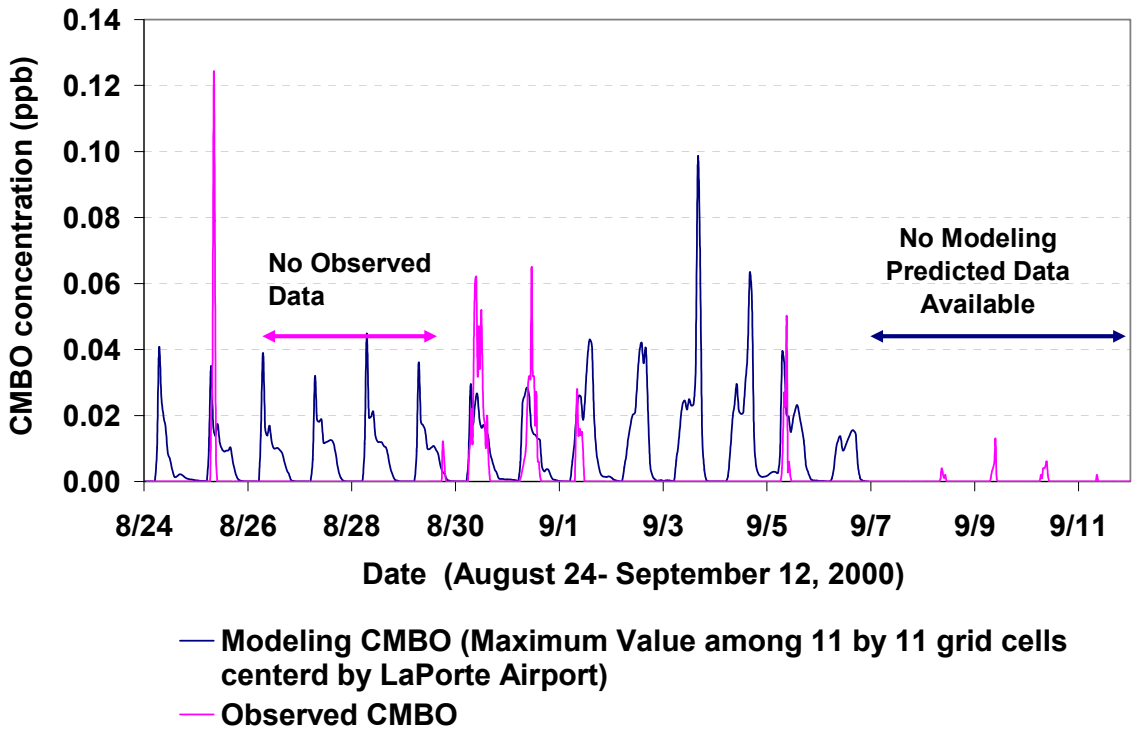

Figure 4.1 Time series of CMBO mixing ratios of (a) maximum predicted enhancement among 11 by 11 modeling 4km grid cells around La Porte airport and of (b) observed value at the grid cell of La Porte Airport

In order to examine the effect of emission estimates on these discrepancies, a series of model sensitivity studies were performed. Since CMBO is a product of the reaction between atomic chlorine and isoprene, the CMBO concentrations predicted by the model depend on both predicted chlorine emissions and predicted isoprene concentrations. Therefore, to assess the accuracy of the chlorine emission inventory based on CMBO concentrations, it is necessary to assess the accuracy of the isoprene emission estimates. Isoprene concentrations, measured at several monitoring sites, were compared with the model-predicted isoprene concentrations at the grid cells where monitoring sites are located. The data for the Aldine, Bayland Park, Clinton, Deer Park,

and La Porte Airport sites are shown in Figure 4.2. Model-predictions are available for the period August 24th through September 6th; observations are available for various days at the different sites. For sites where model-predicted concentrations and observations are not available on the same days, the overall trends in isoprene concentrations can be compared. The model-predicted isoprene concentration is generally greater than the observed isoprene concentration by a factor of 2 or more. A series of model sensitivity studies were performed to assess the nature of the discrepancy, the results are described in detail by Song et al. (2005). The primary conclusion drawn from the sensitivity analyses was that the isoprene over-prediction created an overestimation bias, of approximately a factor of 2 to 3, for the predictions of CMBO. This means that the model under-prediction of CMBO, reported in Figure 4.1, likely represents an even greater under-prediction of the chlorine inventory than would be the case if the model predictions of isoprene were correct.

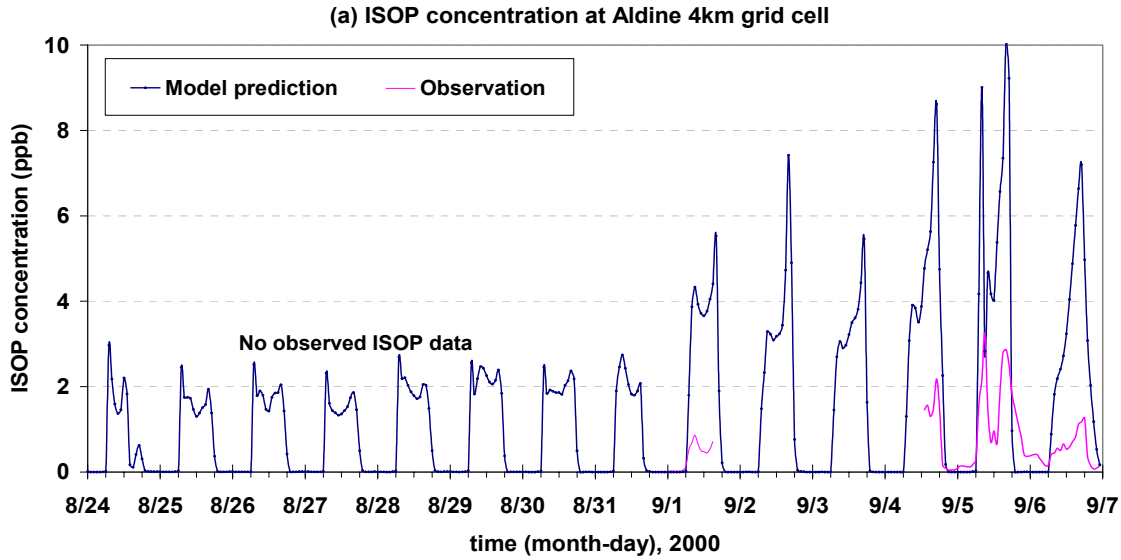

Figure 4.2 Comparison of model predicted and observed isoprene (ISOP) concentrations at several monitoring sites and its grid cell (4km resolution), (a) Aldine monitoring site, (b) Bayland Park monitoring sites, (c) Clinton monitoring site, (d) Deer Park monitoring site, and (e) La Porte Airport monitoring site

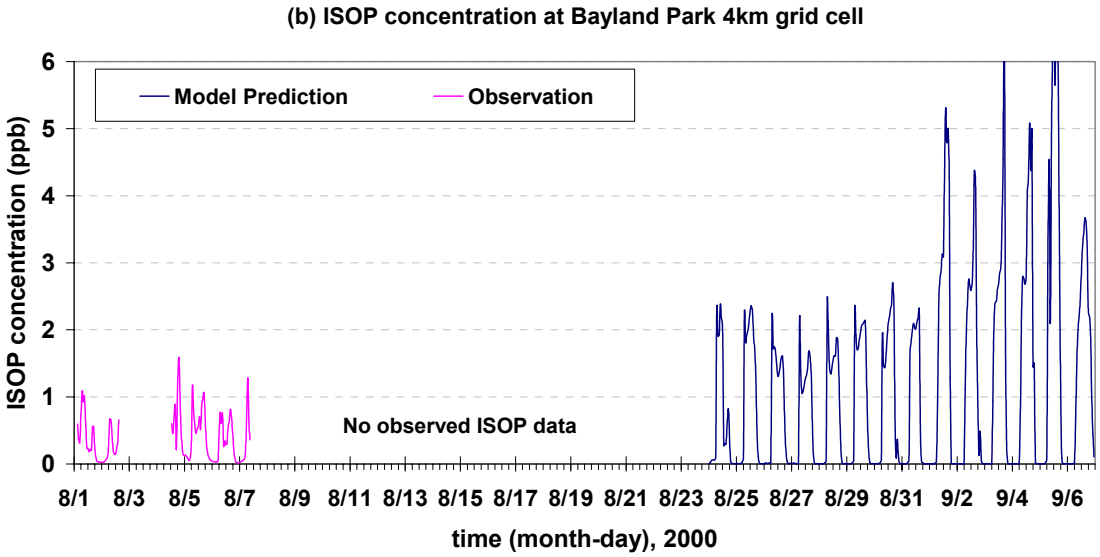

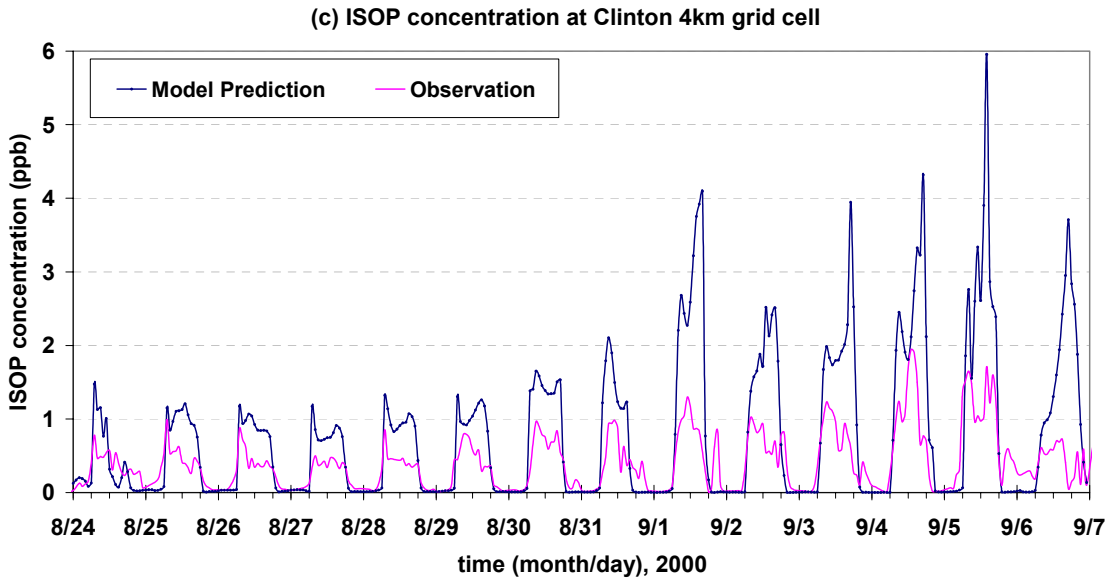

Figure 4.2 (Cont'd) Comparison of model predicted and observed isoprene (ISOP) concentrations at several monitoring sites and its grid cell (4km resolution), (a) Aldine monitoring site, (b) Bayland Park monitoring sites, (c) Clinton monitoring site, (d) Deer Park monitoring site, and (e) La Porte Airport monitoring site

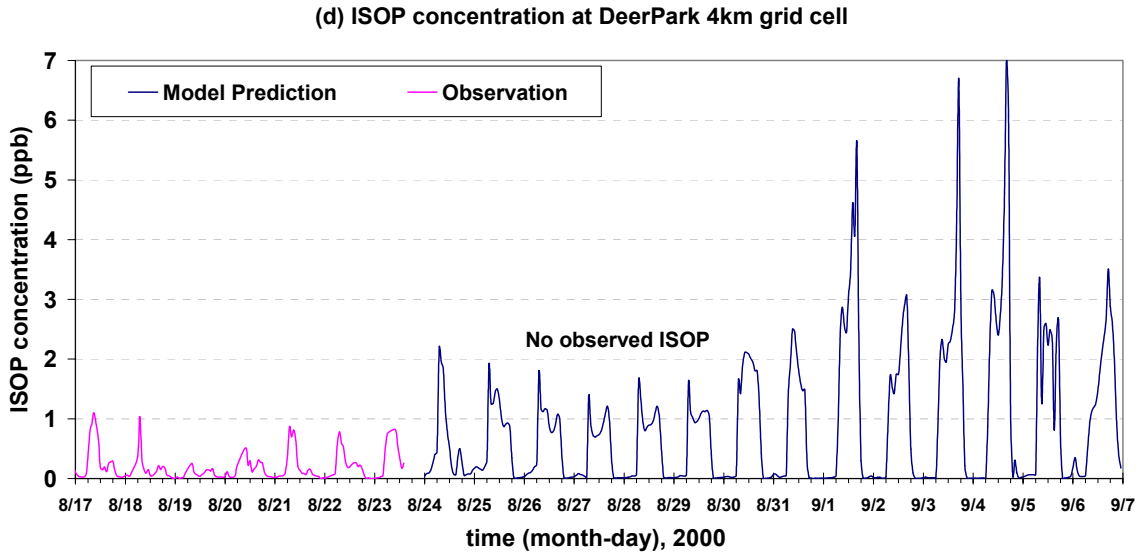

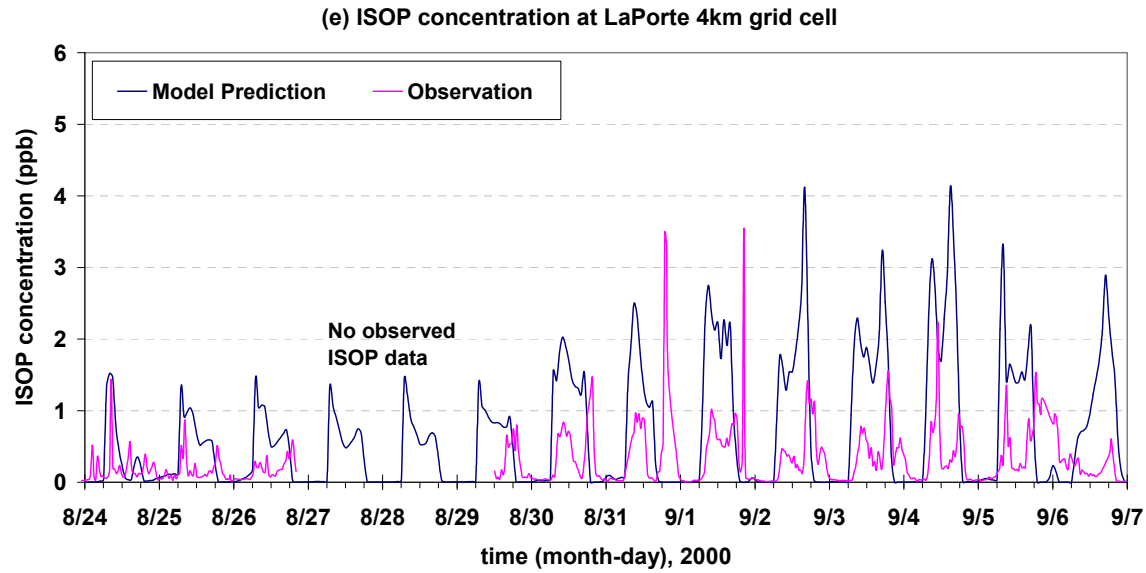

Figure 4.2 (Cont'd) Comparison of model predicted and observed isoprene (ISOP) concentrations at several monitoring sites and its grid cell (4km resolution), (a) Aldine monitoring site, (b) Bayland Park monitoring sites, (c) Clinton monitoring site, (d) Deer Park monitoring site, and (e) La Porte Airport monitoring site

4.3 Comparison of model predicted and observed concentrations of Ozone with and without the incorporation of chlorine chemistry into the modeling

Comparisons between modeled and observed ozone concentrations, with and without the incorporation of chlorine chemistry into the photochemical modeling, are summarized in Table 4.2. Normalized bias and normalized gross errors for La Porte, Deer Park, and Bayland Park monitoring sites were calculated for the entire episode (August 22- September 6). When chlorine chemistry is incorporated into the model, the underprediction bias for ozone concentration is reduced. Figure 4.3 shows time series for ozone concentrations at the locations where some of these under-predictions of ozone concentrations in the base case simulations occur. While the addition of chlorine emissions and chlorine chemistry does not completely eliminate the underprediction bias for ozone concentrations, the effect is directionally correct.

Table 4.2 Comparison of model performance between case with chlorine emissions and basecase without chlorine emissions, at three sites; La Porte, Deer Park, and Bayland Park

	Data Pair w/ Observation > 60.0ppb											
Statistics	**Normalized Bias**						**Normalized Gross Error**					
EPA Range	**±(5-15)%**						**(30-35)%**					
Monitoring sites	La Porte		Deer Park		Bayland Park		La Porte		Deer Park		Bayland Park	
Scenario	Cl	base	Cl	base	Cl	base	Cl	base	Cl	base	Cl	base
8/22-9/6	-6.45	-8.87	0.011	-4.14	-20.32	-23.64	21.84	21.86	20.44	20.36	23.85	26.20

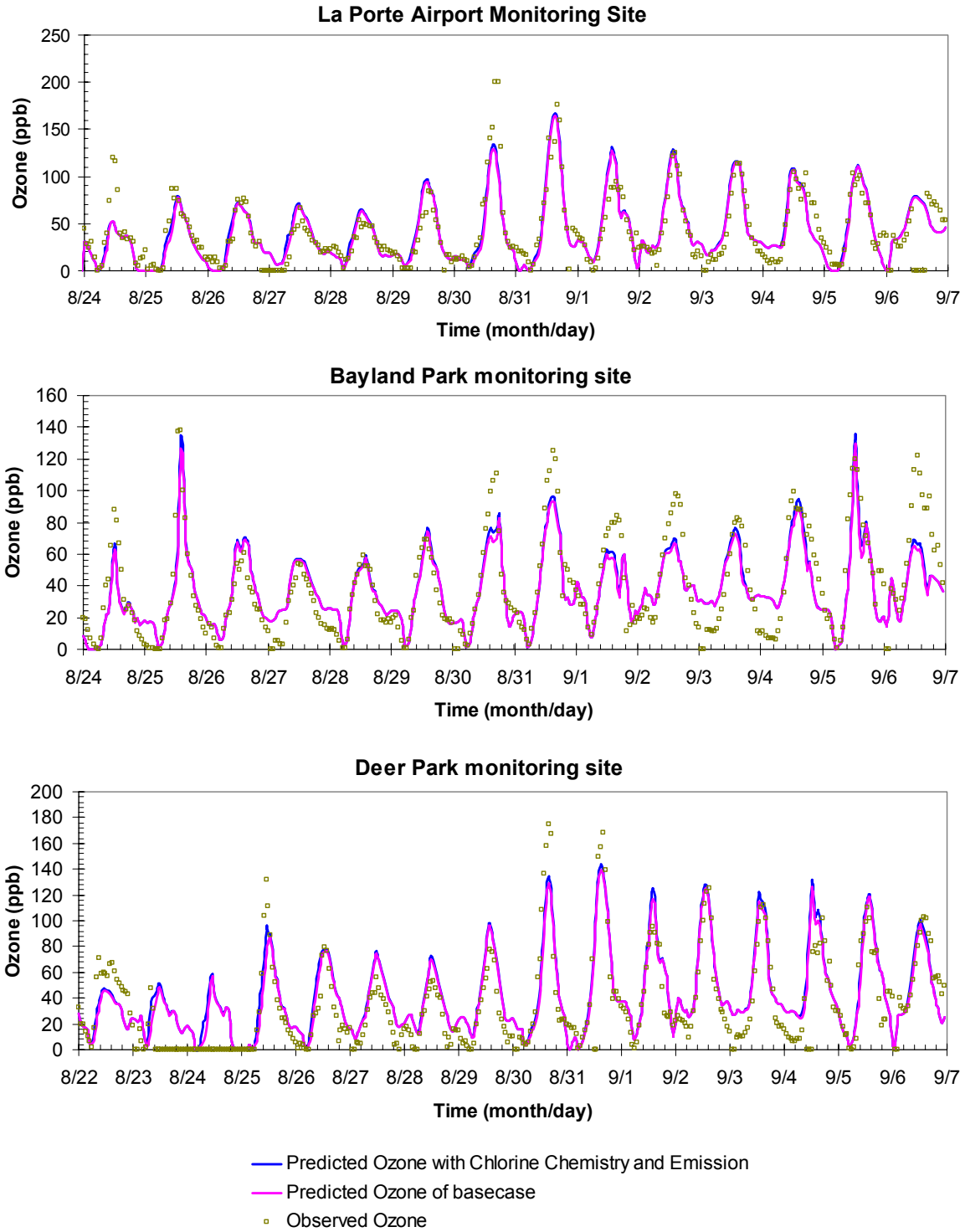

Figure 4.3 Time series for ozone concentrations at the locations where some of these und er-predictions of ozone concentrations in the base case simulations occur (La Porte, Bayla nd Park, and Deer Park monitoring sites)

4.4 Sensitivity of CMBO concentration predictions to emission estimates

More detailed comparisons between modeled and observed concentrations of isoprene and CMBO were performed for August 25th and 30th. August 25th and 30th were chosen for more detailed analysis because the high ozone concentrations and high observed CMBO concentrations occurred on these days.

Time series of observed and model-predicted CMBO concentrations on August 25th and 30th are shown in Figure 4.4. CMBO concentrations are underpredicted by the model by approximately a factor of two or more. If the model predictions of isoprene were more accurate, the underpredictions of CMBO would be even greater.

The sensitivity of predicted CMBO concentrations to variations in the strength of chlorine emission sources (cooling towers, swimming pools, industrial point sources, and seasalt) was examined. The sensitivity analyses were done by doubling tower emissions, doubling swimming pool emissions, doubling industrial point source emissions, and increasing seasalt emissions by a factor of 10. The differences in CMBO mixing ratios between each of the sensitivity runs and the basecase run were calculated. Figures 4.5, 4.6, and 4.7 show the results of the sensitivity analyses. Figures 4.5 and 4.6 report differences in CMBO concentrations between the model predictions with added chlorine emissions and the concentrations predicted using the base case chlorine emissions. Figure 4.5 shows the maximum CMBO mixing ratios near La Porte while Figure 4.6 shows the maximum CMBO mixing ratio for the entire domain. Figure 4.7 shows the total CMBO mixing ratios for the various emission scenarios (basecase chlorine emission inventory + increased chlorine emission from each source) near La Porte.

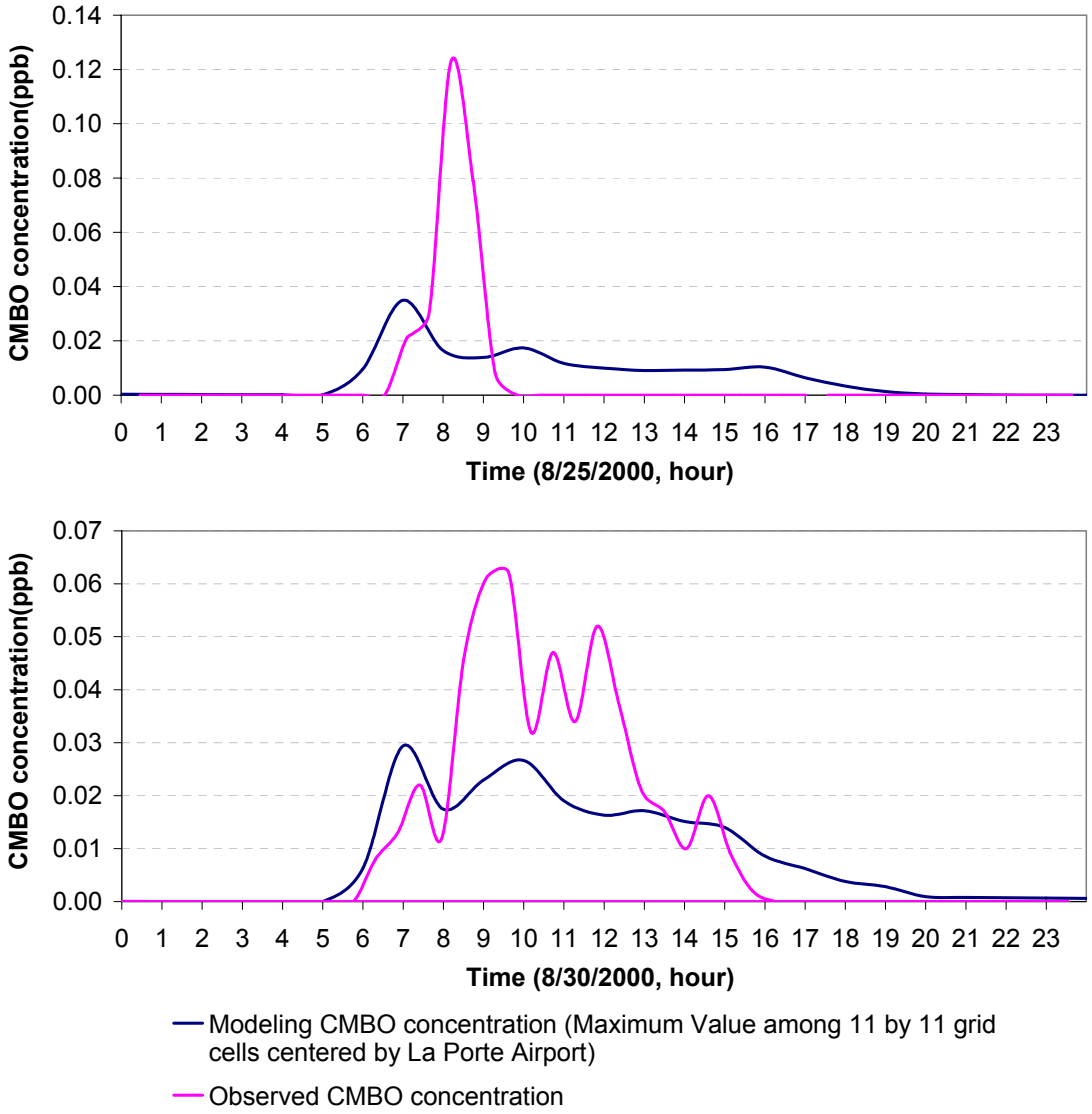

Figure 4.4 Time series of observed and model-predicted CMBO concentration at La Porte Airport grid cell on August 25th and 30th, 2000

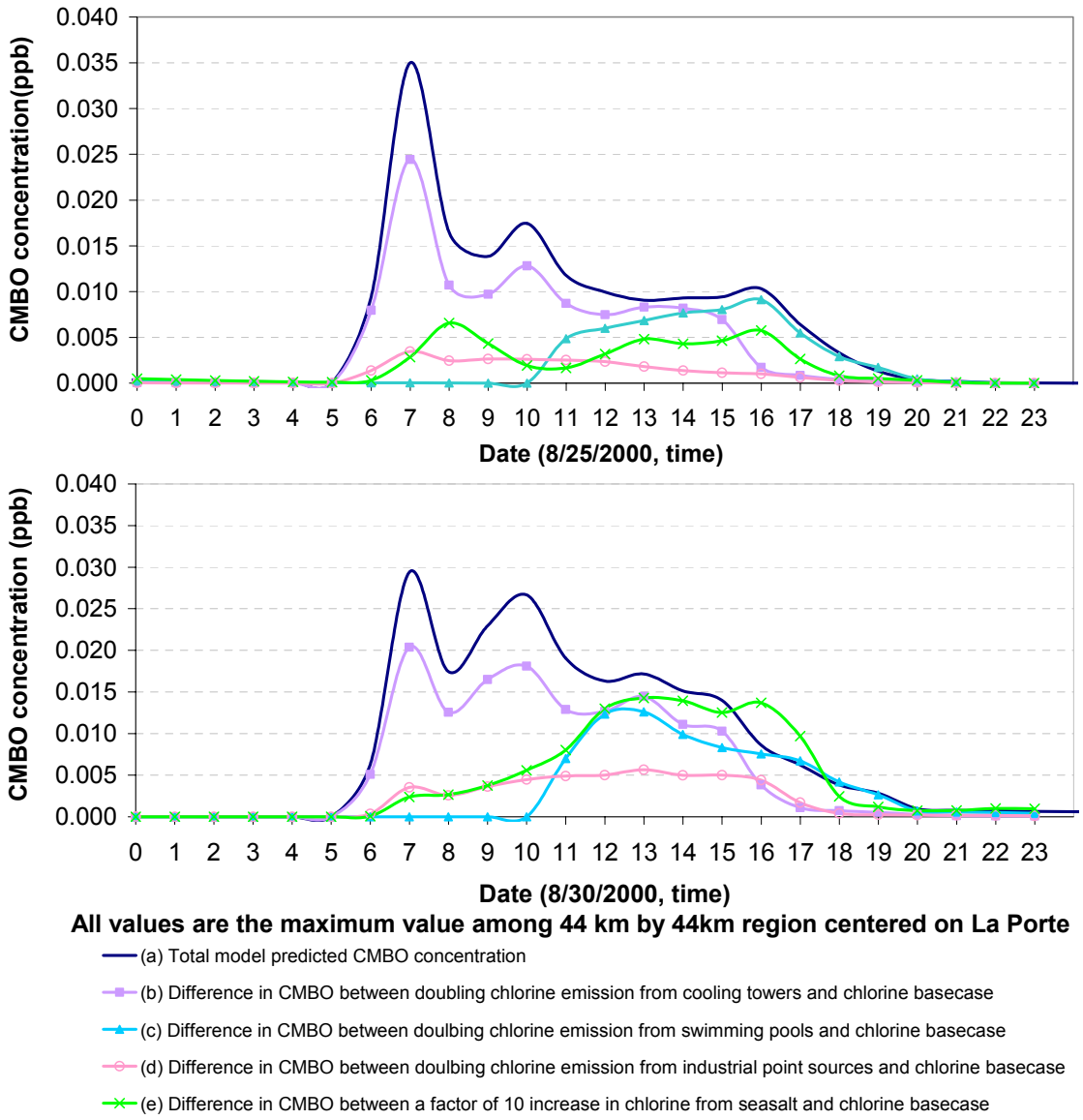

Figure 4.5 CMBO mixing ratio predicted for La Porte Airport (Maximum value among 11 by 11 grid cells centered by La Porte Airport) based on various emission scenarios; Differences in CMBO concentrations between the model predictions with added chlorine emissions and the base case are reported (CMBO mixing ratio predicted using chlorine basecase with increased emissions added in the specified category - CMBO mixing ratio predicted using of chlorine basecase emissions)

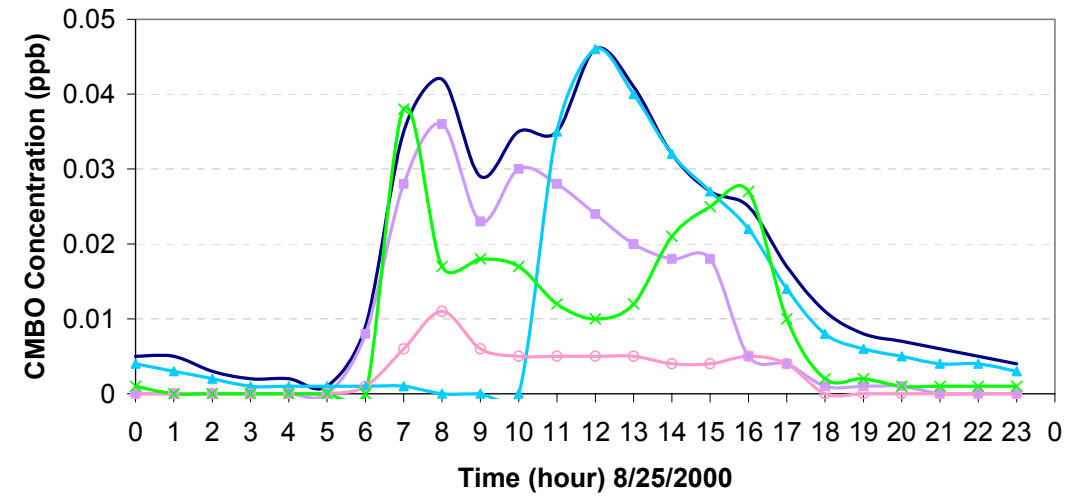

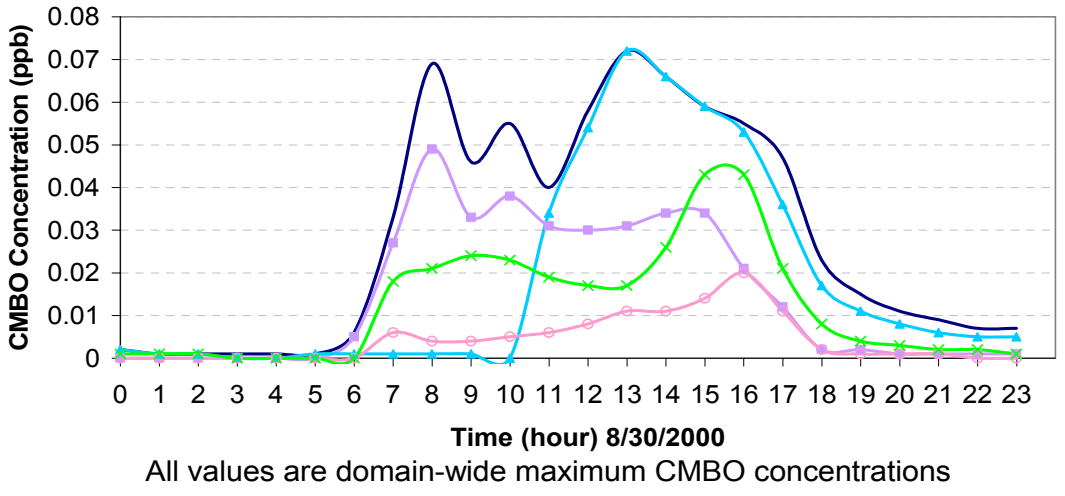

(a) Total model predicted CMBO concentration

(b) Difference in CMBO between doubling chlorine emission from cooling towers and chlorine basecase

(c) Difference in CMBO between doubling chlorine emission from swimming pools and chlorine basecase

(d) Difference in CMBO between doubling chlorine emission from point sources and chlorine basecase

(e) Difference in CMBO between a factor of 10 increase in chlorine from seasalt and chlorine basecase

Figure 4.6 Maximum CMBO mixing ratio predicted for the modeling domain; Differences in CMBO concentrations between the model predictions with added chlorine emissions and the base case are reported (CMBO mixing ratio predicted using chlorine basecase with increased emissions added in the specified category - CMBO mixing ratio predicted using of chlorine basecase emissions)

The sensitivity analyses reported in Figures 4.5, 4.6 and 4.7 indicate that emissions from cooling towers dominate the CMBO formation in the morning hours. The spatial distribution of the differences in CMBO concentrations (reported in Table C-1 in Appendix C) also suggest that the cooling tower emissions have the greatest impact on CMBO concentrations near La Porte. In contrast, the emissions from other sources have a far more spatially distributed impact on predicted CMBO concentrations.

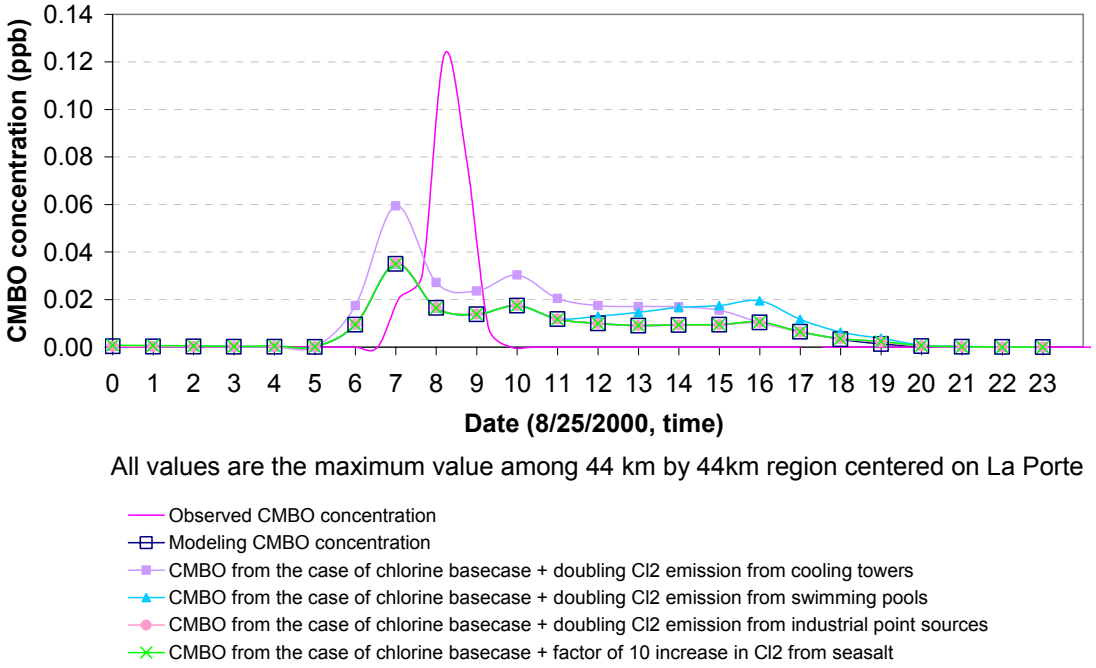

Figure 4.7 CMBO mixing ratio predicted for La Porte Airport (Maximum value among 11 by 11 grid cells centered by La Porte Airport) based on various emission scenarios; Total CMBO concentrations for the model predictions with added chlorine emissions and the base case are reported

One of the strong features of the observed data is a sharp increase in CMBO concentrations on the morning of August 25th. Additional sensitivity analyses were performed to determine whether a transient, point source of chlorine emissions, located near La Porte, could cause this type of feature in the data. In order to examine the potential impacts of a large release of chlorine from an industrial point source, emissions

of Cl_2 were added to the model grid cell (4 km resolution) containing the La Porte Airport. Emissions of 1 ton hr^{-1}, 2 tons hr^{-1}, 4 tons hr^{-1}, and 8 tons hr^{-1} were added at 0800 for a period of one hour. The results are shown in Figures 4.8, 4.9, and 4.10. Figure 4.8 shows total CMBO concentrations at 0800 for the chlorine base case with the added chlorine emissions. Figure 4.9 shows the difference in CMBO mixing ratios between the base case and the base case with the added chlorine emissions. For the base case, the maximum predicted CMBO mixing ratios at La Porte region were 35 pptv at 0700. For the cases with *Cl_2 emissions augmented by 1 ton day^{-1},* the maximum predicted CMBO mixing ratio at La Porte region at 0800 was 37 pptv. For the cases with *Cl_2 emissions augmented by 2 tons day^{-1}, 4 tons day^{-1}, and 8 tons day^{-1}*, the maximum predicted CMBO mixing ratios at 0800 were 68, 112, 139 pptv, relatively. In all of these analyses, the CMBO enhancement is highly localized in La Porte area, and in all the analyses, the temporal trends in CMBO concentrations are similar.

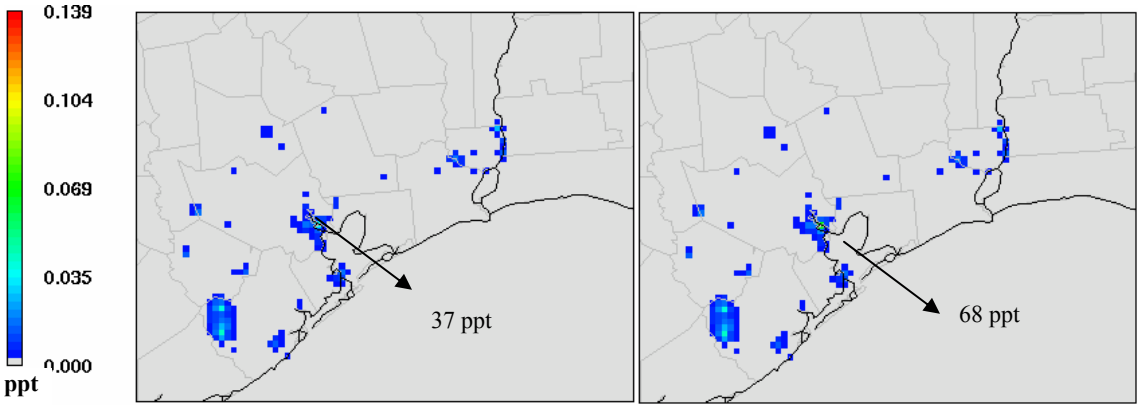

(a) 1ton/day of chlorine release at 0800 at La Porte (b) 2tons/day of chlorine release at 0800 at La Porte

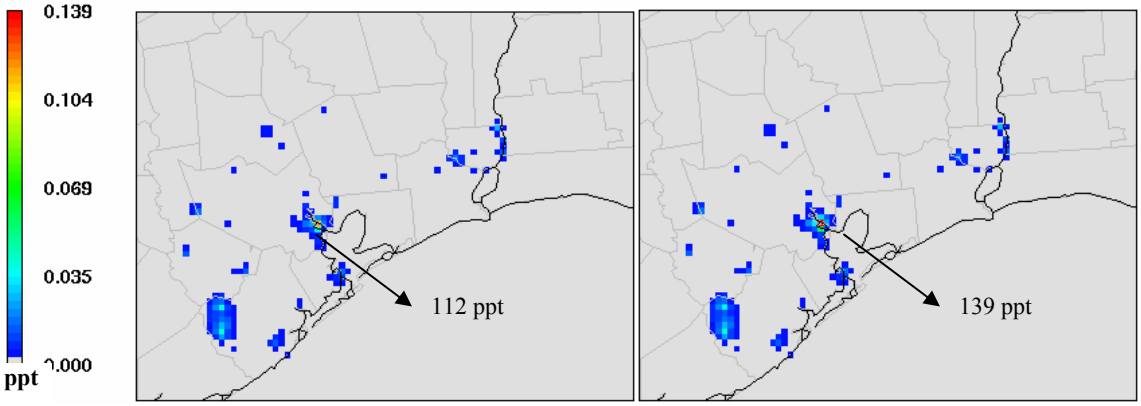

(c) 4tons/day of chlorine release at 0800 at La Porte (d) 8tons/day of chlorine release at 0800 at La Porte

Figure 4.8 Total CMBO mixing ratio from all chlorine sources (base case) augmented by 1 tons day^{-1}, 2 tons day^{-1}, 4 tons day^{-1}, and 8 tons day^{-1}point source release of Cl_2 at 0800 for one hour at the La Porte Airport: The maximum CMBO mixing ratios at La Porte occurred at 0800 for all sensitivity runs.

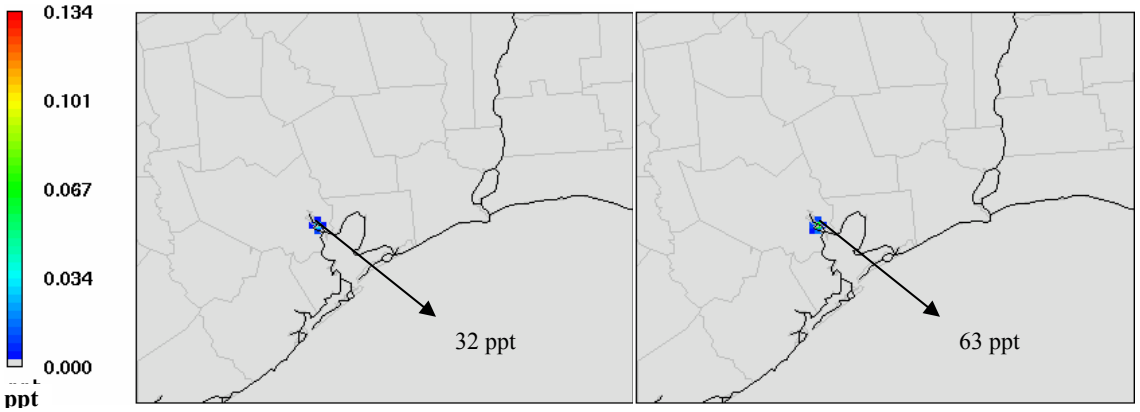

(a) 1ton/day of chlorine release at 0800 at La Porte (b) 2tons/day of chlorine release at 0800 at La Porte

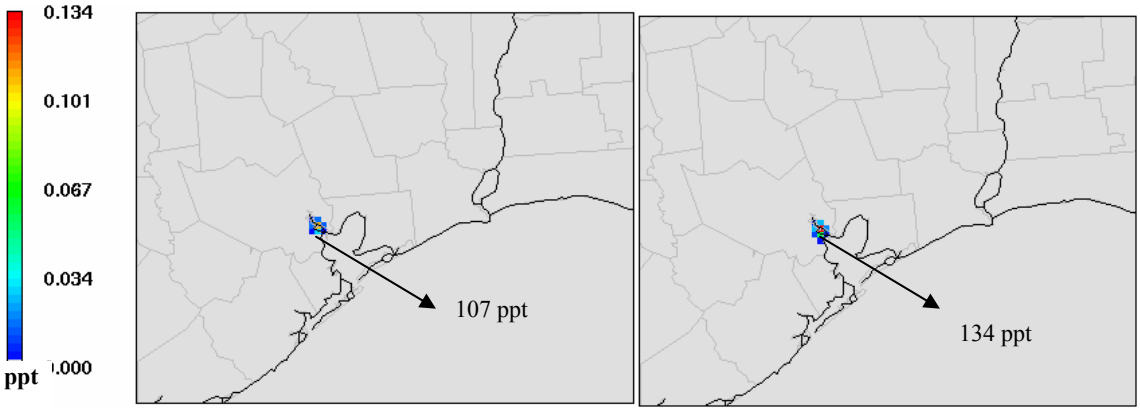

(c) 4tons/day of chlorine release at 0800 at La Porte (d) 8tons/day of chlorine release at 0800 at La Porte

Figure 4.9 Difference in CMBO mixing ratio between base case and basecase augmented by 1 tons day^{-1}, 2 tons day^{-1}, 4 tons day^{-1}, and 8 tons day^{-1} of point source release of Cl_2 at 0800 for one hour at the La Porte Airport: The maximum CMBO mixing ratios at La Porte occurred at 0800 for all sensitivity runs.

In order to assess whether the sensitivity to point source emissions depended on location, a chlorine release of 2 tons day^{-1} was added to a grid cell approximately 8 km (2 grid cells) from the La Porte Airport. The CMBO mixing ratios predicted for this case are also shown in Figure 4.10. The CMBO mixing ratio with added chlorine emissions of 2 tons day^{-1} at the location near La Porte was two times larger than the CMBO mixing ratio with added chlorine emissions of 2 tons day^{-1} at La Porte. This means that CMBO

formation is very dependent on the location of emission sources (most likely due to local emissions of isoprene).

Given the uncertainties in locations of chlorine emissions, these results suggest that fine tuning of the emission inventory is not appropriate until the chlorine and isoprene emission inventories are improved. Nevertheless, it is possible to assess the general implications of chlorine emissions for ozone formation.

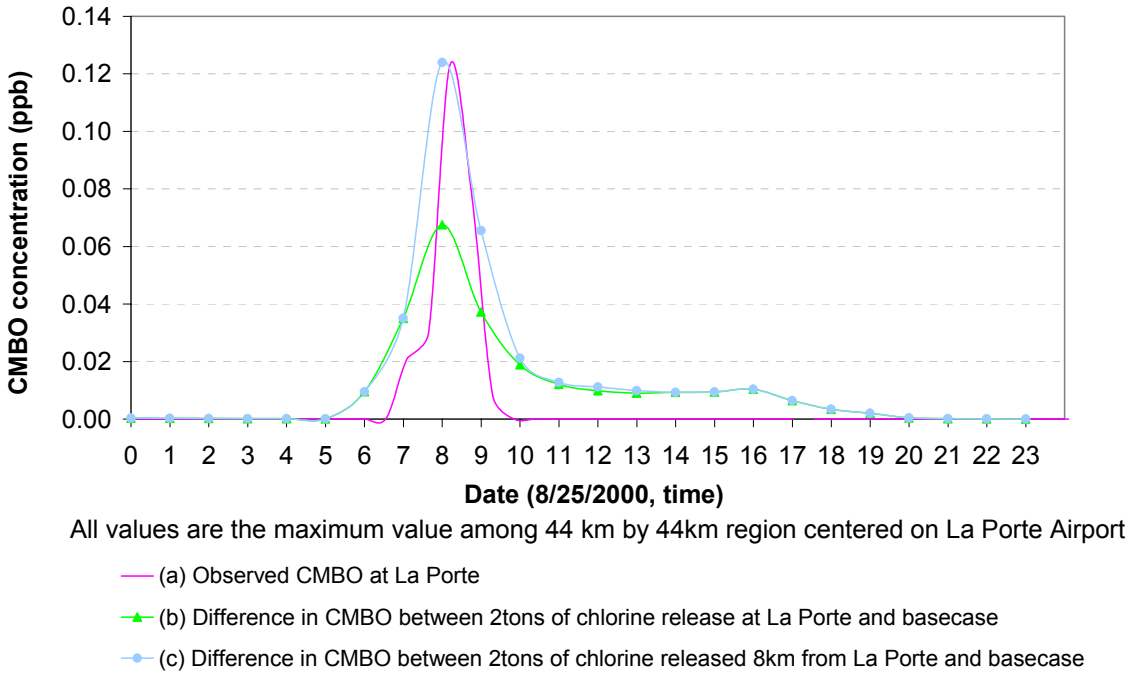

Figure 4.10 Time series of (a) observed CMBO mixing ratio at La Porte, (b) predicted CMBO mixing ratio at La Porte on 25 August 2000 when 2 tons day^{-1} of Cl_2 emission is released at 0800 for one hour at La Porte Airport, (c) CMBO mixing ratio at La Porte when 2 tons day^{-1} of Cl_2 emission is released at 0800 for one hour 8km from La Porte; reported concentrations are the maximum values for the 11 by 11 grid cell region centered on LaPorte

4.5 Enhancement of ozone formation due to chlorine chemistry

The maximum peak ozone enhancements, based on 1-hour averaged concentrations and 8-hour averaged concentrations, due to chlorine emissions (Cl_2 Basecase – Basecase without Cl_2 emissions) are presented in Figure 4.11. The maximum 1-hour averaged ozone enhancement of 72 ppbv was predicted to occur on 25 August 2000 at 0700 and the maximum 8-hour averaged ozone enhancement of 21 ppbv was predicted to occur in Houston Ship Channel area at the same time (time reported as the beginning of the averaging period). Ozone enhancements observed in the morning rapidly disappeared in the afternoon. Relatively small ozone enhancements were predicted (less than 10 ppbv) in the late afternoon. The hourly changes in the differences in 1-hour averaged and 8-hour averaged ozone concentrations on 25 August 2000 are shown in Figures 4.12 and 4.13, respectively.

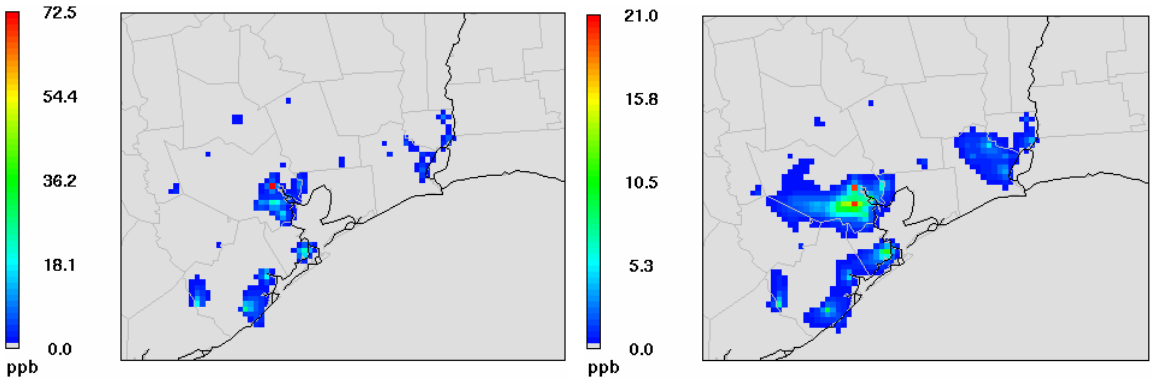

(a) 1- hour averaged ozone concentration (b) 8-hour averaged ozone concentration

Figure 4.11 Maximum change in ozone concentration due to the chlorine emissions at 0700 for (a) 1 hour averaged ozone concentration and at 0700 for (b) 8-hour averaged ozone concentration on 25 August 2000: the difference in predicted ozone concentration between basecase with chlorine emissions (chlorine basecase) and basecase without chlorine emissions is reported.

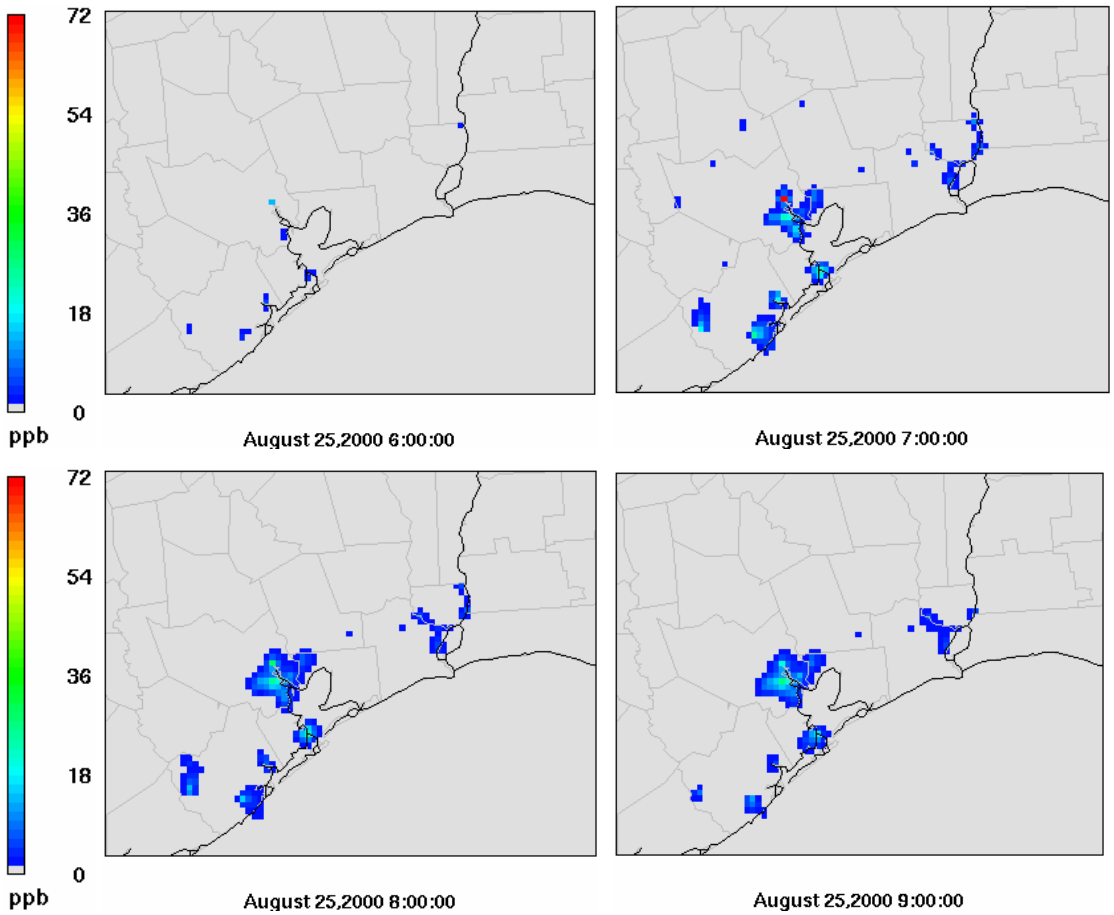

Figure 4.12 Evolution of 1-hour averaged ozone concentrations due to the chlorine emissions on 25 August 2000: Each time represents the beginning of the averaging period for the following one-hour. The difference in ozone concentration between basecase with chlorine emissions (chlorine basecase) and basecase without chlorine emissions is reported.

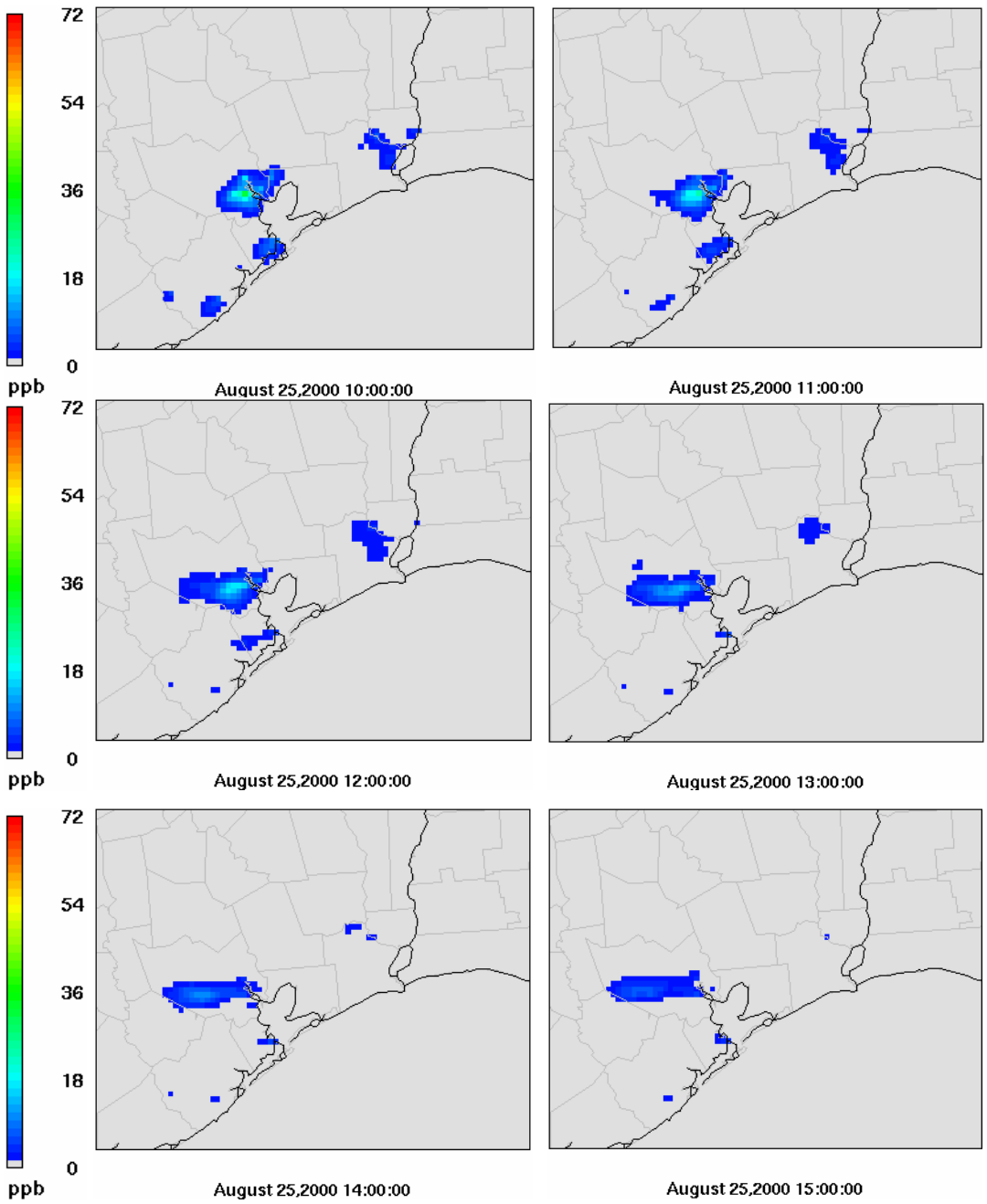

Figure 4.12 (Cont'd) Evolution of 1-hour averaged ozone concentrations on 25 August 2000

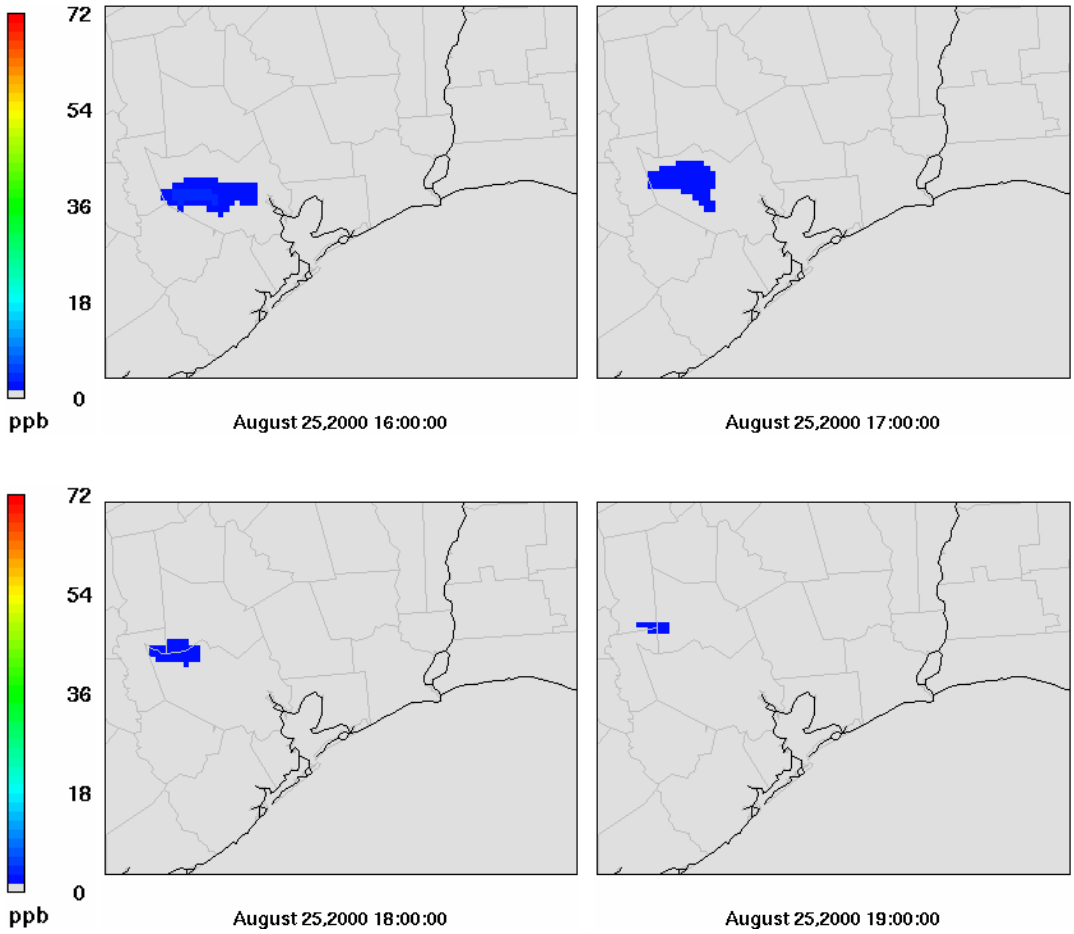

Figure 4.12 (Cont'd) Evolution of 1-hour averaged ozone concentrations on 25 August 2000

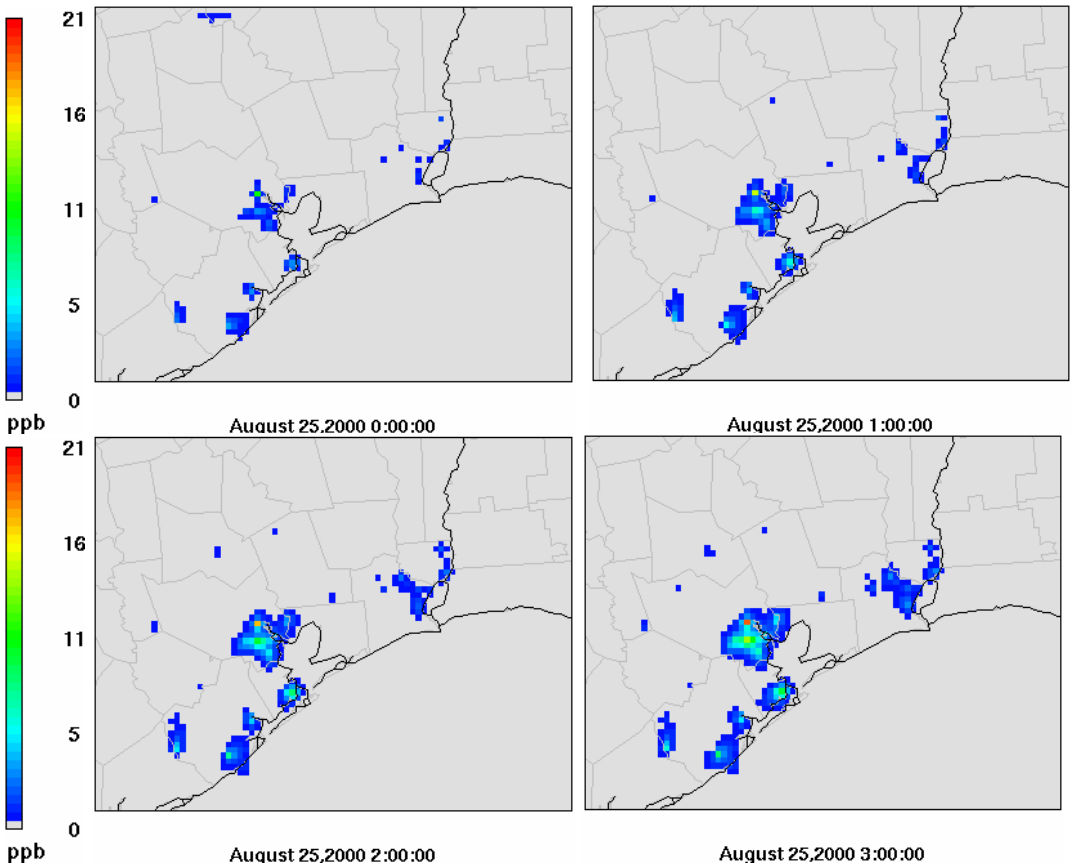

Figure 4.13 Evolution of 8-hour averaged ozone concentrations on 25 August 2000: Each time represent the beginning of the averaging period for the following eight-hour. The difference in ozone concentration between basecase with chlorine emissions (chlorine basecase) and basecase without chlorine emissions is reported.

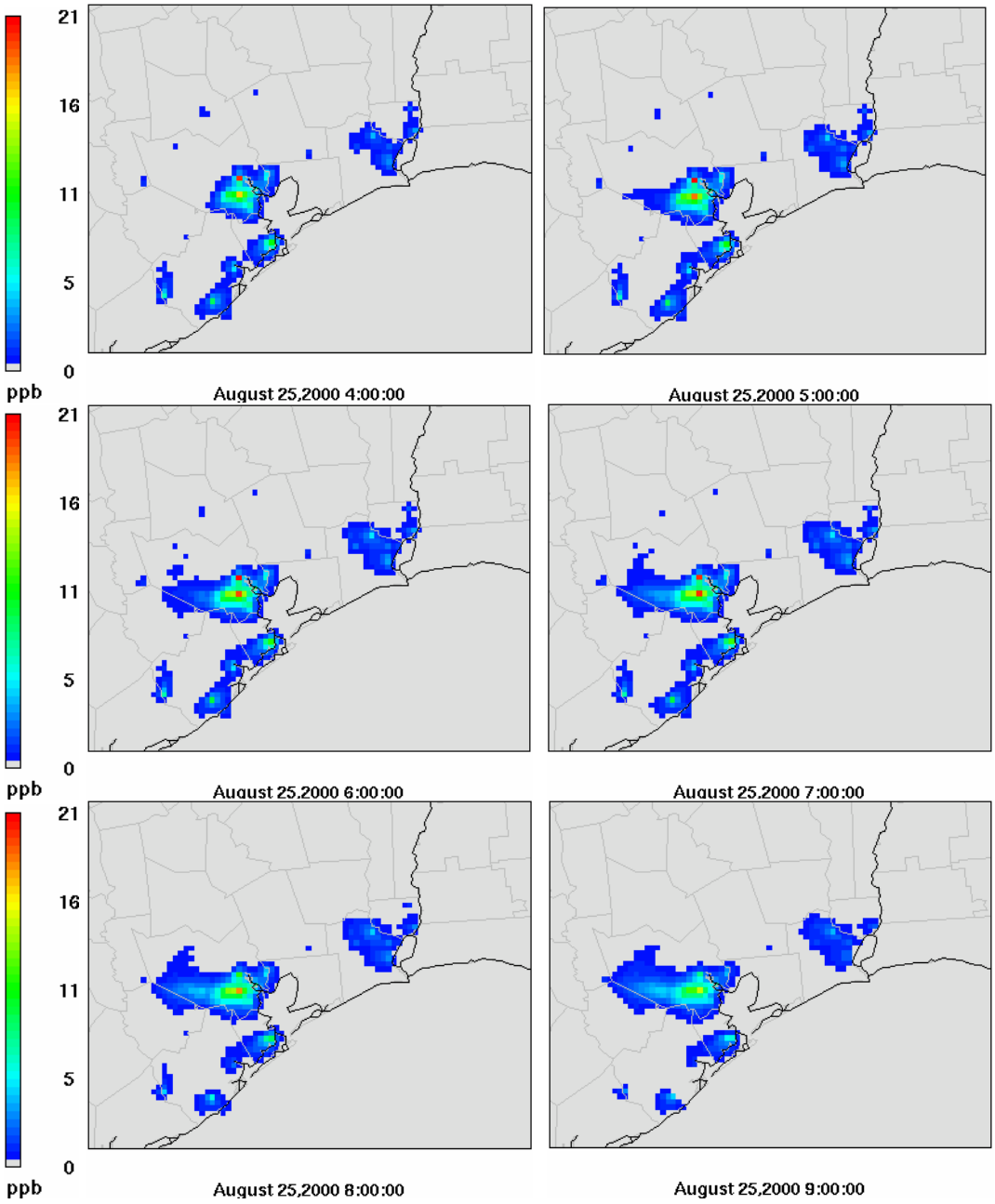

Figure 4.13 (Cont'd) Evolution of 8-hour averaged ozone concentrations on 25 August 2000

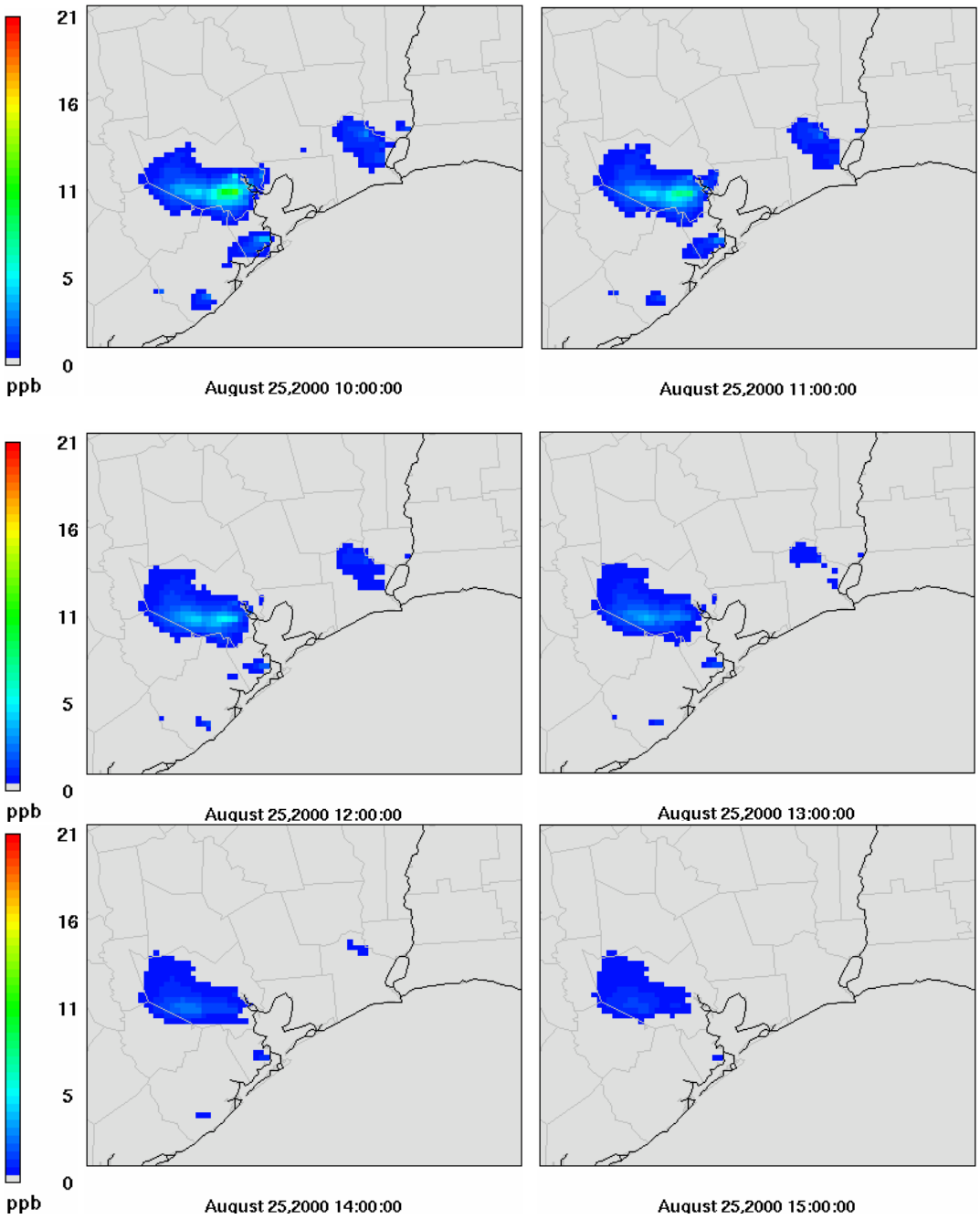

Figure 4.13 (Cont'd) Evolution of 8-hour averaged ozone concentrations on 25 August 2000

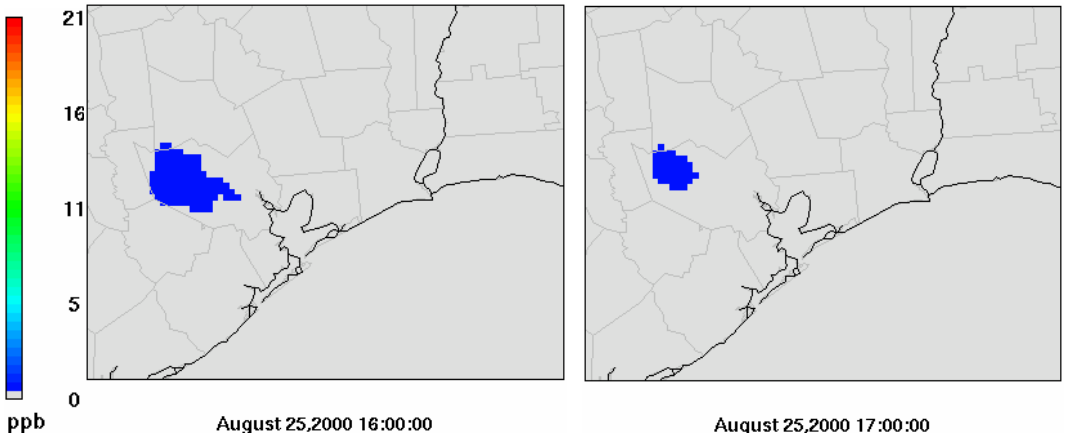

Figure 4.13 (Cont'd) Evolution of 8-hour averaged ozone concentrations on 25 August 2000

The maximum increase in ozone concentration due to the addition of chlorine chemistry is shown for multiple days (August 24, 2000-September 6, 2000) in Figures 4.14 (1-hour averaged concentrations) and 4.15 (8-hour averaged concentrations). On most days the largest increases in ozone concentrations occurred at the La Porte Airport region/Houston area/Ship Channel area. However, on a few days, such as August 24th and 29th the largest increases in ozone concentration due to the addition of chlorine emissions occurred in the Galveston area, and on August 30th and 31st, the largest increases in ozone concentration occurred in the Freeport area. For 1-hour averaged ozone concentrations, the maxima occurred at 0700 on most days in August, and at 0900 or 1000 in on most days in September. In descending order, the days with highest differences in one hour averaged ozone concentrations were August 25th, 26th, 27th, and 30th, respectively.

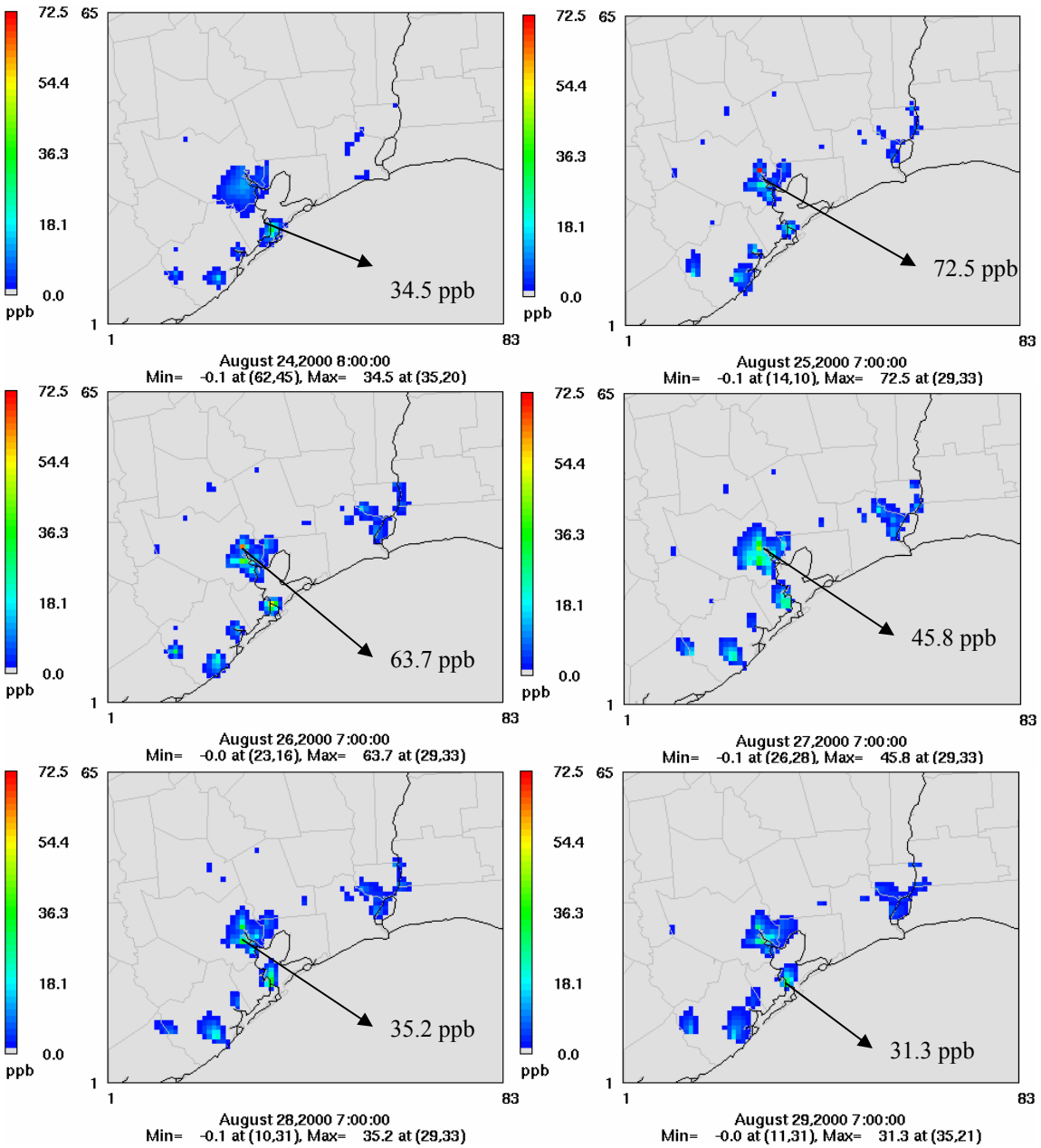

Figure 4.14 Daily maximum enhancement of ozone concentration due to the chlorine chemistry (1-hour averaged ozone concentrations)

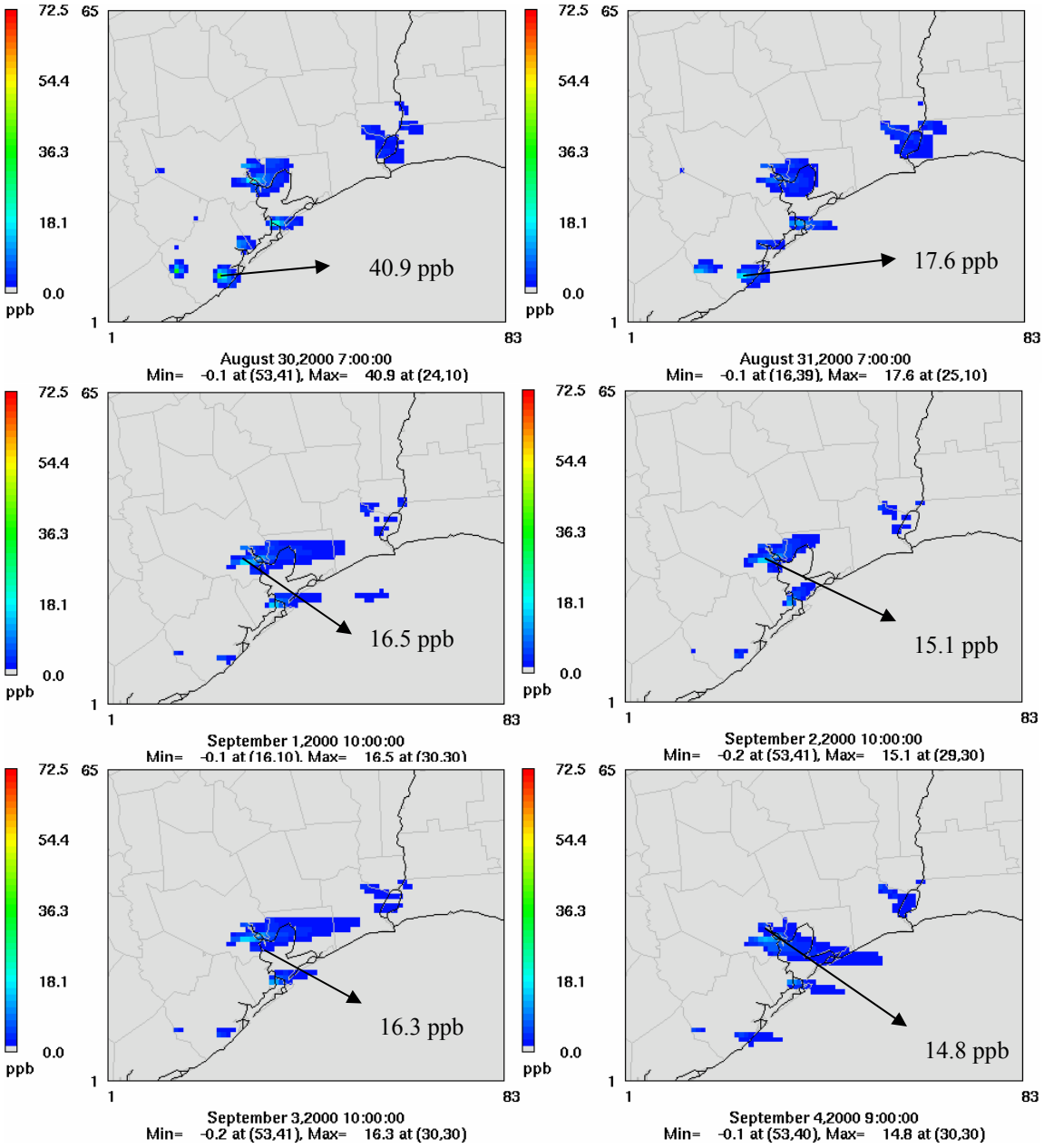

Figure 4.14 (Cont'd) Daily maximum enhancement of ozone concentration due to the chlorine chemistry (1-hour averaged ozone concentrations)

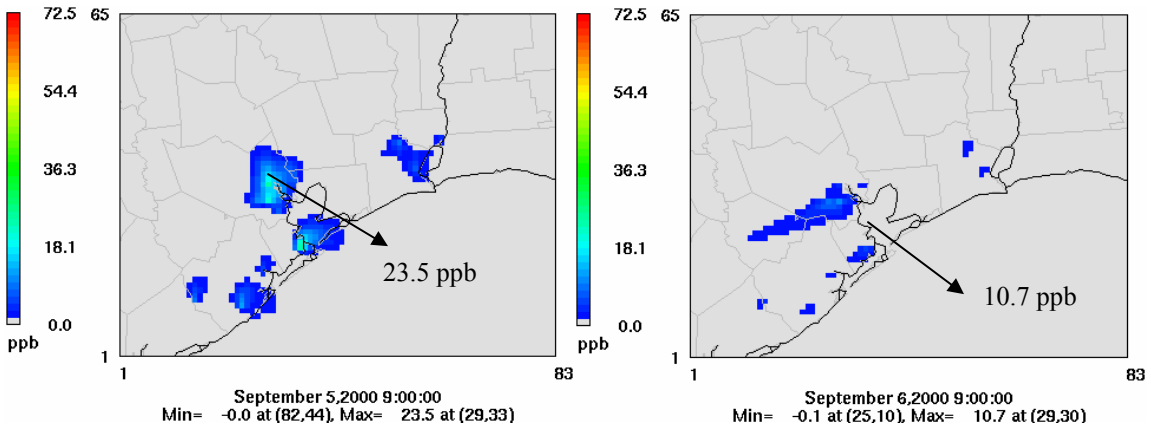

Figure 4.14 (Cont'd) Daily maximum enhancement of ozone concentration due to the chlorine chemistry (1-hour averaged ozone concentrations)

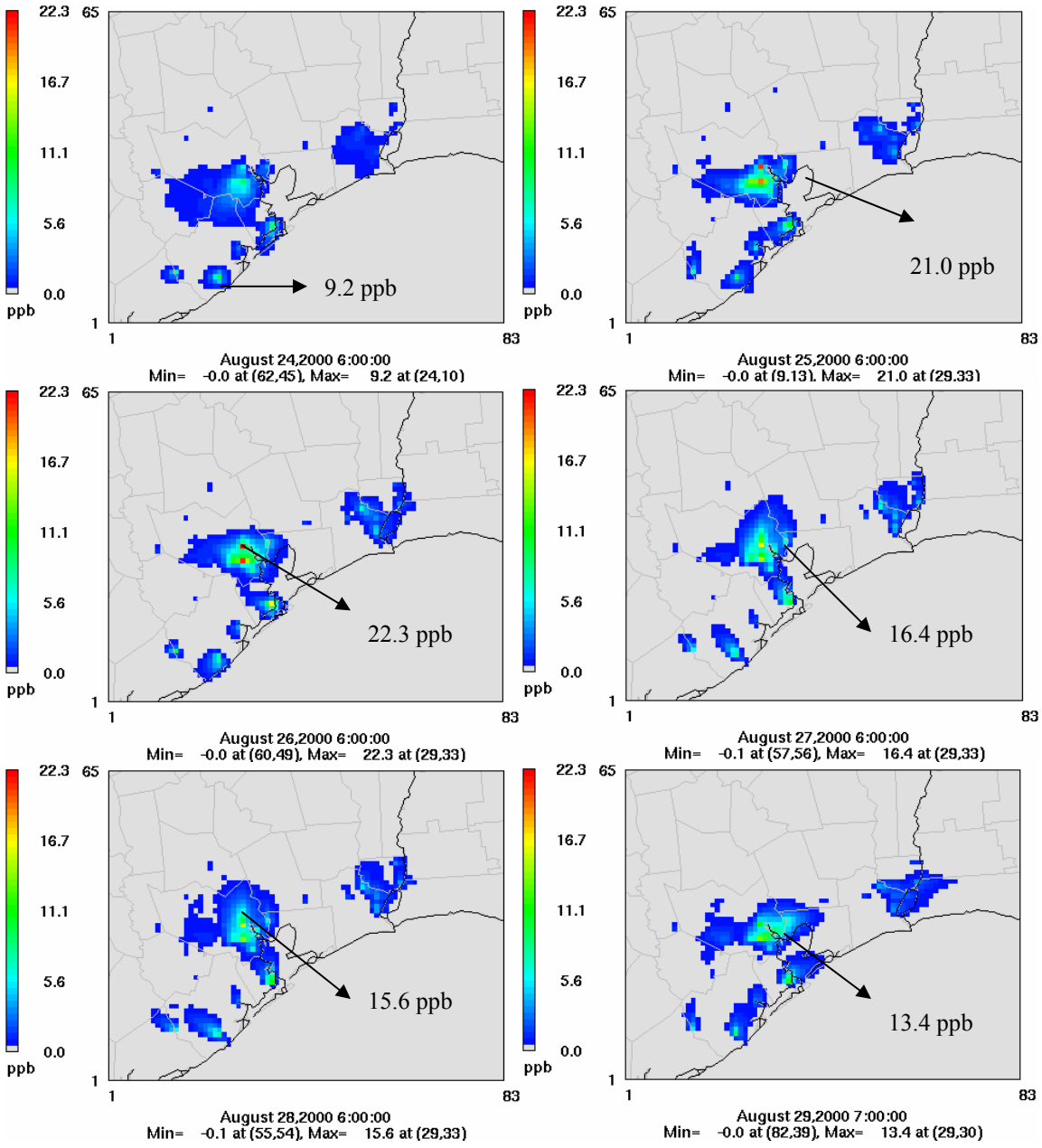

Figure 4.15 Daily maximum enhancement of ozone concentration due to the chlorine chemistry (8-hour averaged ozone concentrations)

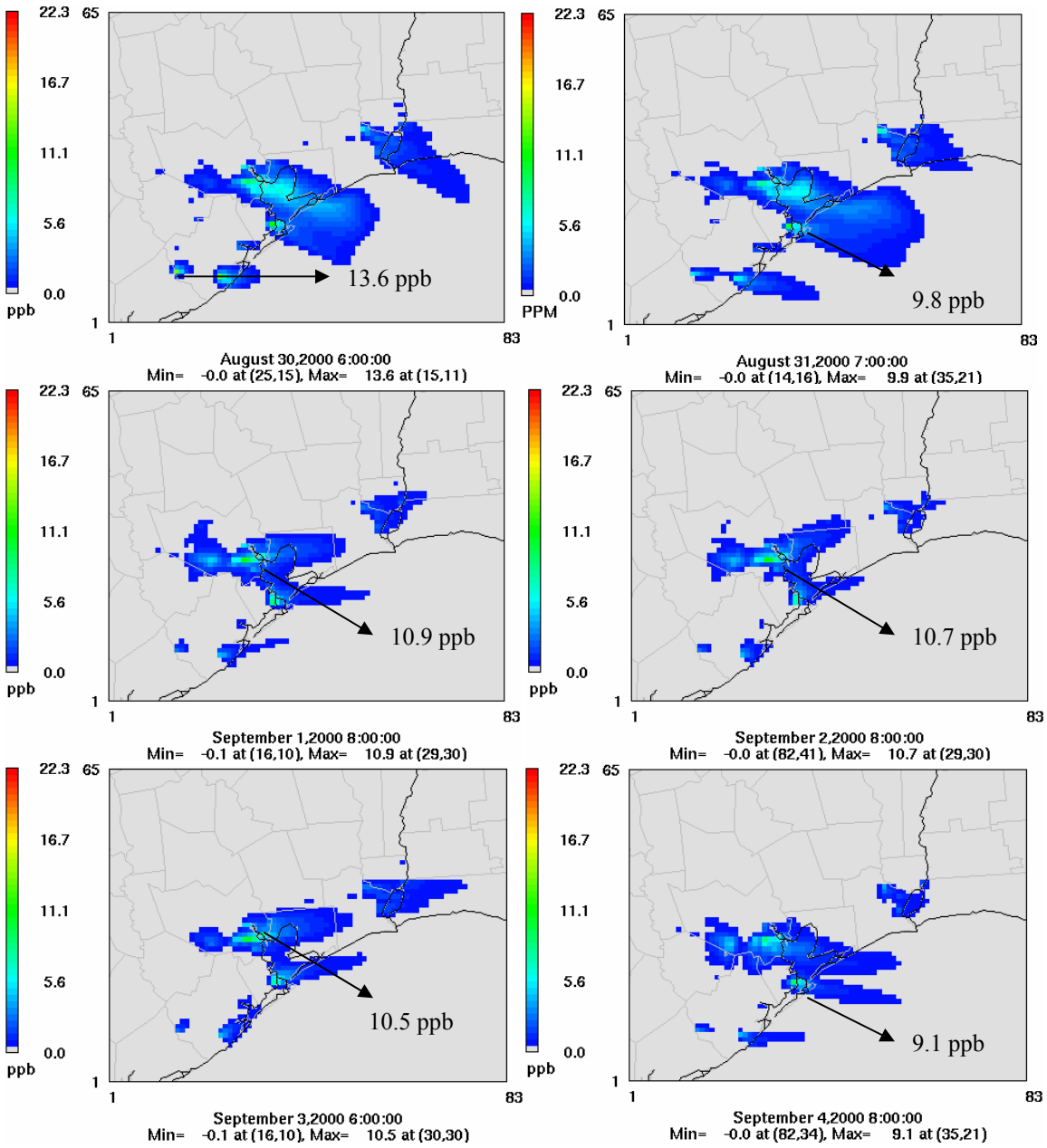

Figure 4.15 (Cont'd) Daily maximum enhancement of ozone concentration due to the chlorine chemistry (8-hour averaged ozone concentrations)

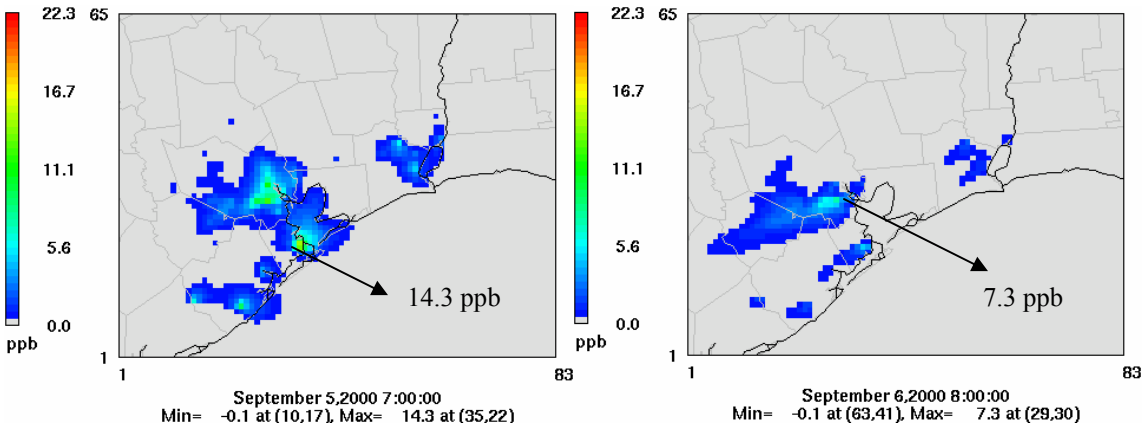

Figure 4.15 (Cont'd) Daily maximum enhancement of ozone concentration due to the chlorine chemistry (8-hour averaged ozone concentrations)

Absolute values of the 1-hour averaged and 8-hour averaged ozone concentrations, together with the differences in ozone concentrations caused by adding chlorine emissions are shown in Figure 4.16 - Figure 4.19. In each of these figures, the plots in the left column represent the total ozone concentration and the plots in the right column represent differences in ozone concentration due to adding chlorine chemistry.

Figures 4.16 (1 hour averages) and 4.17 (8 hour averages) are for the times of day when the daily maximum ozone concentration occurs. The time that the maximum ozone concentration occurred and the magnitude of the maximum ozone concentration are indicated below each plot. During the episode period, the daily maximum 1-hour averaged ozone concentration occurred between 1200 and 1500. The daily maximum 8-hour averaged ozone concentration occurred between 0900 and 1200 (time indicates the start of the averaging period). Figures 4.18 (1 hour averages) and 4.19 (8 hour averages) are for the times of day when the daily maximum difference in ozone concentration occurs.

For Figures 4.16 and 4.18, the scale of the ozone concentration is set from zero to 120 ppbv for 1-hour averaged ozone concentrations since the 1-hour averaged NAAQS is

120ppbv. Therefore, the red color in the plots in Figures 4.16 and 4.18 indicates locations where the ozone concentration is equal to or larger than the NAAQS (120 ppbv). For Figures 4.17 and 4.19, the scale of the ozone concentration is set from zero to 80 ppbv for 8-hour averaged ozone concentrations since the 8-hour averaged NAAQS is 80 ppbv. Therefore, the red color in the plots in the Figures 4.17 and 4.19 indicates locations where the ozone concentration is equal to or larger than the NAAQS criterion (80 ppbv).

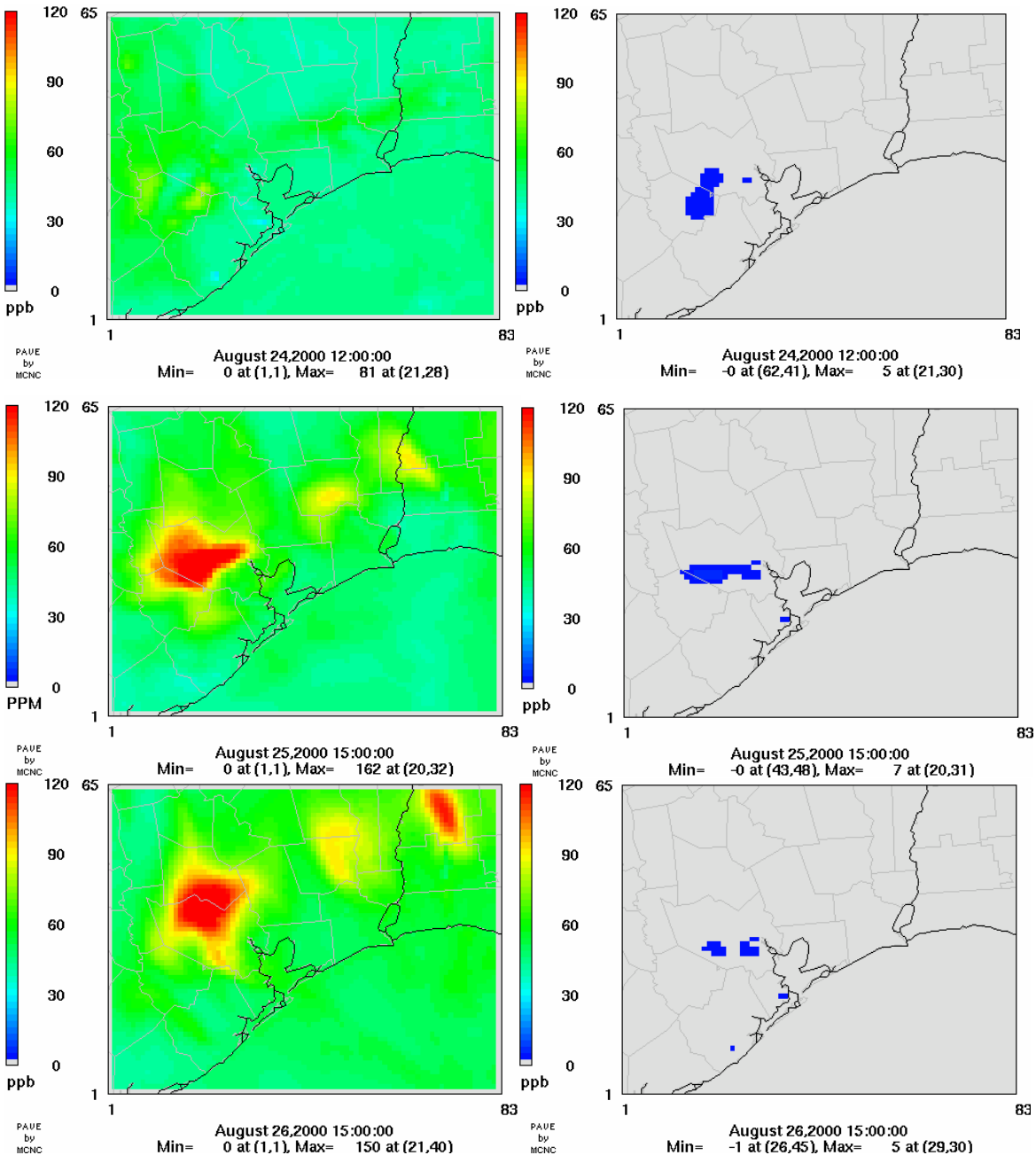

Figure 4.16 One hour averaged ozone concentrations. Left column shows ozone concentrations at the time of the daily maximum. The daily maximum ozone concentration occurs between 1200 and 1500. Peak time and magnitude of the maximum ozone concentrations are indicated below each plot. Right column shows the difference in ozone concentration between the case with chlorine emissions and basecase without chlorine emissions: The scale of the ozone concentration is from zero to 120 ppbv since the 1-hour averaged ozone NAAQS is 120ppbv. Therefore, the red color in the plot shows the location where the ozone concentration is equal or larger than the NAAQS criteria (120ppbv)

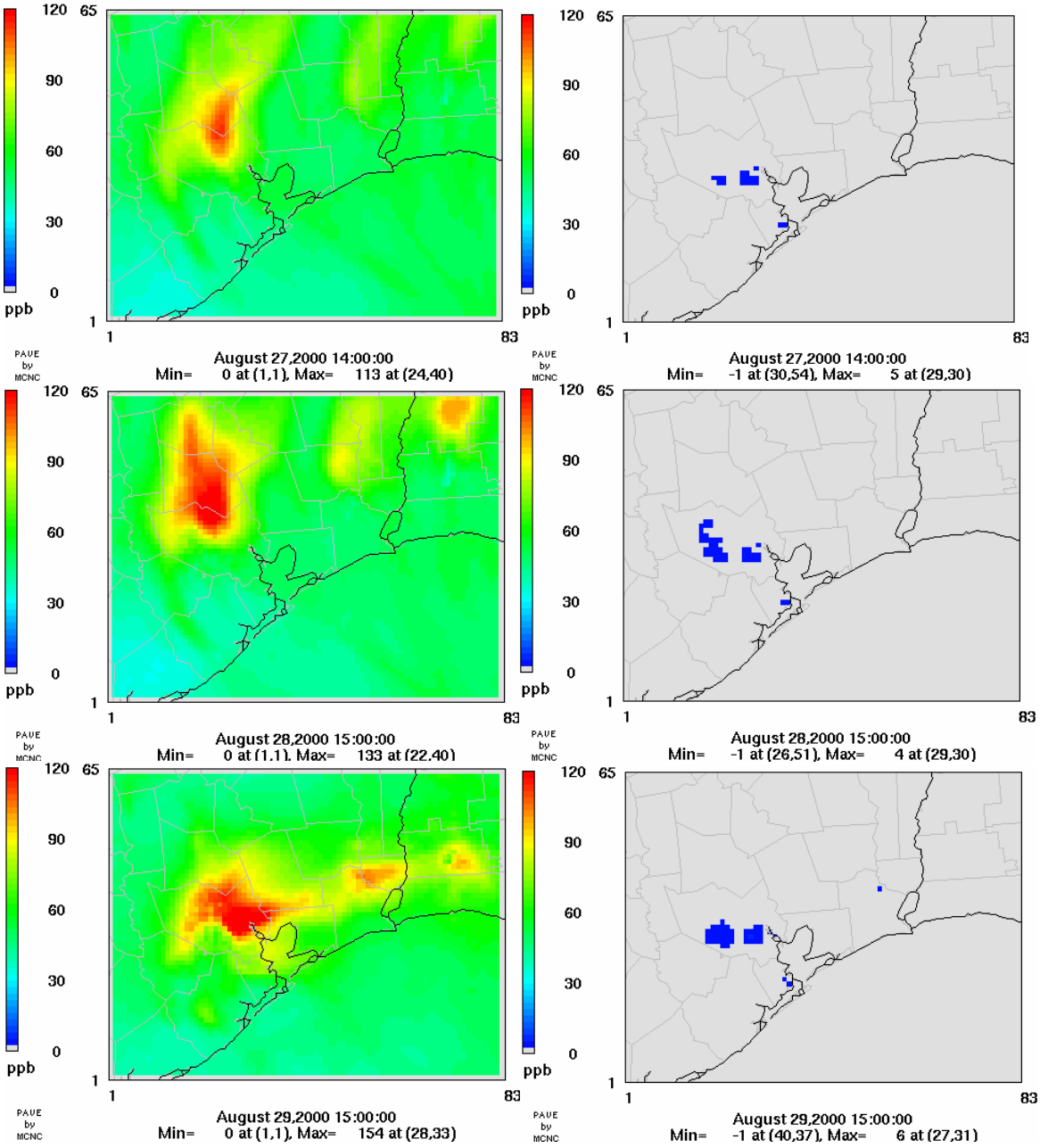

Figure 4.16 (Cont'd) One hour averaged ozone concentrations. Left column shows ozone concentrations at the time of the daily maximum. The daily maximum ozone concentration occurs between 1200 and 1500. Peak time and magnitude of the maximum ozone concentrations are indicated below each plot. Right column shows the difference in ozone concentration between the case with chlorine emissions and basecase without chlorine emissions: The scale of the ozone concentration is from zero to 120 ppbv since the 1-hour averaged ozone NAAQS is 120ppbv. Therefore, the red color in the plot shows the location where the ozone concentration is equal or larger than the NAAQS criteria (120ppbv)

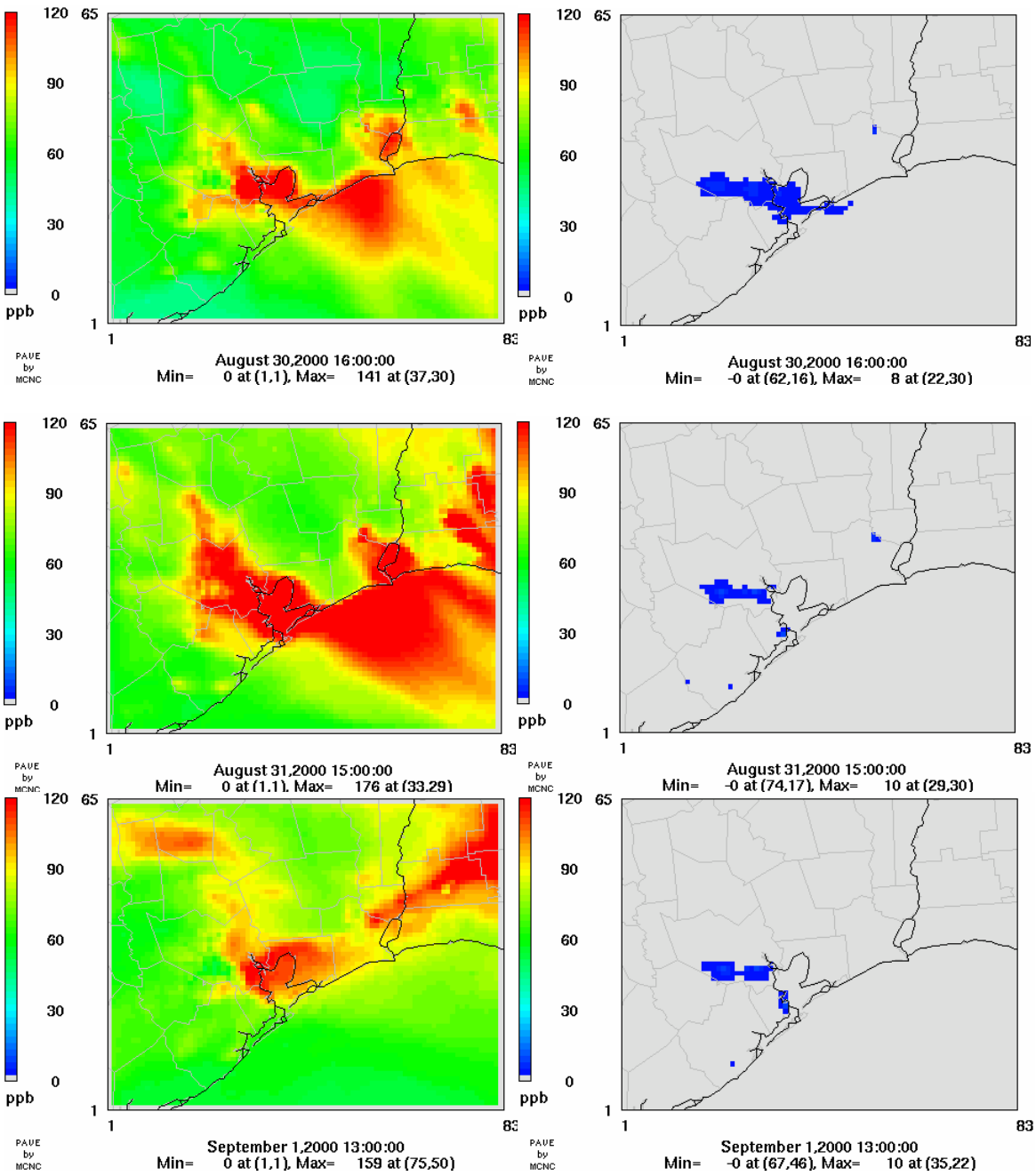

Figure 4.16 (Cont'd) One hour averaged ozone concentrations. Left column shows ozone concentrations at the time of the daily maximum. The daily maximum ozone concentration occurs between 1200 and 1500. Peak time and magnitude of the maximum ozone concentrations are indicated below each plot. Right column shows the difference in ozone concentration between the case with chlorine emissions and basecase without chlorine emissions: The scale of the ozone concentration is from zero to 120 ppbv since the 1-hour averaged ozone NAAQS is 120ppbv. Therefore, the red color in the plot shows the location where the ozone concentration is equal or larger than the NAAQS criteria (120ppbv)

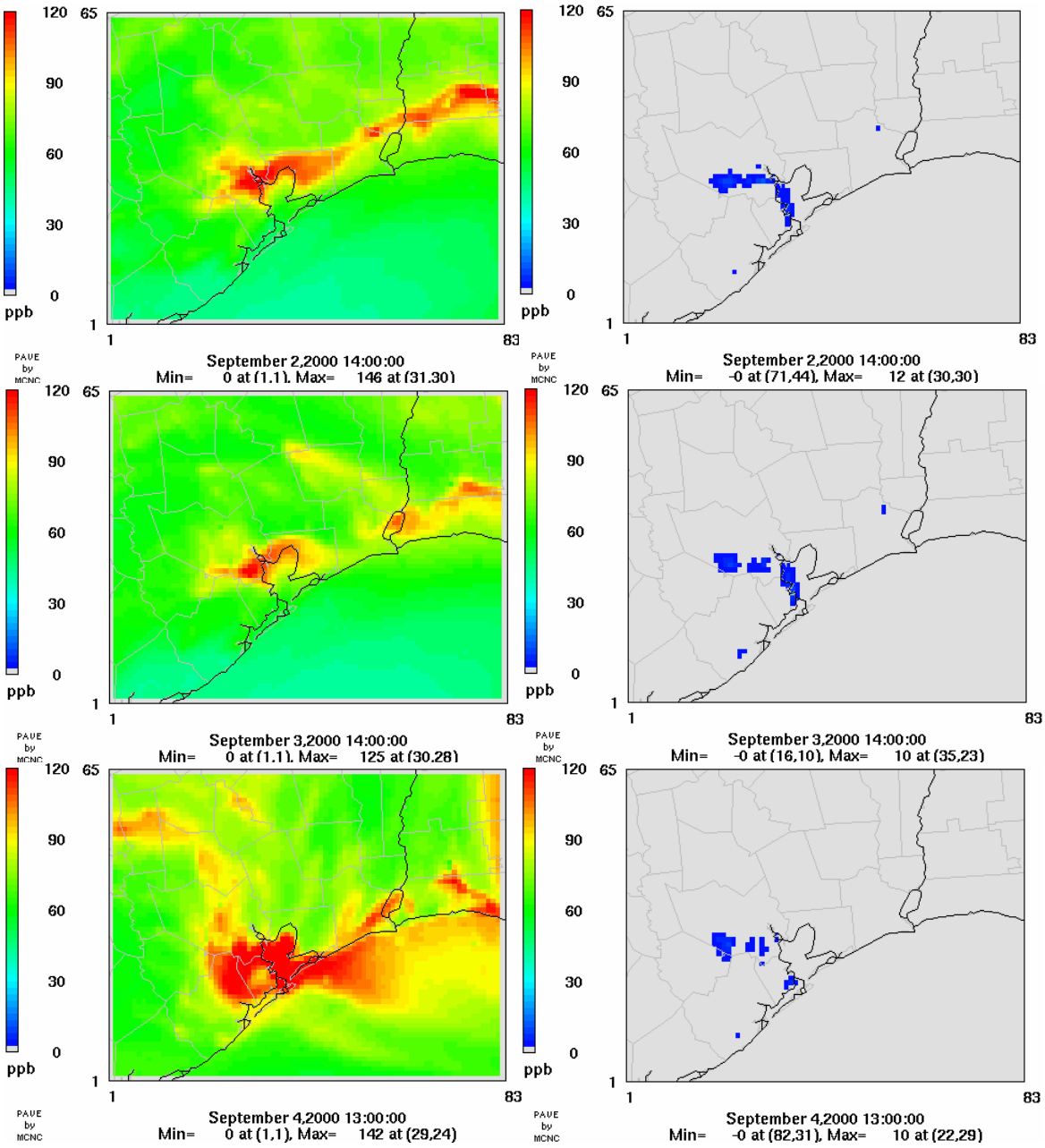

Figure 4.16 (Cont'd) One hour averaged ozone concentrations. Left column shows ozone concentrations at the time of the daily maximum. The daily maximum ozone concentration occurs between 1200 and 1500. Peak time and magnitude of the maximum ozone concentrations are indicated below each plot. Right column shows the difference in ozone concentration between the case with chlorine emissions and basecase without chlorine emissions: The scale of the ozone concentration is from zero to 120 ppbv since the 1-hour averaged ozone NAAQS is 120ppbv. Therefore, the red color in the plot shows the location where the ozone concentration is equal or larger than the NAAQS criteria (120ppbv)

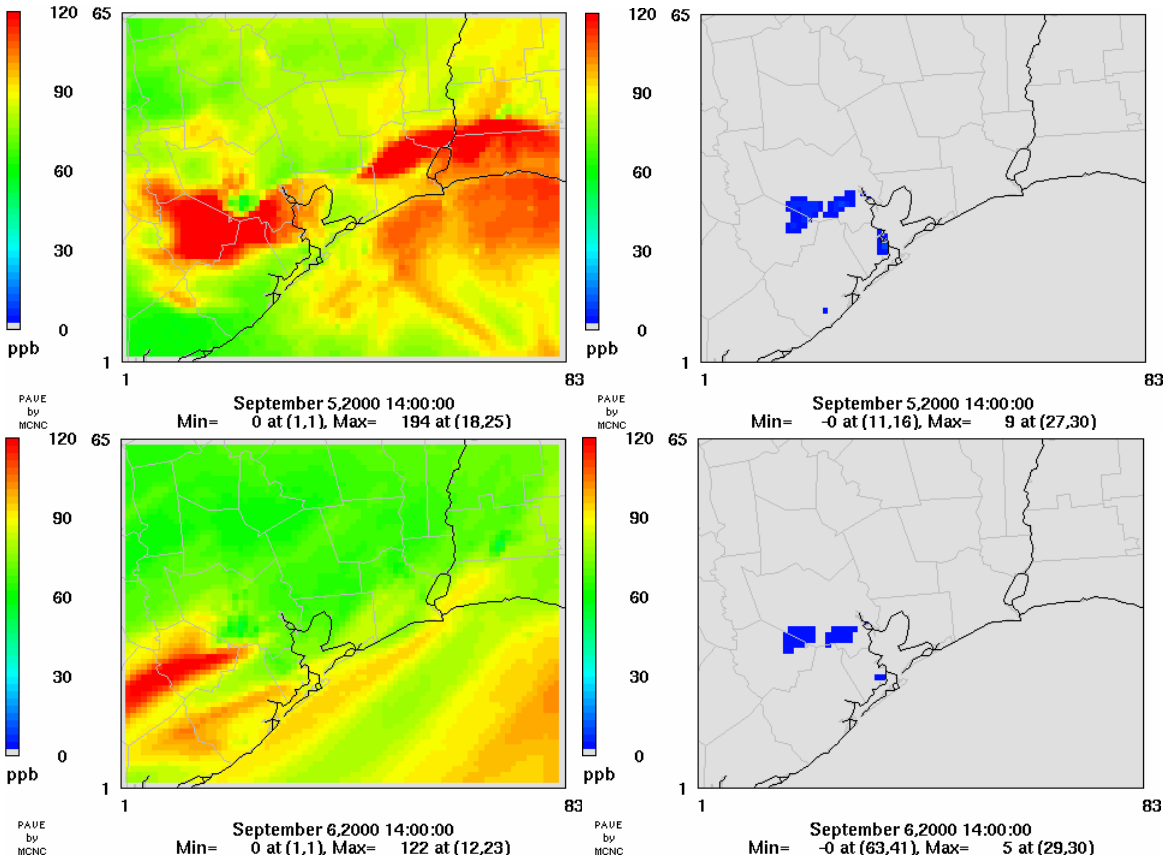

Figure 4.16 (Cont'd) One hour averaged ozone concentrations. Left column shows ozone concentrations at the time of the daily maximum. The daily maximum ozone concentration occurs between 1200 and 1500. Peak time and magnitude of the maximum ozone concentrations are indicated below each plot. Right column shows the difference in ozone concentration between the case with chlorine emissions and basecase without chlorine emissions: The scale of the ozone concentration is from zero to 120 ppbv since the 1-hour averaged ozone NAAQS is 120ppbv. Therefore, the red color in the plot shows the location where the ozone concentration is equal or larger than the NAAQS criteria (120ppbv)

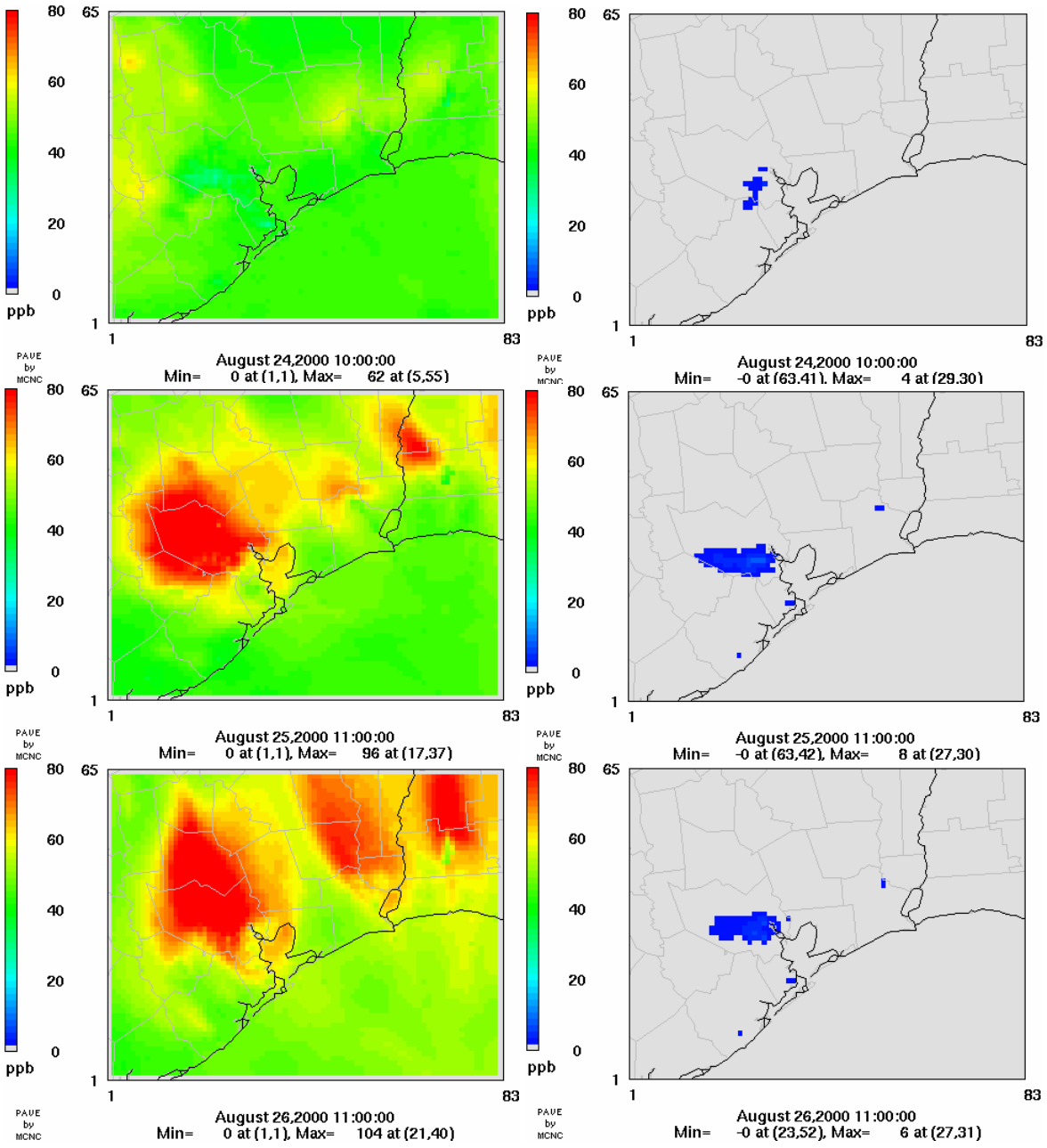

Figure 4.17 Eight hour averaged ozone concentrations. Left column shows ozone concentrations at the time of the daily maximum. The daily maximum ozone concentration occurs between 0900 and 1200. Peak time and magnitude of the maximum ozone concentrations are indicated below each plot. Right column shows the difference in ozone concentration between the case with chlorine emissions and basecase without chlorine emissions: The scale of the ozone concentration is from zero to 80 ppbv since the 8-hour averaged ozone NAAQS is 80ppbv. Therefore, the red color in the plot shows the location where the ozone concentration is equal or larger than the NAAQS (80ppbv)

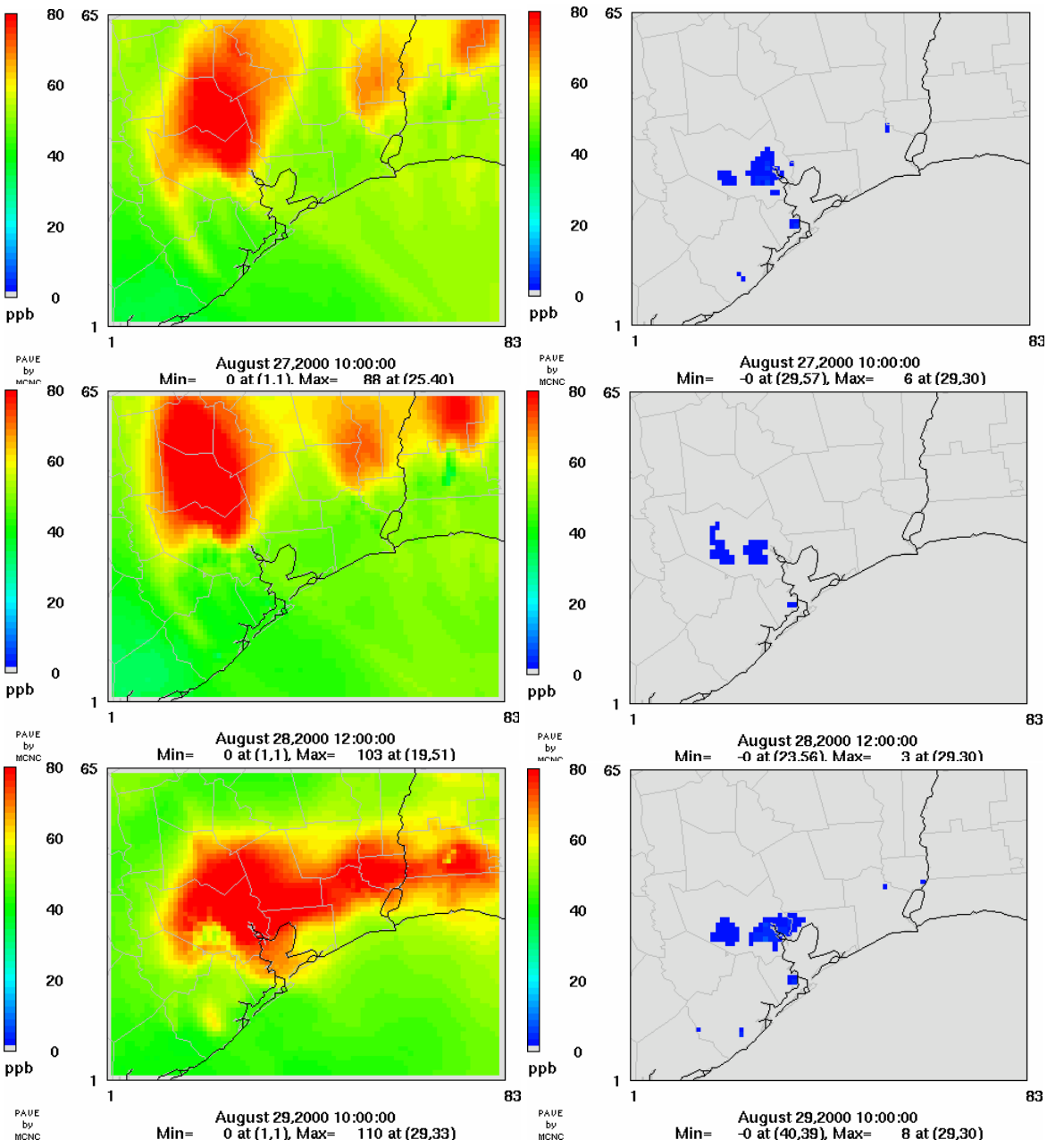

Figure 4.17 (Cont'd) Eight hour averaged ozone concentrations. Left column shows ozone concentrations at the time of the daily maximum. The daily maximum ozone concentration occurs between 0900 and 1200. Peak time and magnitude of the maximum ozone concentrations are indicated below each plot. Right column shows the difference in ozone concentration between the case with chlorine emissions and basecase without chlorine emissions: The scale of the ozone concentration is from zero to 80 ppbv since the 8-hour averaged ozone NAAQS is 80ppbv. Therefore, the red color in the plot shows the location where the ozone concentration is equal or larger than the NAAQS (80ppbv)

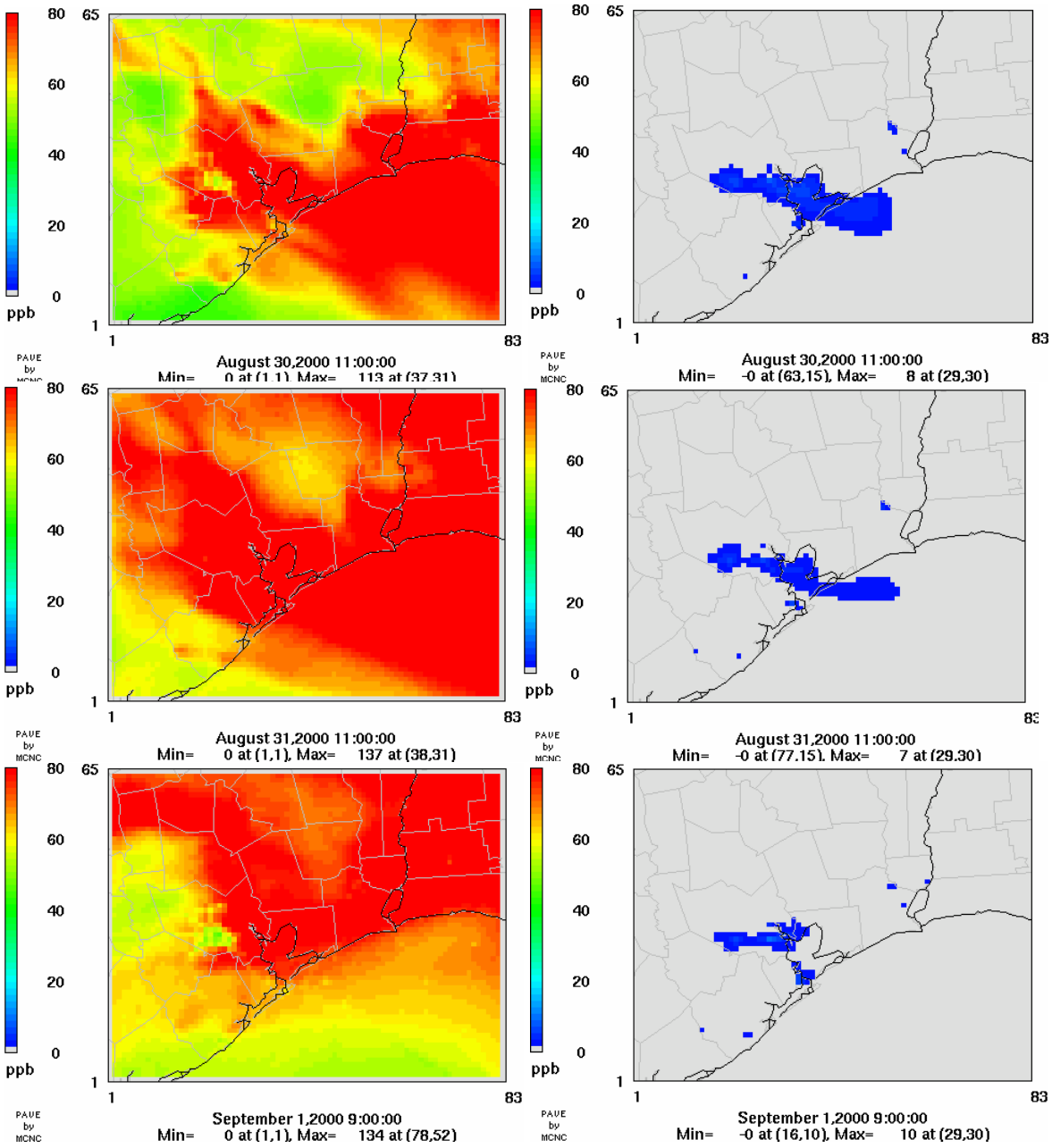

Figure 4.17 (Cont'd) Eight hour averaged ozone concentrations. Left column shows ozone concentrations at the time of the daily maximum. The daily maximum ozone concentration occurs between 0900 and 1200. Peak time and magnitude of the maximum ozone concentrations are indicated below each plot. Right column shows the difference in ozone concentration between the case with chlorine emissions and basecase without chlorine emissions: The scale of the ozone concentration is from zero to 80 ppbv since the 8-hour averaged ozone NAAQS is 80ppbv. Therefore, the red color in the plot shows the location where the ozone concentration is equal or larger than the NAAQS (80ppbv)

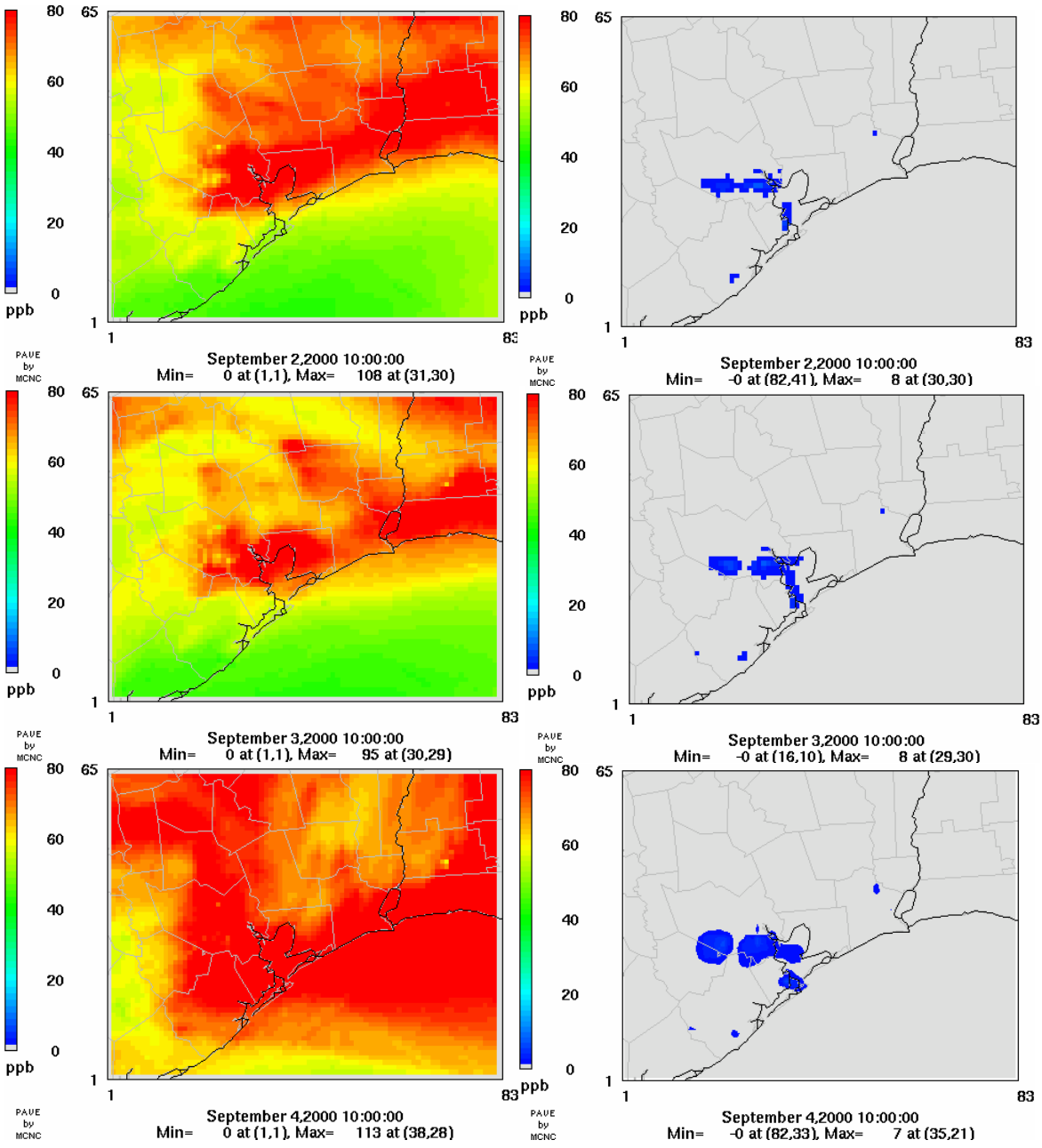

Figure 4.17 (Cont'd) Eight hour averaged ozone concentrations. Left column shows ozone concentrations at the time of the daily maximum. The daily maximum ozone concentration occurs between 0900 and 1200. Peak time and magnitude of the maximum ozone concentrations are indicated below each plot. Right column shows the difference in ozone concentration between the case with chlorine emissions and basecase without chlorine emissions: The scale of the ozone concentration is from zero to 80 ppbv since the 8-hour averaged ozone NAAQS is 80ppbv. Therefore, the red color in the plot shows the location where the ozone concentration is equal or larger than the NAAQS (80ppbv)

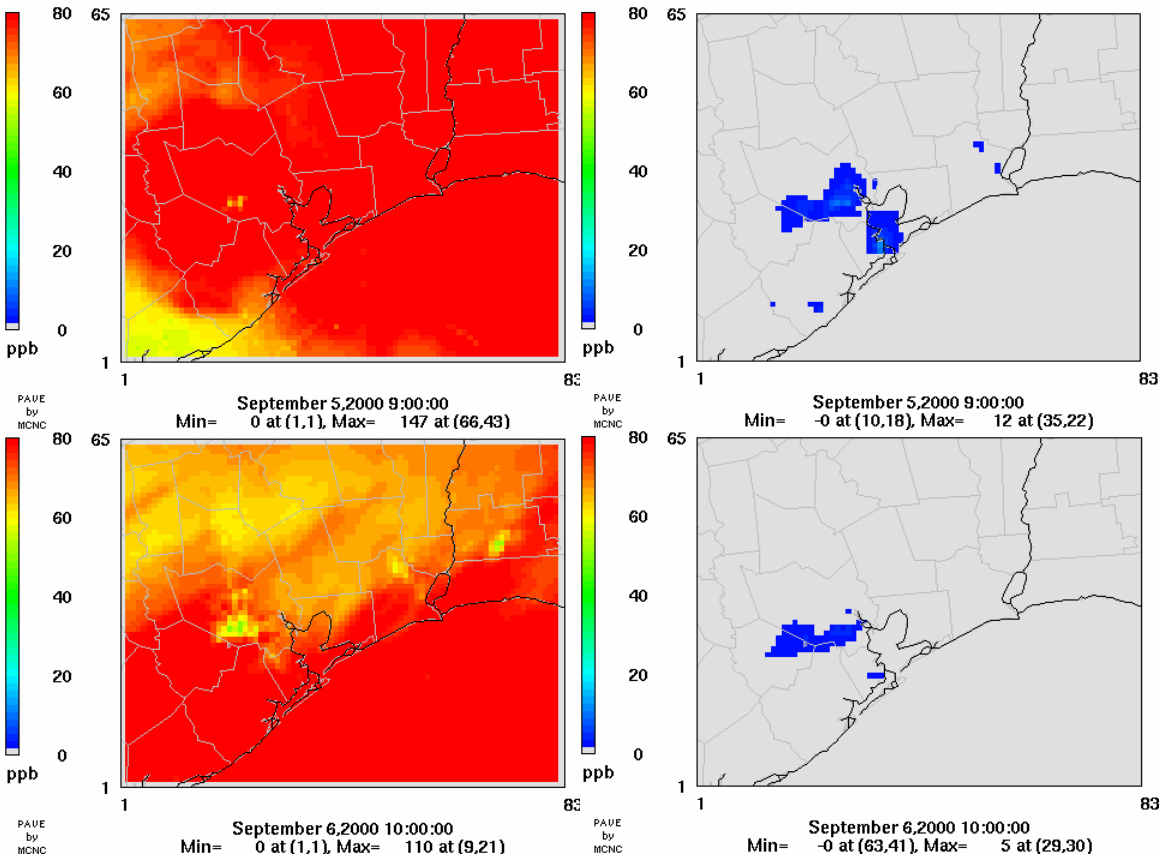

Figure 4.17 (Cont'd)Eight hour averaged ozone concentrations. Left column shows ozone concentrations at the time of the daily maximum. The daily maximum ozone concentration occurs between 0900 and 1200. Peak time and magnitude of the maximum ozone concentrations are indicated below each plot. Right column shows the difference in ozone concentration between the case with chlorine emissions and basecase without chlorine emissions: The scale of the ozone concentration is from zero to 80 ppbv since the 8-hour averaged ozone NAAQS is 80ppbv. Therefore, the red color in the plot shows the location where the ozone concentration is equal or larger than the NAAQS (80ppbv)

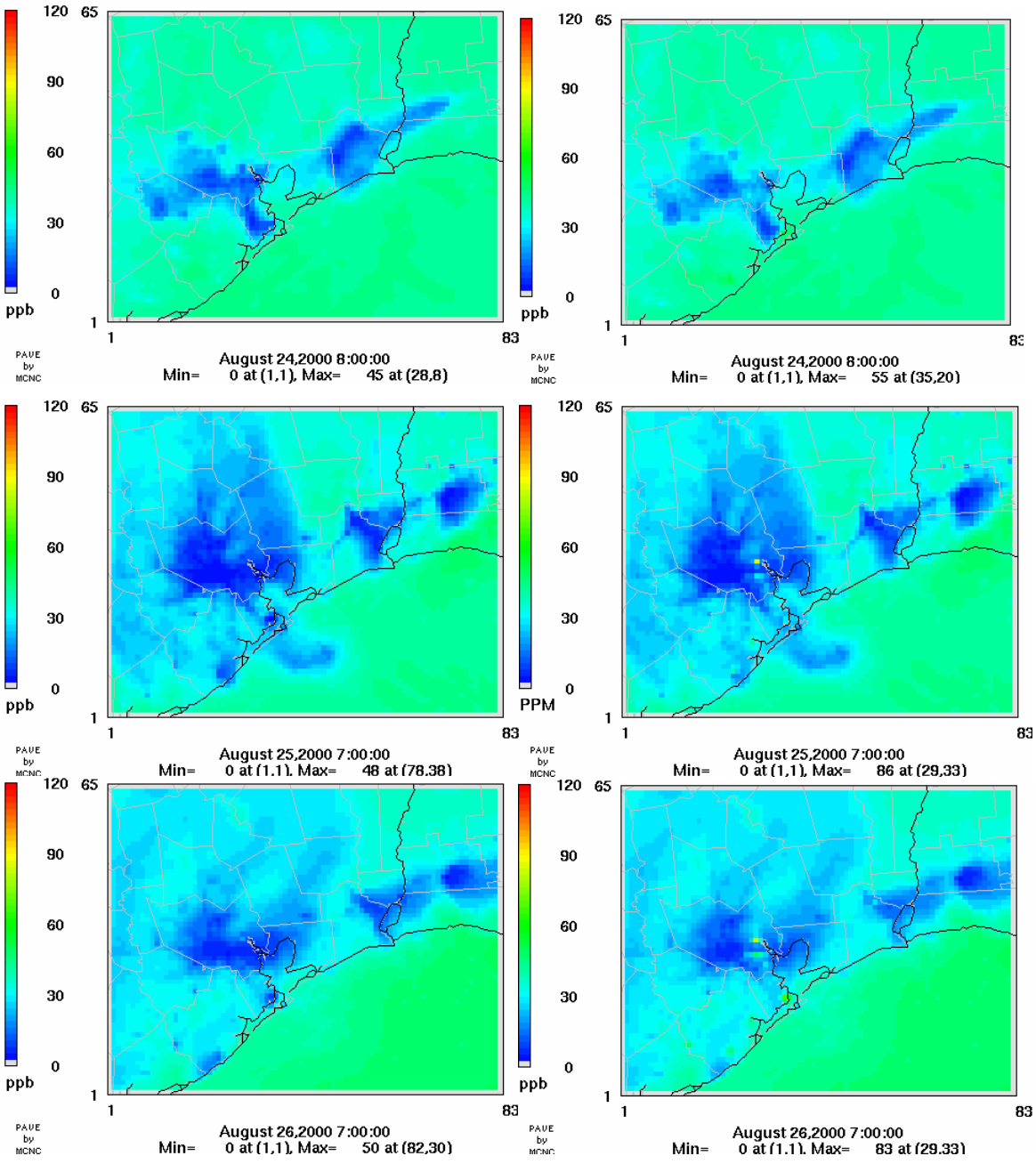

Figure 4.18 One hour averaged ozone concentrations. Left column shows total ozone concentrations, assuming no chlorine emissions, at the time of the maximum difference in ozone concentration caused by chlorine emissions. Peak time and magnitude of the maximum ozone concentrations are indicated below each plot. Right column shows the total ozone concentration for the case with chlorine emissions at the same time of day. The scale of the ozone concentration is from zero to 120 ppbv since the 1-hour averaged ozone NAAQS is 120ppbv. Therefore, the red color in the plot shows the location where the ozone concentration is equal or larger than the NAAQS criteria (120ppbv)

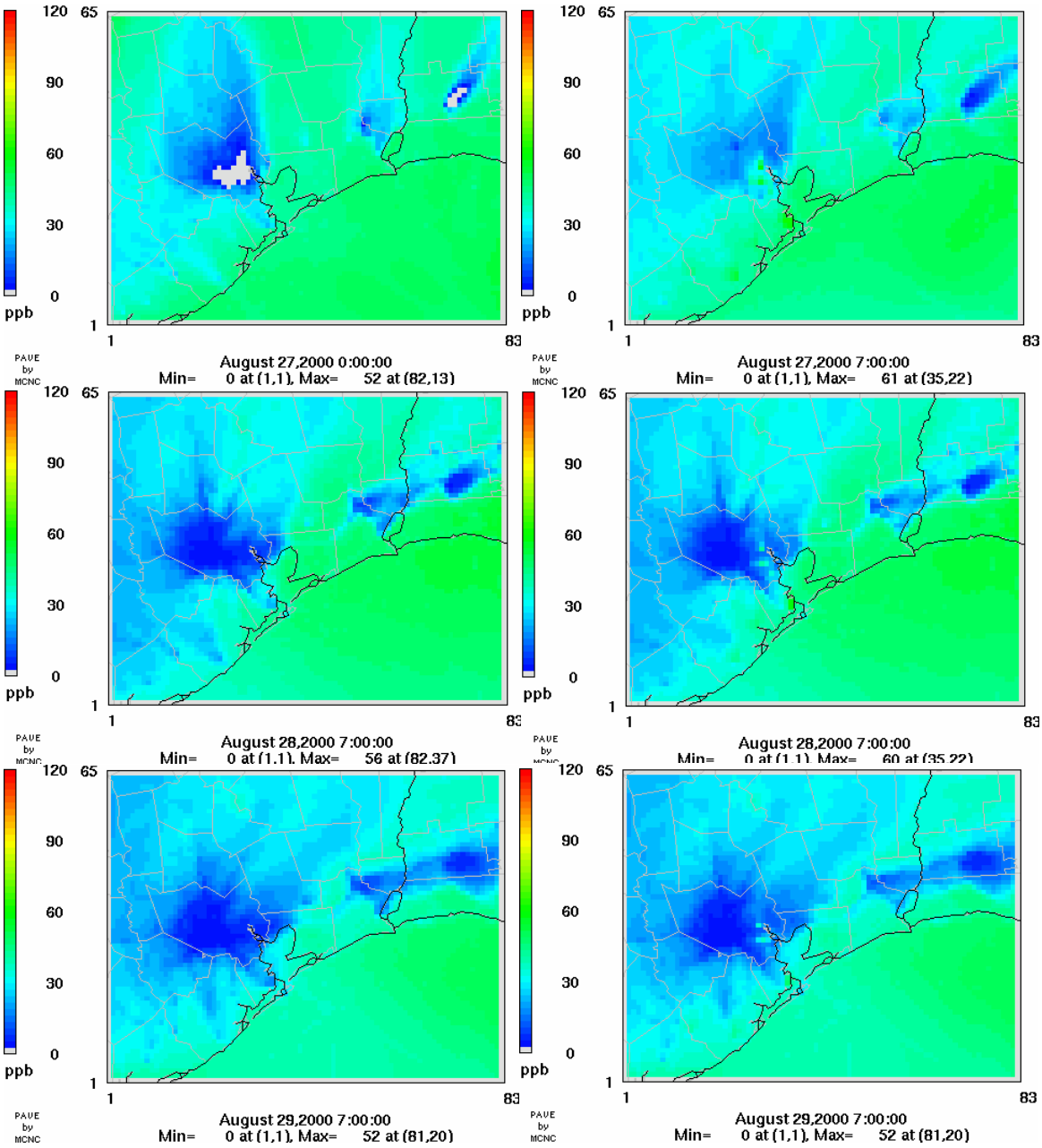

Figure 4.18 (Cont'd) One hour averaged ozone concentrations. Left column shows total ozone concentrations, assuming no chlorine emissions, at the time of the maximum difference in ozone concentration caused by chlorine emissions. Peak time and magnitude of the maximum ozone concentrations are indicated below each plot. Right column shows the total ozone concentration for the case with chlorine emissions at the same time of day. The scale of the ozone concentration is from zero to 120 ppbv since the 1-hour averaged ozone NAAQS is 120ppbv. Therefore, the red color in the plot shows the location where the ozone concentration is equal or larger than the NAAQS criteria (120ppbv)

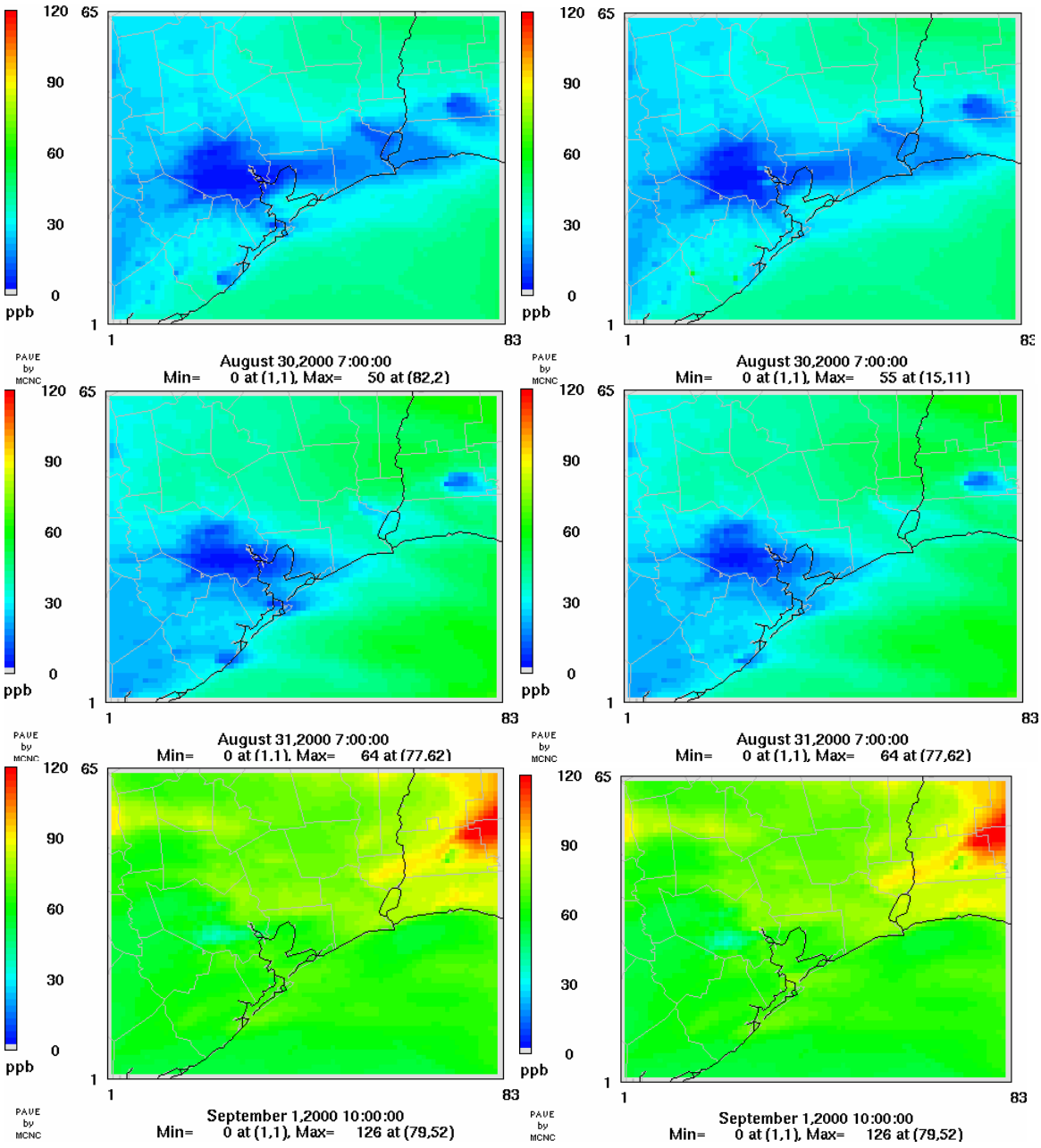

Figure 4.18 (Cont'd) One hour averaged ozone concentrations. Left column shows total ozone concentrations, assuming no chlorine emissions, at the time of the maximum difference in ozone concentration caused by chlorine emissions. Peak time and magnitude of the maximum ozone concentrations are indicated below each plot. Right column shows the total ozone concentration for the case with chlorine emissions at the same time of day. The scale of the ozone concentration is from zero to 120 ppbv since the 1-hour averaged ozone NAAQS is 120ppbv. Therefore, the red color in the plot shows the location where the ozone concentration is equal or larger than the NAAQS criteria (120ppbv)

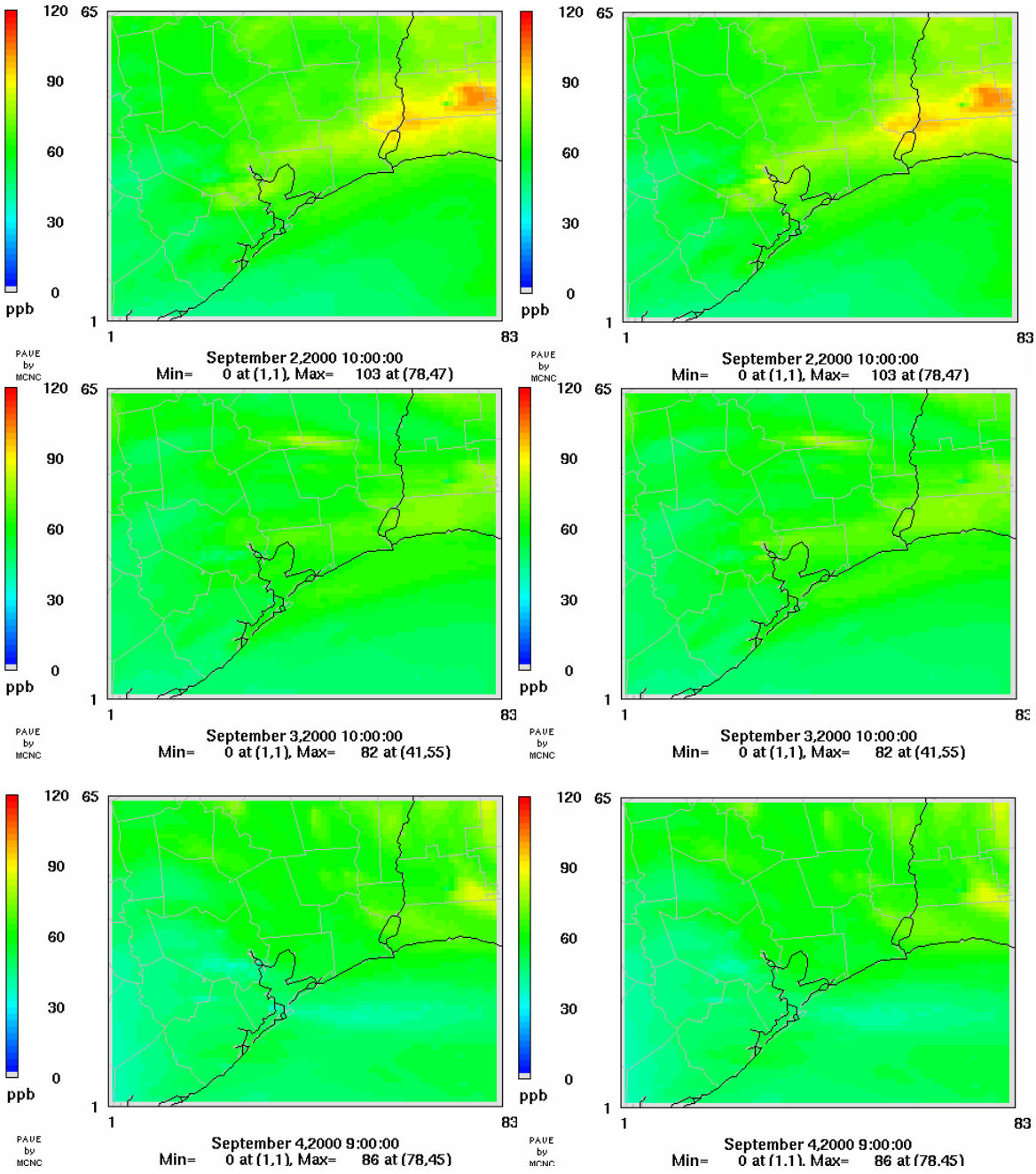

Figure 4.18 (Cont'd) One hour averaged ozone concentrations. Left column shows total ozone concentrations, assuming no chlorine emissions, at the time of the maximum difference in ozone concentration caused by chlorine emissions. Peak time and magnitude of the maximum ozone concentrations are indicated below each plot. Right column shows the total ozone concentration for the case with chlorine emissions at the same time of day. The scale of the ozone concentration is from zero to 120 ppbv since the 1-hour averaged ozone NAAQS is 120ppbv. Therefore, the red color in the plot shows the location where the ozone concentration is equal or larger than the NAAQS criteria (120ppbv)

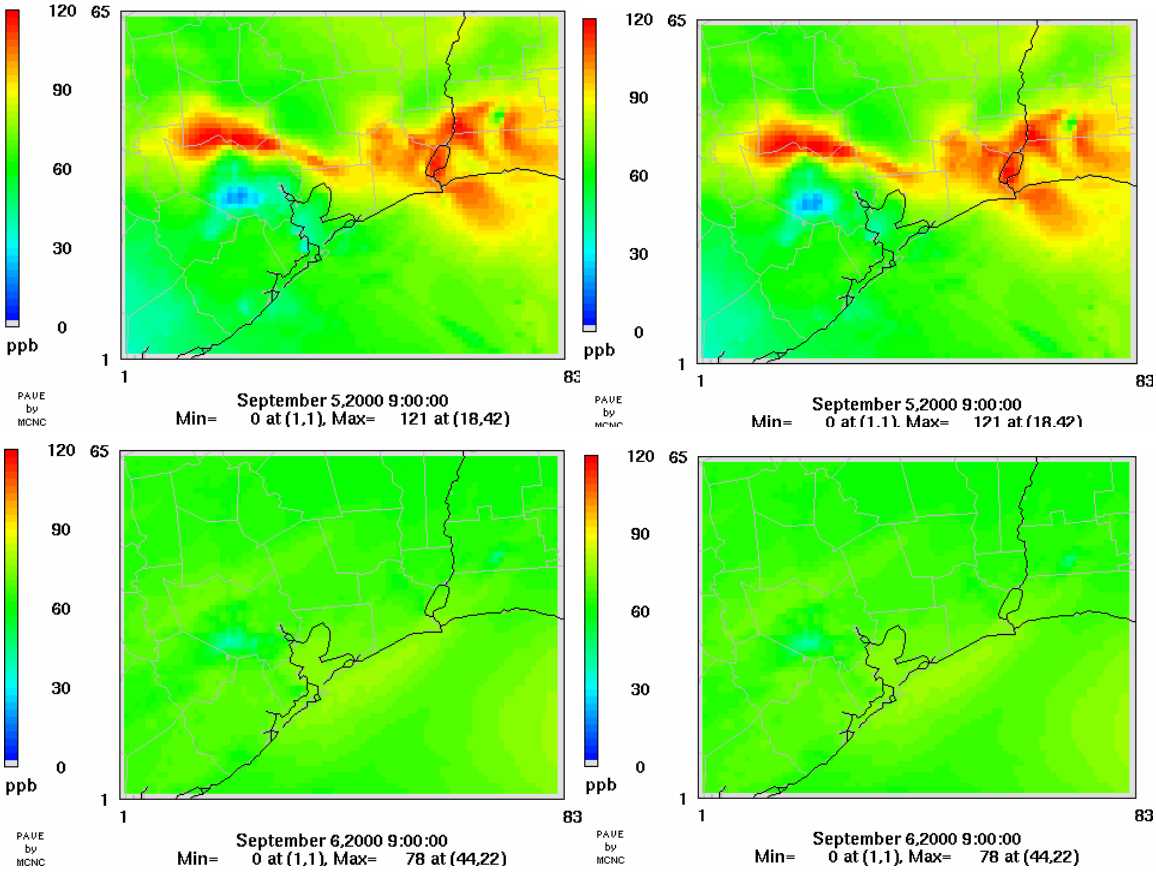

Figure 4.18 (Cont'd) One hour averaged ozone concentrations. Left column shows total ozone concentrations, assuming no chlorine emissions, at the time of the maximum difference in ozone concentration caused by chlorine emissions. Peak time and magnitude of the maximum ozone concentrations are indicated below each plot. Right column shows the total ozone concentration for the case with chlorine emissions at the same time of day. The scale of the ozone concentration is from zero to 120 ppbv since the 1-hour averaged ozone NAAQS is 120ppbv. Therefore, the red color in the plot shows the location where the ozone concentration is equal or larger than the NAAQS criteria (120ppbv)

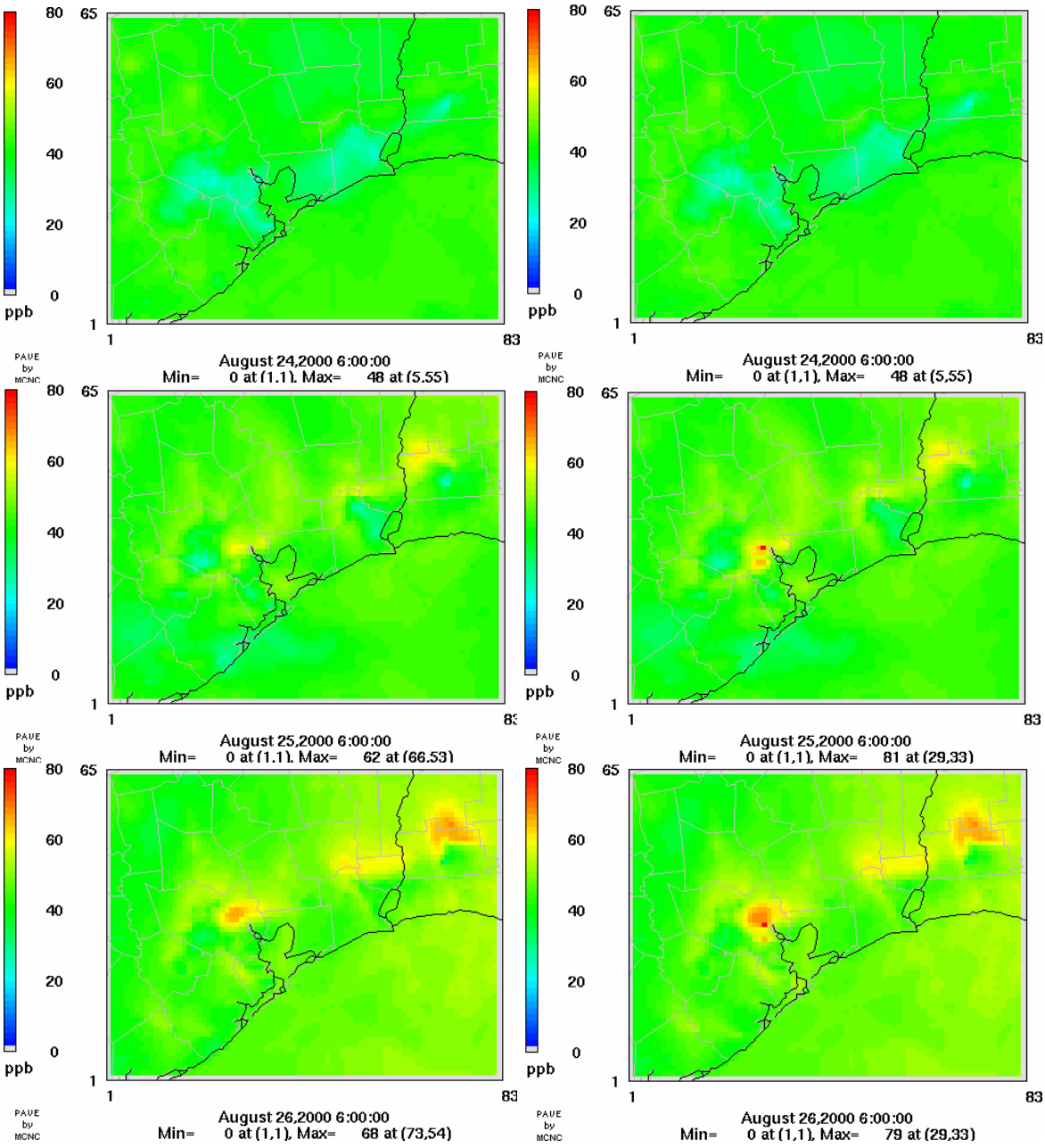

Figure 4.19 Eight hour averaged ozone concentrations. Left column shows total ozone concentrations, assuming no chlorine emissions, at the time of the maximum difference in ozone concentration caused by chlorine emissions. Peak time and magnitude of the maximum ozone concentrations are indicated below each plot. Right column shows the total ozone concentration for the case with chlorine emissions at the same time of day. The scale of the ozone concentration is from zero to 120 ppbv since the 1-hour averaged ozone NAAQS is 120ppbv. Therefore, the red color in the plot shows the location where the ozone concentration is equal or larger than the NAAQS criteria (120ppbv)

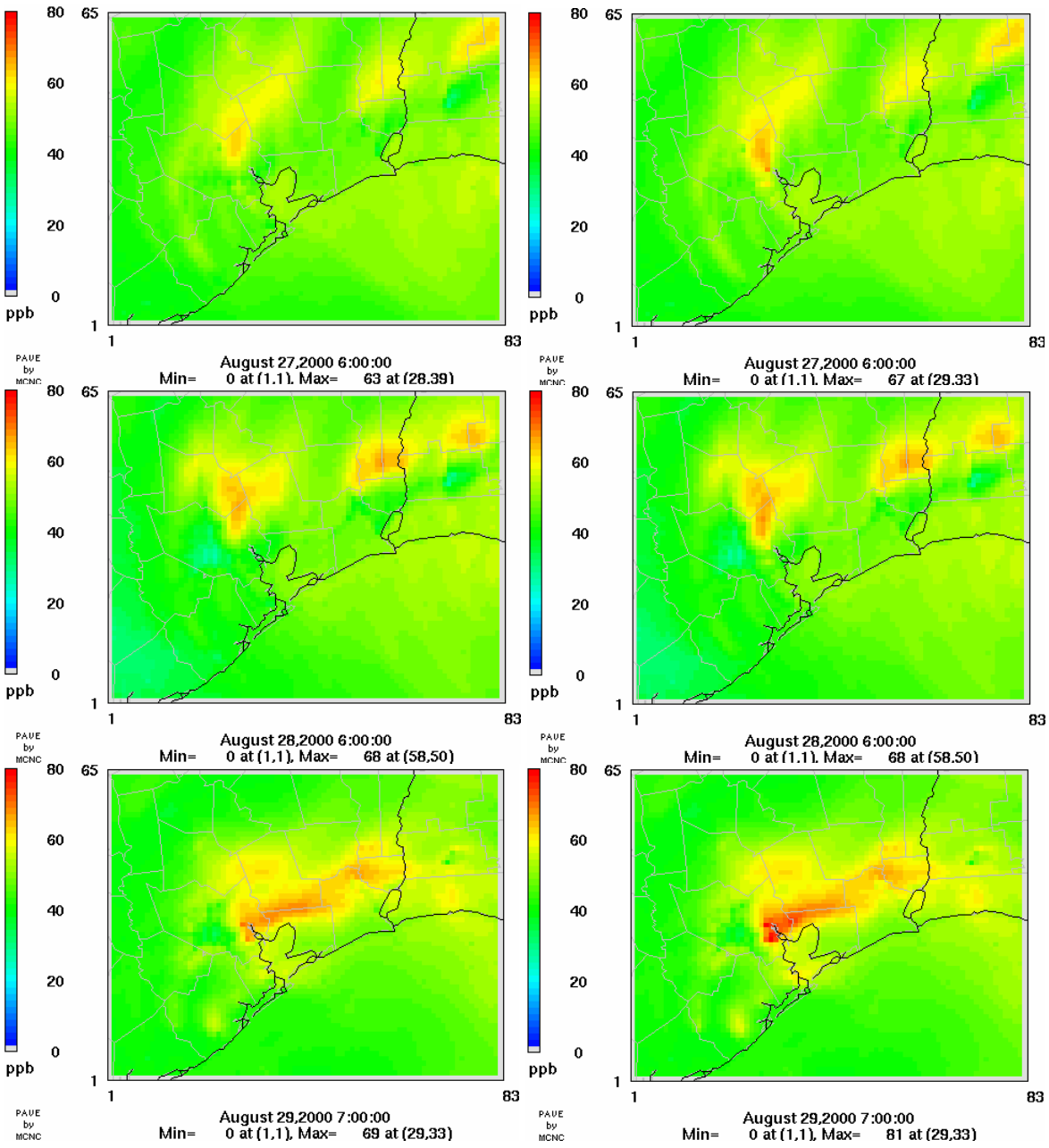

Figure 4.19 (Cont'd) Eight hour averaged ozone concentrations. Left column shows total ozone concentrations, assuming no chlorine emissions, at the time of the maximum difference in ozone concentration caused by chlorine emissions. Peak time and magnitude of the maximum ozone concentrations are indicated below each plot. Right column shows the total ozone concentration for the case with chlorine emissions at the same time of day. The scale of the ozone concentration is from zero to 120 ppbv since the 1-hour averaged ozone NAAQS is 120ppbv. Therefore, the red color in the plot shows the location where the ozone concentration is equal or larger than the NAAQS criteria (120ppbv)

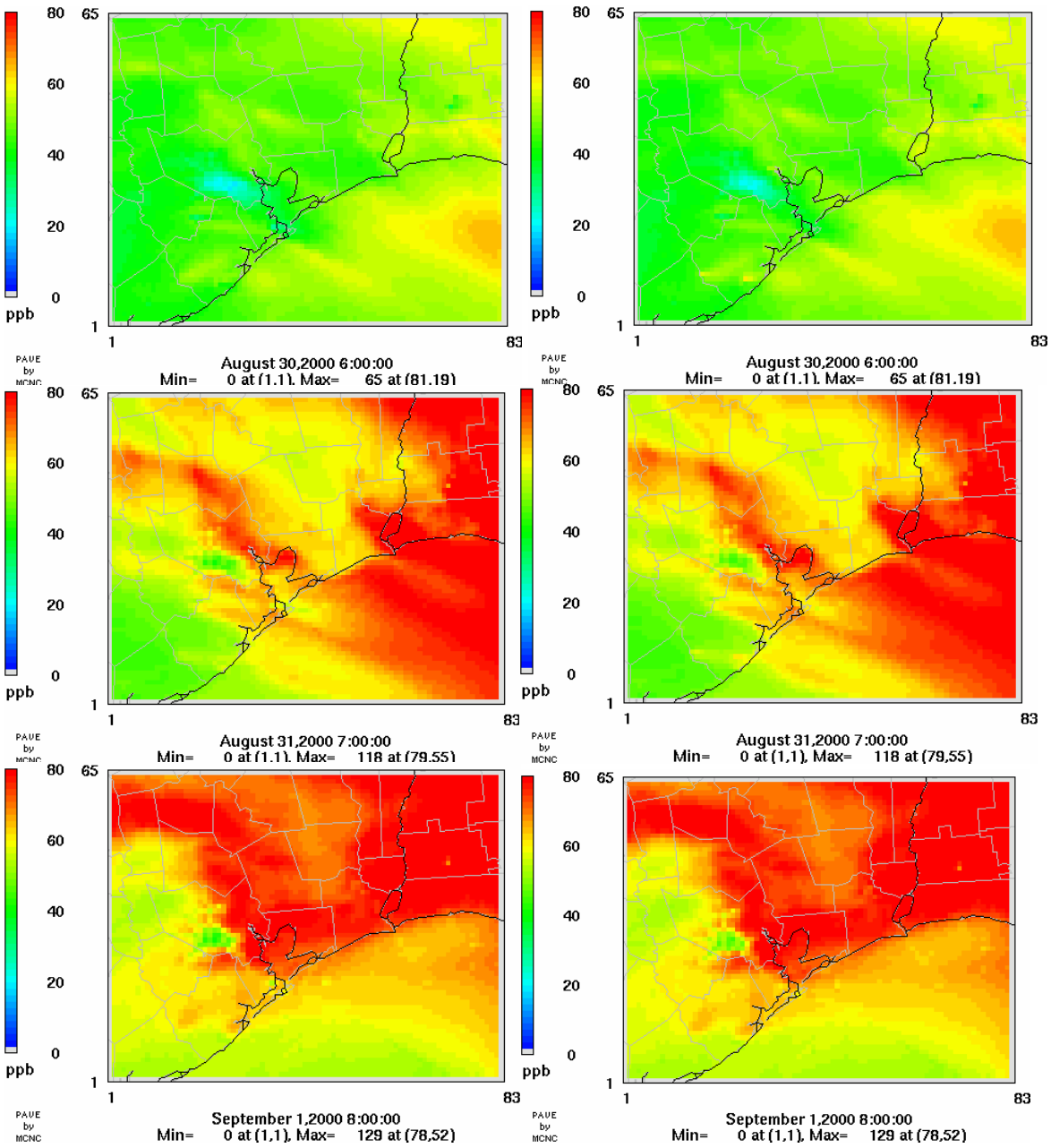

Figure 4.19 (Cont'd) Eight hour averaged ozone concentrations. Left column shows total ozone concentrations, assuming no chlorine emissions, at the time of the maximum difference in ozone concentration caused by chlorine emissions. Peak time and magnitude of the maximum ozone concentrations are indicated below each plot. Right column shows the total ozone concentration for the case with chlorine emissions at the same time of day. The scale of the ozone concentration is from zero to 120 ppbv since the 1-hour averaged ozone NAAQS is 120ppbv. Therefore, the red color in the plot shows the location where the ozone concentration is equal or larger than the NAAQS criteria (120ppbv)

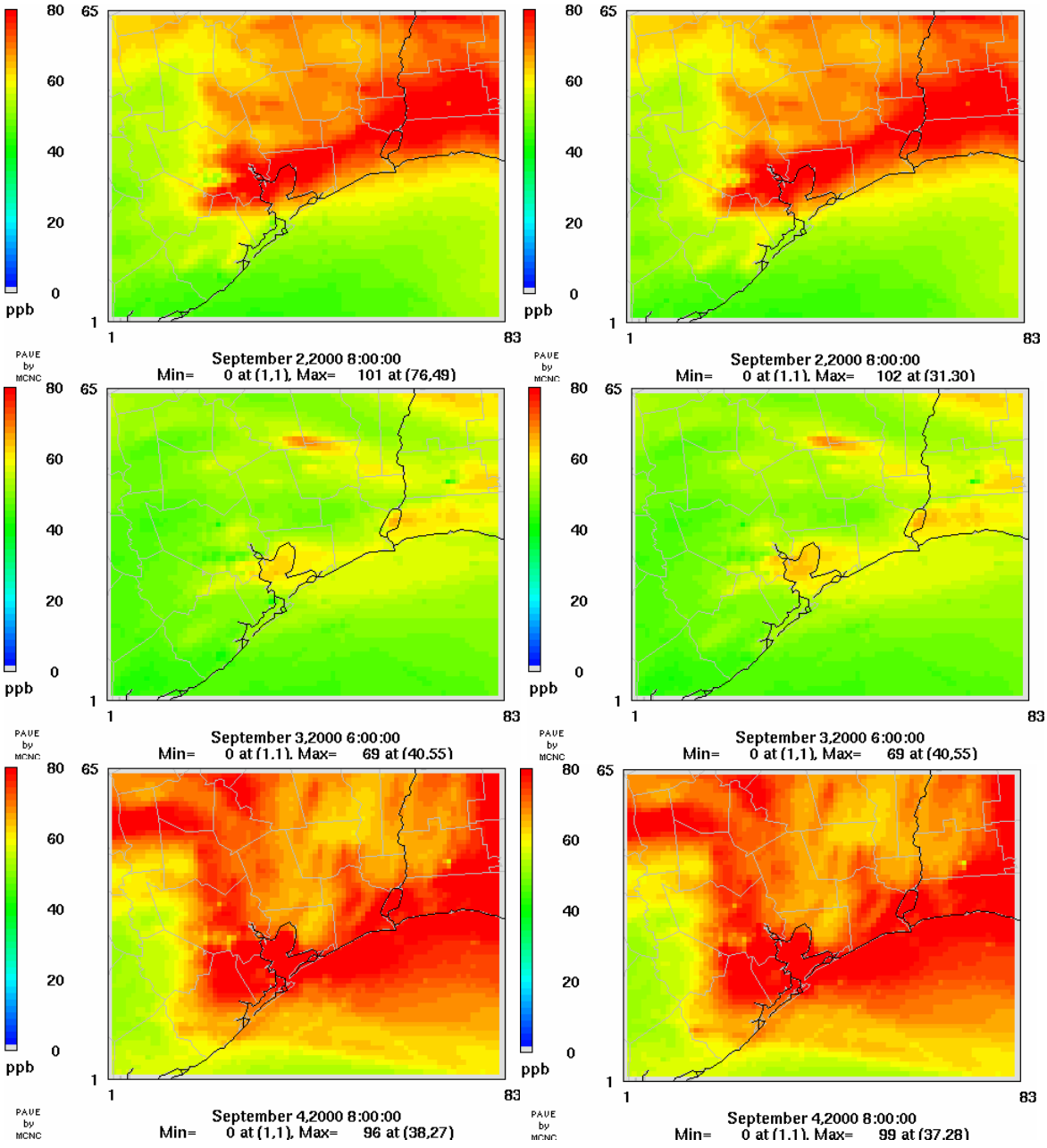

Figure 4.19 (Cont'd) Eight hour averaged ozone concentrations. Left column shows total ozone concentrations, assuming no chlorine emissions, at the time of the maximum difference in ozone concentration caused by chlorine emissions. Peak time and magnitude of the maximum ozone concentrations are indicated below each plot. Right column shows the total ozone concentration for the case with chlorine emissions at the same time of day. The scale of the ozone concentration is from zero to 120 ppbv since the 1-hour averaged ozone NAAQS is 120ppbv.

Therefore, the red color in the plot shows the location where the ozone concentration is equal or larger than the NAAQS criteria (120ppbv)

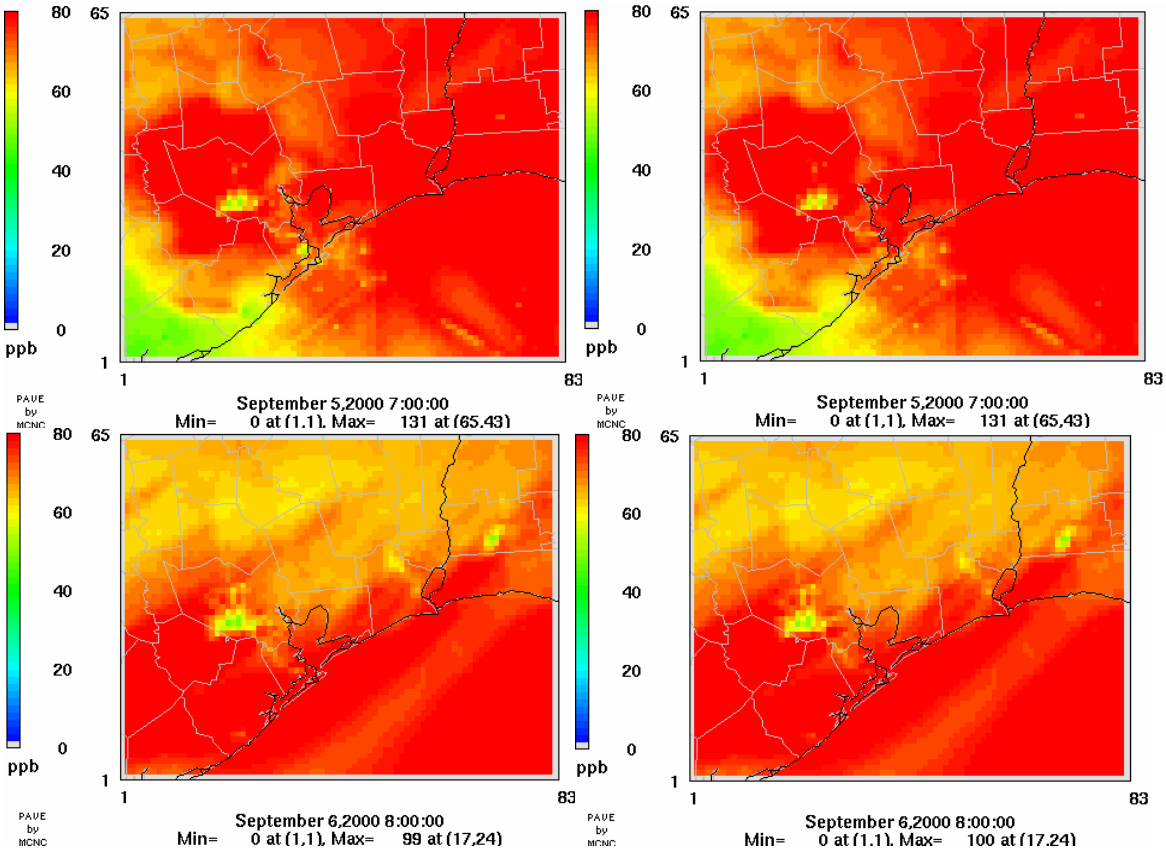

Figure 4.19 (Cont'd) Eight hour averaged ozone concentrations. Left column shows total ozone concentrations, assuming no chlorine emissions, at the time of the maximum difference in ozone concentration caused by chlorine emissions. Peak time and magnitude of the maximum ozone concentrations are indicated below each plot. Right column shows the total ozone concentration for the case with chlorine emissions at the same time of day. The scale of the ozone concentration is from zero to 120 ppbv since the 1-hour averaged ozone NAAQS is 120ppbv. Therefore, the red color in the plot shows the location where the ozone concentration is equal or larger than the NAAQS criteria (120ppbv)

4.6 Impacts of emission estimates on the spatial and temporal distributions of O_3 formation

The sensitivities of ozone formation to changes in the emissions of the various chlorine sources are shown in Figure 4.20 for 1-hour averaged ozone concentrations and in Figure 4.21 for 8-hour averaged ozone concentrations. The sensitivity of predicted ozone concentrations to variations in the strength of chlorine emissions from cooling towers, swimming pools, industrial point sources, and seasalt was examined. The sensitivity analyses were done by doubling tower emissions, doubling swimming pool emissions, doubling industrial point source emissions, and increasing seasalt emissions by a factor of 10. The differences in ozone concentrations between each of the sensitivity runs and the simulation with basecase chlorine emissions were calculated. Figures 4.20 and 4.21 are for August 25th.

Chlorine emissions from cooling towers had the largest impacts on both 1-hour and 8-hour averaged ozone mixing ratios in the region. Peak ozone enhancement from doubling chlorine emissions of cooling towers is 42 ppbv (1- hour averaged) and 19 ppbv (8-hour averaged) both at 0700 in the Houston Ship Channel area. Chlorine emission from swimming pools causes 5 ppbv of enhancement of the maximum ozone concentration at 1400 (1-hour averaged) and 3 ppbv of enhancement of maximum ozone concentration at 1100 (8-hour average) in urban Houston. Increased chlorine emissions from industrial point sources contribute 2 ppbv of additional ozone in the Houston – Ship Channel area at 0800 (1-hour averaged) and 0700 (8-hour average). A ten-fold increase of seasalt chlorine emission makes 2-3 ppbv of ozone enhancement in the Ship Channel area and along the coastline at 0700 (1-hour averaged) and 0600 (8-hour average).

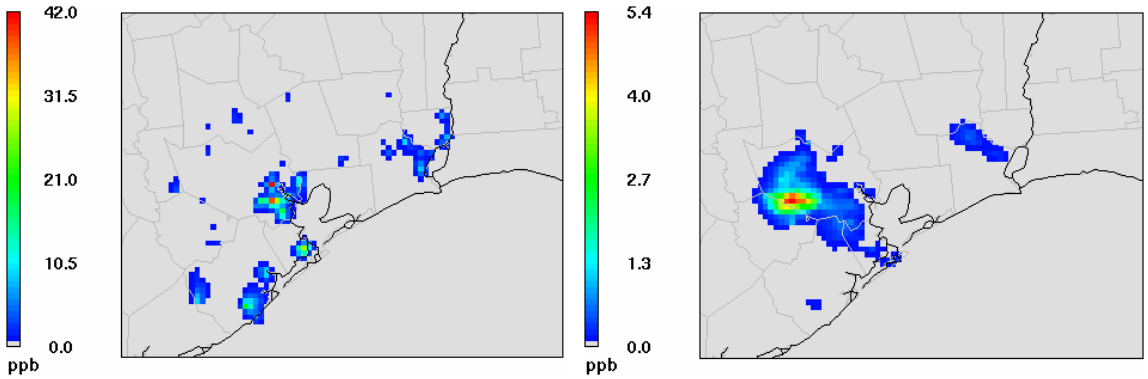

(a) doubling cooling towers emissions at 0700 (b) doubling swimming pools emissions at 1400

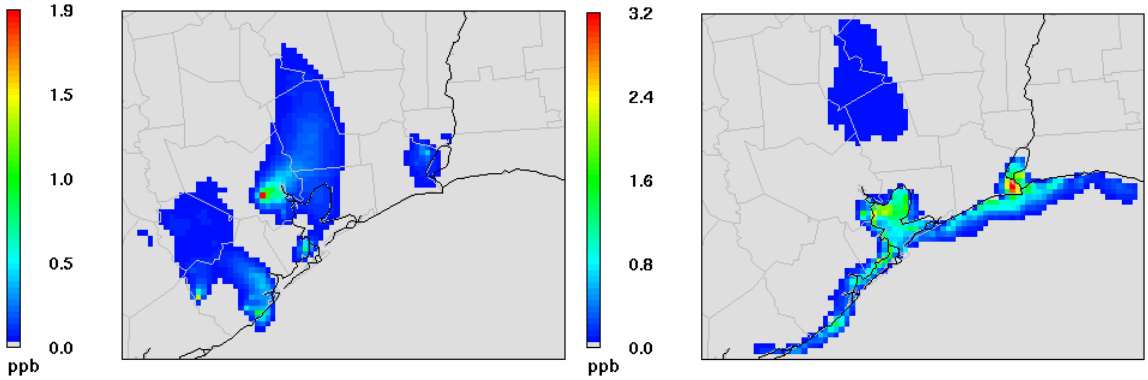

(c) doubling industrial point source emissions at 0800(d)ten times increase released by seasalt emission at 0700

Figure 4.20 Difference between maximum predicted 1- hour averaged O_3 mixing ratios on August 25th for chlorine basecase and chlorine basecase augmented by (a) doubling cooling tower emissions, (b) doubling swimming pools emissions, (c) doubling industrial point source emissions, and by (d) a factor of 10 increase in chlorine released by sea salt emissions

: Maximum difference in ozone concentrations occurred (a) at 0700 for cooling towers, (b) at 1400 for swimming pools, (c) at 0800 for industrial point sources, and (d) at 0700 for seasalt emissions.

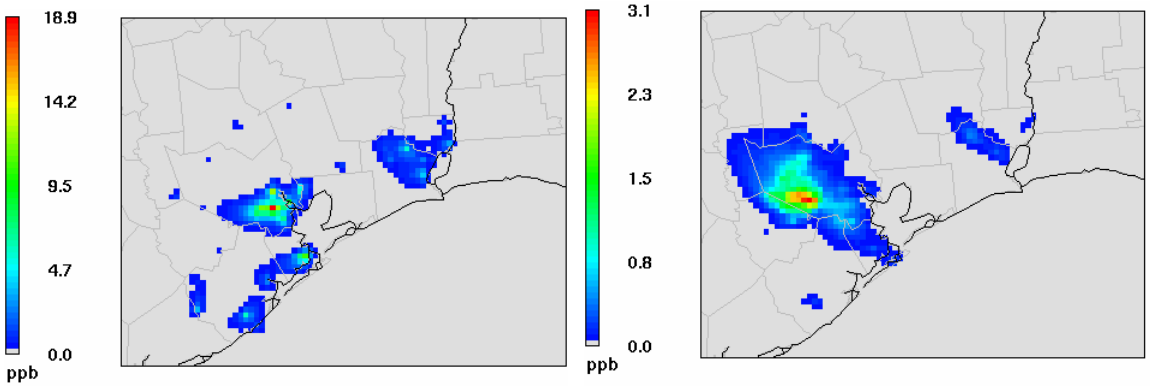

(a) doubling cooling towers emissions at 0700 (b) doubling swimming pools emissions at 1100

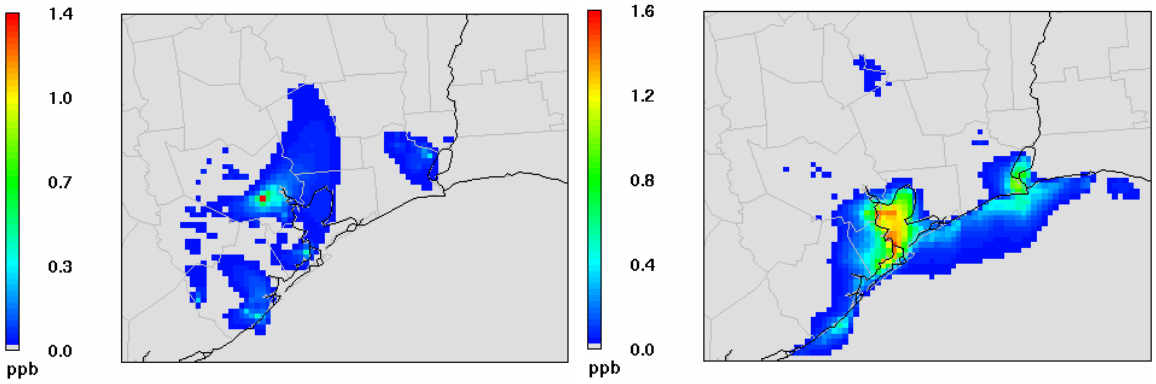

(c)doubling industrial point source emissions at 0700 (d)ten times increase released by seasalt emissions at 0600

Figure 4.21 Difference between maximum predicted 8- hour O_3 mixing ratios on August 25th for chlorine basecase and chlorine basecase augmented by (a) doubling cooling tower emissions, (b) doubling swimming pools emissions, (c) doubling industrial point source emissions, and by (d) a factor of 10 increase in chlorine released by sea salt emissions

: Maximum difference in ozone concentrations occurred (a) at 0700 for cooling towers, (b) at 1100 for swimming pools, (c) at 0700 for industrial point sources, and (d) at 0600 for seasalt emissions.

Figure 4.22 and 4.23 show (a) absolute ozone concentration and differences in ozone concentrations between chlorine basecase and chlorine basecase augmented by (b) doubling cooling tower emissions, (c) doubling swimming pools emissions at the time of the day when the maximum ozone concentration occurs. Figure 4.22 is based on 1-hour averaged ozone concentration and Figure 4.23 is based on 8-hour averaged ozone concentration. Only August 25th is shown in these Figures. Other days are shown in Figures C-1 and C-2 in Appendix C. Since the ozone enhancements due to doubling industrial point source emissions and increasing chlorine released by sea salt by a factor of 10 are small compared to the effects of cooling tower and swimming pool emissions, only ozone enhancement by cooling tower and swimming pools are indicated here.

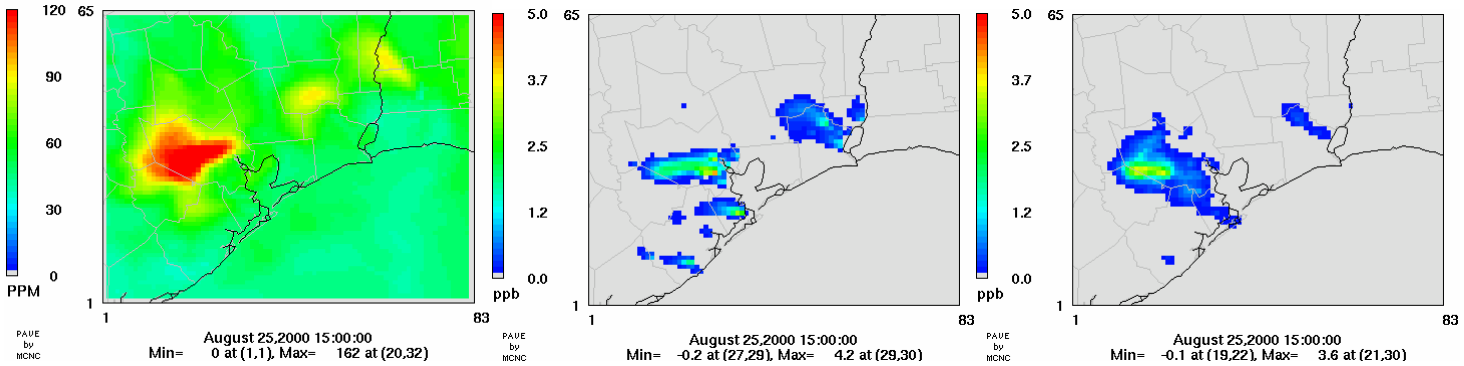

a) absolute ozone concentration b) doubling cooling tower emissions c) doubling swimming pool emissions

Figure 4.22 1-hour averaged absolute ozone concentration and difference in 1-hour averaged ozone concentrations between chlorine basecase and chlorine basecase augmented by (b) doubling cooling tower emissions, (c) doubling swimming pools emissions at the time of the day when the maximum ozone concentration occurs.

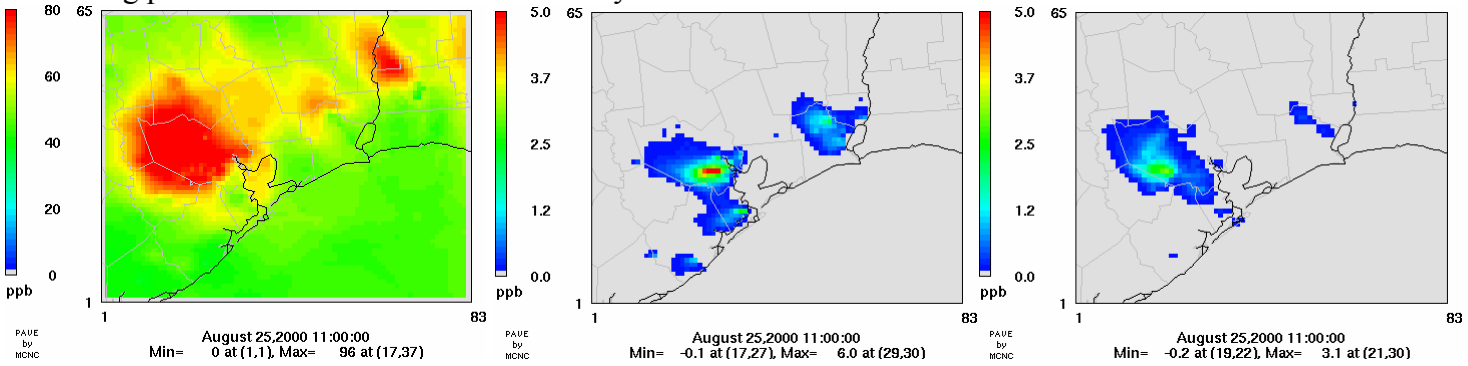

a) absolute ozone concentration b) doubling cooling tower emissions c) doubling swimming pool emissions

Figure 4.23 8-hour averaged absolute ozone concentration and difference in 8-hour averaged ozone concentrations between chlorine basecase and chlorine basecase augmented by (b) doubling cooling tower emissions, (c) doubling swimming pools emissions at the time of the day when the maximum ozone concentration occurs.

Differences in predicted O_3 concentrations for 1-hour averaged and 8-hour averaged between *Cl_2 basecase* and *Cl_2 basecase augmented by a 1 tons day^{-1}, 2 tons day^{-1}, 4 tons day^{-1}, and 8 tons day^{-1} point source release of Cl_2* are shown in Figures 4.24 and 4.25. The maximum peak predicted ozone enhancements are 80 ppbv, 100 ppbv, 80 ppbv, and 68 ppbv for 1-hour averaged concentrations and 21 ppbv, 27 ppbv, 29 ppbv, and 30 ppbv for 8-hour averaged concentrations for 1 tons day^{-1}, 2 tons day^{-1}, 4 tons day^{-1}, and 8 tons day^{-1} of point source release of Cl_2,. The O_3 enhancement is highly localized and located in the same area as the point source release. As point source chlorine emissions become greater than 2 tons day^{-1}, the enhancement of the peak ozone concentration is decreased. This may be because chlorine begins to consume ozone, rather than increase hydrocarbon reactivity.

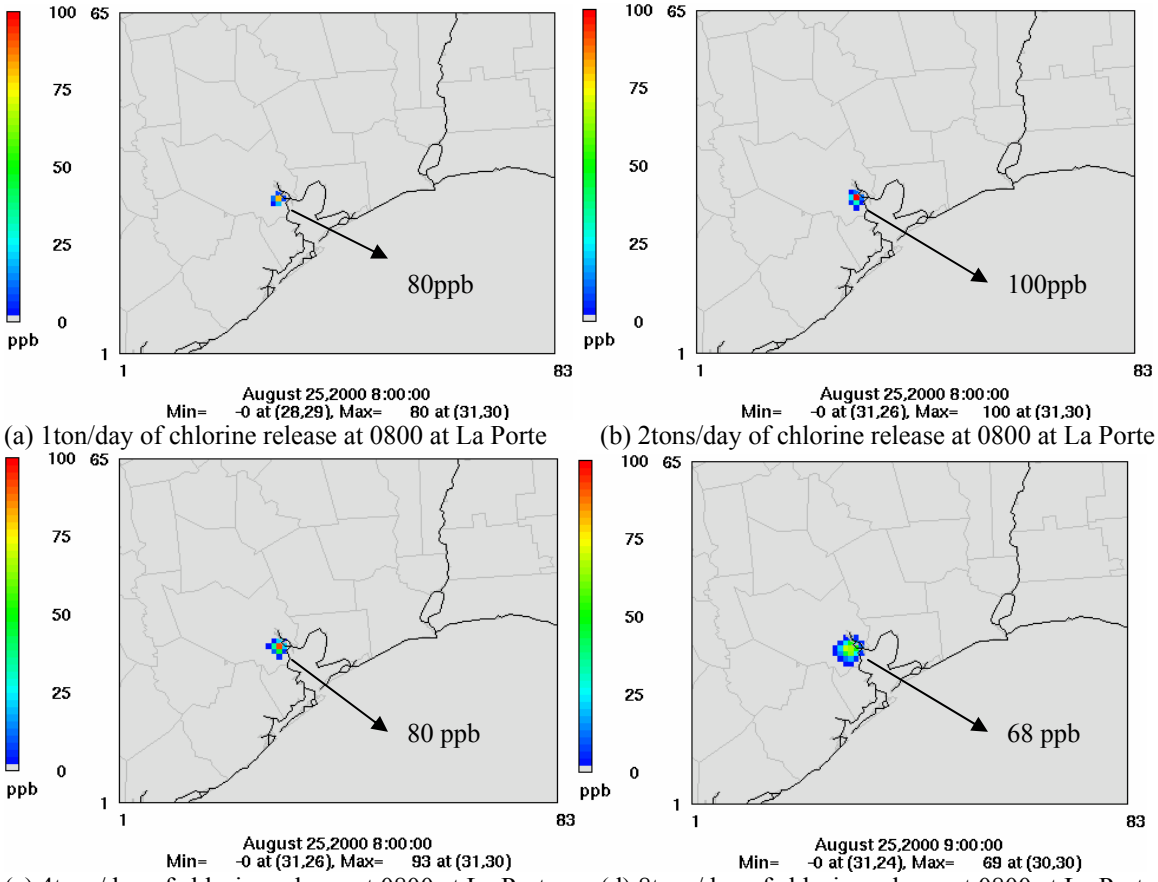

(a) 1ton/day of chlorine release at 0800 at La Porte

(b) 2tons/day of chlorine release at 0800 at La Porte

(c) 4tons/day of chlorine release at 0800 at La Porte

(d) 8tons/day of chlorine release at 0800 at La Porte

Figure 4.24 Difference in 1-hour averaged predicted maximum O_3 concentration between chlorine base case and chlorine basecase augmented by (a) 1 tons day^{-1}, (b) 2 tons day^{-1}, (c) 4 tons day^{-1}, and (d) 8 tons day^{-1} of point source release of Cl_2 at 0800 for one hour at the La Porte Airport

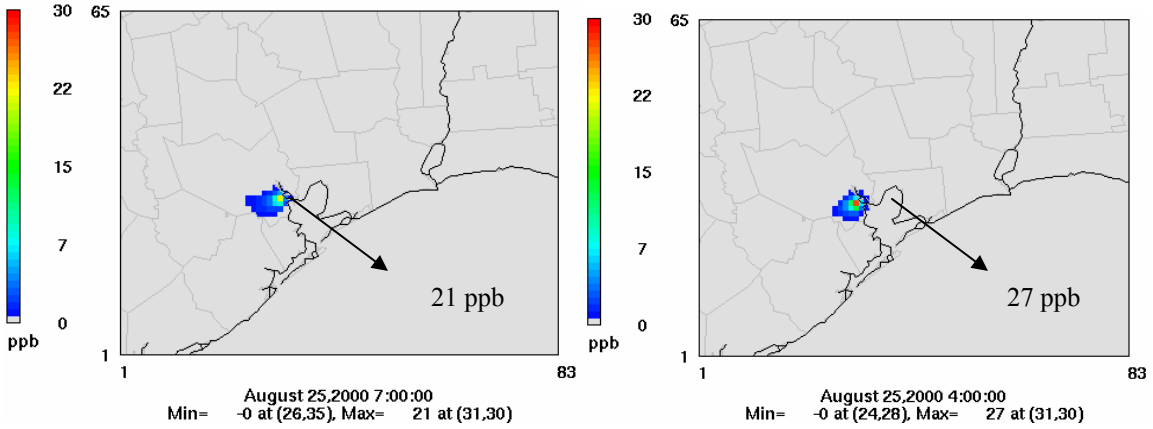

(a) 1ton/day of chlorine release at 0800 at La Porte (b) 2tons/day of chlorine release at 0800 at La Porte

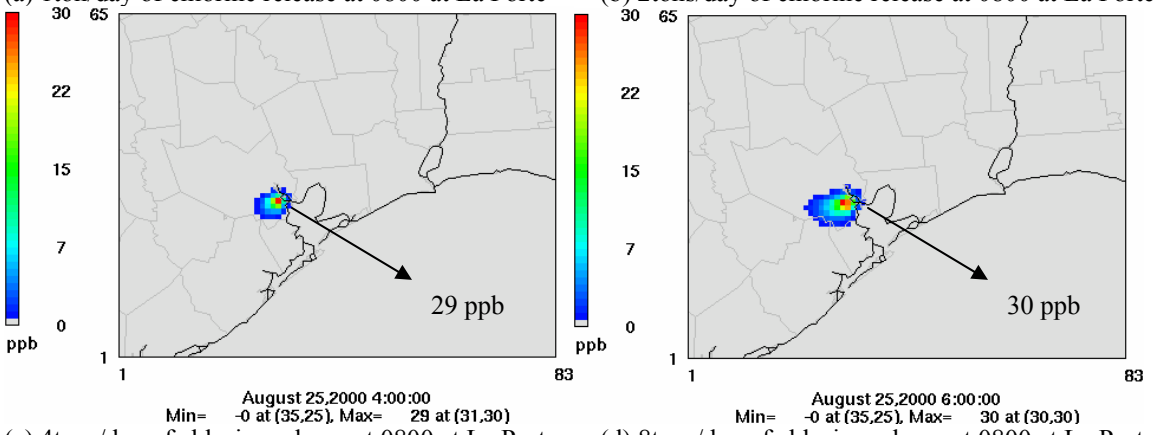

(c) 4tons/day of chlorine release at 0800 at La Porte (d) 8tons/day of chlorine release at 0800 at La Porte

Figure 4.25 Difference in 8-hour averaged predicted maximum O_3 concentration between chlorine base case and chlorine basecase augmented by (a) 1 tons day^{-1}, (b) 2 tons day^{-1}, (c) 4 tons day^{-1}, and (d) 8 tons day^{-1} of point source release of Cl_2 at 0800 for one hour at the La Porte Airport

Figure 4.26 shows the difference in predicted O_3 concentration between chlorine base case and chlorine base case augmented by 2 tons day^{-1}of point source release of Cl_2 at 0800 for one hour near the La Porte Airport (4km apart from La Porte). Peak differences in ozone concentrations for 1 hour averaged and 8 hour averaged are 115 ppbv and 29 ppbv, respectively, which is similar to the peak differences in ozone concentrations that occur due to the 2 ton day^{-1}of point source release of Cl_2 at 0800 at the La Porte Airport. This contrasts with the findings in section 4.4, where it was found that the CMBO mixing ratio with added chlorine emissions of 2 tons day^{-1} at the location

near La Porte was two times larger than the CMBO mixing ratio with added chlorine emissions of 2 tons day^{-1} at La Porte. This means that while CMBO formation is very dependent of the location of emission sources (most likely due to local emissions of isoprene), ozone formation is not as sensitive to the location of the release. Figure 4.27 shows the maximum difference of ozone concentrations between basecase without chlorine and chlorine basecase augmented by augmented by (a) 1 tons day^{-1}, (b) 2 tons day^{-1}, (c) 4 tons day^{-1}, and (d) 8 tons day^{-1} of point source release of Cl_2 at 0800 for one hour in the La Porte Airport. The difference between Figure 4.24 and 4.27 is that whether all the chlorine emissions are included or not; Figure 4.27 has all the chlorine emissions including augmented point source release of chlorine at La Porte.

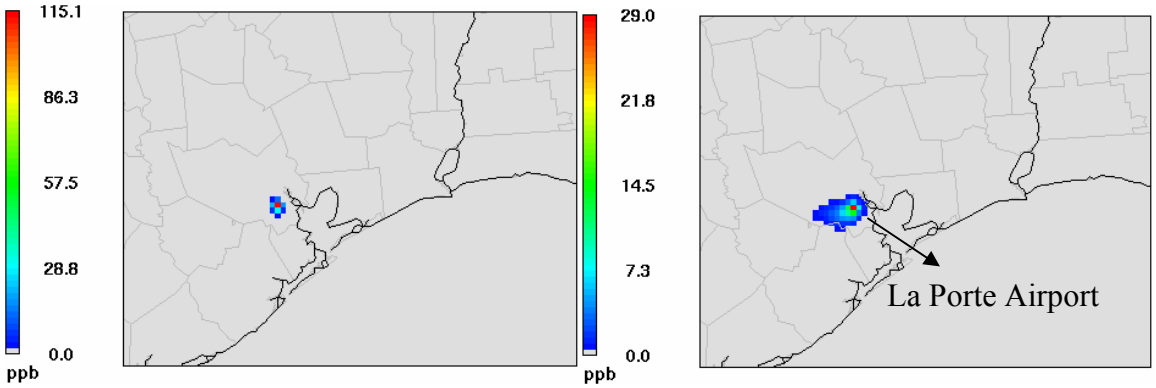

(a) 1-hour averaged ozone concentration at 0800 (b) 8-hour averaged ozone concentration at 0800

Figure 4.26 Maximum difference in predicted O_3 concentration between chlorine base case and chlorine basecase augmented by 2 tons day^{-1}of point source release of Cl_2 at 0800 for one hour near La Porte Airport (4km apart from La Porte) for (a) 1 hour averaged and (b) 8 hour averaged ozone concentrations

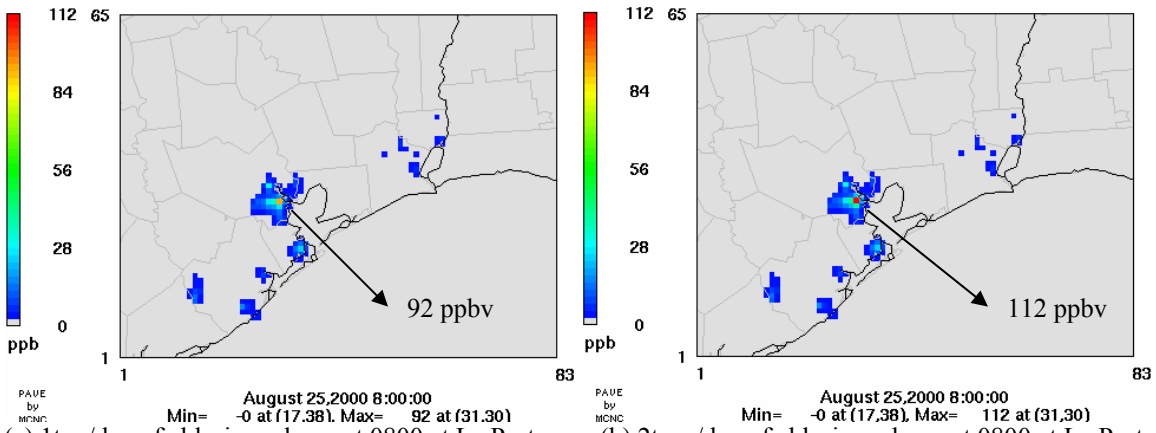

(a) 1ton/day of chlorine release at 0800 at La Porte

(b) 2tons/day of chlorine release at 0800 at La Porte

(c) 4tons/day of chlorine release at 0800 at La Porte

(d) 8tons/day of chlorine release at 0900 at La Porte

Figure 4.27 Maximum differences of ozone concentrations between basecase without chlorine and chlorine basecase augmented by augmented by (a) 1 tons day^{-1}, (b) 2 tons day^{-1}, (c) 4 tons day^{-1}, and (d) 8 tons day^{-1} of point source release of Cl_2 at 0800 for one hour in the La Porte Airport.

4.7 Summary

Regional-scale photochemical modeling suggests that chlorine radical chemistry enhances ozone formation in southeastern Texas. A chlorine emission inventory was estimated in order to predict ozone enhancement. Comparisons of observed CMBO mixing ratios in ambient air and model-predicted CMBO mixing ratios suggests that the emission inventory is reasonable, but likely requires some adjustments. Adjustments to the inventory, however, are very sensitive to the spatial and temporal characteristics of the emissions. Because data on the spatial and temporal distributions of chlorine emissions are limited, and because of the limited ambient data with which spatially variability in CMBO concentrations can be characterized, further analyses will be performed using the base chlorine inventory. Modeling analyses performed with this inventory indicate that chlorine emissions lead to maximum predicted 1-hour and 8-hour averaged ozone enhancements in the Galveston and Houston area of 73 ppbv and 21 ppbv, respectively.

Chapter 5: Control Strategy Evaluation

A hypothesis to be examined in this thesis is that chlorine emissions influence the relative effectiveness of ozone control strategies in the Houston/Galveston area. Since chlorine emissions lead to considerable ozone enhancement, chlorine emissions may also influence the relative effectiveness of ozone control strategies. In order to examine this possibility, ozone enhancements due to chlorine chemistry were determined at a variety of VOC and NO_x emission levels. Specifically, peak ozone concentrations were determined for simulations with 0%, 25%, 50%, 75%, and 100% reductions from the base case simulation in anthropogenic NO_x. All 5 of these scenarios were examined for anthropogenic VOC emission reductions, from the base case simulation, of 0%, 25%, 50%, 75%, and 100%. This matrix of 25 simulations was examined both with and without chlorine chemistry. Ozone isopleth plots (commonly called EKMA diagrams), shown in Figures 5.1 and 5.2 were used to summarize the results.

The isopleths for different days have different shapes, because of the diverse range of meteorological conditions that occurred during the episode. All of the days are described in Appendix D. For this work, the results for August 25 are examined in more detail. Isopleths for one-hour averaged ozone concentrations, with and without chlorine emissions, are compared in Figure 5.1. The isopleths report the domain-wide maximum concentration of ozone at the VOC and NO_x emission levels reported in the diagram; not all of these maxima occur at the same geographical location. In order to reach an ozone concentration of 125 ppb (NAAQS for 1-hour averaged ozone concentrations) on August 25, emission reductions of 27% for VOCs and 71% for NO_x are required, in the simulation without chlorine emissions and chemistry. When chlorine chemistry is included, emission reductions of 33% for VOCs and 72% for NO_x are required to reach an ozone concentration of 125 ppb. Thus, introducing 10^4 kg/day of chlorine emissions

can be considered as being roughly equivalent to adding 5% ($5*10^4$ kg/day) to the VOC emissions.

Isopleths for eight-hour averaged ozone concentrations are shown in Figure 5.2. Comparing the results of the simulations with and without chlorine chemistry reveals that adding chlorine chemistry is equivalent to a 10% NO_x reduction, or a 4% VOC reduction. The case without chlorine chemistry requires a 75% reduction in NO_x emissions or a 46% reduction in VOC emissions in order to reach 85 ppb (NAAQS for 8-hour averaged ozone concentration). The simulations with chlorine chemistry require an 85% reduction in NO_x emissions or a 50% reduction in VOC emissions in order to reach 85 ppb. Thus, introducing 10^4 kg/day of chlorine emissions can be considered as being roughly equivalent to adding 4% ($4*10^4$ kg/day) to the VOC emissions or 10 % to the NO_x emissions.

As shown in Figure 5.1, there was little difference in the response of domain-wide maximum one-hour averaged ozone concentrations to NO_x emission reductions in the simulations with and without chlorine chemistry. However, chlorine chemistry has an influence on the effectiveness of NO_x emission reductions for maximum eight-hour averaged ozone concentrations. The reason for this difference is associated with the spatial location of the domain-wide maximum ozone concentration. For the 1-hour averaged ozone concentrations, simulations with and without chlorine chemistry have maximum concentrations near downtown Houston at 1400hr or 1500hr, depending on the magnitude of NO_x emission reductions. For 8-hour averaged ozone concentrations, the maximum concentrations of simulations without chlorine chemistry occurred near downtown Houston at 1000hr or 1100hr. However, for simulations with chlorine chemistry included, the maximum ozone concentration occurred in the industrial source region (Ship Channel area) at 0700hr. In the base case, ozone produced in the industrial

source region is rapidly titrated by available NO. As NO is reduced, early morning ozone concentrations in the source region increase rapidly, but never exceed the domain-wide, peak one-hour averaged concentration. The morning ozone concentration peaks in the source region, caused by chlorine emissions, are sufficient, however, to change the location of the maximum eight-hour averaged ozone concentration.

Generally, for most days shown in Appendix D, adding chlorine chemistry and emissions necessitates a 2-5 percent increase in the level of VOC and NO_x emission reductions required to achieve 1-hour and 8-hour averaged maximum ozone concentrations that achieve the NAAQS.

(a) Case without chlorine (2000/08/25) (b) Case with chlorine (2000/08/25)

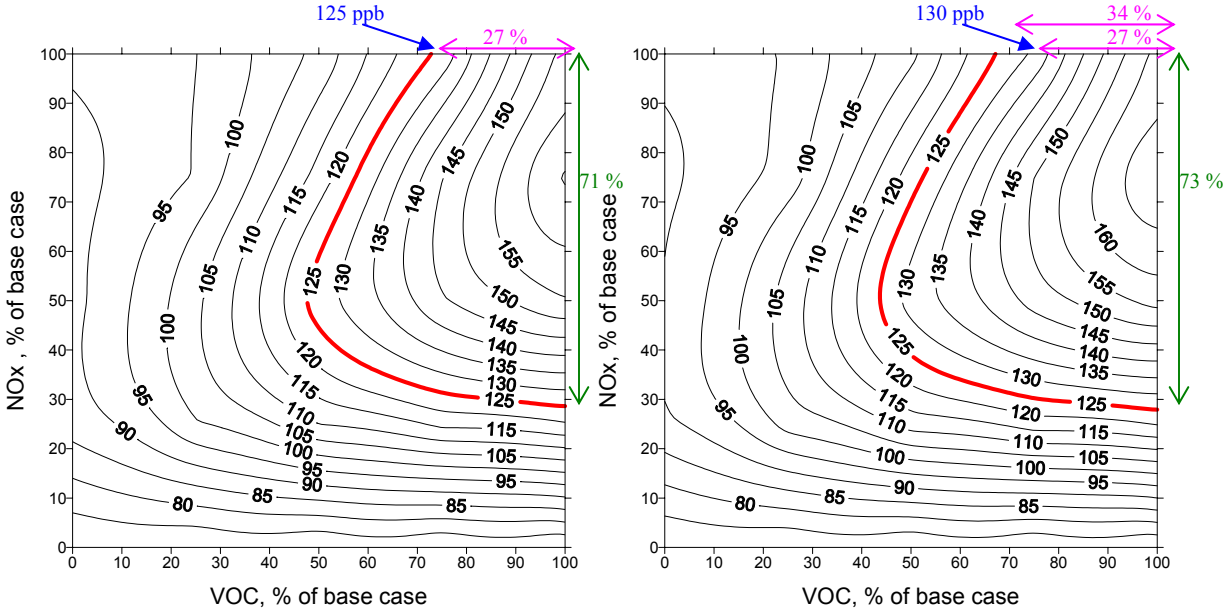

Figure 5.1 Isopleth diagrams for 1-hour averaged domain-wide maximum ozone concentrations with various amounts of NOx/VOCs reduction:(a) case without chlorine on August 25, (b) case with chlorine on August 25

(a) Case without chlorine (2000/08/25) (b) Case with chlorine (2000/08/25)

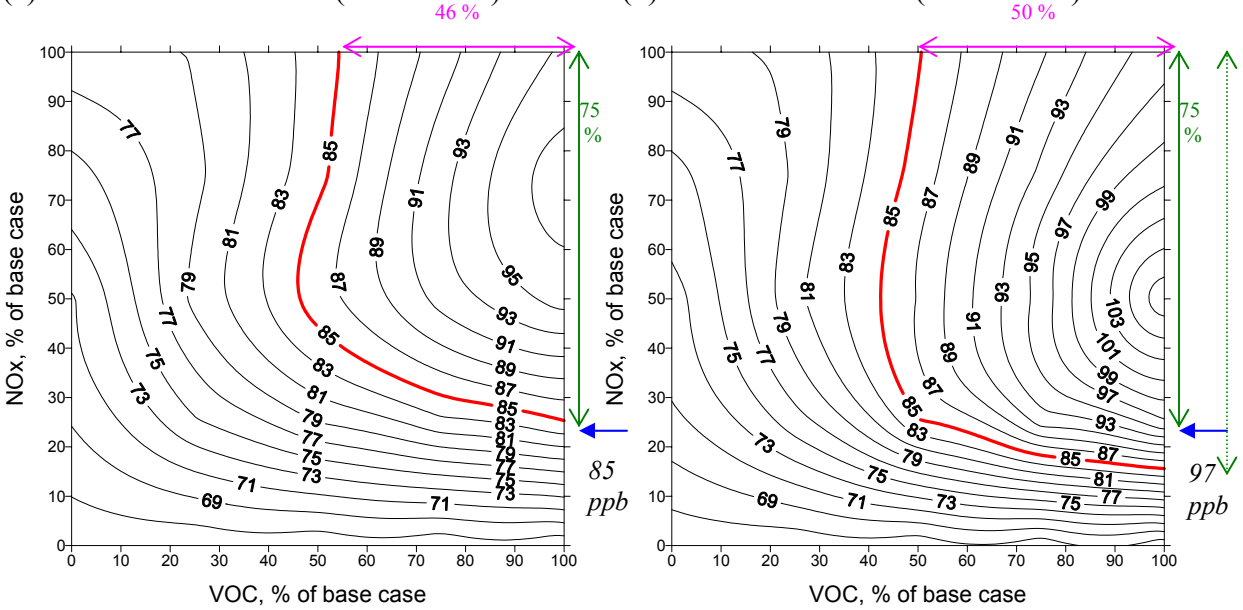

Figure 5.2 Isopleth diagrams for 8-hour averaged domain-wide maximum ozone concentrations with various amounts of NOx/VOCs reduction:(a) case without chlorine on August 25, (b) case with chlorine on August 25

Chapter 6: The Role of Anthropogenic Chlorine Emissions in Particulate Matter Formation in Southeast Texas

6.1 Atmospheric Chemistry of Atmospheric Ammonium Chloride

Previous chapters have examined the role of anthropogenic chlorine chemistry in the production of gas phase oxidants, such as ozone, in southeast Texas. These chlorine emissions can also play a role in fine particulate matter formation through the production of HCl. The primary reaction pathway for molecular chlorine releases during daylight hours is photolysis. The resulting atomic chlorine rapidly abstracts hydrogen from hydrocarbons, producing HCl. Hydrochloric acid ($HCl_{(g)}$) then reacts with ammonia ($NH_{3(g)}$), producing particulate $NH_4Cl_{(s)}$:

$$NH_{3(g)} + HCl_{(g)} \leftrightarrow NH_4Cl_{(s)} \qquad (6.1)$$

The equilibrium constant for this reaction at 298K is $2.12*10^{17}$ $mol^2kg^{-2}atm^{-2}$, as compared to $4.0*10^{17}$ $mol^2kg^{-2}atm^{-2}$ for the ammonia-nitric acid-ammonium nitrate reaction and $>>10^{17}$ $mol^2kg^{-2}atm^{-2}$ for the ammonia-sulfuric acid-ammonium sulfate reaction (Seinfeld and Pandis, 1998). Thus, significant quantities of ammonium chloride will only form if sufficient ammonia is available to neutralize both atmospheric sulfuric acid and nitric acid.

Sulfuric acid is created by oxidation of SO_2 in the atmosphere by hydrogen peroxide (H_2O_2), OH radicals, or on surfaces. If ammonia (NH_3) is present, the sulfuric acid is neutralized to form aerosol phase solids including $(NH_4)_3H(SO_4)_2$ (letovicite), $(NH_4)_2SO_4$ and NH_4HSO_4, as well as aqueous solutions of NH_4^+, SO_4^{2-}, HSO_4^- and $NH_3(aq)$. The reaction between ammonia and sulfate is:

$$2NH_4^+ + SO_4^{2-} \leftrightarrow (NH_4)_2SO_{4(s)} \qquad (6.2)$$

If ammonia is present only at low concentrations, sulfuric acid exists in the aerosol phase in the form of H_2SO_4. As NH_3 concentration increases, sulfuric acid converts to HSO_4^- and its salts, and SO_4^{2-} and its salts (Pavlovic, 2005).

In the presence of ammonia, nitric acid and water, ammonium nitrate may be formed:

$$NH_{3(g)} + HNO_{3(g)} \leftrightarrow NH_4NO_{3(s)} \qquad (6.3)$$

This can be observed in areas characterized by high ammonia and nitric acid concentrations and low sulfate concentrations. In southeast Texas, where ammonia, nitric acid, sulfuric acid, water and chloride are all present (Equations 6.1, 6.2, and 6.3), there is a complex equilibrium partitioning of materials in the gas and particle phases.

This equilibrium has two major regimes of interest, ammonia-rich and ammonia-poor. If [TA], [TS], and [TN] are the total (gas + aqueous + solid) molar concentrations of ammonia, sulfate, and nitrate, respectively, then the two cases are (Seinfeld and Pandis, 1998):

1. Ammonia-poor, [TA] < 2[TS]
2. Ammonia-rich, [TA] > 2[TS]

Under ammonia poor conditions, the equilibrium partitioning favors the formation of ammonium sulfate over the formation of ammonium chloride or ammonium nitrate, if there is insufficient ammonia to neutralize the sulfuric acid, very little ammonium nitrate or ammonium chloride will form. Under ammonia rich conditions, there is excess ammonia, so that the aerosol phase will be neutralized to a large extent. The ammonia that does not react with sulfate will be available to react with chloride and nitrate to produce ammonium chloride or ammonium nitrate. The CAMx simulations, described earlier in this thesis, provide a framework for modeling the competition between sulfate, nitrate, and chloride for the available ammonia.

The CAMx simulations reported in this chapter use the same inputs and modeling domain reported in previous chapters of this thesis, along with detailed inventories of ammonia and sulfur dioxide emissions. The ammonia emission inventory used in this dissertation was based on both the emission inventory developed by Corsi et al. (2000) for non-point source ammonia emissions in the State of Texas and the national ammonia emissions inventory developed by Carnegie Mellon University (CMU) in 2004. Pavlovic (2005) added point source emission to the inventory developed by Corsi et al (2000), merged the CMU inventory with the inventory for the State of Texas, and allocated the emissions spatially using surrogates from land use and land cover (LULC) data, as well as population and urban area shape files. According to Pavlovic (2005), 80 % of all ammonia emissions in Texas come from livestock and animal feeding operations. Additional significant sources of ammonia emissions are mostly distributed over agricultural land and population/urban land categories. Ammonia emitted from point sources are generally much smaller than those from non-point sources. The major sources of sulfur dioxide (SO_2) are point sources. Pavlovic (2005) also developed a comprehensive, spatially allocated inventory of SO_2 emissions. Details of the ammonia and sulfur dioxide emissions inventories can be found in Pavlovic (2005).

6.2 Aerosol Chemistry Mechanism and HCl Emission Inventory

To predict the effect of chlorine emissions and chemistry on particle formation, a detailed mechanism available in CAMx (Mechanism 4_CMU scheme) was used. Mechanism 4 is described in detail in the CAMx documentation (www.camx.com). The mechanism includes gas phase chemistry along with the aerosol formation chemistry, however, the gas phase chemistry in Mechanism 4 does not include gas phase chlorine chemistry. The only chlorine containing species in Mechanism 4 is HCl.

Because of the limitations of the chemical mechanisms, a simplifying assumption was required in the modeling of particulate chloride formation. For this work, it was assumed that anthropogenic molecular chlorine emissions would very rapidly photolyze and abstract hydrogen, producing HCl. Justification for this assumption is shown in Figure 6.1, which compares, hour by hour, the total anthropogenic Cl_2 emission rates to predicted HCl concentrations, using the gas phase chlorine mechanism developed by Tanaka et al. (2002). The HCl concentrations closely track the anthropogenic Cl_2 emissions, which indicates HCl is created as soon as molecular chlorine is emitted.

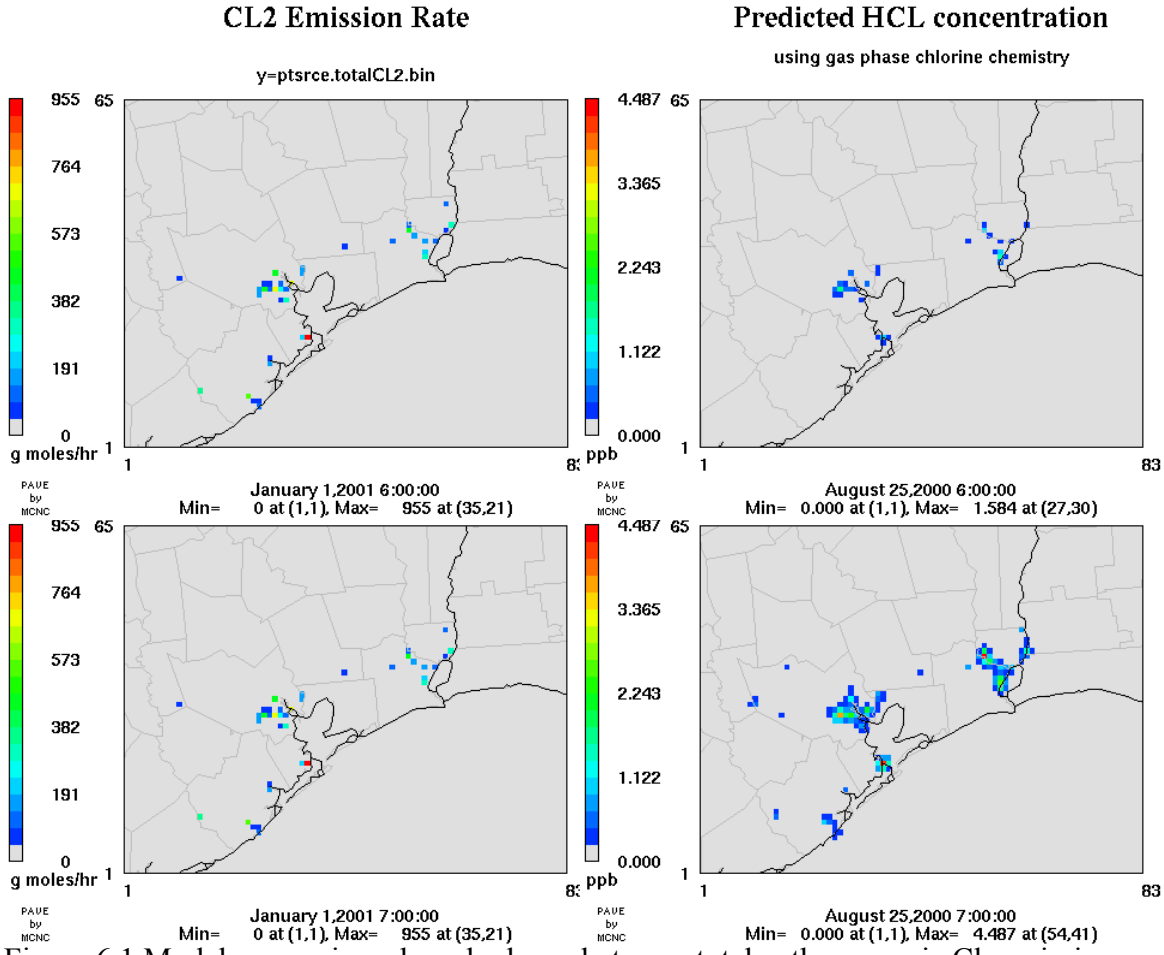

Figure 6.1 Model comparison, hour by hour, between total anthropogenic Cl_2 emission rates (left column) and predicted hydrogen chloride (HCl) concentrations (right column) on August 25, 2000 using Cl_2 emission rates shown in left column

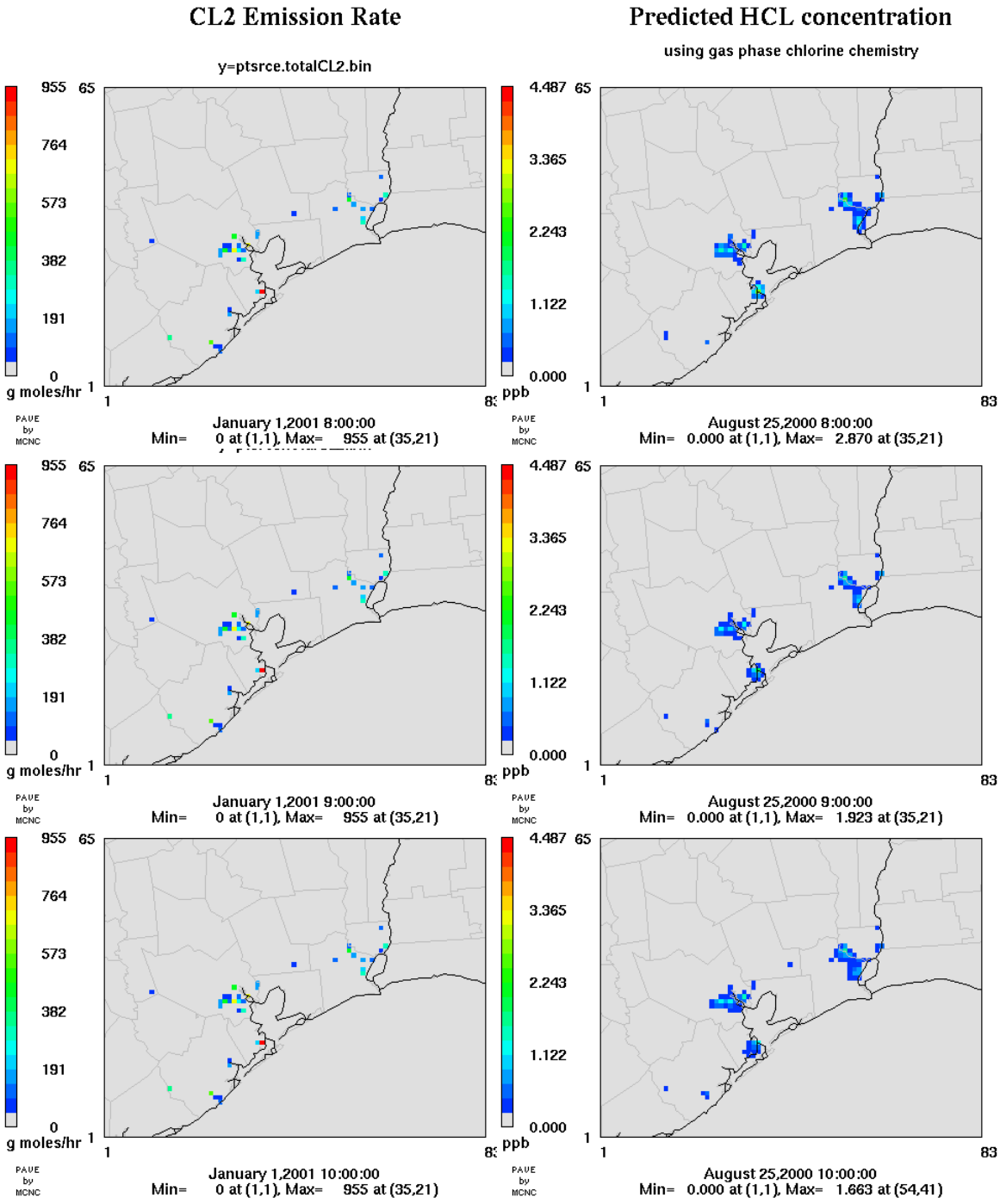

Figure 6.1 (Cont'd) Model comparison, hour by hour, between total anthropogenic Cl_2 emission rates (left column) and predicted hydrogen chloride (HCl) concentrations (right column) on August 25, 2000 using Cl_2 emission rates shown in left column

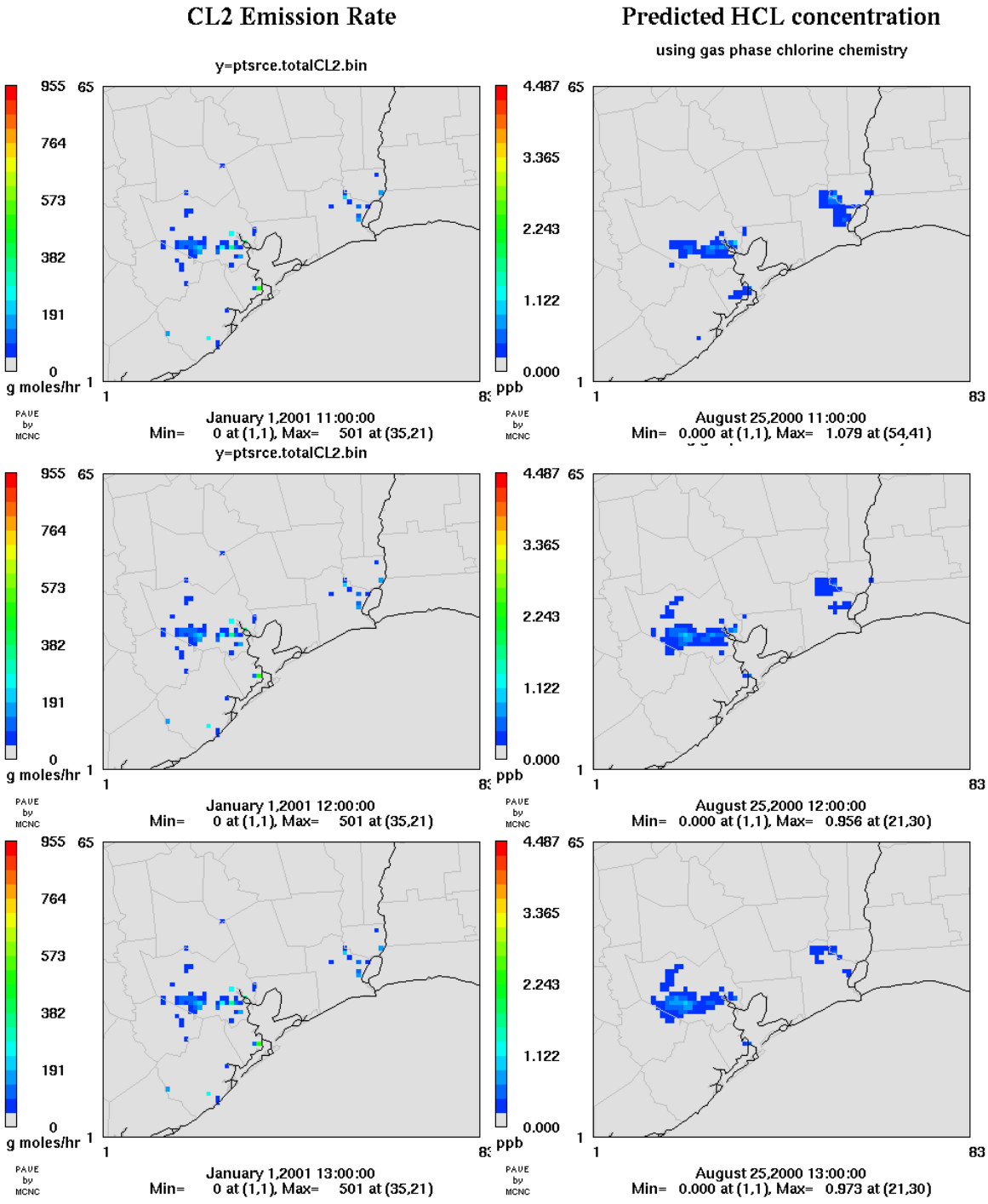

Figure 6.1 (Cont'd) Model comparison, hour by hour, between total anthropogenic Cl_2 emission rates (left column) and predicted hydrogen chloride (HCl) concentrations (right column) on August 25, 2000 using Cl_2 emission rates shown in left column

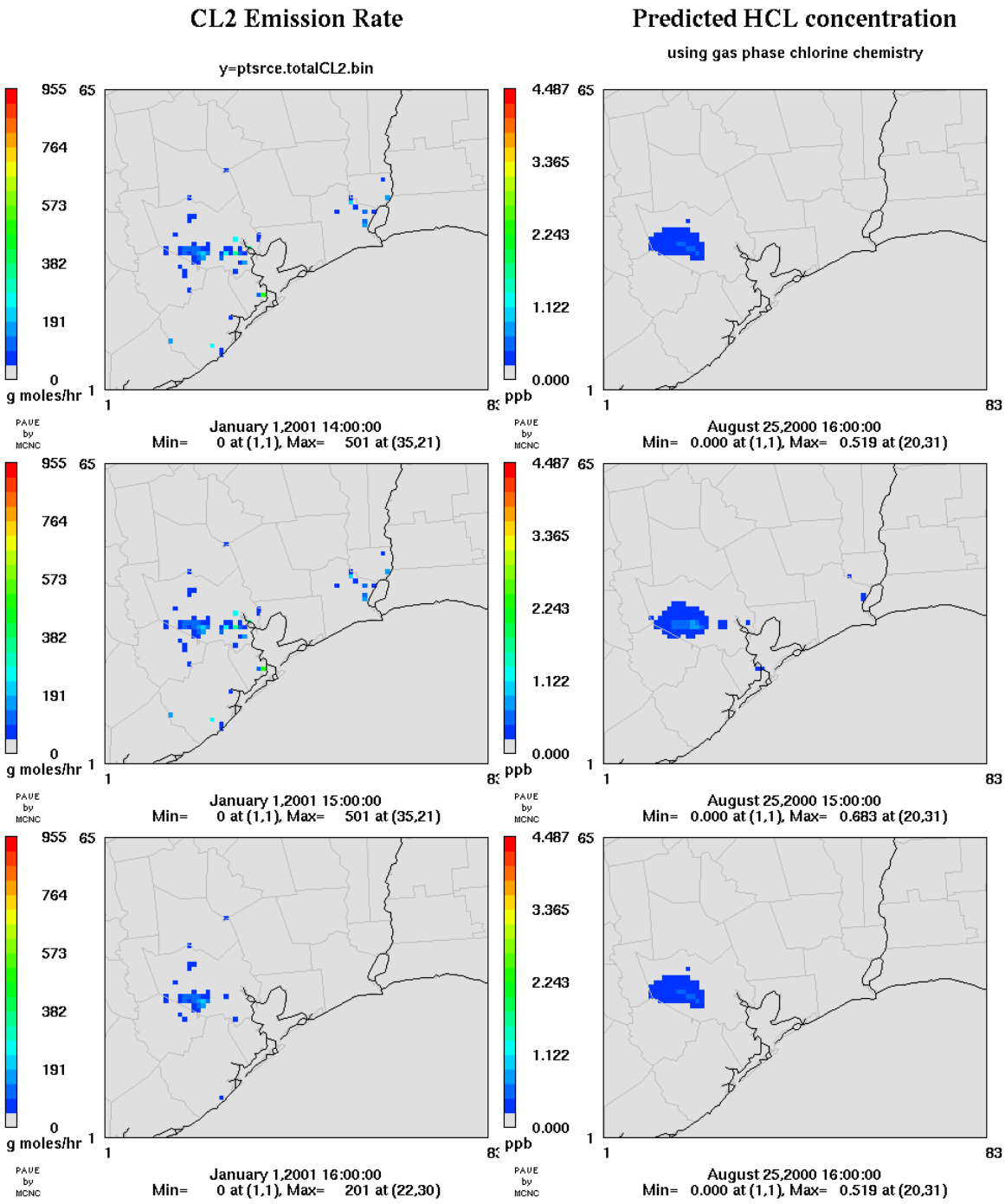

Figure 6.1 (Cont'd) Model comparison, hour by hour, between total anthropogenic Cl_2 emission rates (left column) and predicted hydrogen chloride (HCl) concentrations (right column) on August 25, 2000 using Cl_2 emission rates shown in left column

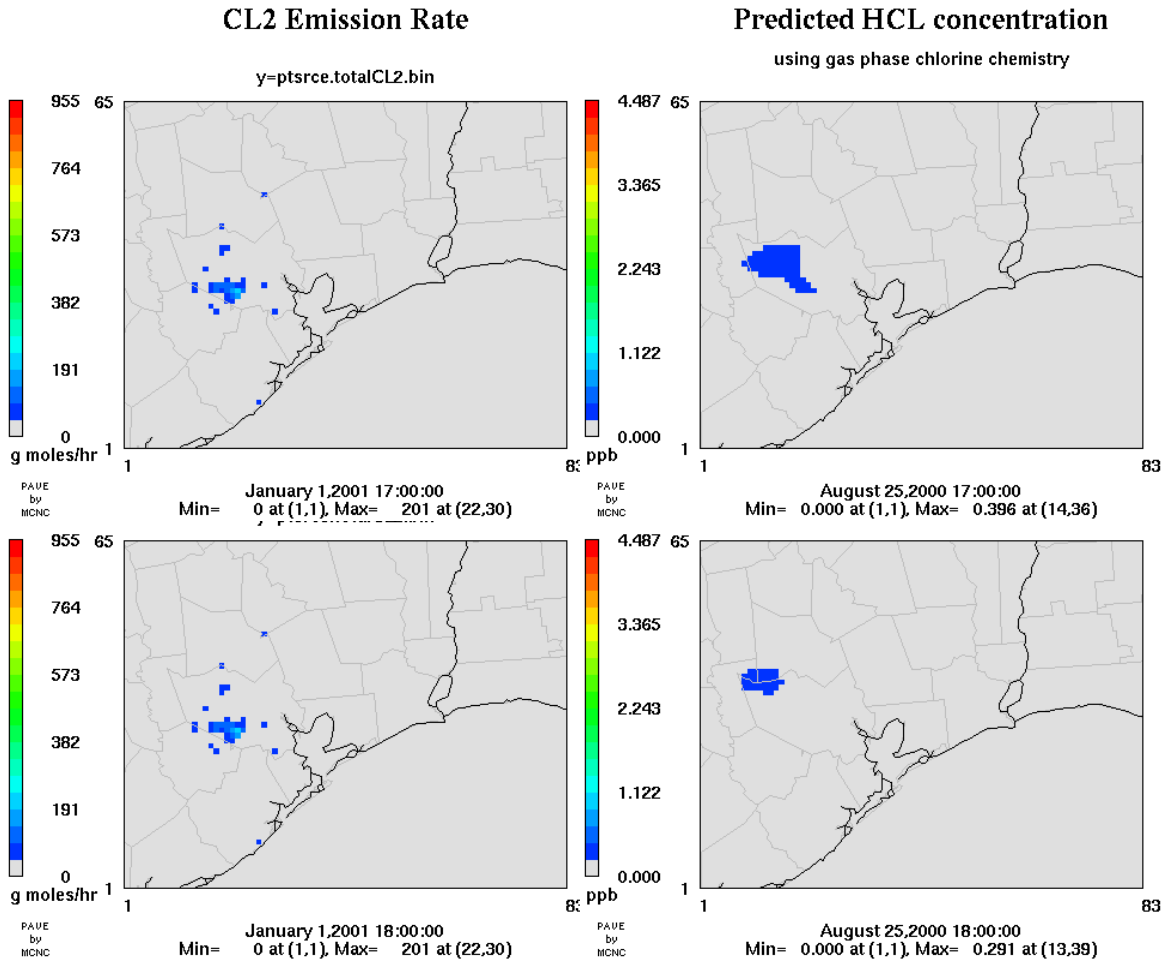

Figure 6.1 (Cont'd) Model comparison, hour by hour, between total anthropogenic Cl_2 emission rates (left column) and predicted hydrogen chloride (HCl) concentrations (right column) on August 25, 2000 using Cl_2 emission rates shown in left column

Converting molecular chlorine emissions into equivalent emissions of chlorine as HCl leads to the temporal and spatial distributions of HCl emissions shown in Figure 6.2. This HCl emission inventory was implemented into the regional photochemical air quality model to predict the formation of chloride containing particulate matter (particle chloride). Direct emissions of HCl from sources other than the sources of molecular chlorine were neglected since point sources of HCl emissions are only 0.5 ~ 1 tons/day,

(see Appendix E, Table E-1), which is more than an order of magnitude lower than molecular chlorine emission rates.

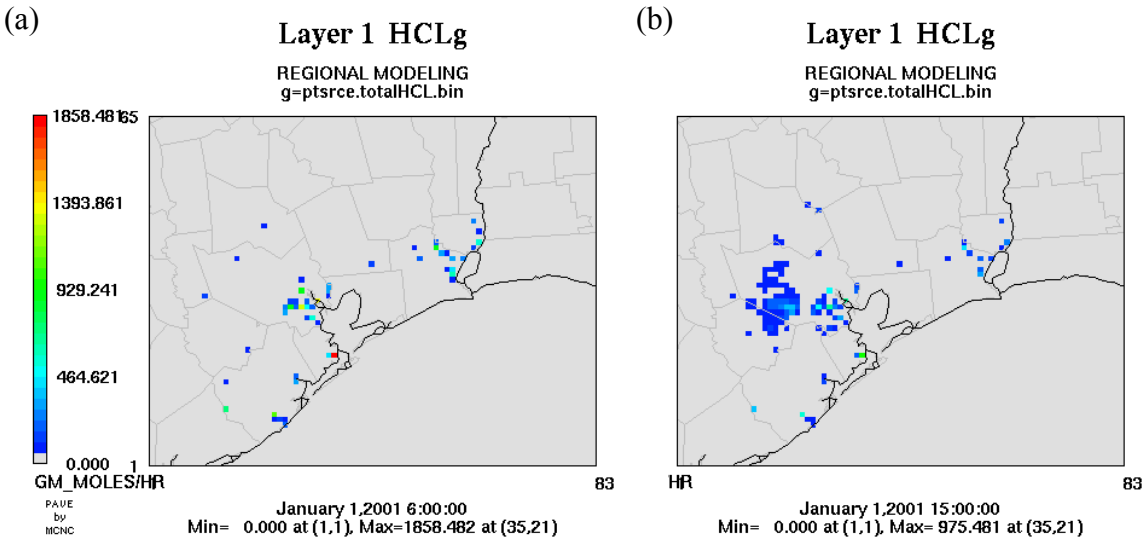

Figure 6.2 Spatial and temporal distribution of HCl emission inventory; Figure (a) represents HCl emission from 0600 hr to 1100 hr, Figure (b) represents HCl emission from 1200 hr to 1500 hr

6.3 Predicted Total Particle Chloride

The spatial distributions of total particle chloride concentrations predicted for August 25 and August 26 are shown in Figure 6.3. Other days in the Episode are shown in Figure E-1 in Appendix E. Total particle chloride in these figures represent PM_{10} (0.039063 µm ~ 10 µm), however, most of the chloride is found in the $PM_{2.5}$ fraction. Particle chloride is formed rapidly at 0600 hr and reaches maximum concentration at 0700 hr for all episode days. Particle chloride concentrations then rapidly decrease, beginning at 0800 hr, and rarely appeared throughout the rest of the day. The maximum predicted total particle chloride occurred near the Ship Channel, and the values vary from 0.1 µg/m^3 to 9 µg/m^3 during the Episode.

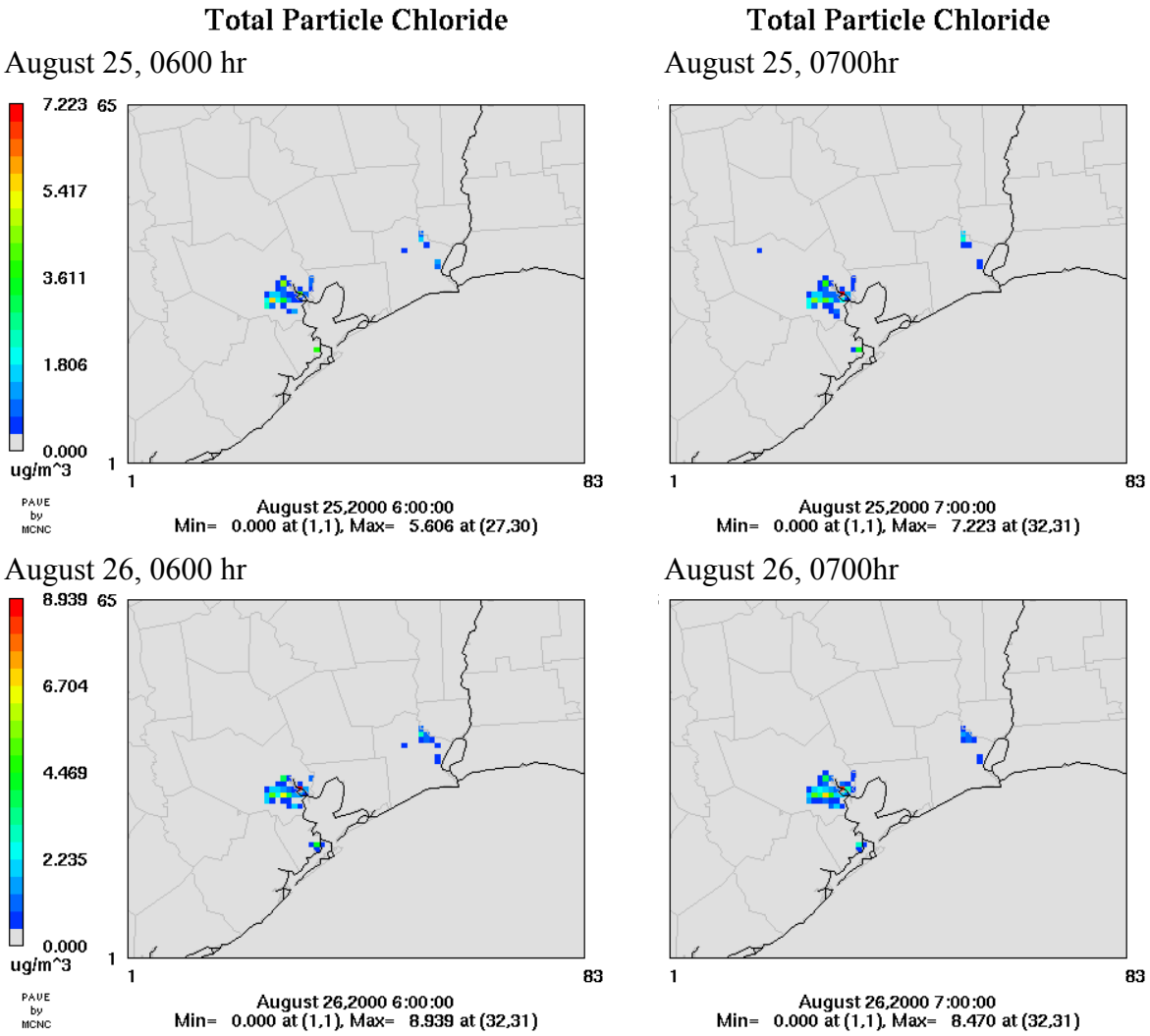

Figure 6.3 Formation of total particle chloride at 0600 and 0700 for August 25 and 26, 2000

6.4 Comparisons of predicted and observed HCl and Particle chloride

Particle and gas phase composition data relevant to the simulations were collected at the La Porte airport monitoring site during the episode period by both Georgia Institute of Technology (GIT) and Aerodyne Research Inc. Aerodyne Research Inc. deployed an aerosol mass spectrometer (AMS) at the La Porte site from 20 August 2000 until 15 September 2000. The AMS obtained chemical composition data on aerosols using a

quadrupole mass spectrometer equipped with electron ionization source. The AMS obtained chemical composition data and particle size distribution data with a 10 minute averaging times for the duration of the study. The Georgia Institute of Technology (GIT) measured particle composition using their Particle Composition Monitor (PCM) which is equipped with 3 separate mass flow controlled channels for the sampling of airborne $PM_{2.5}$ on discrete time scales between 24 and 6 hours, depending on pollution level. Prior to collection of $PM_{2.5}$ on filter media, important inorganic and organic gas species such as NH_3, SO_2 and HNO_3 , as well as semi-volatile polycyclic aromatic compounds (PAH), pesticides, and halogenated species are removed from the sample stream by means of specially coated diffusion tubes (denuders). For gases such as HCl, the concentrations were calculated using the following method:

$$c_{n,gas} = \frac{\{c_{n,ion}(D1) + c_{n,ion}(D2) - 2 * c_{n,ion}(DB)\} * M_n}{\Phi_{n,tot}}$$

where

$c_{n,ion}$*(D1/D2/DB)*: concentration of species *n* from Denuder 1, 2, Blank, respectively

Triple-annuli etched quartz glass denuders(15/24 cm long , 0.06/0.1 seconds residence time at 16.7 liter per minute) are used.

M_n: mass correction factor = $\frac{M_{gas}}{M_{ion}}$ with $M_{gas/ion}$: molar mass of gaseous/conjugated ionic species, respectively

For non-volatile $PM_{2.5}$ such as Na^+, Cl^-, SO_4^{2-} concentrations were calculated as:

$$c_{n,ion} = c_{n,ion}(T) - c_{n,ion}(TB)$$

where

$c_{n,ion}$*(T/TB)*: concentration of species *n* from Teflon filter/blank, respectively.

Model predicted and observed HCl concentrations are shown in Figure 6.4. The observed HCl concentrations are from GIT's PCM and are reported as 6-24 hour averages. The predicted concentrations are reported on both an hourly basis and based on averaging times that correspond to the measurement periods. The agreement between the observed and predicted HCl concentrations is generally good, although the observations do not have a fine enough time resolution to detect the strong morning peaks predicted by the model at 0700.

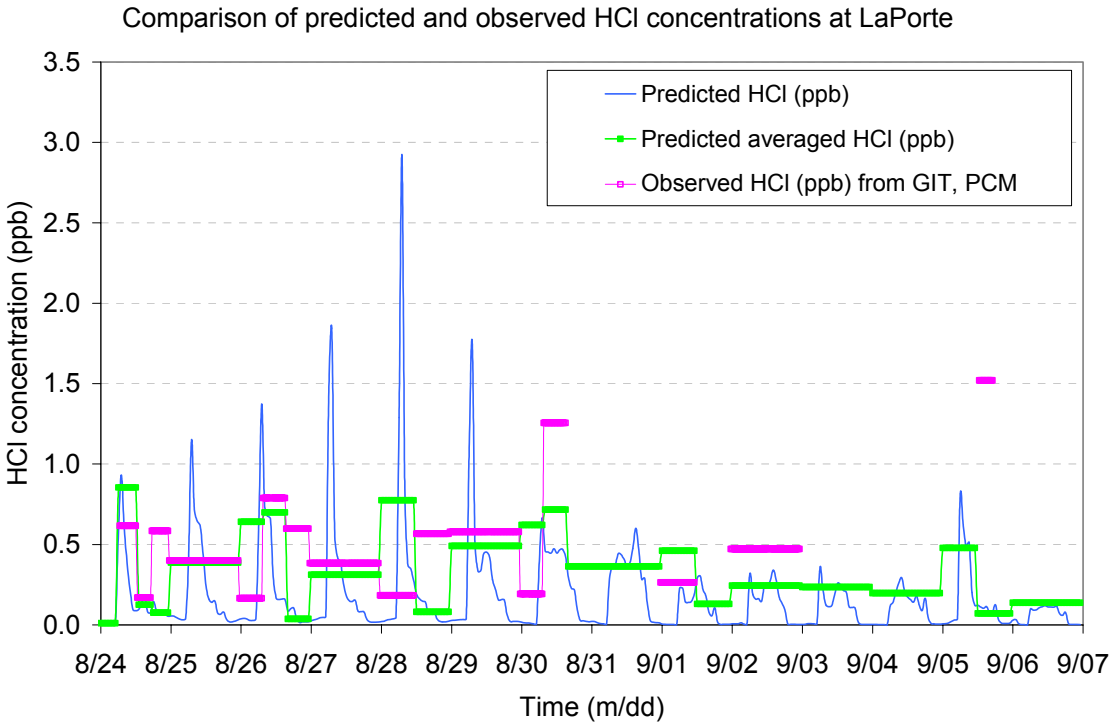

Figure 6.4 Comparison between observed HCl monitored (6-24 hr averages) from GIT's PCM at La Porte and predicted HCl concentration at La Porte (hourly time resolution and average values calculated to correspond to the GIT measurement periods)

In order to examine what the gas-particle partitioning chlorine, observed HCl and observed particle chloride concentrations at La Porte are plotted in Figure 6.5. Both gas and particle concentrations are expressed as ppb (mole basis). On most days, the chlorine remains largely in the gas phase; the exceptions are August 23, which shows a large peak in the concentration of particle chloride from the Aerodyne instrument, and August 30, which shows a large peak in the chloride concentration measured by GIT.

Figure 6.6 shows model predicted HCl and particle chloride (PM2.5) concentrations at each hour at La Porte, and comparisons between predicted and observed particle chloride ($PM_{2.5}$) concentrations at La Porte are shown in Figure 6.7. The model, in general mirrors the observations – little particulate chloride is produced due to the HCl emissions. The model fails to predict some of the largest observed concentrations, however. To determine whether these large concentrations may be due to sea salt, particulate sodium concentrations were examined.

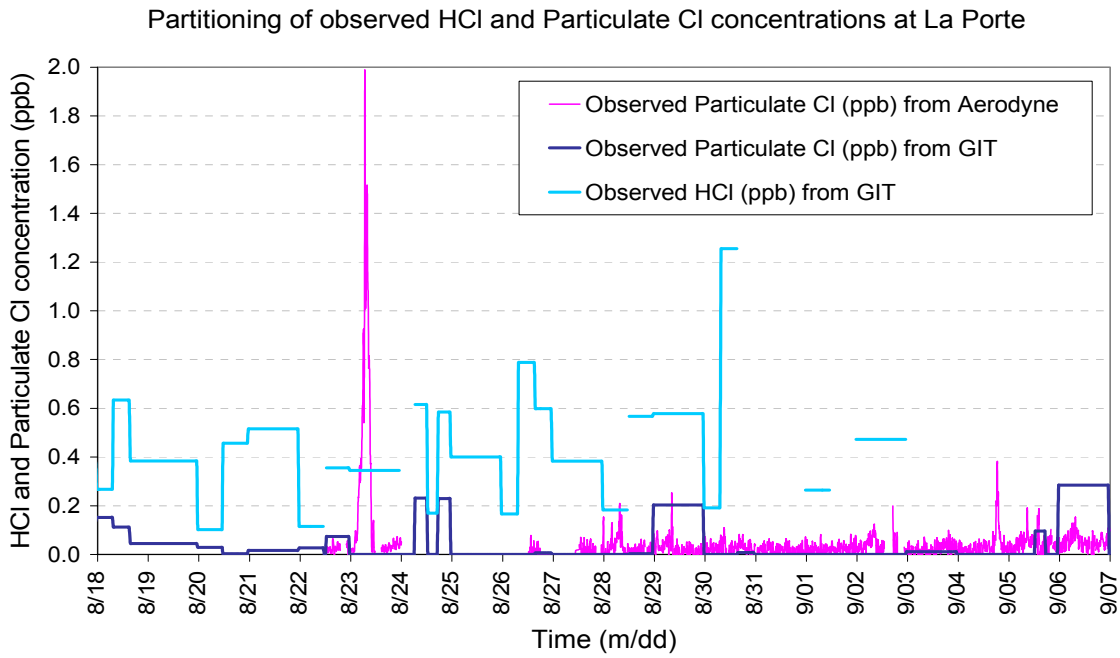

Figure 6.5 Time series of Observed HCl concentration and particle chloride ($PM_{2.5}$) at the equilibrium steady state at each hour at La Porte

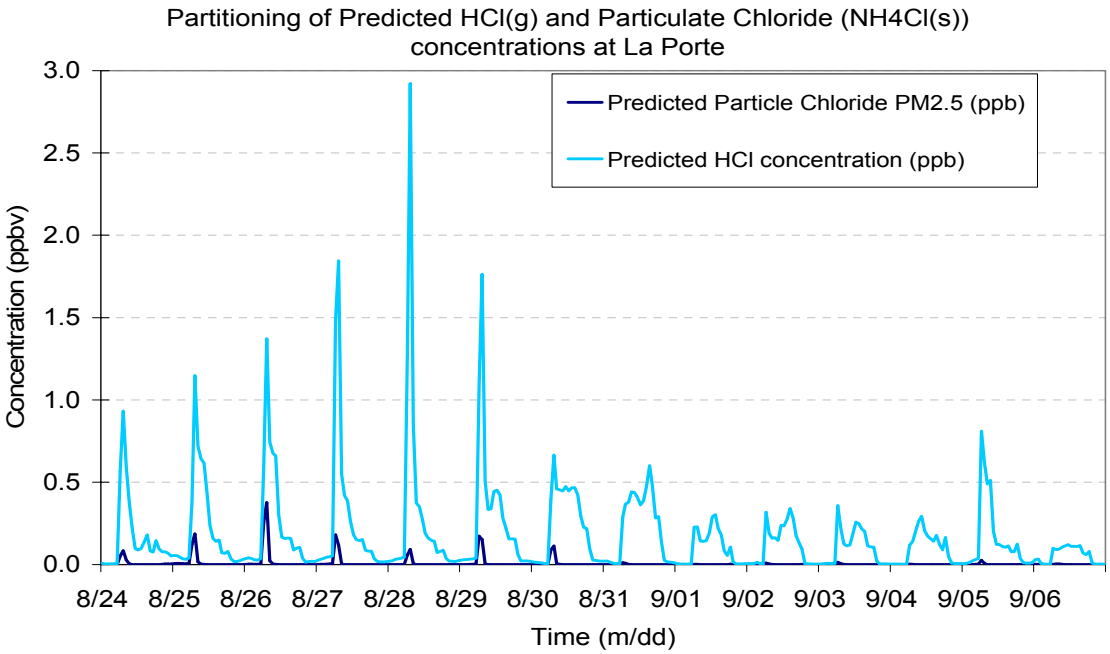

Figure 6.6 Time series of model predicted HCl concentration and particle chloride ($PM_{2.5}$) at the equilibrium steady state at each hour at La Porte

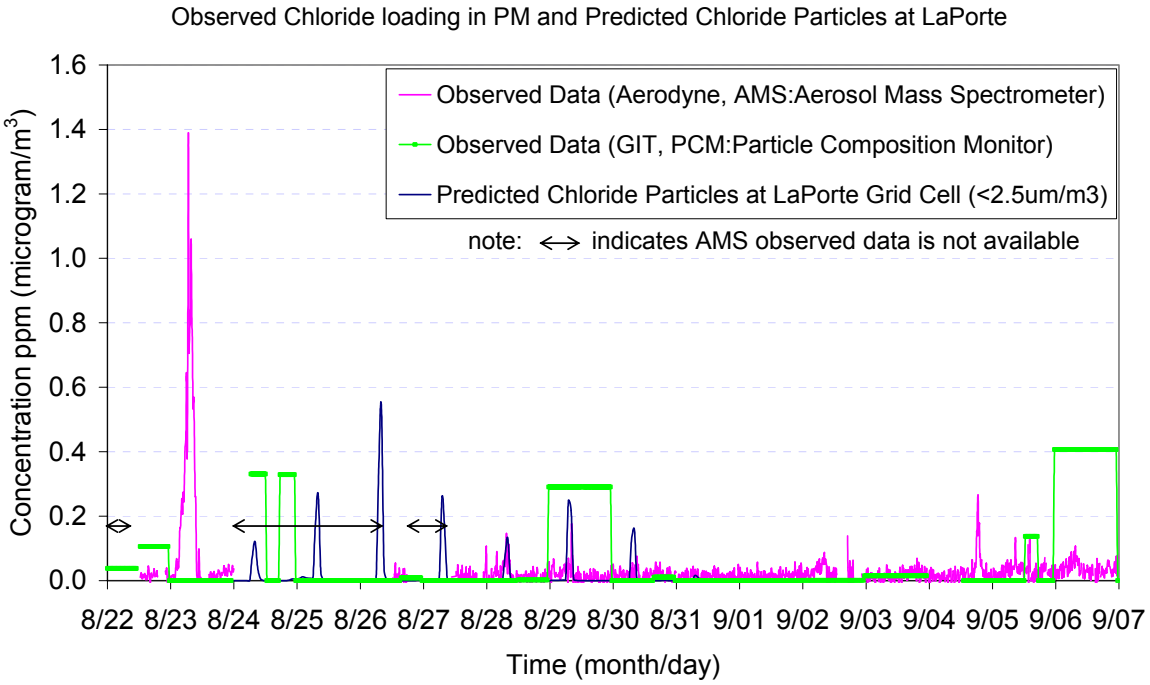

Figure 6.7 Comparison between the predicted particle chloride ($PM_{2.5}$) at La Porte gird cell (4km resolution) and two observed chloride loading in $PM_{2.5}$ from Aerodyne and GIT

6.5 Sodium (Na) composition in Particulate Matter at La Porte

Sodium (Na) is a stable marker of sea salt concentrations, therefore sodium concentrations were examined to determine (1) whether sea salt might explain some of the high particulate chloride concentrations, and (2) whether sea salt (as opposed to anthropogenic chlorine emissions) might contribute to the high HCl concentrations observed in the region.

Figure 6.8 and Figure 6.9 compare the concentrations of sodium and HCl, and the concentrations of sodium and particulate chloride, respectively. Subtracting the molar Na concentration from the molar HCl and particle chloride concentrations provides an estimate of the Cl that originated from anthropogenic chlorine emissions. Observed Na

concentration from Texas Commission on Environmental Quality (TCEQ) (Russell, 2004) is hourly averaged concentration, and the value is less than 0.2 ppb (moles of Na/moles of air) during most days except September 4 through 6. TCEQ oversees the collection of Federal Reference Method (FRM) 24 hr averaged $PM_{2.5}$ mass concentrations, filter-based determinations of $PM_{2.5}$ composition, and near-continuous $PM_{2.5}$ mass concentration data with Tapered Element Oscillating Microbalance (TEOM) samplers. These routine data are reported to EPA and available in the Aerometric Information Retrieval System (AIRS) database (USEPA, 2002; NARSTO, 2005; Russell, 2004). A subset of FRM monitoring sites also measure $PM_{2.5}$ speciation using Partisol – Plus Model 2025 $PM_{2.5}$ Sequential Samplers (Rupprecht & Patashnick Co. Inc.). $PM_{2.5}$ particles are passed in parallel through PTFE (polyterafluoroethylene or Teflon) and quartz fiber filters. Total mass is determined gravimetrically from the PTFE filters. The PTFE filters are also used to quantify mass of chemical elements using Energy Dispersive X-Ray Fluorescence (XRF), and soluble ions using ion chromatography. Detail description of FRM data is found at Russell (2004). Observed averaged Na and HCl concentrations from GIT is approximately 0.19 ppb and 0.42 ppb for August 18 through September 3. Therefore, the observed HCl concentration is 2.2 times higher than observed Na concentration for August 18 through September 3. Since there was fire event for September 4 through 6, these days are ignored for this analysis. Same Na concentration data shown in Figure 6.8 is compared with observed chloride concentration in particulate matters at La Porte as shown in Figure 6.9. If chloride is considered to be lost from the aerosol as the aerosol ages, concentration of chloride and sodium tends to show generally good agreement. Exceptionally, large peak of chloride and little Na concentrations are shown on August 23. It is interpreted that chloride from anthropogenic

HCl emissions contributes to particle chloride formation more than from the seasalt emission.

Besides the La Porte site, Figure 6.10 illustrates Na and Cl concentrations in particulate matter at several CAMS monitoring stations in Houston, Texas (Russell, 2003). Unlike Figure 6.9, TCEQ data from several monitoring sites indicates that chloride concentration in particulate matter is much smaller than Na concentration.

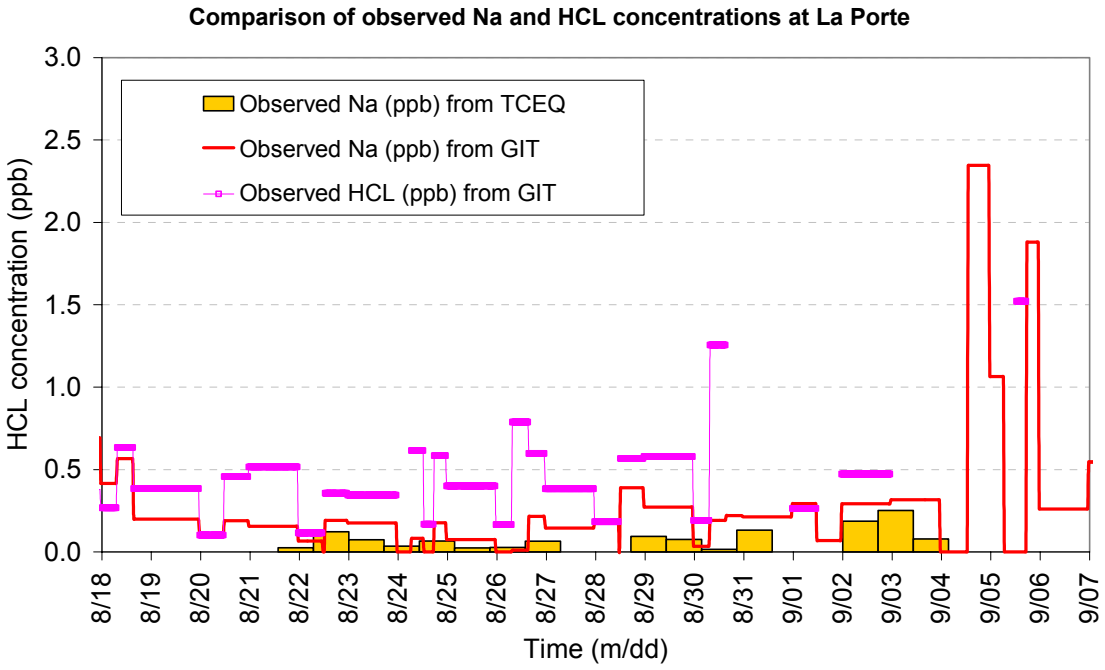

Figure 6.8 Comparison of observed Na and HCl concentrations at La Porte

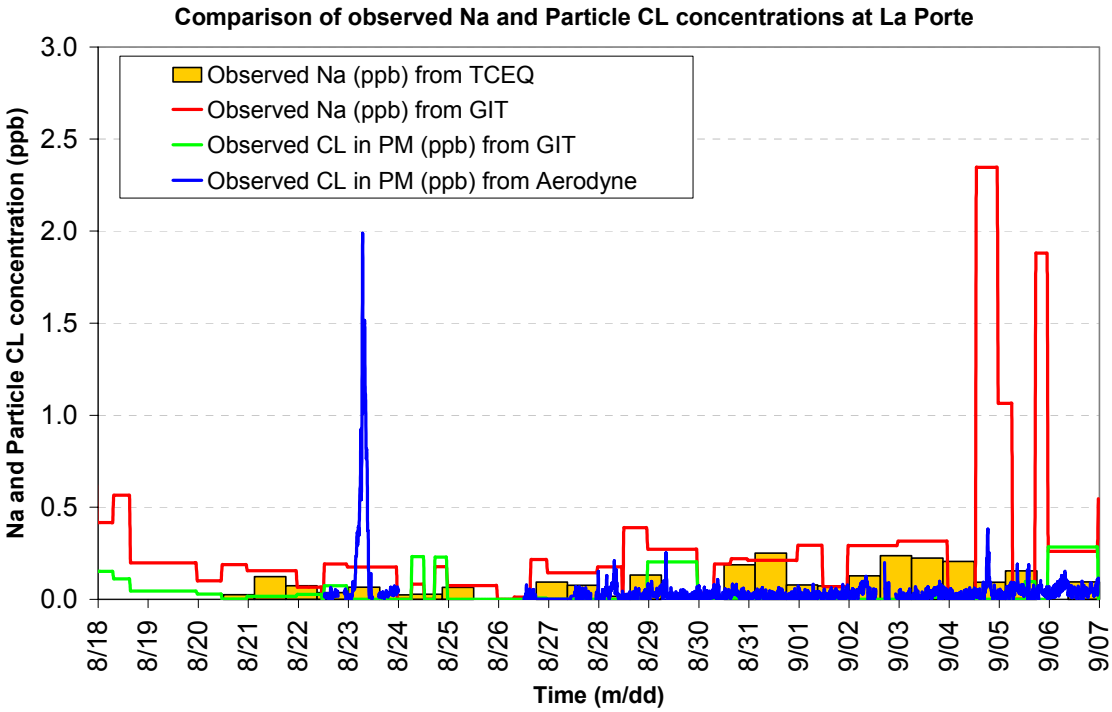

Figure 6.9 Comparison of observed Na and particle chloride concentrations at La Porte

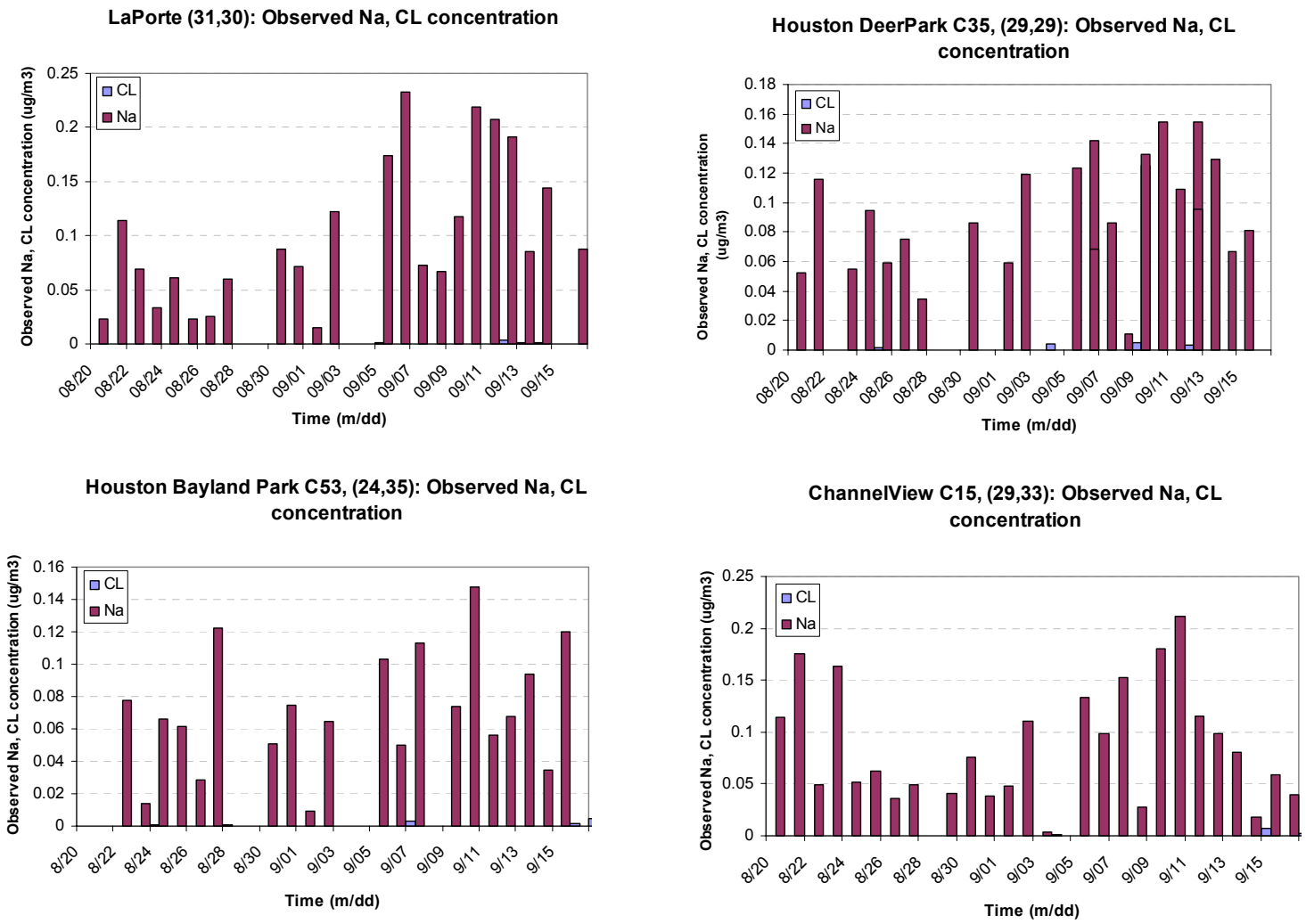

Figure 6.10 Comparison of observed Na and chloride concentrations in PM at CAMS monitoring sites in Houston, TX

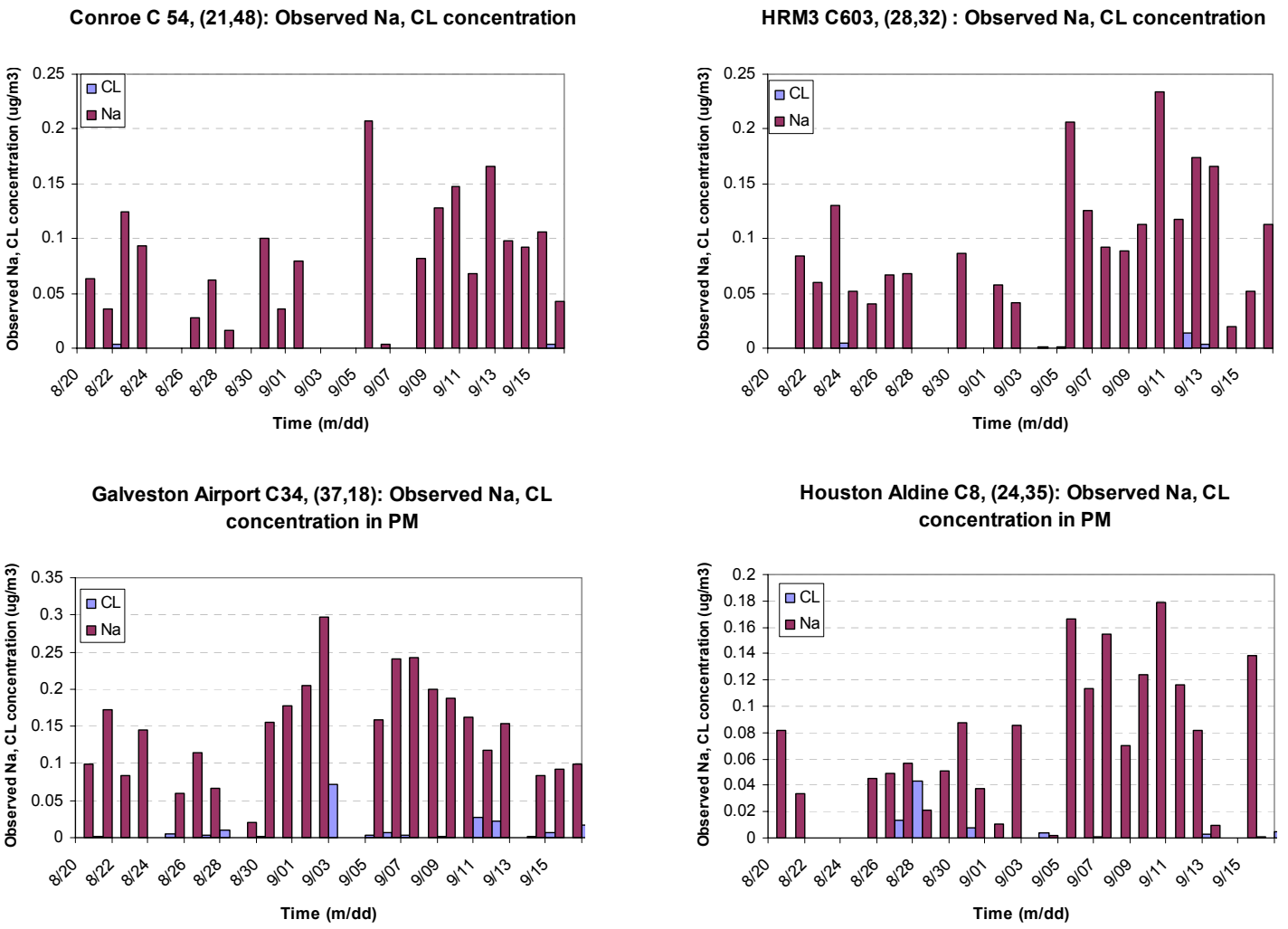

Figure 6.10 (Cont'd) Comparison of observed Na and chloride concentrations in PM at CAMS monitoring sites in Houston, TX

6.6 Competition of chloride, Sulfate, and Nitrate with Ammonia in Formation of Particulate Matter at La Porte

As discussed Section 6.1, HCl competes with nitric and sulfuric acid for available atmospheric ammonia, and therefore the formation of ammonium chloride is strongly affected by whether the atmosphere is ammonia-rich or ammonia-poor. In order to examine how this competition influences particle chloride formation, times series of particulate chemical species concentrations (particle chloride, particle ammonium, particle nitrate, and particle sulfate) at the La Porte grid cell and times series of gaseous chemical species concentrations (hydrochloric acid, nitric acid, ammonia, and sulfate/ sulfuric acid) at the La Porte grid cell were examined. The data are shown in Figures 6.11 and 6.12. The time series show that ammonium chloride only forms when there is an exceess of ammonia and ammonium nitrate concentrations are relatively high. For example, the mornings of August 25, 26, and 27 (Figures 6.13 and 6.14) show ammonia-rich conditions; high concentrations of particle nitrate and particle chloride are created in the morning, since sulfate concentrations are relatively low. In the afternoons of August 25, 26, and 27, as sulfate concentrations increase, both particulate nitrate and particulate chloride show very low concentrations. After August 31, ammonia-poor conditions occurred in both the mornings and the afternoons (Figure 6.15 and 6.16). For these days, very little particle chloride and particle nitrate are created.

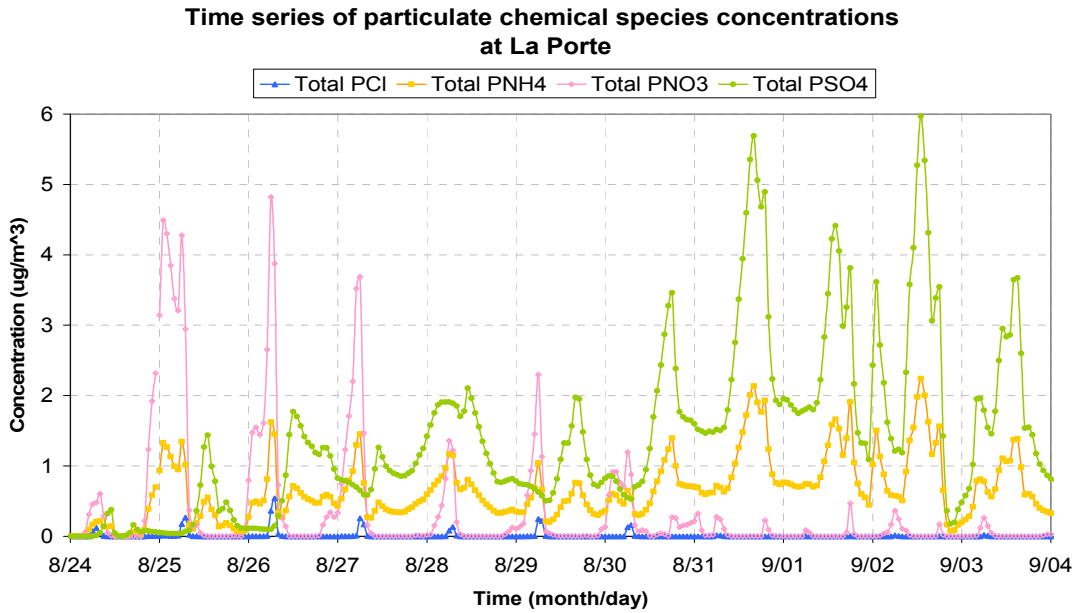

Figure 6.11 Times series of particulate chemical species concentrations such as particle chloride (PCl), particle ammonium (PNH_4), particle nitrate (PNO_3), and particle sulfate (PSO_4) at La Porte grid cell

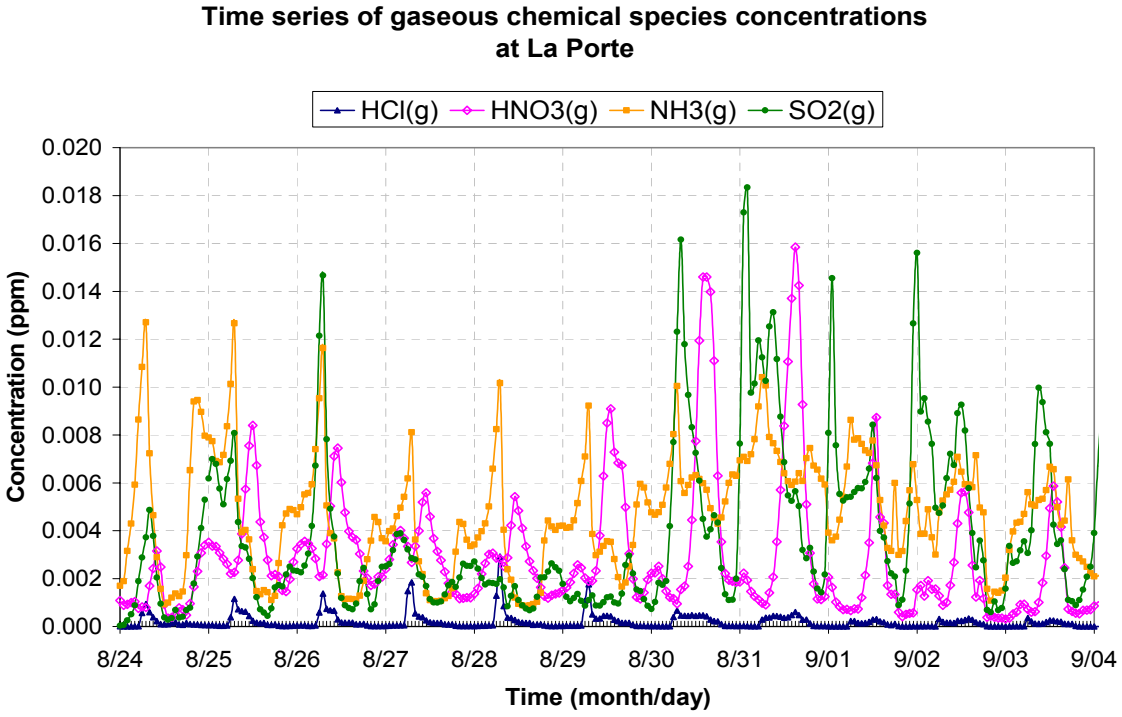

Figure 6.12 Times series of gaseous chemical species concentrations such as hydrochloric acid (HCl), nitric acid (HNO_3), ammonia (NH_3), and sulfate (SO_2) at La Porte grid cell

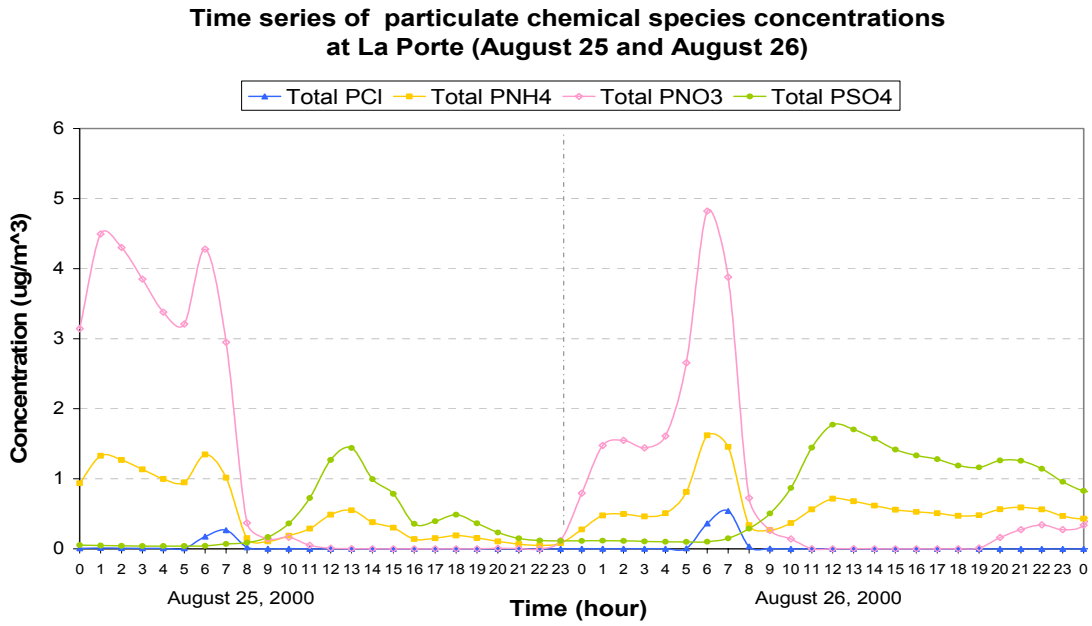

Figure 6.13 Times series of particulate chemical species concentrations such as particle chloride (PCl), particle ammonium (PNH_4), particle nitrate (PNO_3), and particle sulfate (PSO_4) on August 25 and August 26 at La Porte grid cell

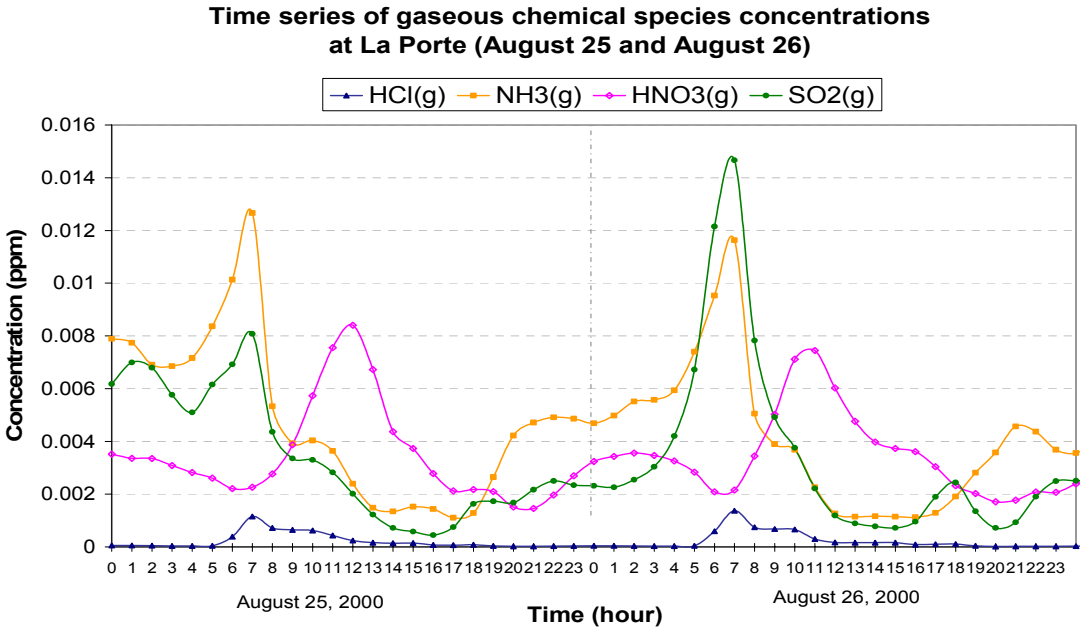

Figure 6.14 Times series of gaseous chemical species concentrations such as hydrochloric acid (HCl), nitric acid (HNO_3), ammonia (NH_3), and sulfate (SO_2) on August 25 and August 26 at La Porte grid cell

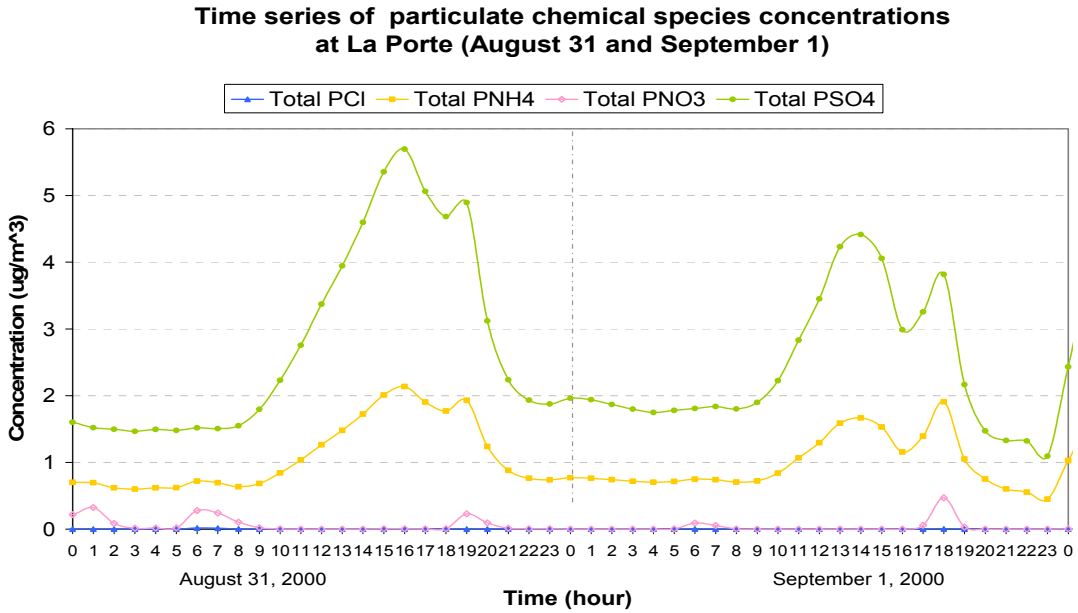

Figure 6.15 Times series of particulate chemical species concentrations such as particle chloride (PCl), particle ammonium (PNH_4), particle nitrate (PNO_3), and particle sulfate (PSO_4) on August 31 and September 1 at La Porte grid cell

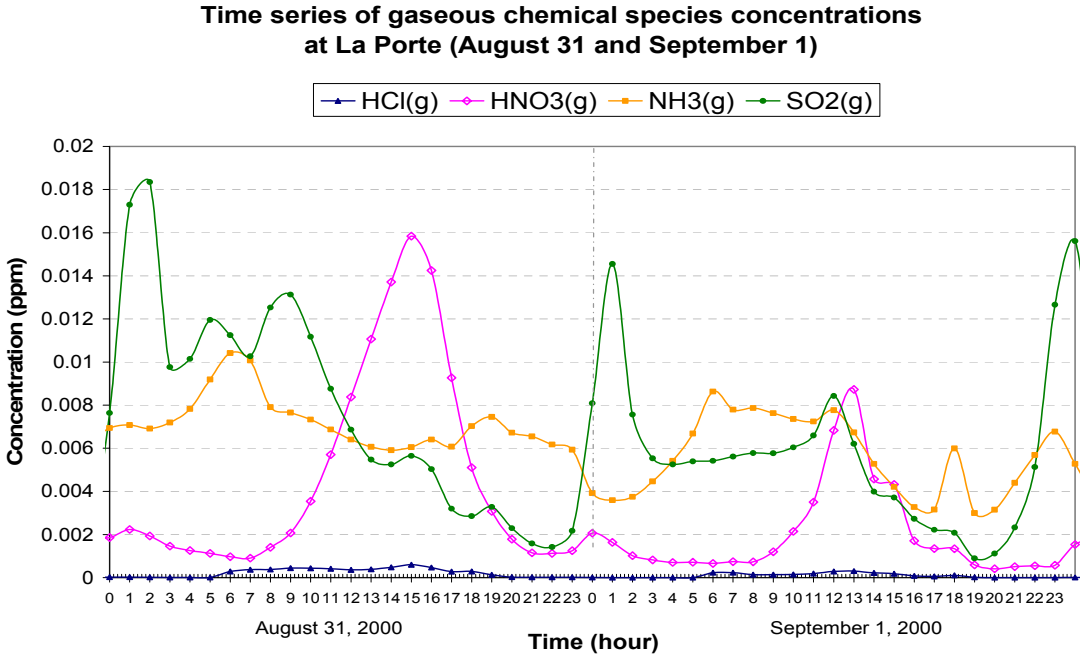

Figure 6.16 Times series of gaseous chemical species concentrations such as hydrochloric acid (HCl), nitric acid (HNO_3), ammonia (NH_3), and sulfate (SO_2) on August 31 and September 1 at La Porte grid cell

6.7 Competition of chloride, Sulfate, and Nitrate with Ammonia in Formation of Particulate Matter at the Grid Cell Where Maximum Predicted Particulate Chloride is Occurred During the Entire Episode

The maximum predicted total particle chloride occurred near the Ship Channel (grid cell number (32, 31) based on 4km resolution) with the values of 8.9 $\mu g/m^3$ at 0600 on August 26. This magnitude of particle chloride indicates maximum impact of chlorine emissions on particulate matter formation in southeast Texas.

In order to examine how this competition influences particle chloride formation, times series of particulate chemical species concentrations (particle chloride, particle ammonium, particle nitrate, and particle sulfate) at the (32, 31) grid cell and times series of gaseous chemical species concentrations (hydrochloric acid, nitric acid, ammonia, and sulfate/ sulfuric acid) at the same grid cell were examined. The data are shown in Figures 6.17 and 6.18. Details of August 26 and 25 (the most and second largest peaks were occurred) are shown in Figures 6.19 and 6.20.

The large peaks of particle chloride are occurred on August 25 and 26 because there is enough excess of ammonia and ammonium nitrate concentration to react with chloride. The trend of particle ammonium follows a trend of particle chloride on those days. However, the particle chloride created on August 27 and 28 is less than August 25 and 26 although August 27 and 28 have more sufficient ammonia concentration and less sulfate concentration than August 25 and 26 have. Therefore, the time series of August 27 and 28 indicates that only the ratio of ammonia and sulfate cannot explain driving force of formation of particle chloride because August 27 and 28 have more sufficient ammonia concentration and less sulfate concentration than August 25 and 26 have.

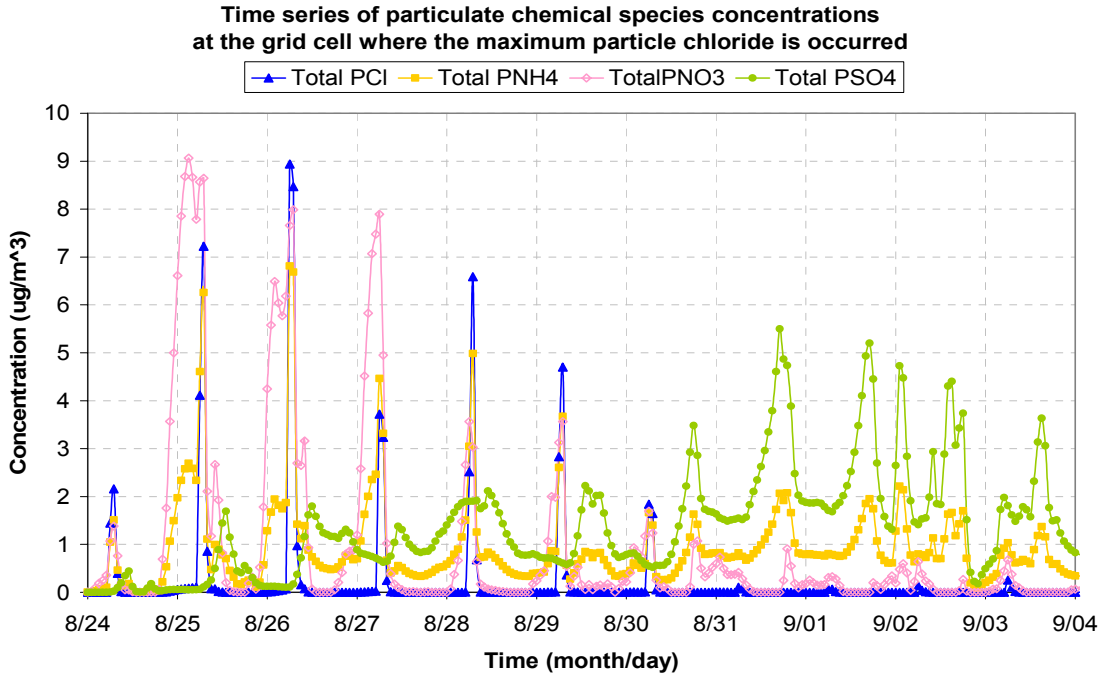

Figure 6.17 Time series of particulate chemical species concentrations at the grid cell where the maximum particle chloride is occurred

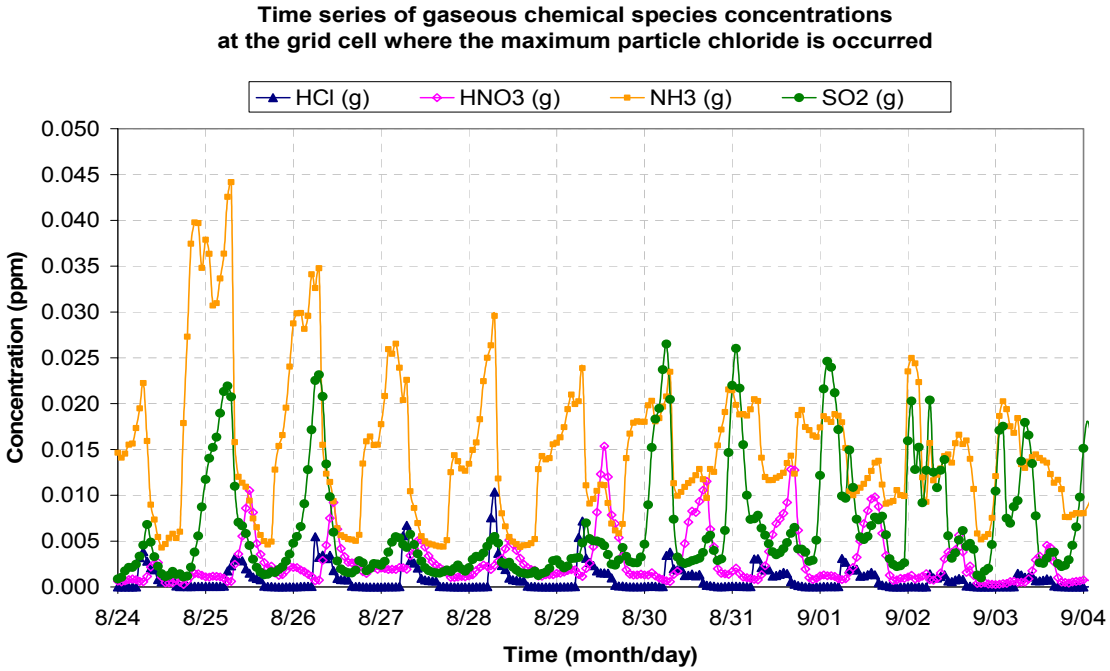

Figure 6.18 Time series of gaseous chemical species concentrations at the grid cell where the maximum particle chloride is occurred

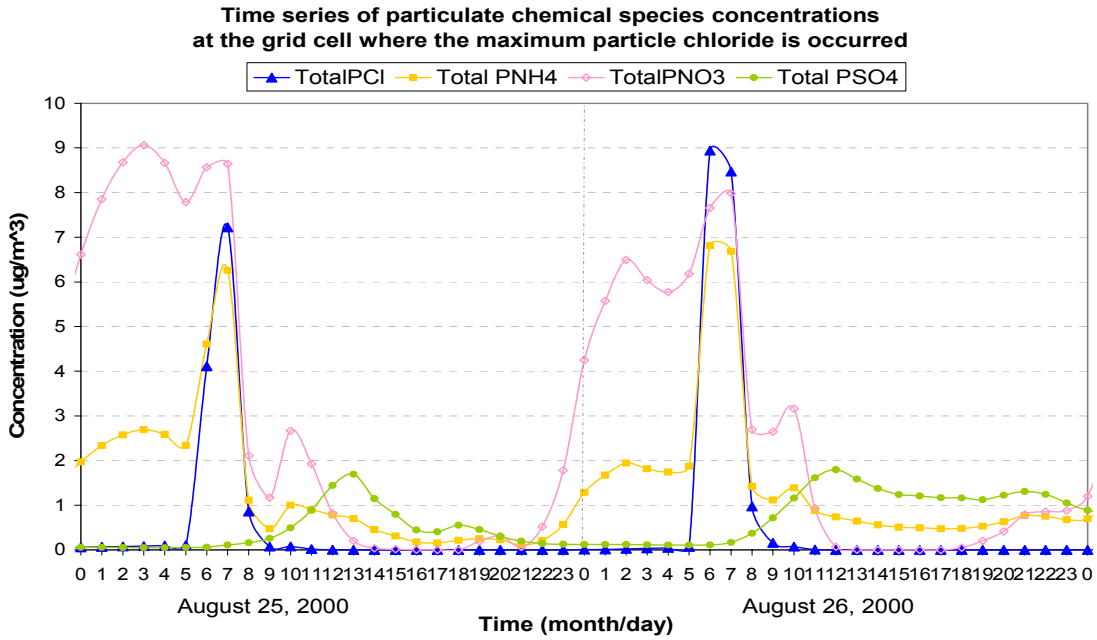

Figure 6.19 Time series of particulate chemical species concentrations on August 25 and 26 at the grid cell where the maximum particle chloride is occurred

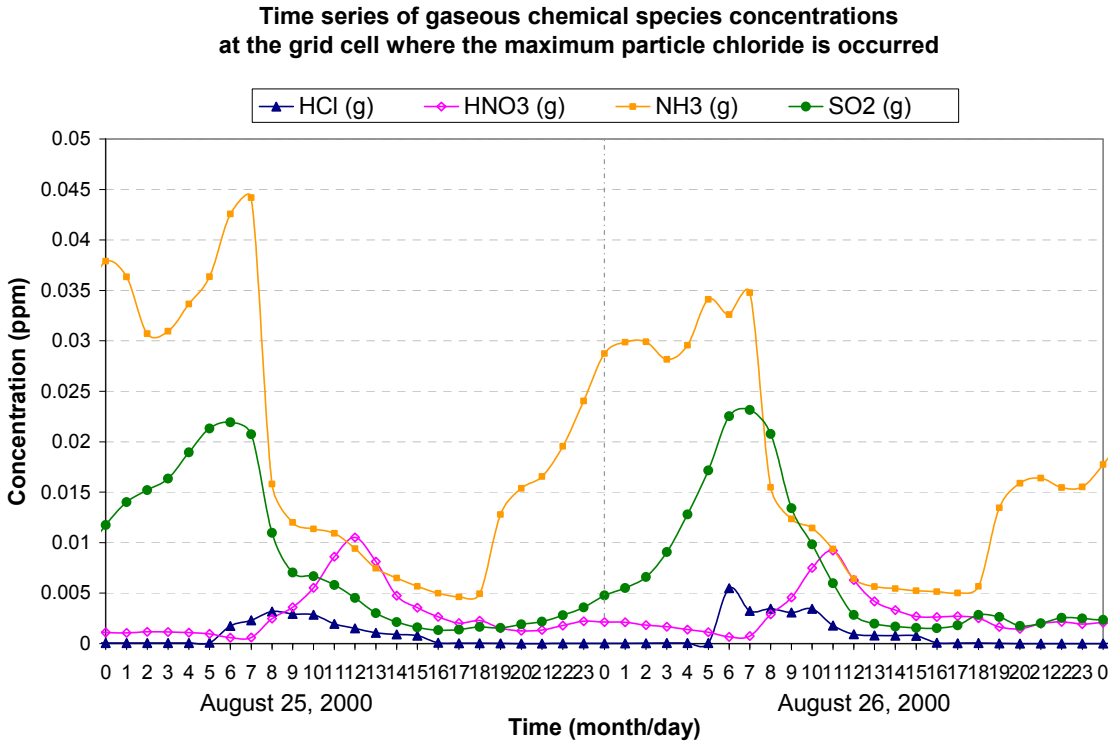

Figure 6.20 Time series of gaseous chemical species concentrations on August 25 and 26 at the grid cell where the maximum particle chloride is occurred

Chapter 7: Conclusions and Recommendations

The objectives of this thesis were to examine whether anthropogenic chlorine emissions estimates play a major role in ozone and particulate matter formation and whether chlorine emissions influence the relative effectiveness of ozone control strategies in the Houston/Galveston area.

The major findings of this study include the following:

1. Chlorine emissions have a significant effect on ozone formation in Houston/Galveston area. Chlorine chemistry has the potential to enhance 1-hour averaged ozone mixing ratios by up to 10-72 ppbv in the industrial areas of Houston in the morning and by 5-12 ppbv within and north of the Houston urban area in the afternoon, based on the current emission inventory. Chlorine chemistry has the potential to enhance 8-hour averaged ozone mixing ratio by up to 7-21 ppbv in the industrial areas of Houston.
2. Emissions of atomic chlorine precursors in southeast Texas are approximately 10 tons/day, although considerable uncertainty remains about the exact magnitude, spatial distribution and temporal distribution of the emissions. Comparisons of predicted and measured concentrations of molecular markers of chlorine chemistry (CMBO) suggest that chlorine emission estimates developed in this work may be low. CMBO formation is very dependent on the location of emission sources; however, and therefore insufficient data are available to perform emission adjustments.
3. Different sources of chlorine emissions have different effects on ozone formation. Cooling towers were primarily responsible for the morning enhancements in ozone mixing ratios, while swimming pools were responsible for the afternoon

enhancements. Chlorine emissions from cooling towers had the largest impacts on both 1-hour and 8-hour averaged ozone mixing ratios in the region. Peak ozone enhancements, associated with doubling chlorine emissions from cooling towers is 42 ppbv (1- hour averaged) and 19 ppbv (8-hour averaged).

4. By determining peak ozone enhancements due to chlorine emissions at a variety of VOC and NO_x emission levels, it was demonstrated that adding chlorine chemistry and emissions necessitates a 2-5 percent increase in the level of VOC and NO_x emission reductions required to achieve 1-hour and 8-hour averaged maximum ozone concentrations that achieve the NAAQS.
5. The maximum predicted particle chloride concentrations, due to anthropogenic chlorine emissions, occurred near the Ship Channel, and the values varied from 0.1 $\mu g/m^3$ to 9 $\mu g/m^3$
6. Anthropogenic chlorine emissions contribute to high HCl concentrations observed in the La Porte region and to particle chloride formation more than sea salt emissions.

The following studies are recommended:

1. Reducing uncertainties associated with emission estimates from cooling towers and swimming pools should be focal points of future research. Future studies should specifically address (1) characterization of the spatial distribution of cooling towers and identification of facility practices associated with chlorination, and (2) improvement in spatial surrogates for residential pools and quantification of the rate of chlorine volatilization.
2. In order to examine the accuracy of the chlorine emission inventory, CMBO measurements should be conducted in the areas where chlorine emissions are

predicted, and a more accurate isoprene emission inventory needs to be established.

3. Gas phase chlorine chemical mechanism and aerosol chlorine chemical mechanism should be merged and incorporated into the regional photochemical 3-D model in order to predict the impact of molecular chlorine emissions on both ozone and particle chloride formation.
4. Night-time chlorine chemistry should be studied to assess whether the chlorine emissions are stored as reservoir species or whether they are converted to unreactive forms at night.

Appendix A

Chemical Mechanism and Chemical Parameters

Table A-1 Gas Phase Chlorine Chemical Mechanism (Chemical Mechanism 1)
: CB4 with reactive chlorine chemistry, 110 reactions and 48 species (34 state gasses and 14 radicals)

1	NO2			=	1	NO	1	O			
2	O			=	1	O3					
3	O3	NO		=	1	NO2					
4	O	NO2		=	1	NO					
5	O	NO2		=	1	NO3					
6	O	NO		=	1	NO2					
7	NO2	O3		=	1	NO3					
8	O3			=	1	O					
9	O3			=	1	O1D					
10	O1D			=	1	O					
11	O1D	H2O		=	2	OH					
12	O3	OH		=	1	HO2					
13	O3	HO2		=	1	OH					
14	NO3			=	0.89	NO2	0.89	O	0.11	NO	
15	NO3	NO		=	2	NO2					
16	NO3	NO2		=	1	NO	1	NO2			
17	NO3	NO2		=	1	N2O5					
18	N2O5	H2O		=	2	HNO3					
19	N2O5			=	1	NO3	1	NO2			
20	NO	NO		=	2	NO2					
21	NO	NO2	H2O	=	2	HONO					
22	NO	OH		=	1	HONO					
23	HONO			=	1	NO	1	OH			
24	OH	HONO		=	1	NO2					
25	HONO	HONO		=	1	NO	1	NO2			
26	NO2	OH		=	1	HNO3					
27	OH	HNO3		=	1	NO3					
28	HO2	NO		=	1	OH	1	NO2			
29	HO2	NO2		=	1	PNA					
30	PNA			=	1	HO2	1	NO2			
31	OH	PNA		=	1	NO2					
32	HO2	HO2		=	1	H2O2					
33	HO2	HO2	H2O	=	1	H2O2					
34	H2O2			=	2	OH					
35	OH	H2O2		=	1	HO2					
36	OH	CO		=	1	HO2					
37	FORM	OH		=	1	HO2	1	CO			
38	FORM			=	2	HO2	1	CO			
39	FORM			=	1	CO					
40	FORM	O		=	1	OH	1	HO2	1	CO	
41	FORM	NO3		=	1	HNO3	1	HO2	1	CO	
42	ALD2	O		=	1	C2O3	1	OH			

43	ALD2	OH	=	1	C2O3					
44	ALD2	NO3	=	1	C2O3	1	HNO3			
45	ALD2		=	1	FORM	2	HO2	1	CO	
				1	XO2					
46	C2O3	NO	=	1	FORM	1	NO2	1	HO2	
				1	XO2					
47	C2O3	NO2	=	1	PAN					
48	PAN		=	1	C2O3	1	NO2			
49	C2O3	C2O3	=	2	FORM	2	XO2	2	HO2	
50	C2O3	HO2	=	0.79	FORM	0.79	XO2	0.79	HO2	
				0.79	OH					
51	OH		=	1	FORM	1	XO2	1	HO2	
52	PAR	OH	=	0.87	XO2	0.13	XO2N	0.11	HO2	
				0.11	ALD2	-0.11	PAR	0.76	ROR	
53	ROR		=	0.96	XO2	1.1	ALD2	0.94	HO2	
				-2.1	PAR	0.04	XO2N			
54	ROR		=	1	HO2					
55	ROR	NO2	=	1	NTR					
56	O	OLE	=	0.63	ALD2	0.38	HO2	0.28	XO2	
				0.3	CO	0.2	FORM	0.02	XO2N	
				0.22	PAR	0.2	OH			
57	OH	OLE	=	1	FORM	1	ALD2	-1	PAR	
				1	XO2	1	HO2			
58	O3	OLE	=	0.5	ALD2	0.74	FORM	0.22	XO2	
				0.1	OH	0.33	CO	0.44	HO2	
				-1	PAR					
59	NO3	OLE	=	0.91	XO2	1	FORM	0.09	XO2N	
				1	ALD2	1	NO2	-1	PAR	
60	O	ETH	=	1	FORM	1.7	HO2	1	CO	
				0.7	XO2	0.3	OH			
61	OH	ETH	=	1	XO2	1.56	FORM	0.22	ALD2	
				1	HO2					
62	O3	ETH	=	1	FORM	0.42	CO	0.12	HO2	
63	TOL	OH	=	0.44	HO2	0.08	XO2	0.36	CRES	
				0.56	TO2					
64	TO2	NO	=	0.9	NO2	0.9	HO2	0.9	OPEN	
				0.1	NTR					
65	TO2		=	1	CRES	1	HO2			
66	OH	CRES	=	0.4	CRO	0.6	XO2	0.6	HO2	
				0.3	OPEN					
67	CRES	NO3	=	1	CRO	1	HNO3			
68	CRO	NO2	=	1	NTR					
69	OPEN		=	1	C2O3	1	HO2	1	CO	
70	OPEN	OH	=	1	XO2	2	CO	2	HO2	
				1	C2O3	1	FORM			
71	OPEN	O3	=	0.03	ALD2	0.62	C2O3	0.7	FORM	
				0.03	XO2	0.69	CO	0.08	OH	

				0.76	HO2	0.2	MGLY			
72	OH	XYL	=	0.7	HO2	0.5	XO2	0.2	CRES	
				0.8	MGLY	1.1	PAR	0.3	TO2	
73	OH	MGLY	=	1	XO2	1	C2O3			
74	MGLY		=	1	C2O3	1	HO2	1	CO	
75	O	ISOP	=	0.75	ISPD	0.5	FORM	0.25	XO2	
				0.25	HO2	0.25	C2O3	0.25	PAR	
76	OH	ISOP	=	0.912	ISPD	0.629	FORM	0.991	XO2	
				0.912	HO2	0.088	XO2N			
77	O3	ISOP	=	0.65	ISPD	0.6	FORM	0.2	XO2	
				0.066	HO2	0.266	OH	0.2	C2O3	
				0.15	ALD2	0.35	PAR	0.066	CO	
78	NO3	ISOP	=	0.2	ISPD	0.8	NTR	1	XO2	
				0.8	HO2	0.2	NO2	0.8	ALD2	
				2.4	PAR					
79	XO2	NO	=	1	NO2					
80	XO2	XO2	=							
81	XO2N	NO	=	1	NTR					
82	SO2	OH	=	1	SULF	1	HO2			
83	SO2		=	1	SULF					
84	MEOH	OH	=	1	FORM	1	HO2			
85	ETOH	OH	=	1	HO2	1	ALD2			
86	XO2	HO2	=							
87	XO2N	HO2	=							
88	XO2N	XO2N	=							
89	XO2	XO2N	=							
90	OH	HO2	=							
91	CRO		=							
92	OH	ISPD	=	1.565	PAR	0.167	FORM	0.713	XO2	
				0.503	HO2	0.334	CO	0.168	MGLY	
				0.273	ALD2	0.498	C2O3			
93	O3	ISPD	=	0.114	C2O3	0.15	FORM	0.85	MGLY	
				0.154	HO2	0.268	OH	0.064	XO2	
				0.02	ALD2	0.36	PAR	0.225	CO	
94	NO3	ISPD	=	0.357	ALD2	0.282	FORM	1.282	PAR	
				0.925	HO2	0.643	CO	0.85	NTR	
				0.075	C2O3	0.075	XO2	0.15	HNO3	
95	ISPD		=	0.333	CO	0.067	ALD2	0.9	FORM	
				0.832	PAR	1.033	HO2	0.7	XO2	
				0.967	C2O3					
96	NO2	ISOP	=	0.2	ISPD	0.8	NTR	1	XO2	
				0.8	HO2	0.2	NO	0.8	ALD2	
				2.4	PAR					
97	CL2		=	2	CL					
98	HOCL		=	1	OH	1	CL			
99	CL	O3	=	1	CLO	1	O2			
100	CLO	NO	=	1	CL	1	NO2			

101	CLO	HO2	=	1	HOCL	1	O2			
102	CL	PAR	=	1	HCL	0.87	XO2	0.13	XO2N	
				0.11	RCHO	0.76	ROR	-0.11	PAR	
103	CL	OLE	=	1	FMCL	1	RCHO	2	XO2	
				1	HO2	-1	PAR			
104	CL		=	1	HCL	1	XO2	1	FORM	
				1	HO2					
105	CL	ETH	=	1	FORM	2	XO2	1	FMCL	
				1	HO2					
106	CL	ISOP	=	0.15	HCL	1	XO2	1	HO2	
				0.28	ICL1					
107	OH	ICL1	=	1	ICL2					
108	CL	BUTA	=	1	XO2	1	HO2	0.7	BCL1	
109	OH	BCL1	=	1	BCL2					
110	CLO	CLO	=	0.3	CL2	1.4	CL			

Table A-2 Gas Phase Chlorine Chemical Parameters (Chemparam 1)

```
CAMx Version       |VERSION4.0
Mechanism ID       |1
Description        |CB4 (mechanism 3) with chlorine chemistry
No of gas species  |34
No of aero species |0
No of reactions    |110
Prim photo rxns    |6 1 38 39 9 45 95
No of sec photo rxn|8
ID, prim ID, scale | 8  1  0.053
                   |14  1 33.9
                   |23  1  0.1975
                   |34 39  0.189
                   |69 38  9.04
                   |74 38  9.64
                   |97  1   0.264
                   |98 95 143.0
```

Species Records

	Gas Spec	lower bnd	H-law	T-fact	Diffrat	Reactvty	Rscale
1	NO	1.00E-15	1.90e-03	-1480.	1.29	0.0	1.
2	NO2	1.00E-09	1.00e-02	-2516.	1.60	0.1	1.
3	O3	1.00E-09	1.10e-02	-2415.	1.63	1.0	1.
4	PAN	1.00E-09	3.60e+00	-5910.	2.59	0.1	1.
5	NXOY	1.00E-12	3.20e+04	-8706.	2.45	0.1	0.
6	OLE	1.00E-09	5.00e-03	0.	1.80	0.0	1.
7	PAR	1.00E-04	1.00e-03	0.	2.00	0.0	1.
8	TOL	1.00E-09	1.20e+00	0.	2.26	0.0	1.
9	XYL	1.00E-09	1.40e+00	0.	2.43	0.0	1.
10	FORM	1.00E-09	6.30e+03	-6492.	1.29	0.0	1.
11	ALD2	1.00E-09	6.30e+03	-6492.	1.56	0.0	1.
12	ETH	1.00E-09	1.00e-02	0.	1.25	0.0	1.
13	CRES	1.00E-09	2.70e+03	-6492.	2.45	0.0	1.
14	MGLY	1.00E-09	2.70e+03	-6492.	2.00	0.0	1.
15	OPEN	1.00E-12	2.70e+03	-6492.	2.47	0.0	1.
16	PNA	1.00E-09	2.00e+04	-5910.	2.09	0.0	1.
17	CO	1.00E-04	1.00e-10	0.	1.25	0.0	1.
18	HONO	1.00E-09	5.90e+01	-4781.	1.62	0.1	1.
19	H2O2	1.00E-09	7.40e+04	-6643.	1.37	1.0	1.
20	HNO3	1.00E-09	2.00e+05	-8707.	1.87	0.0	0.
21	ISOP	1.00E-09	1.00e-02	0.	1.94	0.0	1.
22	MEOH	1.00E-09	2.20e+02	-4932.	1.33	0.0	1.
23	ETOH	1.00E-09	2.20e+02	-4932.	1.60	0.0	1.
24	ISPD	1.00E-09	6.30e+03	-6492.	1.97	0.0	1.
25	NTR	1.00E-09	9.40e+03	-8706.	2.72	0.0	1.
26	CL2	1.00E-15	1.82e-02	0.	1.98	0.0	1.

27	HOCL	1.00E-12	6.62e+02	0.	1.71	0.0	1.
28	FMCL	1.00E-12	1.50e+01	0.	1.89	0.0	1.
29	HCL	1.00E-12	4.72e+01	0.	1.42	0.0	0.
30	ICL1	1.00E-12	1.50e+01	0.	2.09	0.0	1.
31	ICL2	1.00E-12	1.50e+01	0.	2.09	0.0	1.
32	BUTA	1.00E-12	1.00e-02	0.	1.73	0.0	1.
33	BCL1	1.00E-12	1.50e+01	0.	2.41	0.0	1.
34	BCL2	1.00E-12	1.50e+01	0.	2.41	0.0	1.

Reaction Records

Rxn	Typ	Order	Parameters (1 to 12, depending upon Typ)	
1	1	1	0.0000E+00	
2	2	2	4.3233E+06	-1.1750E+03
3	2	2	2.6640E+01	1.3700E+03
4	1	2	1.3750E+04	
5	2	2	2.3090E+03	-6.8700E+02
6	2	2	2.4380E+03	-6.0200E+02
7	2	2	4.7310E-02	2.4500E+03
8	1	1	0.0000E+00	
9	1	1	0.0000E+00	
10	2	2	4.2500E+10	-3.9000E+02
11	1	2	3.2600E+05	
12	2	2	1.0000E+02	9.4000E+02
13	2	2	2.9990E+00	5.8000E+02
14	1	1	0.0000E+00	
15	2	2	4.4167E+04	-2.5000E+02
16	2	2	5.9010E-01	1.2300E+03
17	2	2	1.8530E+03	-2.5600E+02
18	1	2	1.9000E-06	
19	2	1	2.7760E+00	1.0897E+04
20	2	2	1.5390E-04	-5.3000E+02
21	1	3	1.6000E-11	
22	2	2	9.7990E+03	-8.0600E+02
23	1	1	0.0000E+00	
24	1	2	9.7700E+03	
25	1	2	1.5000E-05	
26	2	2	1.6817E+04	-7.1300E+02
27	2	2	2.1790E+02	-1.0000E+03
28	2	2	1.2270E+04	-2.4000E+02
29	1	2	0.0000E+00	
30	1	1	0.0000E+00	
31	1	1	0.0000E+00	
32	2	2	4.1440E+03	-1.1500E+03
33	2	3	2.1810E-01	-5.8000E+03
34	1	1	0.0000E+00	
35	2	2	2.5200E+03	1.8700E+02
36	1	2	3.2200E+02	
37	1	2	1.5000E+04	

38	1	1	0.0000E+00	
39	1	1	0.0000E+00	
40	2	2	2.3700E+02	1.5500E+03
41	1	2	9.3000E-01	
42	2	2	6.3600E+02	9.8600E+02
43	2	2	2.4000E+04	-2.5000E+02
44	1	2	3.7000E+00	
45	1	1	0.0000E+00	
46	2	2	2.8200E+04	1.8000E+02
47	2	2	1.3700E+04	-3.8000E+02
48	2	1	2.5400E-02	1.3500E+04
49	1	2	3.7000E+03	
50	1	2	9.6000E+03	
51	2	1	2.1000E+01	1.7100E+03
52	1	2	1.2030E+03	
53	2	1	1.3710E+05	8.0000E+03
54	1	1	9.5450E+04	
55	1	2	2.2000E+04	
56	2	2	5.9200E+03	3.2400E+02
57	2	2	4.2000E+04	-5.0400E+02
58	2	2	1.8000E-02	2.1050E+03
59	1	2	1.1350E+01	
60	2	2	1.0800E+03	7.9200E+02
61	2	2	1.1920E+04	-4.1100E+02
62	2	2	2.7000E-03	2.6330E+03
63	2	2	9.1500E+03	-3.2200E+02
64	1	2	1.2000E+04	
65	1	1	2.5000E+02	
66	1	2	6.1000E+04	
67	1	2	3.2500E+04	
68	1	2	2.0000E+04	
69	1	1	0.0000E+00	
70	1	2	4.4000E+04	
71	2	2	1.5000E-02	5.0000E+02
72	2	2	3.6200E+04	-1.1600E+02
73	1	2	2.6000E+04	
74	1	1	0.0000E+00	
75	1	2	5.3200E+04	
76	1	2	1.4760E+05	
77	1	2	1.9000E-02	
78	1	2	9.9600E+02	
79	1	2	1.2000E+04	
80	2	2	2.0000E+03	-1.3000E+03
81	1	2	1.2000E+04	
82	2	2	1.1100E+03	-1.6000E+02
83	1	1	8.1667E-05	
84	1	2	1.6000E+03	

85	2	2	4.3000E+03	-1.7600E+02		
86	2	2	8.9000E+03	-1.3000E+03		
87	2	2	8.9000E+03	-1.3000E+03		
88	2	2	2.0000E+03	-1.3000E+03		
89	2	2	4.0000E+03	-1.3000E+03		
90	2	2	1.6260E+05	-2.5000E+02		
91	1	1	2.7778E-04			
92	1	2	4.9667E+04			
93	1	2	1.0500E-02			
94	1	2	1.4780E+00			
95	1	1	0.0000E+00			
96	1	2	2.2000E-04			
97	1	1	0.0000E+00			
98	1	1	0.0000E+00			
99	3	2	4.2569E+04	-2.6000E+02	0.0000E+00	3.0000E+02
100	3	2	9.1010E+03	2.9500E+02	0.0000E+00	3.0000E+02
101	3	2	6.7523E+02	7.1000E+02	0.0000E+00	3.0000E+02
102	1	2	9.3834E+04			
103	2	2	8.4000E+05	-5.0400E+02		
104	3	1	1.8060E+04	-1.2400E+03	0.0000E+00	2.7300E+02
105	2	2	1.5019E+05	-4.1100E+02		
106	1	2	6.6420E+05			
107	1	2	2.8044E+04			
108	1	2	6.1992E+05			
109	1	2	5.3136E+04			
110	2	2	2.4100E+01	2.0000E+03		

Table A-3 Aerosol Chemistry Chemical Mechanism (Chemical Mechanism 4)
: CB4 with extensions for aerosol modeling, including a biogenic olefin(OLE2) for terpenes, four condensable organic gasses, secondary organic aerosol formation, and inorganic aerosol chemistry/thermodynamics. 100 reactions and 46 gas species (34 state gasses, 12 radicals). Number of aerosol species is 13 for the CMU scheme.

1	NO2			=	1	NO	1	O			
2	O			=	1	O3					
3	O3	NO		=	1	NO2					
4	O	NO2		=	1	NO					
5	O	NO2		=	1	NO3					
6	O	NO		=	1	NO2					
7	NO2	O3		=	1	NO3					
8	O3			=	1	O					
9	O3			=	1	O1D					
10	O1D			=	1	O					
11	O1D	H2O		=	2	OH					
12	O3	OH		=	1	HO2					
13	O3	HO2		=	1	OH					
14	NO3			=	0.89	NO2	0.89	O	0.11	NO	
15	NO3	NO		=	2	NO2					
16	NO3	NO2		=	1	NO	1	NO2			
17	NO3	NO2		=	1	N2O5					
18	N2O5	H2O		=	2	HNO3					
19	N2O5			=	1	NO3	1	NO2			
20	NO	NO		=	2	NO2					
21	NO	NO2	H2O	=	2	HONO					
22	NO	OH		=	1	HONO					
23	HONO			=	1	NO	1	OH			
24	OH	HONO		=	1	NO2					
25	HONO	HONO		=	1	NO	1	NO2			
26	NO2	OH		=	1	HNO3					
27	OH	HNO3		=	1	NO3					
28	HO2	NO		=	1	OH	1	NO2			
29	HO2	NO2		=	1	PNA					
30	PNA			=	1	HO2	1	NO2			
31	OH	PNA		=	1	NO2					
32	HO2	HO2		=	1	H2O2					
33	HO2	HO2	H2O	=	1	H2O2					
34	H2O2			=	2	OH					
35	OH	H2O2		=	1	HO2					
36	OH	CO		=	1	HO2					
37	FORM	OH		=	1	HO2	1	CO			
38	FORM			=	2	HO2	1	CO			
39	FORM			=	1	CO					
40	FORM	O		=	1	OH	1	HO2	1	CO	

41	FORM	NO3	=	1	HNO3	1	HO2	1	CO	
42	ALD2	O	=	1	C2O3	1	OH			
43	ALD2	OH	=	1	C2O3					
44	ALD2	NO3	=	1	C2O3	1	HNO3			
45	ALD2		=	1	FORM	2	HO2	1	CO	
				1	XO2					
46	C2O3	NO	=	1	FORM	1	NO2	1	HO2	
				1	XO2					
47	C2O3	NO2	=	1	PAN					
48	PAN		=	1	C2O3	1	NO2			
49	C2O3	C2O3	=	2	FORM	2	XO2	2	HO2	
50	C2O3	HO2	=	0.79	FORM	0.79	XO2	0.79	HO2	
				0.79	OH					
51	OH		=	1	FORM	1	XO2	1	HO2	
52	PAR	OH	=	0.87	XO2	0.13	XO2N	0.11	HO2	
				0.11	ALD2	-0.11	PAR	0.76	ROR	
				0.0024	CG3					
53	ROR		=	0.96	XO2	1.1	ALD2	0.94	HO2	
				-2.1	PAR	0.04	XO2N			
54	ROR		=	1	HO2					
55	ROR	NO2	=	1	NTR					
56	O	OLE	=	0.63	ALD2	0.38	HO2	0.28	XO2	
				0.3	CO	0.2	FORM	0.02	XO2N	
				0.22	PAR	0.2	OH	0.0024	CG3	
57	OH	OLE	=	1	FORM	1	ALD2	-1	PAR	
				1	XO2	1	HO2	0.0024	CG3	
58	O3	OLE	=	0.5	ALD2	0.74	FORM	0.22	XO2	
				0.1	OH	0.33	CO	0.44	HO2	
				-1	PAR	0.0024	CG3			
59	NO3	OLE	=	0.91	XO2	1	FORM	0.09	XO2N	
				1	ALD2	1	NO2	-1	PAR	
				0.0024	CG3					
60	O	ETH	=	1	FORM	1.7	HO2	1	CO	
				0.7	XO2	0.3	OH			
61	OH	ETH	=	1	XO2	1.56	FORM	0.22	ALD2	
				1	HO2					
62	O3	ETH	=	1	FORM	0.42	CO	0.12	HO2	
63	TOL	OH	=	0.44	HO2	0.08	XO2	0.36	CRES	
				0.56	TO2	0.07	CG1	0.137	CG2	
64	TO2	NO	=	0.9	NO2	0.9	HO2	0.9	OPEN	
				0.1	NTR					
65	TO2		=	1	CRES	1	HO2			
66	OH	CRES	=	0.4	CRO	0.6	XO2	0.6	HO2	
				0.3	OPEN	0.036	CG3			
67	CRES	NO3	=	1	CRO	1	HNO3	0.036	CG3	
68	CRO	NO2	=	1	NTR					
69	OPEN		=	1	C2O3	1	HO2	1	CO	

70	OPEN	OH	=	1	XO2	2	CO	2	HO2	
				1	C2O3	1	FORM			
71	OPEN	O3	=	0.03	ALD2	0.62	C2O3	0.7	FORM	
				0.03	XO2	0.69	CO	0.08	OH	
				0.76	HO2	0.2	MGLY			
72	OH	XYL	=	0.7	HO2	0.5	XO2	0.2	CRES	
				0.8	MGLY	1.1	PAR	0.3	TO2	
				0.044	CG1	0.192	CG2			
73	OH	MGLY	=	1	XO2	1	C2O3			
74	MGLY		=	1	C2O3	1	HO2	1	CO	
75	O	ISOP	=	0.75	ISPD	0.5	FORM	0.25	XO2	
				0.25	HO2	0.25	C2O3	0.25	PAR	
76	OH	ISOP	=	0.912	ISPD	0.629	FORM	0.991	XO2	
				0.912	HO2	0.088	XO2N			
77	O3	ISOP	=	0.65	ISPD	0.6	FORM	0.2	XO2	
				0.066	HO2	0.266	OH	0.2	C2O3	
				0.15	ALD2	0.35	PAR	0.066	CO	
78	NO3	ISOP	=	0.2	ISPD	0.8	NTR	1	XO2	
				0.8	HO2	0.2	NO2	0.8	ALD2	
				2.4	PAR					
79	XO2	NO	=	1	NO2					
80	XO2	XO2	=							
81	XO2N	NO	=	1	NTR					
82	SO2	OH	=	1	SULF	1	HO2			
83	SO2		=	1	SULF					
84	MEOH	OH	=	1	FORM	1	HO2			
85	ETOH	OH	=	1	HO2	1	ALD2			
86	XO2	HO2	=							
87	XO2N	HO2	=							
88	XO2N	XO2N	=							
89	XO2	XO2N	=							
90	OH	HO2	=							
91	CRO		=							
92	OH	ISPD	=	1.565	PAR	0.167	FORM	0.713	XO2	
				0.503	HO2	0.334	CO	0.168	MGLY	
				0.273	ALD2	0.498	C2O3			
93	O3	ISPD	=	0.114	C2O3	0.15	FORM	0.85	MGLY	
				0.154	HO2	0.268	OH	0.064	XO2	
				0.02	ALD2	0.36	PAR	0.225	CO	
94	NO3	ISPD	=	0.357	ALD2	0.282	FORM	1.282	PAR	
				0.925	HO2	0.643	CO	0.85	NTR	
				0.075	C2O3	0.075	XO2	0.15	HNO3	
95	ISPD		=	0.333	CO	0.067	ALD2	0.9	FORM	
				0.832	PAR	1.033	HO2	0.7	XO2	
				0.967	C2O3					
96	NO2	ISOP	=	0.2	ISPD	0.8	NTR	1	XO2	
				0.8	HO2	0.2	NO	0.8	ALD2	

				2.4	PAR				
97	O	OLE2	=	0.63	ALD2	0.38	HO2	0.28	XO2
				0.3	CO	0.2	FORM	0.02	XO2N
				0.22	PAR	0.2	OH	0.136	CG4
98	OH	OLE2	=	1	FORM	1	ALD2	-1	PAR
				1	XO2	1	HO2	0.136	CG4
99	O3	OLE2	=	0.5	ALD2	0.74	FORM	0.22	XO2
				0.1	OH	0.33	CO	0.44	HO2
				-1	PAR	0.136	CG4		
100	NO3	OLE2	=	0.91	XO2	1	FORM	0.09	XO2N
				1	ALD2	1	NO2	-1	PAR
				0.136	CG4				

Table A-4 Aerosol Chemistry Chemical Parameters (Chemparam 4_CMU scheme)

```
CAMx Version        |VERSION4.1
Mechanism ID        |4 CMU
Description         |Mech 3 plus Size-Resolved Aerosols (Full-Science PM Module)
No of gas species   |34
#aero, dt, bins     |13 15.0 4 0.039063 0.15625 0.625 2.5 10.0
No of reactions     |100
Prim photo rxns     |6 1 38 39 9 45 95
No of sec photo rxn|6
ID, prim ID, scale | 8  1  0.053
                    |14  1 33.9
                    |23  1  0.1975
                    |34 39  0.189
                    |69 38  9.04
                    |74 38  9.64
Species Records
     Gas Spec    lower bnd     H-law    T-fact    Diffrat  Reactvty    Rscale
  1  NO          1.00E-15  1.90e-03    -1480.       1.29       0.0        1.
  2  NO2         1.00E-09  1.00e-02    -2516.       1.60       0.1        1.
  3  O3          1.00E-09  1.10e-02    -2415.       1.63       1.0        1.
  4  PAN         1.00E-09  3.60e+00    -5910.       2.59       0.1        1.
  5  NXOY        1.00E-12  3.20e+04    -8706.       2.45       0.1        0.
  6  OLE         1.00E-09  5.00e-03        0.       1.80       0.0        1.
  7  PAR         1.00E-04  1.00e-03        0.       2.00       0.0        1.
  8  TOL         1.00E-09  1.20e+00        0.       2.26       0.0        1.
  9  XYL         1.00E-09  1.40e+00        0.       2.43       0.0        1.
 10  FORM        1.00E-09  6.30e+03    -6492.       1.29       0.0        1.
 11  ALD2        1.00E-09  6.30e+03    -6492.       1.56       0.0        1.
 12  ETH         1.00E-09  1.00e-02        0.       1.25       0.0        1.
 13  CRES        1.00E-09  2.70e+03    -6492.       2.45       0.0        1.
 14  MGLY        1.00E-09  2.70e+03    -6492.       2.00       0.0        1.
 15  OPEN        1.00E-12  2.70e+03    -6492.       2.47       0.0        1.
 16  PNA         1.00E-09  2.00e+04    -5910.       2.09       0.0        1.
 17  CO          1.00E-04  1.00e-10        0.       1.25       0.0        1.
 18  HONO        1.00E-09  5.90e+01    -4781.       1.62       0.1        1.
 19  H2O2        1.00E-09  7.40e+04    -6643.       1.37       1.0        1.
 20  HNO3        1.00E-09  2.00e+05    -8707.       1.87       0.0        0.
 21  ISOP        1.00E-09  1.00e-02        0.       1.94       0.0        1.
 22  MEOH        1.00E-09  2.20e+02    -4932.       1.33       0.0        1.
 23  ETOH        1.00E-09  2.20e+02    -4932.       1.60       0.0        1.
 24  ISPD        1.00E-09  6.30e+03    -6492.       1.97       0.0        1.
 25  NTR         1.00E-09  9.40e+03    -8706.       2.72       0.0        1.
 26  SO2         1.00E-09  1.00e+05    -3156.       1.89       0.0        1.
 27  SULF        1.00E-12  1.00e+10        0.       1.00       0.0        0.
 28  NH3         1.00E-09  2.00e+04    -3400.       0.97       0.0        1.
```

29	HCL	1.00E-12	1.00e+05	0.	1.42	0.0	0.
30	OLE2	1.00E-12	5.00e-03	0.	1.80	0.0	1.
31	CG1	1.00E-12	2.70e+03	-6492.	2.50	0.0	1.
32	CG2	1.00E-12	2.70e+03	-6492.	2.50	0.0	1.
33	CG3	1.00E-12	2.70e+03	-6492.	2.50	0.0	1.
34	CG4	1.00E-12	2.70e+03	-6492.	2.50	0.0	1.

	Aero Spec	lower bnd	Density
1	SOA1	1.00E-09	1.0
2	SOA2	1.00E-09	1.0
3	SOA3	1.00E-09	1.0
4	SOA4	1.00E-09	1.0
5	POA	1.00E-09	1.0
6	PEC	1.00E-09	2.0
7	CRST	1.00E-09	3.0
8	PH20	1.00E-09	1.0
9	PCL	1.00E-09	2.0
10	NA	1.00E-09	2.0
11	PNH4	1.00E-09	1.5
12	PNO3	1.00E-09	1.5
13	PSO4	1.00E-09	1.5

Reaction Records

Rxn	Typ	Order	Parameters (1 to 12, depending upon Typ)	
1	1	1	0.0000E+00	
2	2	2	4.3233E+06	-1.1750E+03
3	2	2	2.6640E+01	1.3700E+03
4	1	2	1.3750E+04	
5	2	2	2.3090E+03	-6.8700E+02
6	2	2	2.4380E+03	-6.0200E+02
7	2	2	4.7310E-02	2.4500E+03
8	1	1	0.0000E+00	
9	1	1	0.0000E+00	
10	2	2	4.2500E+10	-3.9000E+02
11	1	2	3.2600E+05	
12	2	2	1.0000E+02	9.4000E+02
13	2	2	2.9990E+00	5.8000E+02
14	1	1	0.0000E+00	
15	2	2	4.4167E+04	-2.5000E+02
16	2	2	5.9010E-01	1.2300E+03
17	2	2	1.8530E+03	-2.5600E+02
18	1	2	3.8400E-07	
19	2	1	2.7760E+00	1.0897E+04
20	2	2	1.5390E-04	-5.3000E+02
21	1	3	1.6000E-11	
22	2	2	9.7990E+03	-8.0600E+02
23	1	1	0.0000E+00	
24	1	2	9.7700E+03	
25	1	2	1.5000E-05	

```
26    4   2     9.4640E-02     0.0000E+00 -3.2000E+00   3.0000E+02   3.5470E+04   0.0000E+00
-1.3000E+00   3.0000E+02   6.0000E-01   1.0000E+00
27    2   2     2.1790E+02    -1.0000E+03
28    2   2     1.2270E+04    -2.4000E+02
29    1   2     0.0000E+00
30    1   1     0.0000E+00
31    1   1     0.0000E+00
32    2   2     4.1440E+03    -1.1500E+03
33    2   3     2.1810E-01    -5.8000E+03
34    1   1     0.0000E+00
35    2   2     2.5200E+03     1.8700E+02
36    7   2     2.2170E+02     0.0000E+00   0.0000E+00   3.0000E+02   1.3300E-04   0.0000E+00
0.0000E+00   3.0000E+02
37    1   2     1.5000E+04
38    1   1     0.0000E+00
39    1   1     0.0000E+00
40    2   2     2.3700E+02     1.5500E+03
41    1   2     9.3000E-01
42    2   2     6.3600E+02     9.8600E+02
43    2   2     2.4000E+04    -2.5000E+02
44    1   2     3.7000E+00
45    1   1     0.0000E+00
46    2   2     2.8200E+04     1.8000E+02
47    2   2     1.3700E+04    -3.8000E+02
48    2   1     2.5400E-02     1.3500E+04
49    1   2     3.7000E+03
50    1   2     9.6000E+03
51    2   2     1.6290E+01     1.7750E+03
52    1   2     1.2030E+03
53    2   1     1.3710E+05     8.0000E+03
54    1   1     9.5450E+04
55    1   2     2.2000E+04
56    2   2     5.9200E+03     3.2400E+02
57    2   2     4.2000E+04    -5.0400E+02
58    2   2     1.8000E-02     2.1050E+03
59    1   2     1.1350E+01
60    2   2     1.0800E+03     7.9200E+02
61    2   2     1.1920E+04    -4.1100E+02
62    2   2     2.7000E-03     2.6330E+03
63    2   2     9.1500E+03    -3.2200E+02
64    1   2     1.2000E+04
65    1   1     2.5000E+02
66    1   2     6.1000E+04
67    1   2     3.2500E+04
68    1   2     2.0000E+04
69    1   1     0.0000E+00
70    1   2     4.4000E+04
```

```
71   2  2    1.5000E-02    5.0000E+02
72   2  2    3.6200E+04   -1.1600E+02
73   1  2    2.6000E+04
74   1  1    0.0000E+00
75   1  2    5.3200E+04
76   1  2    1.4760E+05
77   1  2    1.9000E-02
78   1  2    9.9600E+02
79   1  2    1.2000E+04
80   2  2    2.0000E+03   -1.3000E+03
81   1  2    1.2000E+04
82   4  2    1.0910E-02    0.0000E+00 -3.3000E+00  3.0000E+02  2.2170E+03  0.0000E+00
0.0000E+00  3.0000E+02  6.0000E-01  1.0000E+00
83   1  1    0.0000E+00
84   1  2    1.6000E+03
85   2  2    4.3000E+03   -1.7600E+02
86   2  2    8.9000E+03   -1.3000E+03
87   2  2    8.9000E+03   -1.3000E+03
88   2  2    2.0000E+03   -1.3000E+03
89   2  2    4.0000E+03   -1.3000E+03
90   2  2    1.6260E+05   -2.5000E+02
91   1  1    2.7778E-04
92   1  2    4.9667E+04
93   1  2    1.0500E-02
94   1  2    1.4780E+00
95   1  1    0.0000E+00
96   1  2    2.2000E-04
97   2  2    5.9200E+03    3.2400E+02
98   2  2    4.2000E+04   -5.0400E+02
99   2  2    1.8000E-02    2.1050E+03
100  1  2    1.1350E+01
```

Appendix B

Point source emissions of molecular chlorine were identified in eleven counties in Southeastern Texas using the Toxic Release Inventory (TRI) compiled by the United States Environmental Protective Agency (USEPA, www.epa.gov/tri). These counties were Jefferson, Brazoria, Galveston, Orange, Harris, Fort Bend, Montgomery, Liberty, Chambers, Waller, and Hardin. Data was for 2000.

Of the 11 counties, Jefferson, Brazoria, Galveston, Orange and Harris County had facilities with significant (around 1000 pounds per year (ppy)) chlorine releases. The largest emissions of chlorine gas were recorded in Harris, Brazoria, Jefferson, and Galveston counties which registered 108 tpy (221568 ppy), 70 tpy (141897 ppy), 35 tpy (70341 ppy), and 16 tpy (32040 ppy) respectively. The chlorine emissions reported in Chambers, Orange, and Liberty counties were approximately 7000 ppy, 2000ppy, and 1000ppy respectively. Fort Bend, and Montgomery counties had molecular chlorine emissions of less than 1000 ppy. Waller and Hardin County had no documented chlorine emissions. Major point sources (>1000 ppy) from the eleven counties from the TRI data are compiled in Table B-1 through Table B-7.

Table B-1 Point source releases of molecular chlorine in Brazoria County

Facility	Latitude	Longitude	2000 TRI reported releases lb/yr	TCEQ PSDB lb/yr	Proposed Emission Rate lb/yr	Proposed Emission Rate t/d
Air Liquide America Corp.	28.99167	-95.3333	3000		3000	0.00411
Chevron Phillips Chemical Co.LP	29.06889	-95.7467	13981	8198	13981	0.01915
Rhodia Rare Earths Inc.	28.99014	-95.3588		657	657	0.0009
Shintech Incorporated	28.99702	-95.3575		365	365	0.0005
Dow Chemical Co. Clute	28.99212	-95.3995		40040	40040	0.054849
Dow Chemical Co. Freeport	28.98611	-95.3789	77000	68686	77000	0.105479
Phillips 66 Co.	29.06889	-95.7467	5317	6854	6854	0.009389

Sweeny Complex						
Total					141897	0.194377

Table B-2 Point source releases of molecular chlorine in Chamber County

Facility	Latitude	Longitude	2000 TRI reported releases lb/yr	TCEQ PSDB lb/yr	Proposed Emission Rate lb/yr	Proposed Emission Rate t/d
Bayer Corporation	29.75934	-106.912	5317	6854	6854	0.009389
Total					6854	0.009389

Table B-3 Point source releases of molecular chlorine in Jefferson County

Facility	Latitude	Longitude	2000 TRI reported releases lb/yr	TCEQ PSDB lb/yr	Proposed Emission Rate lb/yr	Proposed Emission Rate t/d
Air Liquid Nederland ASU Facility	30.002778	-94.038056	1950		1950	0.002671
Atofina Petrochemicals Inc	29.95456	-93.89291		453	453	0.000621
Basf Corp.	29.970833	-94.056944	1550	1971	1971	0.0027
Du PontDow Elastomers Beaumont Plant	30.012222	-94.0275	1791	1796	1796	0.00246
Equistar Chemicals L.P.Port Arthur Plant	29.866667	-93.995833	2880	3322	3322	0.00455
Exxon Mobil Chemical Co.	30.06791	-94.09063		1504	1504	0.00206
Goodyear Tire & Rubber Co.	29.975833	-94.217778	1560		1560	0.002137
Huntsman Corp.-Po/MTBE Plant	29.965278	-93.930556	30260	17031	30260	0.041452
Mobil Chemical Co.Olefins&Aromatics Plant	30.069722	-94.062222	1602		1602	0.002195
Port Arthur A&O Plant Huntsman Corp.	29.892778	-93.973333	25200		25200	0.034521
P D Glycol	30.05776	-94.04239		723	723	0.00099
Total (lb/yr)			66793	26800	70341	0.096357

Table B-4 Point source releases of molecular chlorine in Harris County

Facility	Latitude	Longitude	2000 TRI reported releases lb/yr	TCEQ PSDB lb/yr	Proposed Emission Rate lb/yr	Proposed Emission Rate t/d
Abitibi Consolidated	29.88306	-95.1086	3506		3506	0.004803
Albemarle Corp, Houston Plant	29.73889	-95.1681	2775		2775	0.003801
BP Amoco Chemical Co.	29.73861	-95.1669	936		936	0.001282
Chevron Phillips Chemical Co. Houston Chemical Complex	29.74167	-95.1756	2500		2500	0.003425
Crown Central Petroleum Corp. Houston Refy.	29.72389	-95.2083	63084	93688	93688	0.12834
Donohue Inds.Inc.				1679	1679	0.0023
Dow Chemical Co. La Porte Site	29.70889	-95.0733	912	292	912	0.001249
Dxi Industrial Inc.	29.76333	-95.15	961		961	0.001316
El Dupont De Nemours and Co	29.70311	-95.0369		481.8	481.8	0.00066
Equistar Chemicals - Bayport Chemicals Plant	29.625	-95.075	7400	2599	7400	0.010137
Ethyl Corp	29.73038	-95.1703		379.6	379.6	0.00052
Exxon Mobil Refining Supply & Baytown Refy.	29.73944	-95.0069	847	868.7	868.7	0.00119
GB Biosciences Corp.	29.7625	-95.1667	17909	22572	22572	0.030921
Huntsman Corp. C4/O&O Plant.	29.96528	-93.9306	62860		62860	0.08611
Lubrizol Corp., Deer Park Facility	29.72056	-95.1128	2338	1949	2338	0.003203
Oxy Vinyls L.P. LA Porte- VCM Plant	29.725	-95.075	3910	6300	6300	0.00863
Oxy Vinyls L.P. Deer park C/A	29.72833	-95.1106	2871	3766	3766	0.005159
Safety Kleen DeerPark Inc.	29.72844	-95.0957		1183	1183	0.001621
Shell Oil Co.	29.72291	-107.122		4052	4052	0.005551
PPG Inds. Inc	29.65556	-95.0383	1010		1010	0.001384

Zeneca AG Prods. Inc. Bayport Plant	29.62889	-95.0511	1400	1394	1400	0.001918
Total (lb/yr)			175219	141204	221568	0.303518

Table B-5 Point source releases of molecular chlorine in Galveston County

Facility	Latitude	Longitude	2000 TRI reported releases lb/yr	TCEQ PSDB lb/yr	Proposed Emission Rate lb/yr	Proposed Emission Rate t/d
BP Amoco Texas City Business Unit	29.37444	-94.925	15000	2964	15000	0.020548
Valero Refining Co.	29.36972	-94.9092	17040	14403	17040	0.023342
Total (lb/yr)			32040	17367	32040	0.04389

Table B-6 Point source releases of molecular chlorine in Orange County

Facility	Latitude	Longitude	2000 TRI reported releases lb/yr	TCEQ PSDB lb/yr	Proposed Emission Rate lb/yr	Proposed Emission Rate t/d
Du Pont Sabine River Works	30.05611	-93.7561	2356	1657	2356	0.003227
Total (lb/yr)			2356	1657	2356	0.003227

Table B-7 Point source releases of molecular chlorine in Liberty County

Facility	Latitude	Longitude	2000 TRI reported releases lb/yr	TCEQ PSDB lb/yr	Proposed Emission Rate lb/yr	Proposed Emission Rate t/d
Louisiana-Pacific Corp.	30.40711	-94.961		1226	1226	0.001679
Total (lb/yr)				1226	1226	0.001679

Table B-8 Wastewater treatment facilities in Houston

FACILITY NAME	ADDRESS	PHONE NUMBER
ALMEDA SIMS	12319 1/2 ALMEDA ROAD	713 - 433 - 1717
BELTWAY	10518 BELLAIRE	281 - 498 - 4127
CEDAR BAYOU	2804 HUFFMAN EASTGATE	
CHOCOLATE BAYOU	9600 MARTIN LUTHER KING	
CLINTON PARK	9030 CLINTON DRIVE	713 - 672 - 2433
EASTHAVEN	8545 SCRANTON	713 - 948 - 9060
F.W.S.D.# 23	8219 KELLET	713 - 636 - 8209
GREENRIDGE	6301-#1 W.FUQUA	281 - 437 - 6299
HOMESTEAD	5565 KIRKPATRICK	713 - 675 - 3910
IMPERIAL VALLEY	15500 COTILLION	281 - 448 - 4226
INTERCONTINENTAL	2450 RANKIN	281 - 233 - 2572
KEEGANS BAYOU	9400 WHITE CHAPEL LN.	
METRO CENTRAL	12815 GALVESTON ROAD	
NORTHBELT	14506 SMITH	713 - 441 - 1786
NORTHBOROUGH	13131 NORTH FREEWAY	
NORTHEAST	655 MAXEY ROAD	713 - 453 - 2946
NORTHGATE	303 BENMAR	281 - 875 - 5551
NORTHWEST	5423 MANGUM	713 - 683 - 6789
PARK TEN	16500 PARK ROW	281 - 646 - 6606
SAGEMONT	11700 SAGEARBOR	281 - 922 - 2308
SIMS BAYOU	9500 LAWNDALE	713 - 926 - 1040
SIMS SOUTH	3005 GALVESTON ROAD	713 - 847 - 5158
SOUTHEAST	9610 KINGSPOINT	713 - 731 - 6003
SOUTHWEST	4211 BEECHNUT	713 - 622 - 8031
TURKEY CREEK	1147 ENCLAVE PARKWAY	
UPPER BRAES	13525 OLD WESTHEIMER	281 - 752 - 2231
W.C.I.D.# 47	7410 GALVESTON	713 - 946 - 9057
W.C.I.D.# 76	13535 RIVER TRAIL DR.	281 - 590 - 6219
W.C.I.D.# 111	10601 HUNTINGTON POINT	281 - 568 - 7598
WEST DISTRICT	255 ISOLDE	713 - 468 - 0875
WESTWAY	10273 GENARD	
WHITE OAK	7103 GULF BANK RD.	713 - 937 - 0433
WILLOWBROOK	7101 W. GREENS RD.	281 - 807 - 9586
69TH STREET	2525 MACARIO GARCIA	713 - 671 - 4200
TIDWELL TIMBER	10155 TIDWELL	
M.U.D.# 203	1215 GEARS ROAD	281 - 825 - 8124
M.U.D.# 48	SORTERS ROAD	281 - 358 - 6885
HUNTERWOOD	6230 S.LAKE HOUSTON PKWY	
KINGWOOD CENTRAL	3928 KINGWOOD DR.	
FOREST COVE	729 HAMBLEN RD.	

Appendix C

Figure C-1 Spatial distribution of the difference in CMBO concentrations between the model predictions with added chlorine emissions and the basecase with chlorine emissions are reported: doubling chlorine emissions from (a) cooling tower, (b) swimming pools, and (c) point sources, and (d) a factor of 10 increase in chlorine from seasalt are subtracted by basecase with chlorine emissions

Figure C-2 1-hour averaged absolute ozone concentration and difference in 1-hour averaged ozone concentrations between chlorine basecase and chlorine basecase augmented by (b) doubling cooling tower emissions, (c) doubling swimming pools emissions at the time of the day when the maximum ozone concentration occurs.

Figure C-3 8-hour averaged absolute ozone concentration and difference in 1-hour averaged ozone concentrations between chlorine basecase and chlorine basecase augmented by (b) doubling cooling tower emissions, (c) doubling swimming pools emissions at the time of the day when the maximum ozone concentration occurs.

Figure C-1 Spatial distribution of the difference in CMBO concentrations between the model predictions with added chlorine emissions and the basecase with chlorine emissions are reported: doubling chlorine emissions from (a) cooling tower, (b) swimming pools, and (c) point sources, and (d) a factor of 10 increase in chlorine from seasalt are subtracted by basecase with chlorine emissions

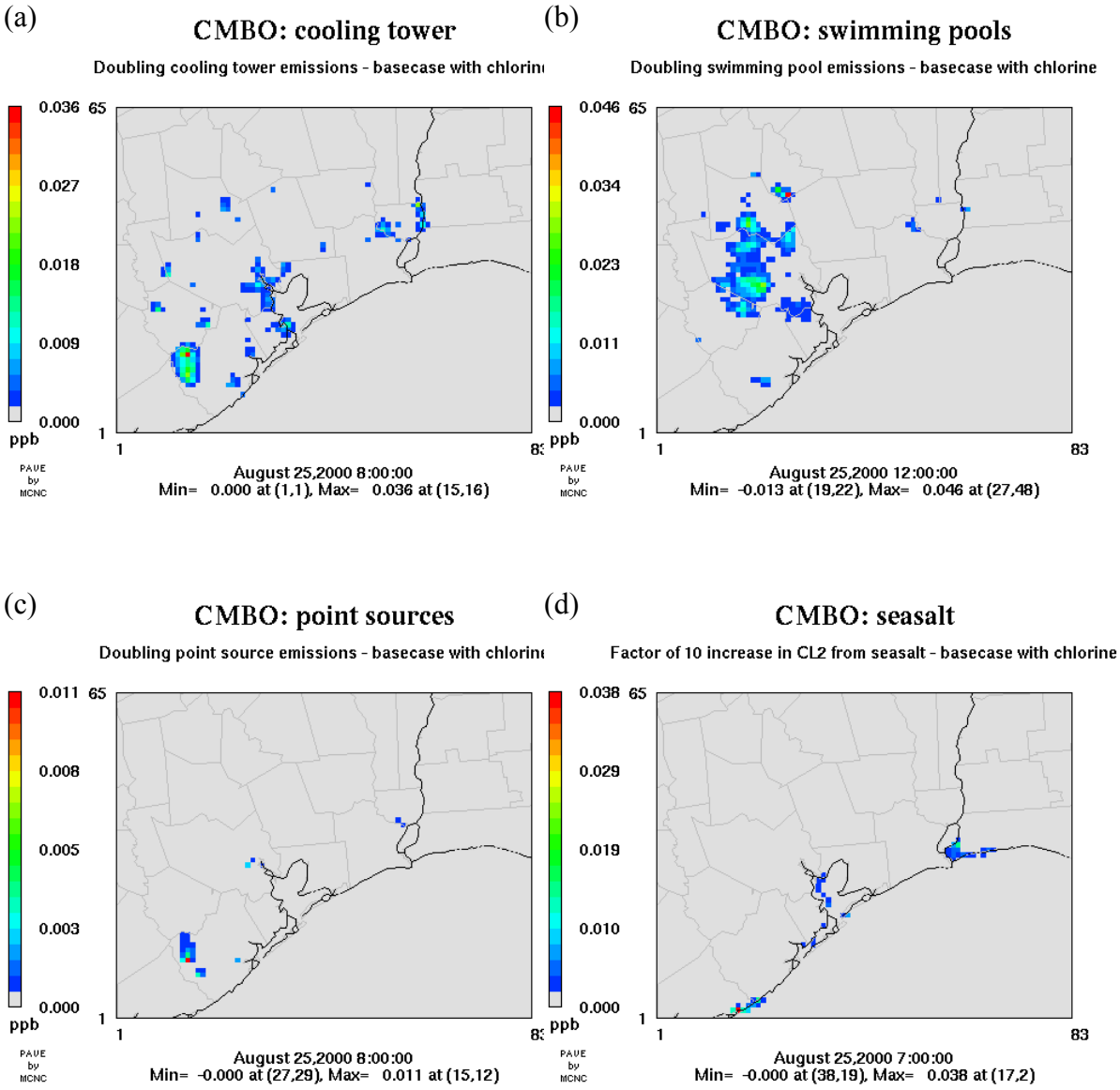

Figure C-2 1-hour averaged absolute ozone concentration and difference in 1-hour averaged ozone concentrations between chlorine basecase and chlorine basecase augmented by (b) doubling cooling tower emissions, (c) doubling swimming pools emissions at the time of the day when the maximum ozone concentration occurs

a)absolute ozone concentration b)ozone formation due to cooling towers c) ozone formation due to swimming pools

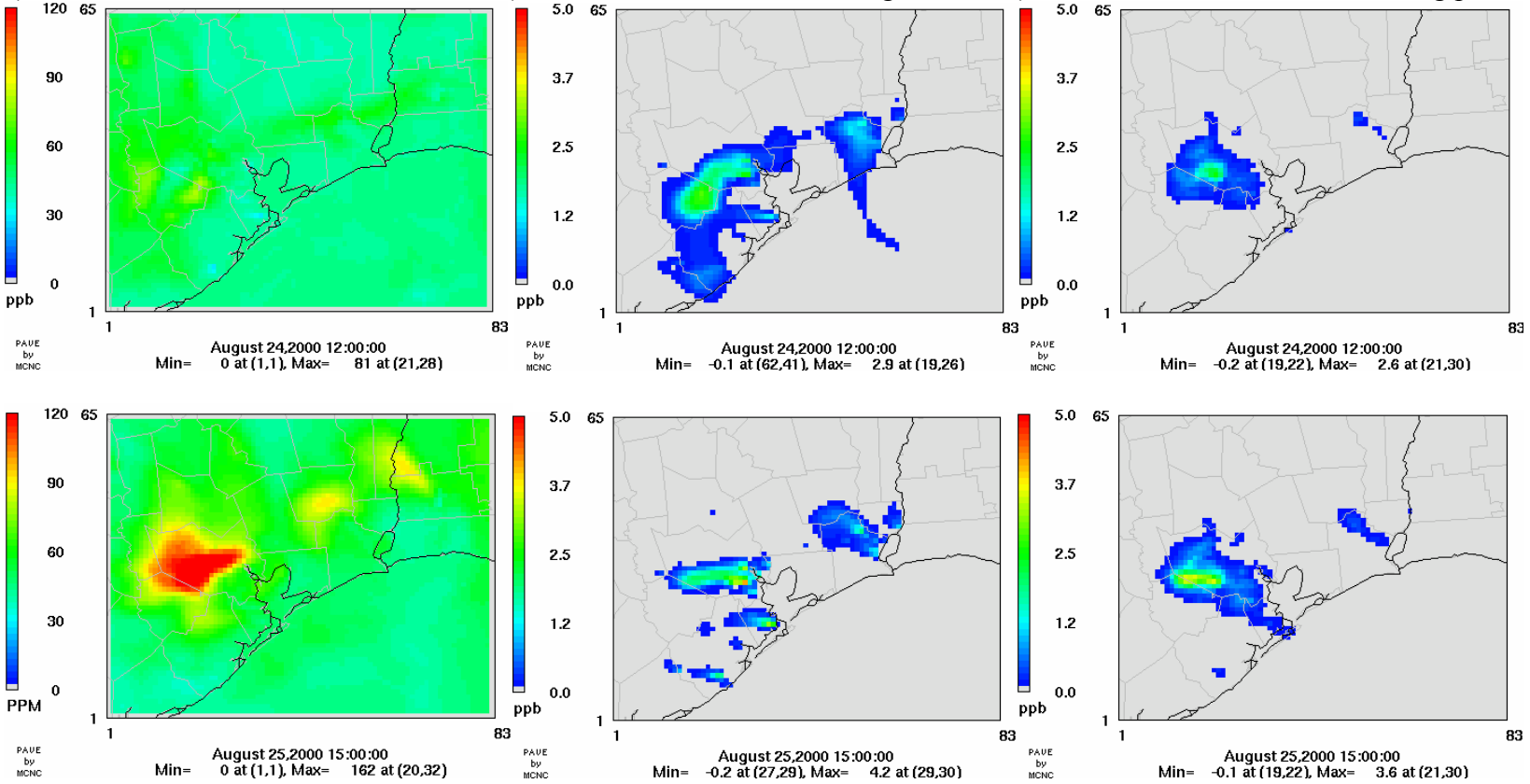

Figure C-2 1-hour averaged absolute ozone concentration and difference in 1-hour averaged ozone concentrations between chlorine basecase and chlorine basecase augmented by (b) doubling cooling tower emissions, (c) doubling swimming pools emissions at the time of the day when the maximum ozone concentration occurs

a)absolute ozone concentration b)ozone formation due to cooling towers c) ozone formation due to swimming pools

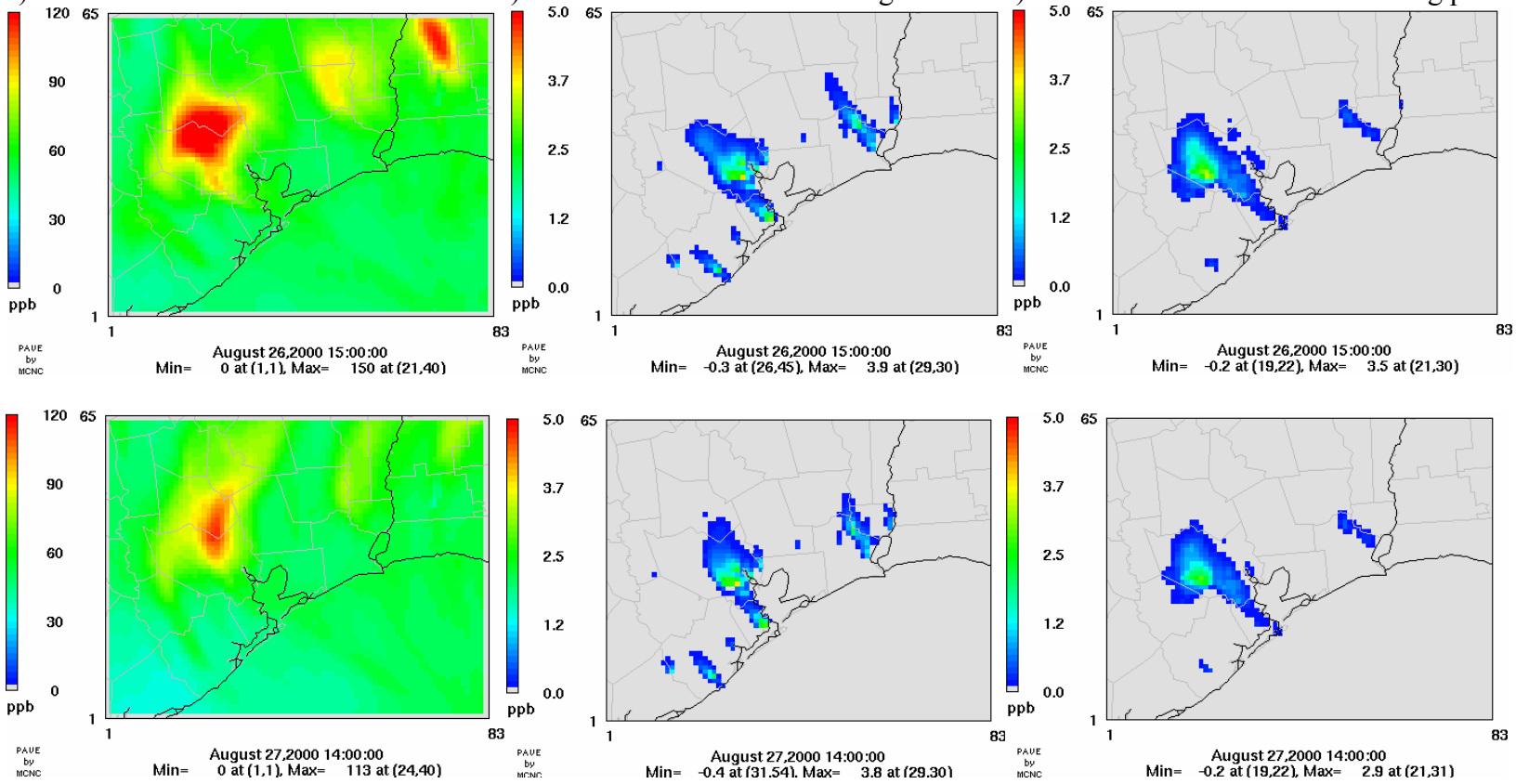

Figure C-2 1-hour averaged absolute ozone concentration and difference in 1-hour averaged ozone concentrations between chlorine basecase and chlorine basecase augmented by (b) doubling cooling tower emissions, (c) doubling swimming pools emissions at the time of the day when the maximum ozone concentration occurs

a)absolute ozone concentration b)ozone formation due to cooling towers c) ozone formation due to swimming pools

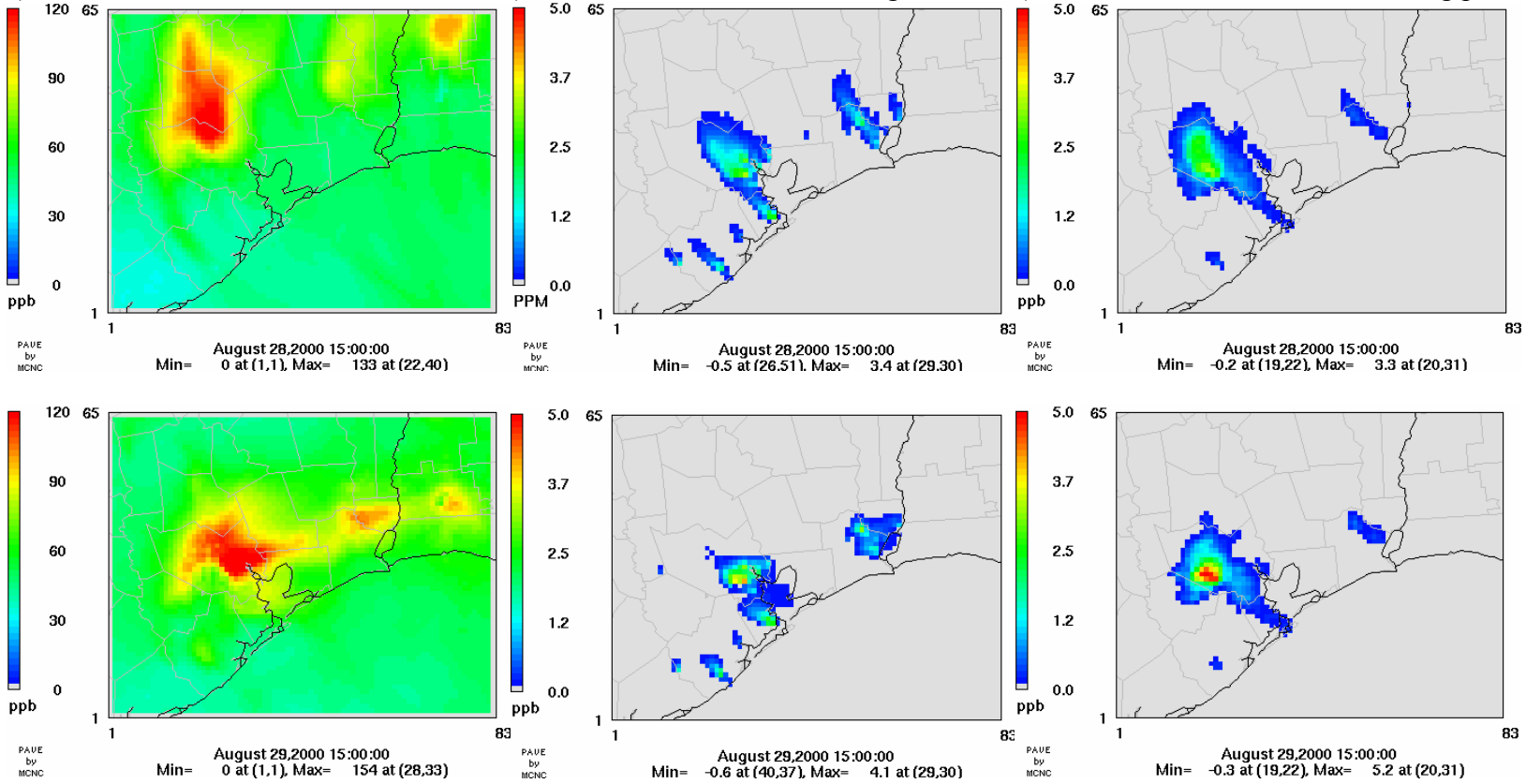

Figure C-2 1-hour averaged absolute ozone concentration and difference in 1-hour averaged ozone concentrations between chlorine basecase and chlorine basecase augmented by (b) doubling cooling tower emissions, (c) doubling swimming pools emissions at the time of the day when the maximum ozone concentration occurs

a)absolute ozone concentration b)ozone formation due to cooling towers c) ozone formation due to swimming pools

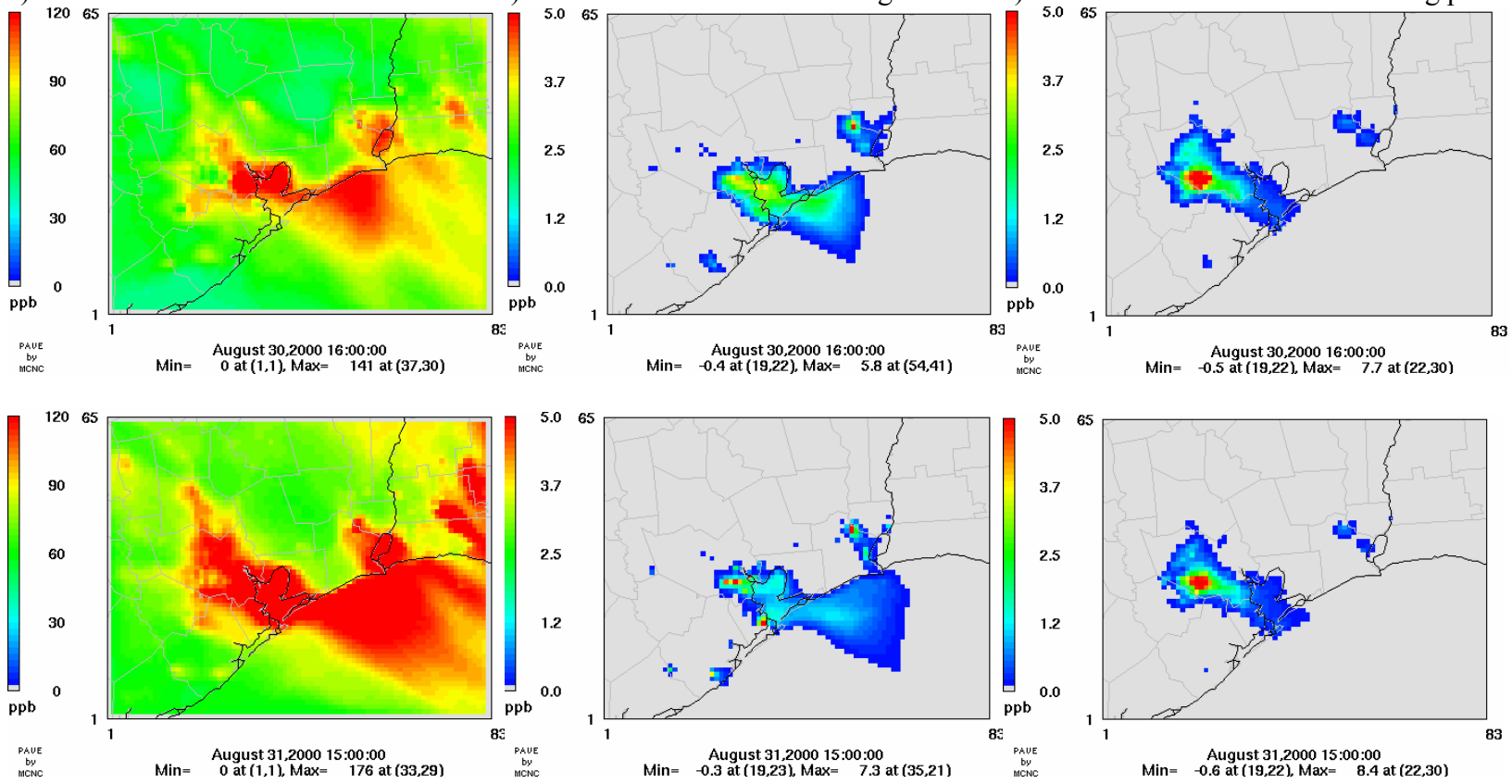

Figure C-2 1-hour averaged absolute ozone concentration and difference in 1-hour averaged ozone concentrations between chlorine basecase and chlorine basecase augmented by (b) doubling cooling tower emissions, (c) doubling swimming pools emissions at the time of the day when the maximum ozone concentration occurs

a)absolute ozone concentration b)ozone formation due to cooling towers c) ozone formation due to swimming pools

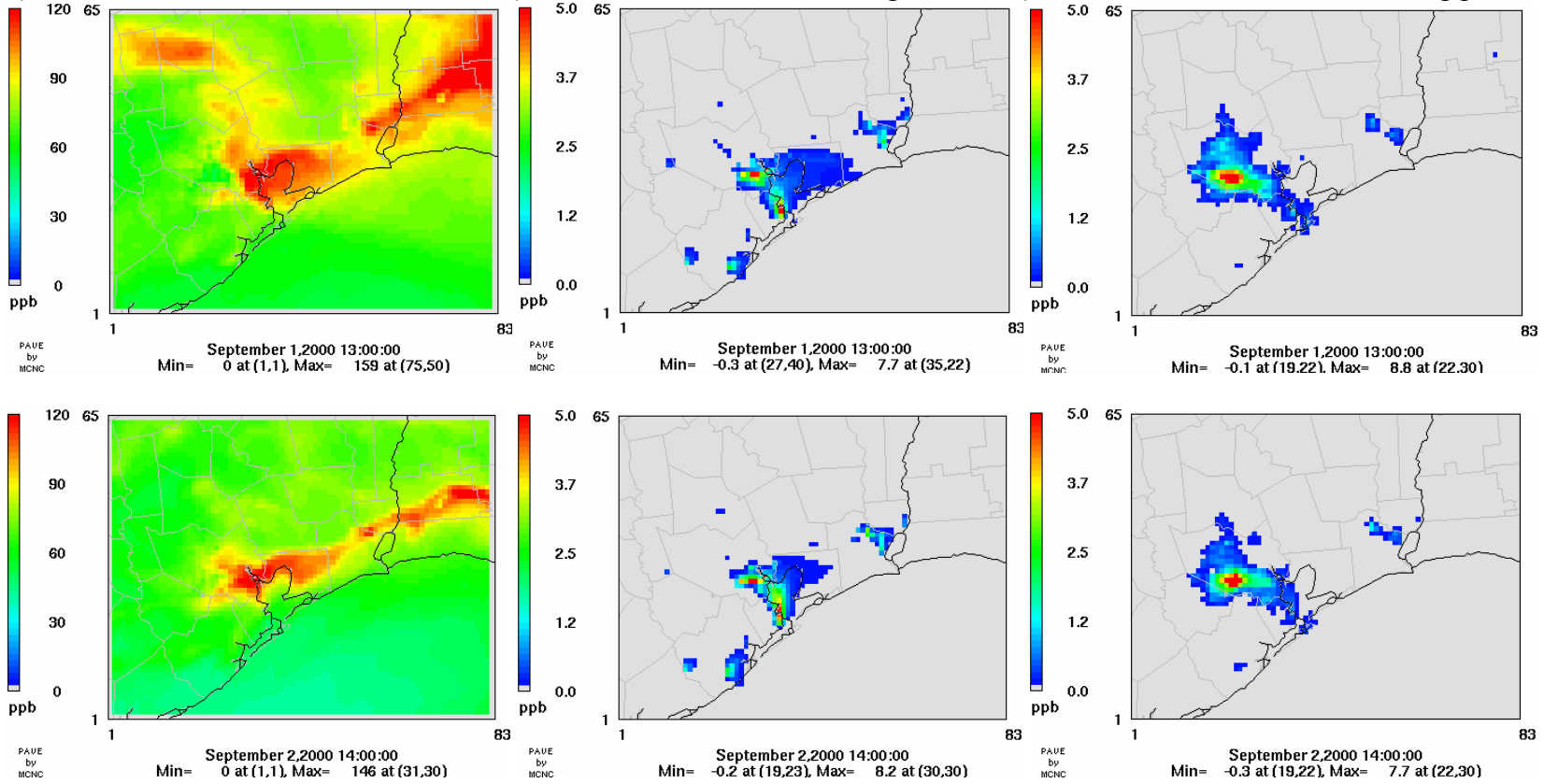

Figure C-2 1-hour averaged absolute ozone concentration and difference in 1-hour averaged ozone concentrations between chlorine basecase and chlorine basecase augmented by (b) doubling cooling tower emissions, (c) doubling swimming pools emissions at the time of the day when the maximum ozone concentration occurs

a)absolute ozone concentration b)ozone formation due to cooling towers c) ozone formation due to swimming pools

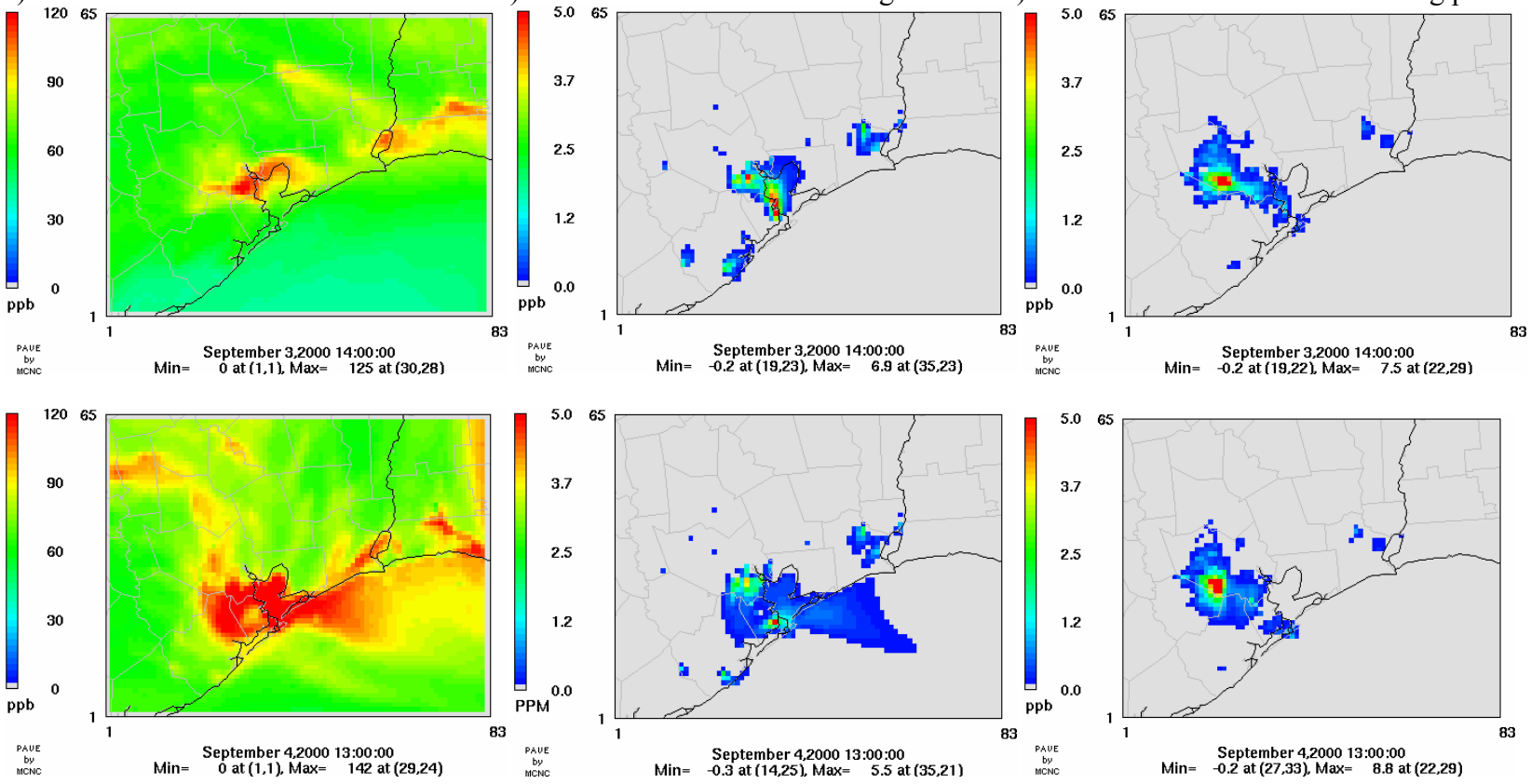

Figure C-2 1-hour averaged absolute ozone concentration and difference in 1-hour averaged ozone concentrations between chlorine basecase and chlorine basecase augmented by (b) doubling cooling tower emissions, (c) doubling swimming pools emissions at the time of the day when the maximum ozone concentration occurs

a)absolute ozone concentration b)ozone formation due to cooling towers c) ozone formation due to swimming pools

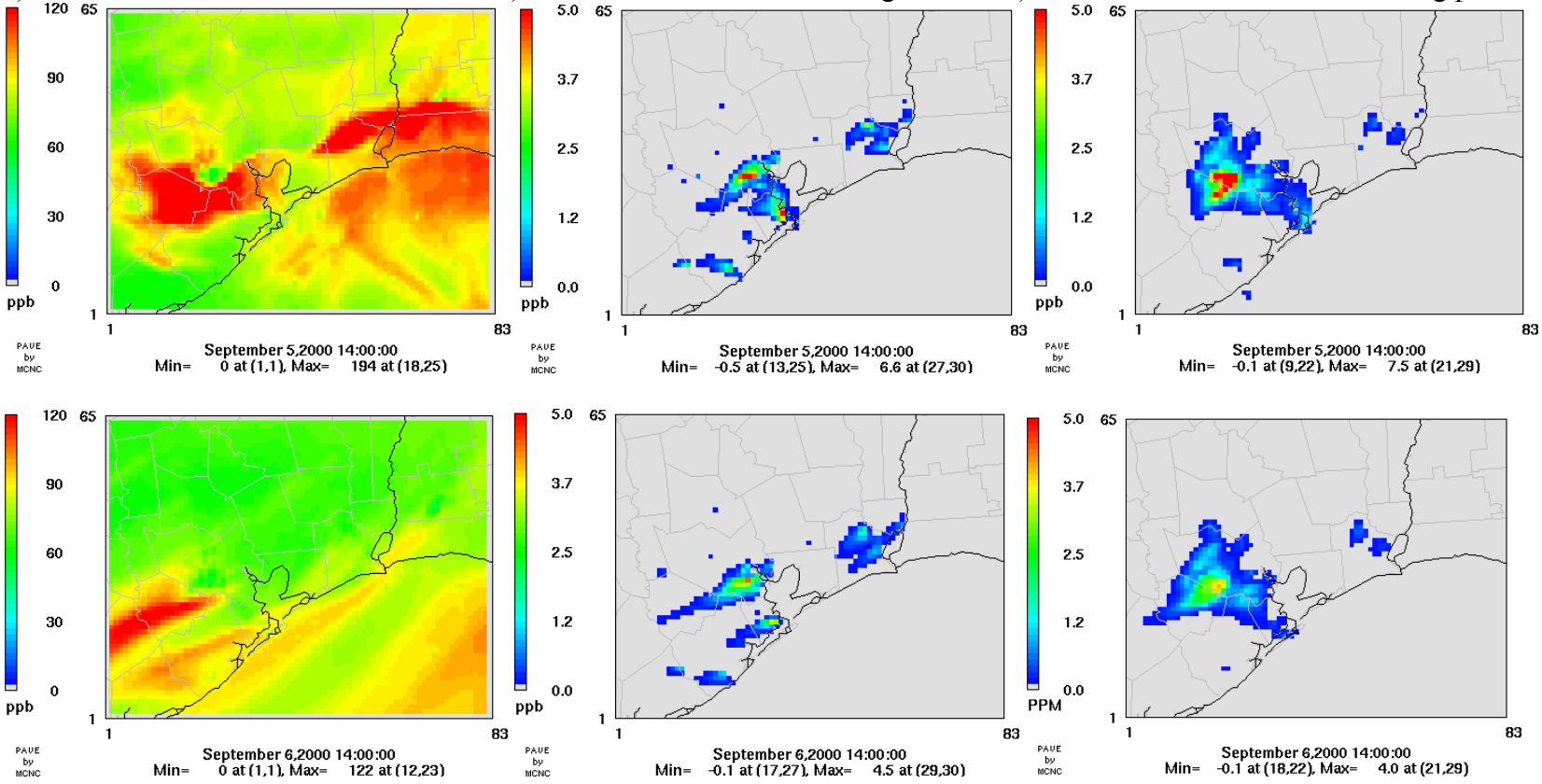

Figure C-3 8-hour averaged absolute ozone concentration and difference in 1-hour averaged ozone concentrations between chlorine basecase and chlorine basecase augmented by (b) doubling cooling tower emissions, (c) doubling swimming pools emissions at the time of the day when the maximum ozone concentration occurs.

a)absolute ozone concentration b)ozone formation due to cooling towers c) ozone formation due to swimming pools

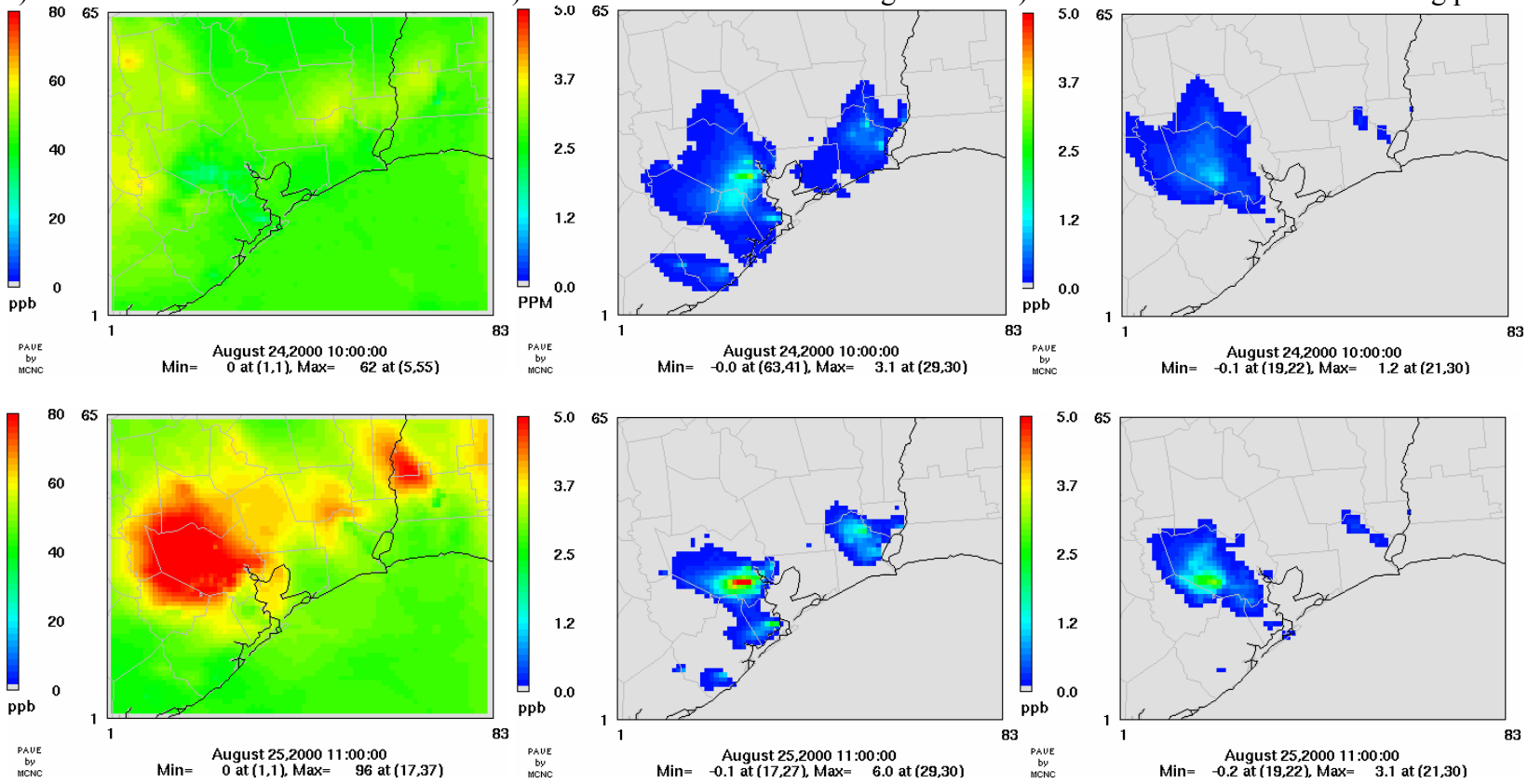

Figure C-3 8-hour averaged absolute ozone concentration and difference in 1-hour averaged ozone concentrations between chlorine basecase and chlorine basecase augmented by (b) doubling cooling tower emissions, (c) doubling swimming pools emissions at the time of the day when the maximum ozone concentration occurs.

a)absolute ozone concentration b)ozone formation due to cooling towers c) ozone formation due to swimming pools

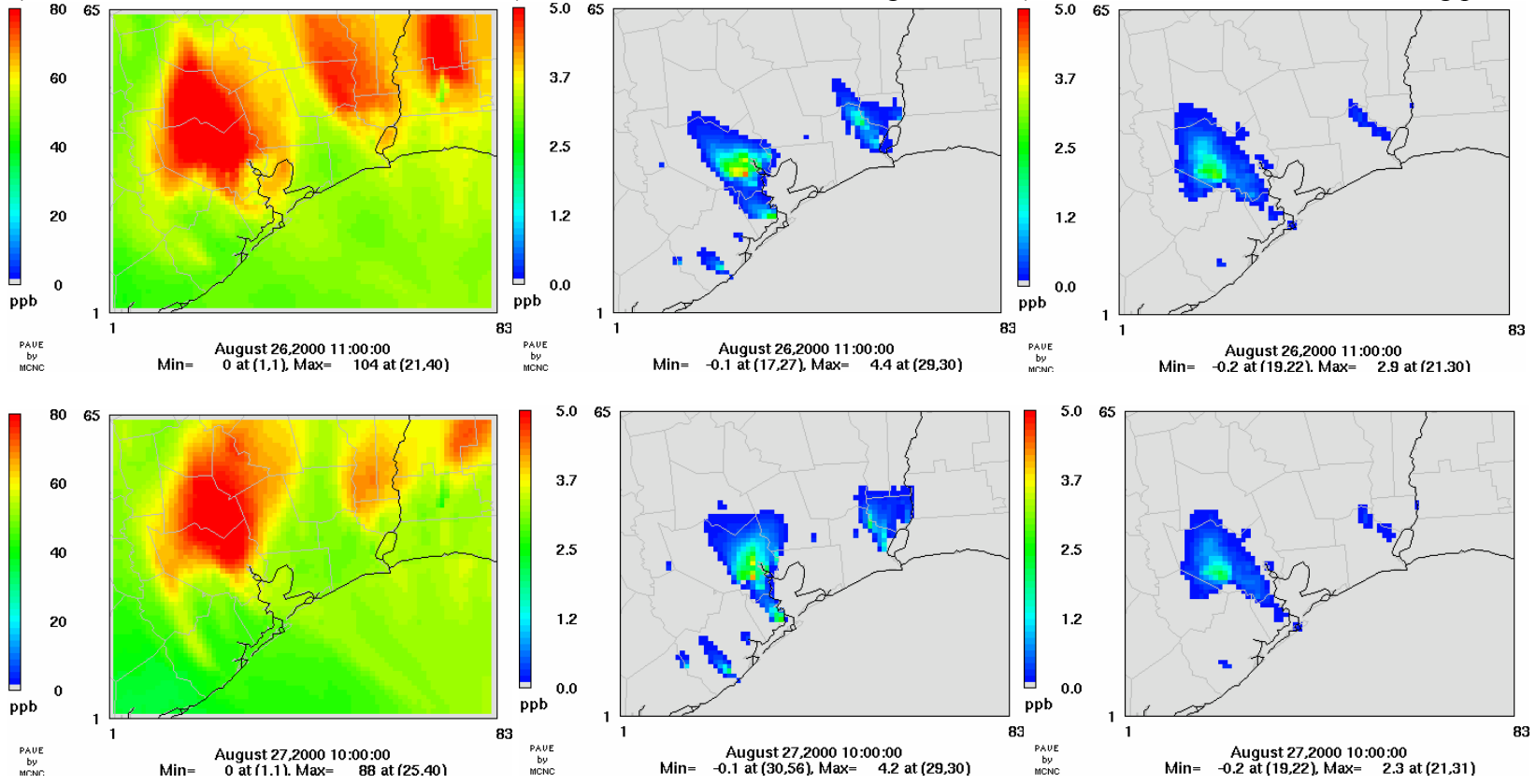

Figure C-3 8-hour averaged absolute ozone concentration and difference in 1-hour averaged ozone concentrations between chlorine basecase and chlorine basecase augmented by (b) doubling cooling tower emissions, (c) doubling swimming pools emissions at the time of the day when the maximum ozone concentration occurs.

a)absolute ozone concentration b)ozone formation due to cooling towers c) ozone formation due to swimming pools

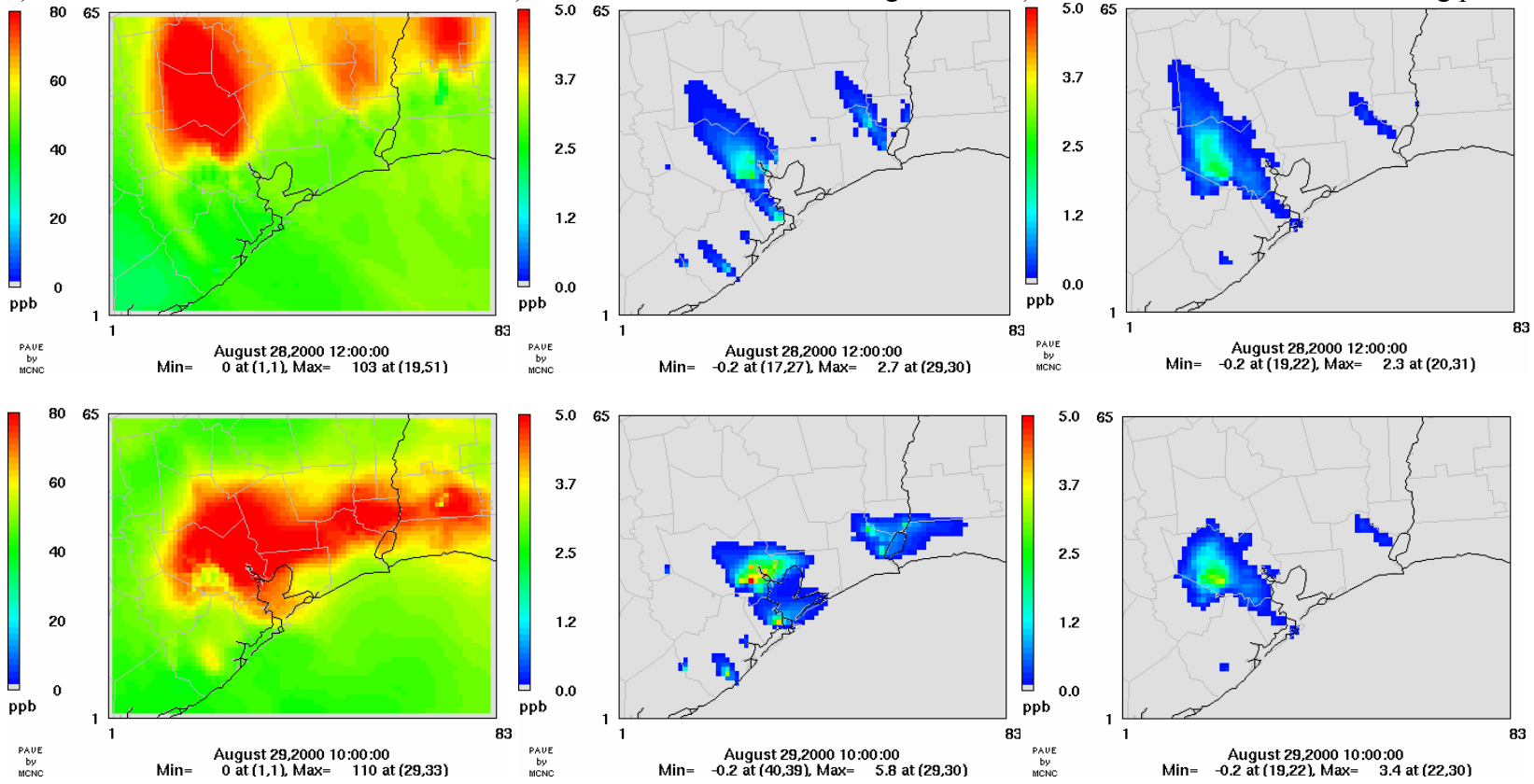

Figure C-3 8-hour averaged absolute ozone concentration and difference in 1-hour averaged ozone concentrations between chlorine basecase and chlorine basecase augmented by (b) doubling cooling tower emissions, (c) doubling swimming pools emissions at the time of the day when the maximum ozone concentration occurs.

a)absolute ozone concentration b)ozone formation due to cooling towers c) ozone formation due to swimming pools

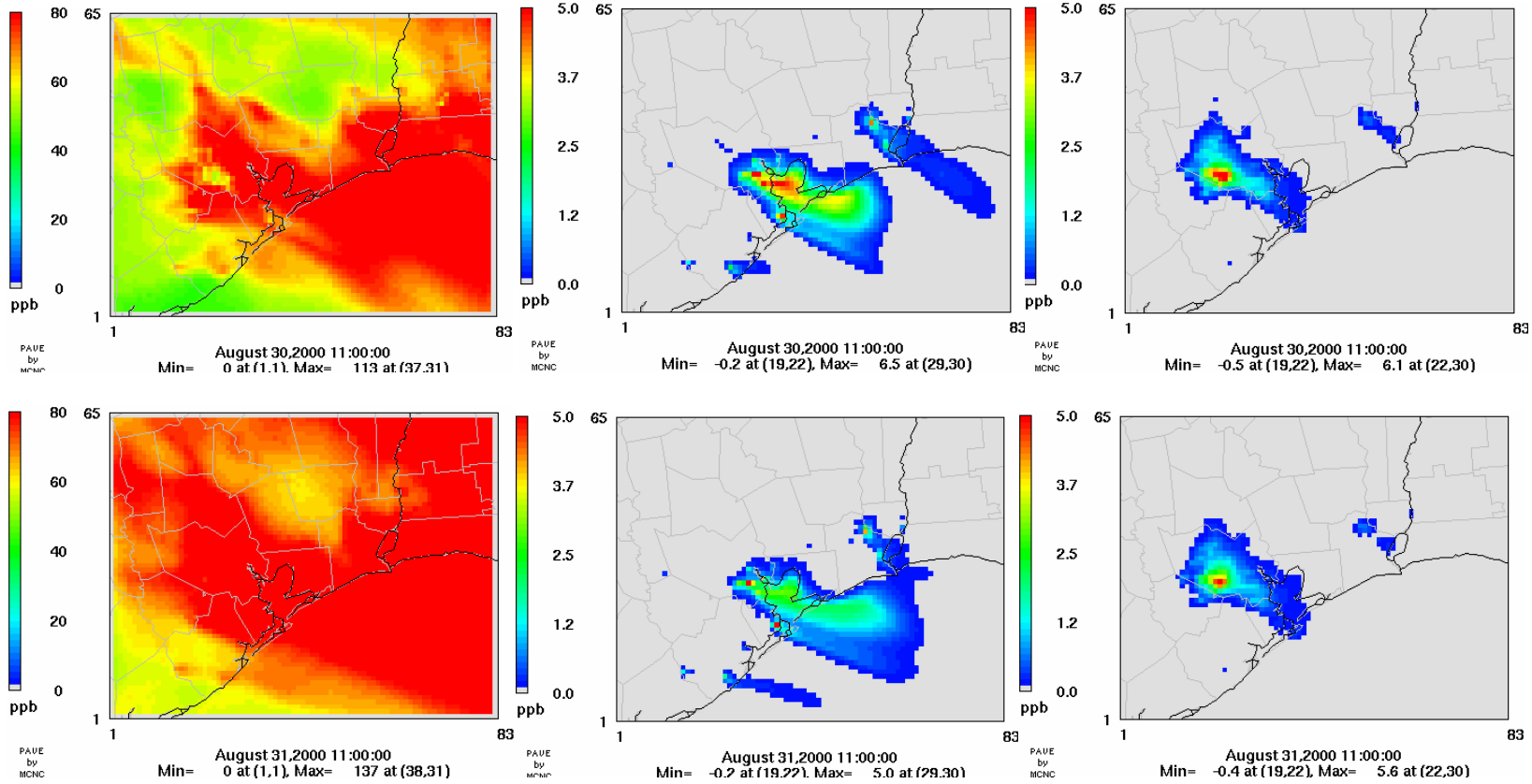

Figure C-3 8-hour averaged absolute ozone concentration and difference in 1-hour averaged ozone concentrations between chlorine basecase and chlorine basecase augmented by (b) doubling cooling tower emissions, (c) doubling swimming pools emissions at the time of the day when the maximum ozone concentration occurs.

a)absolute ozone concentration b)ozone formation due to cooling towers c) ozone formation due to swimming pools

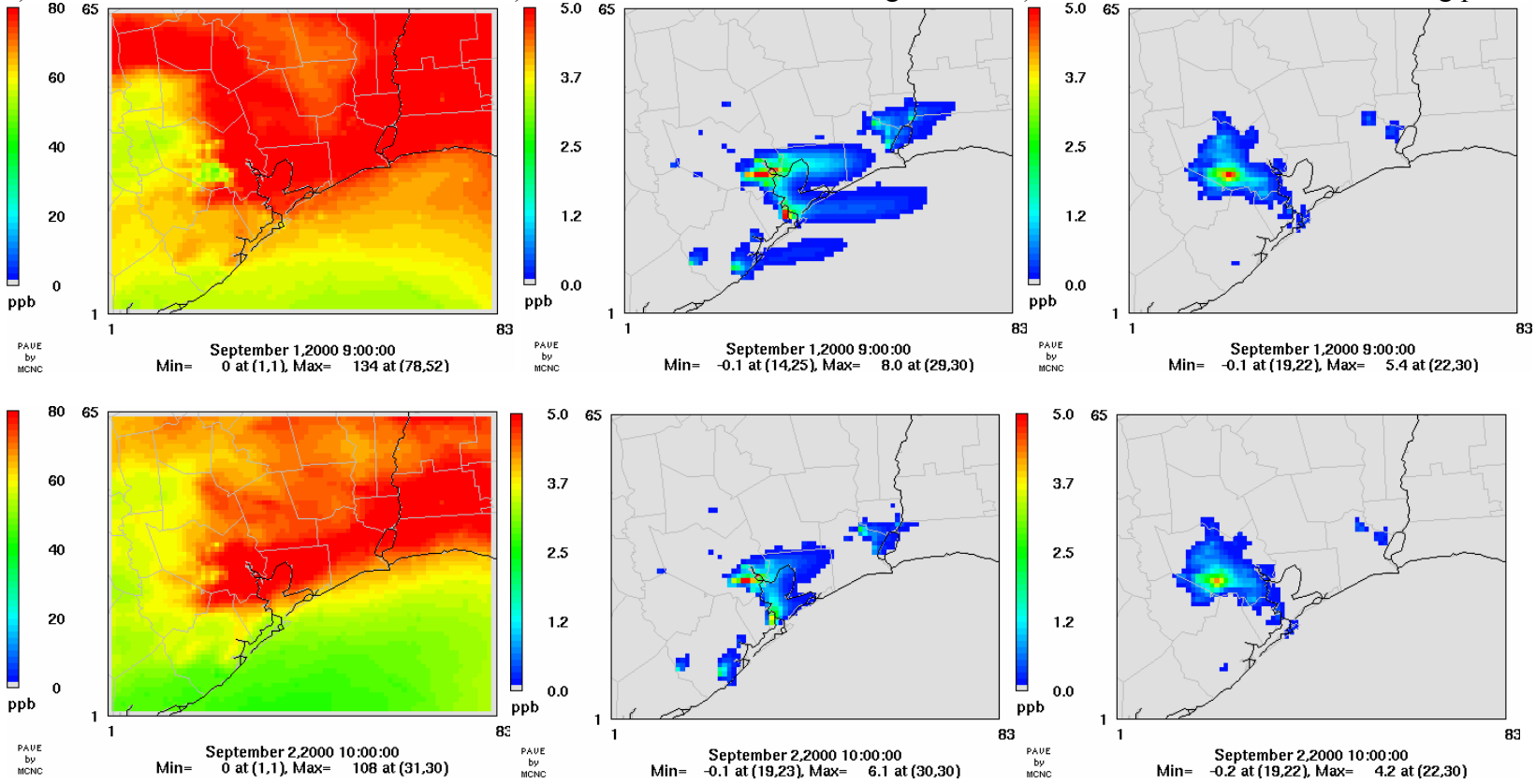

Figure C-3 8-hour averaged absolute ozone concentration and difference in 1-hour averaged ozone concentrations between chlorine basecase and chlorine basecase augmented by (b) doubling cooling tower emissions, (c) doubling swimming pools emissions at the time of the day when the maximum ozone concentration occurs.

a)absolute ozone concentration b)ozone formation due to cooling towers c) ozone formation due to swimming pools

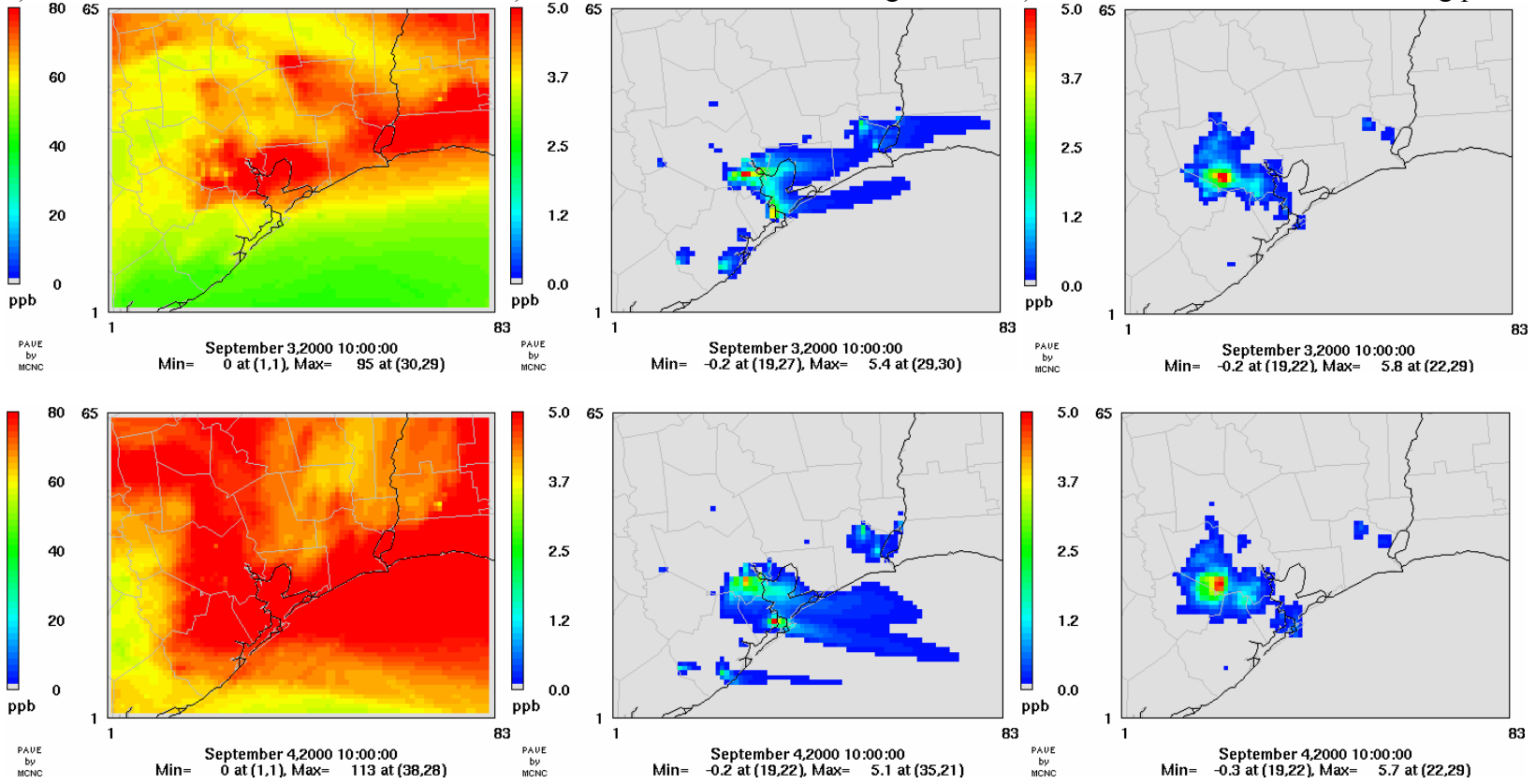

Figure C-3 8-hour averaged absolute ozone concentration and difference in 1-hour averaged ozone concentrations between chlorine basecase and chlorine basecase augmented by (b) doubling cooling tower emissions, (c) doubling swimming pools emissions at the time of the day when the maximum ozone concentration occurs.

a)absolute ozone concentration b)ozone formation due to cooling towers c) ozone formation due to swimming pools

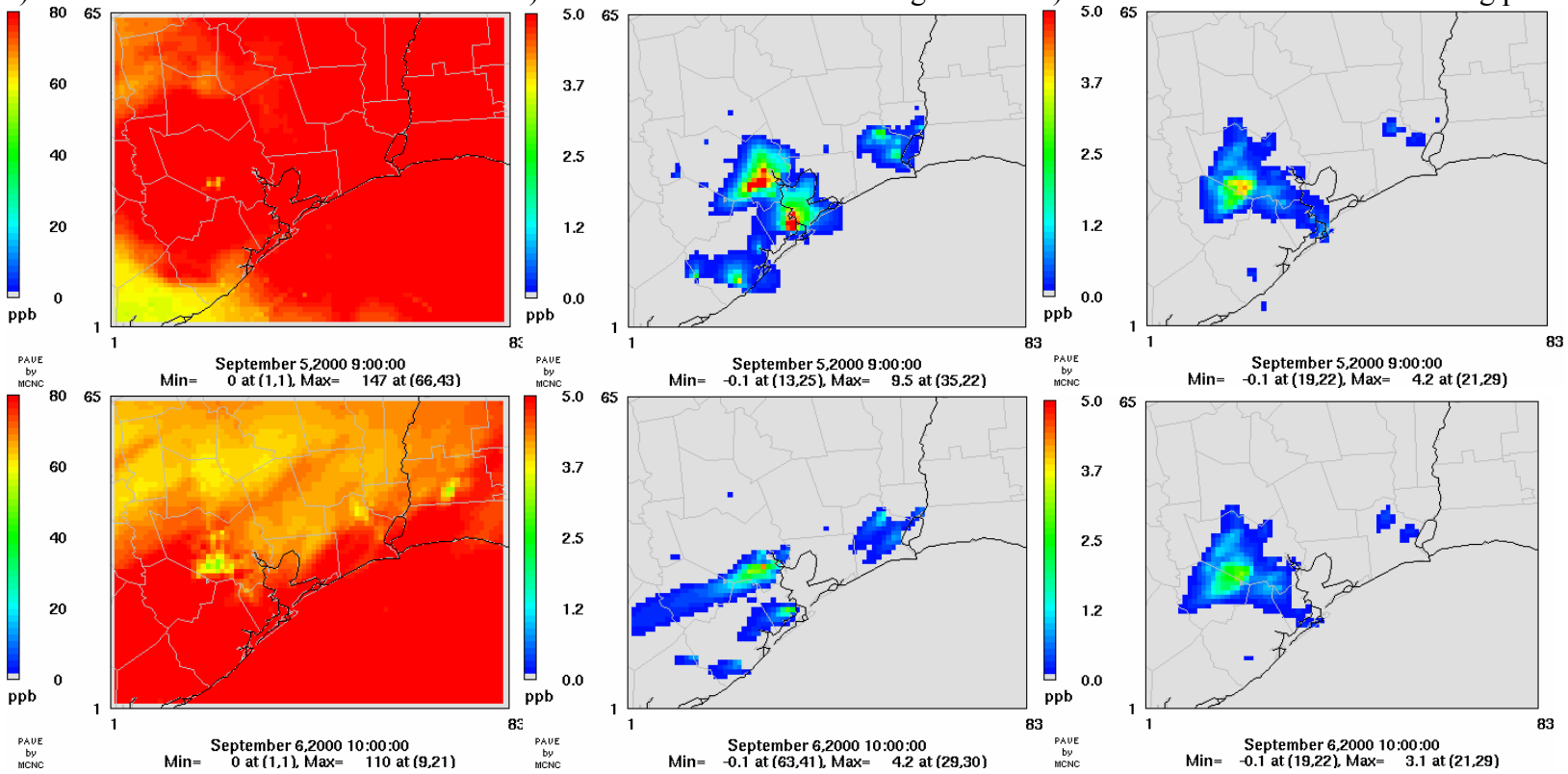

Appendix D

Isopleth diagrams for 1-hour averaged domain-wide maximum ozone concentrations with various amount of NOx/VOCs reduction:(a) case without chlorine, (b) case with chlorine

Isopleth diagrams for 8-hour averaged domain-wide maximum ozone concentrations with various amount of NO_x/VOCs reduction:(c) case without chlorine, (d) case with chlorine

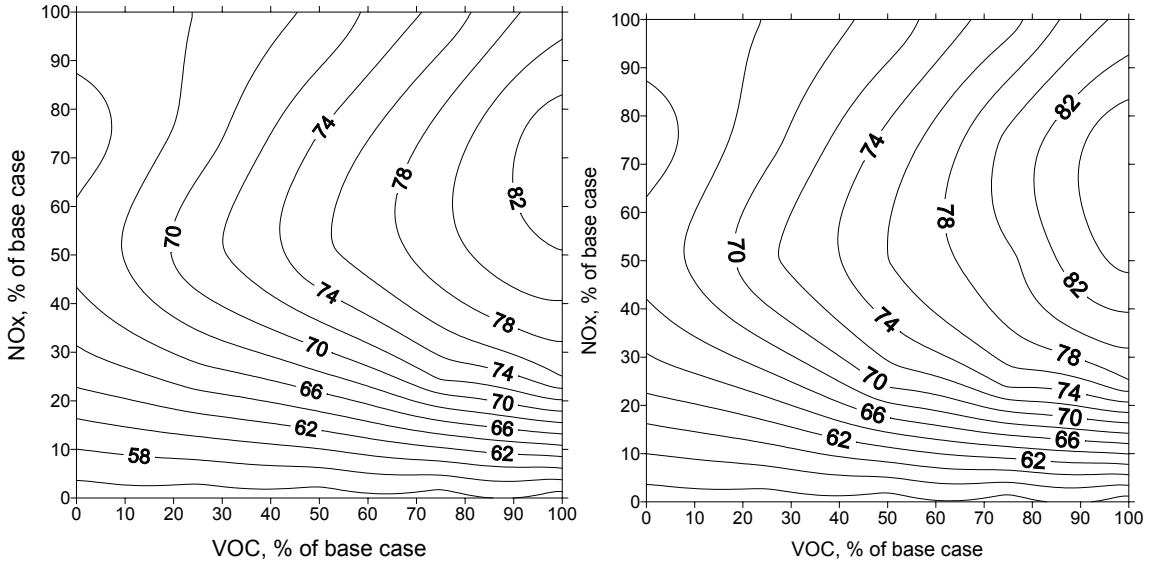

(a) 1-hour averaged ozone of basecase without Cl_2 (b) 1-hour averaged ozone of basecase with Cl_2

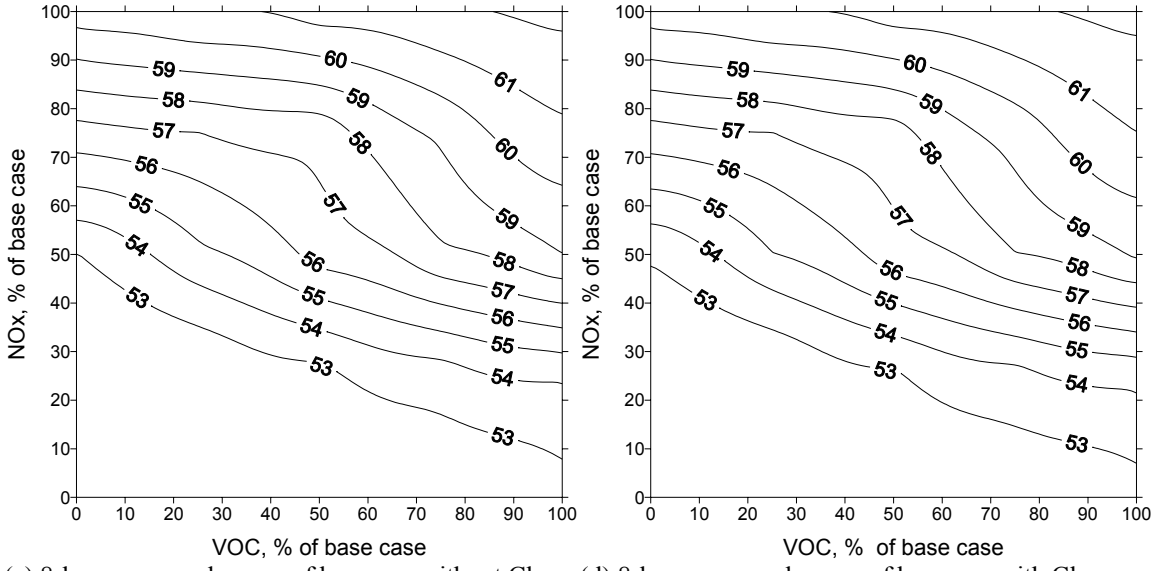

(c) 8-hour averaged ozone of basecase without Cl_2 (d) 8-hour averaged ozone of basecase with Cl_2

Figure D-1 Isopleth diagrams for 1-hour averaged domain-wide maximum ozone concentrations with various amount of NOx/VOCs reduction:(a) case without chlorine on August 24, (b) case with chlorine on August 24, Isopleth diagrams for 8-hour averaged domain-wide maximum ozone concentrations with various amount of NO_x/VOCs reduction:(c) case without chlorine on August 24, (d) case with chlorine on August 24

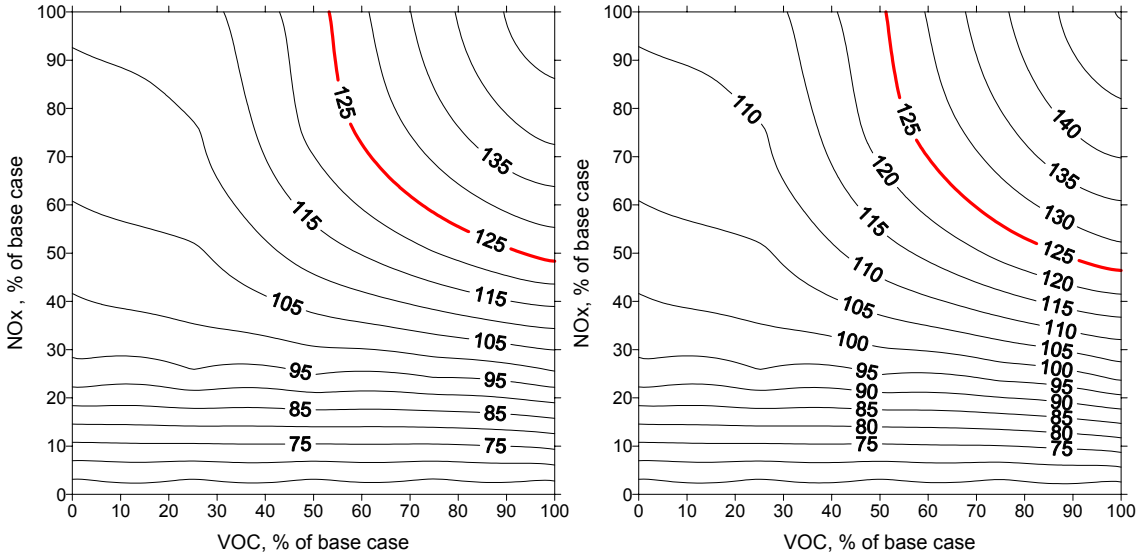

(a) 1-hour averaged ozone of basecase without Cl_2 (b) 1-hour averaged ozone of basecase with Cl_2

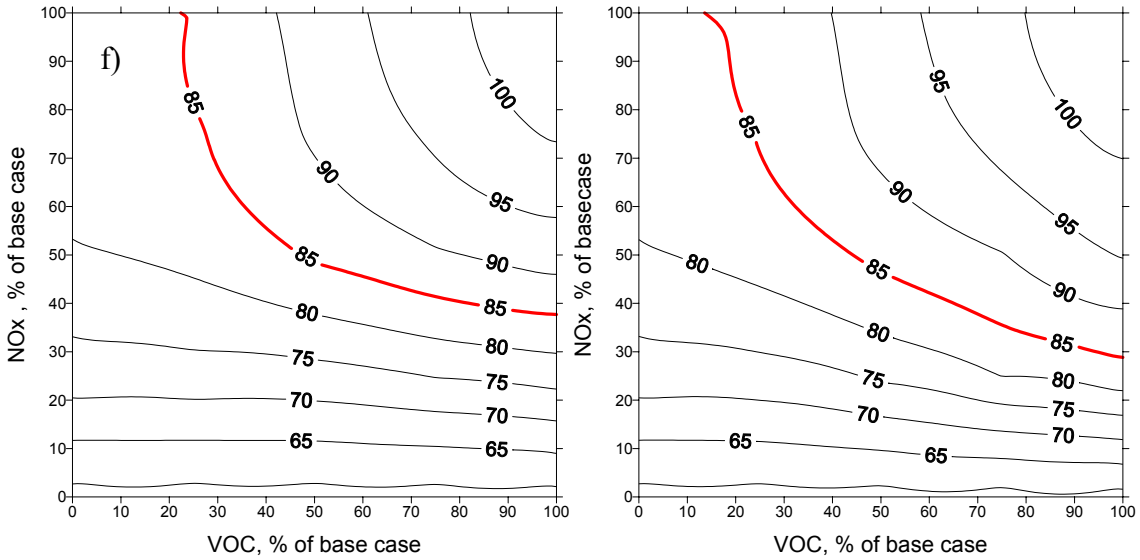

(c) 8-hour averaged ozone of basecase without Cl_2 (d) 8-hour averaged ozone of basecase with Cl_2

Figure D-2 Isopleth diagrams for 1-hour averaged domain-wide maximum ozone concentrations with various amount of NOx/VOCs reduction:(a) case without chlorine on August 26, (b) case with chlorine on August 26, Isopleth diagrams for 8-hour averaged domain-wide maximum ozone concentrations with various amount of NO_x/VOCs reduction:(c) case without chlorine on August 26, (d) case with chlorine on August 26

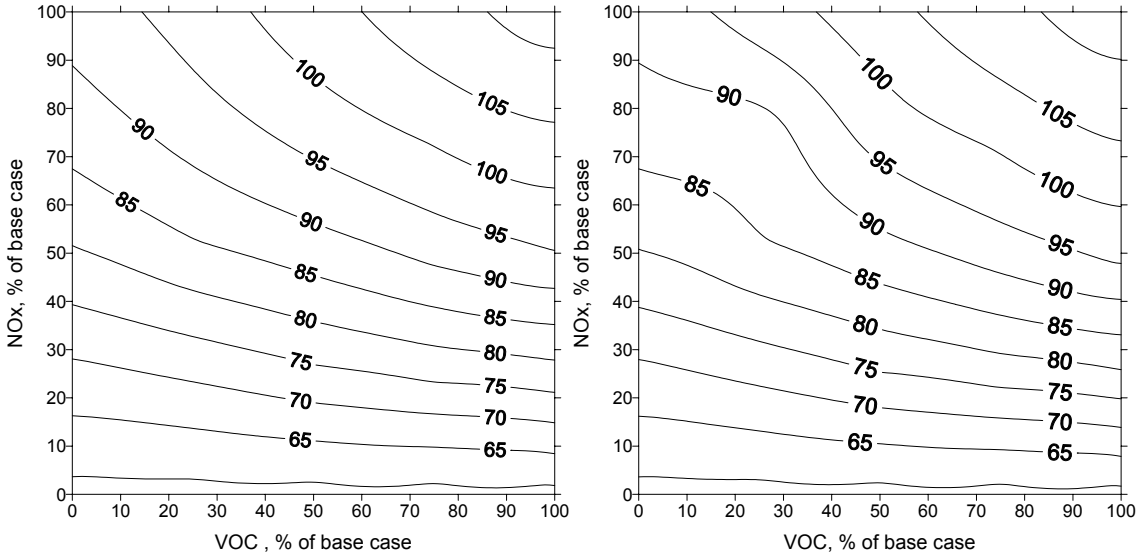

(a) 1-hour averaged ozone of basecase without Cl_2

(b) 1-hour averaged ozone of basecase with Cl_2

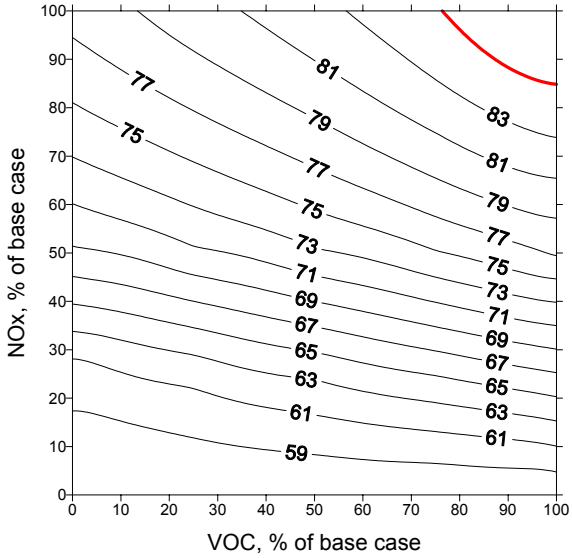

(c) 8-hour averaged ozone of basecase without Cl_2

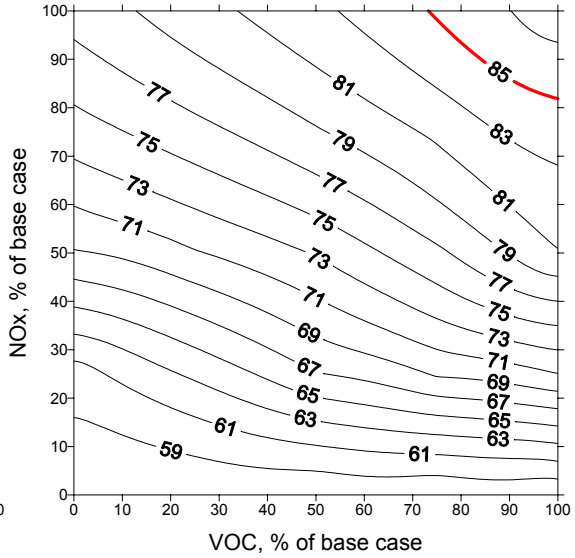

(d) 8-hour averaged ozone of basecase with Cl_2

Figure D-3 Isopleth diagrams for 1-hour averaged domain-wide maximum ozone concentrations with various amount of NOx/VOCs reduction:(a) case without chlorine on August 27, (b) case with chlorine on August 27, Isopleth diagrams for 8-hour averaged domain-wide maximum ozone concentrations with various amount of NO_x/VOCs reduction:(c) case without chlorine on August 27, (d) case with chlorine on August 27

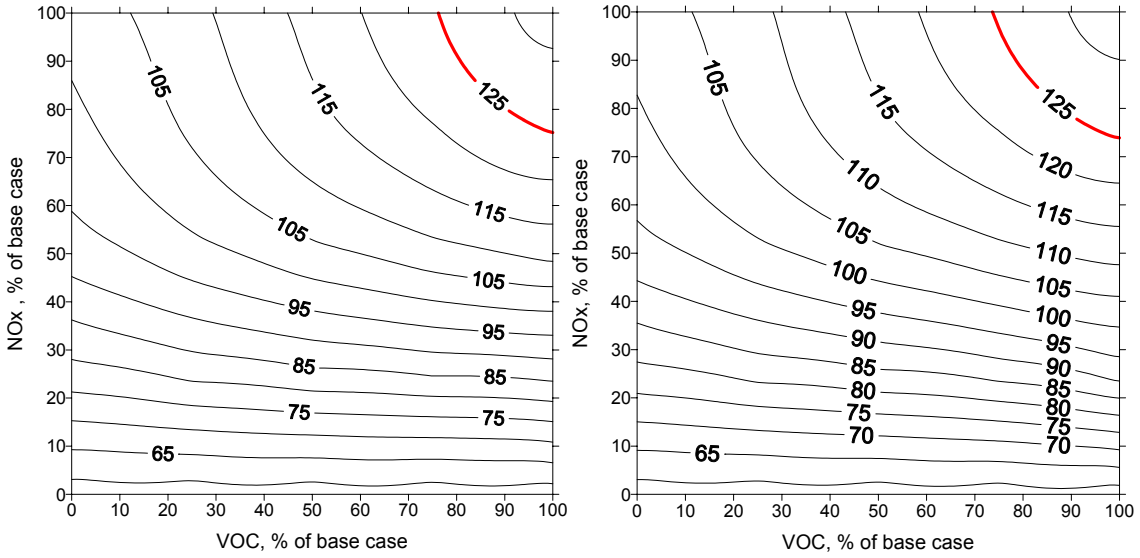

(a) 1-hour averaged ozone of basecase without Cl_2 (b) 1-hour averaged ozone of basecase with Cl_2

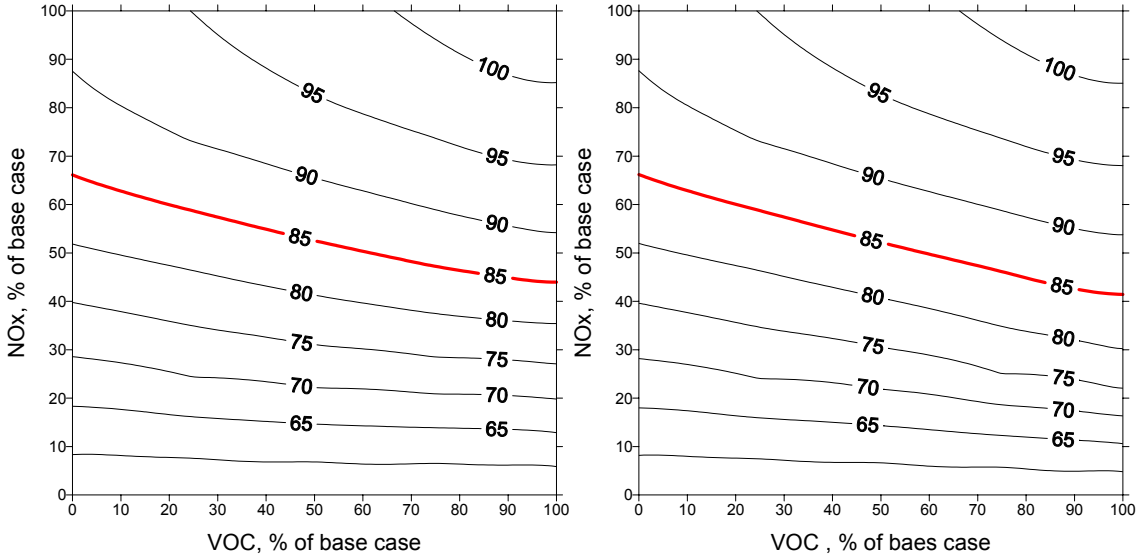

(c) 8-hour averaged ozone of basecase without Cl_2 (d) 8-hour averaged ozone of basecase with Cl_2

Figure D-4 Isopleth diagrams for 1-hour averaged domain-wide maximum ozone concentrations with various amount of NOx/VOCs reduction:(a) case without chlorine on August 28, (b) case with chlorine on August 28, Isopleth diagrams for 8-hour averaged domain-wide maximum ozone concentrations with various amount of NO_x/VOCs reduction:(c) case without chlorine on August 28, (d) case with chlorine on August 28

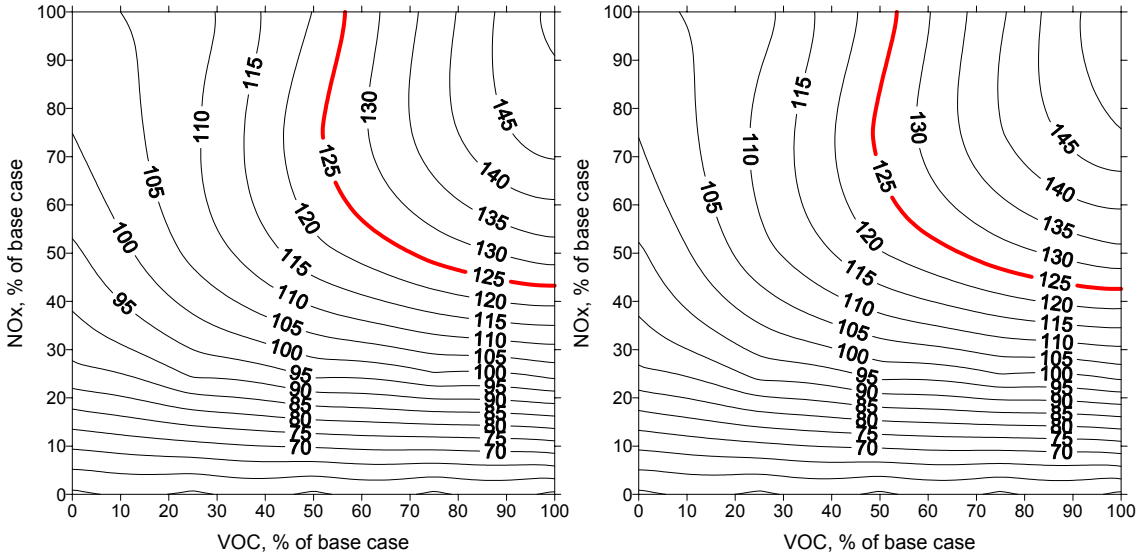

(a) 1-hour averaged ozone of basecase without Cl_2 (b) 1-hour averaged ozone of basecase with Cl_2

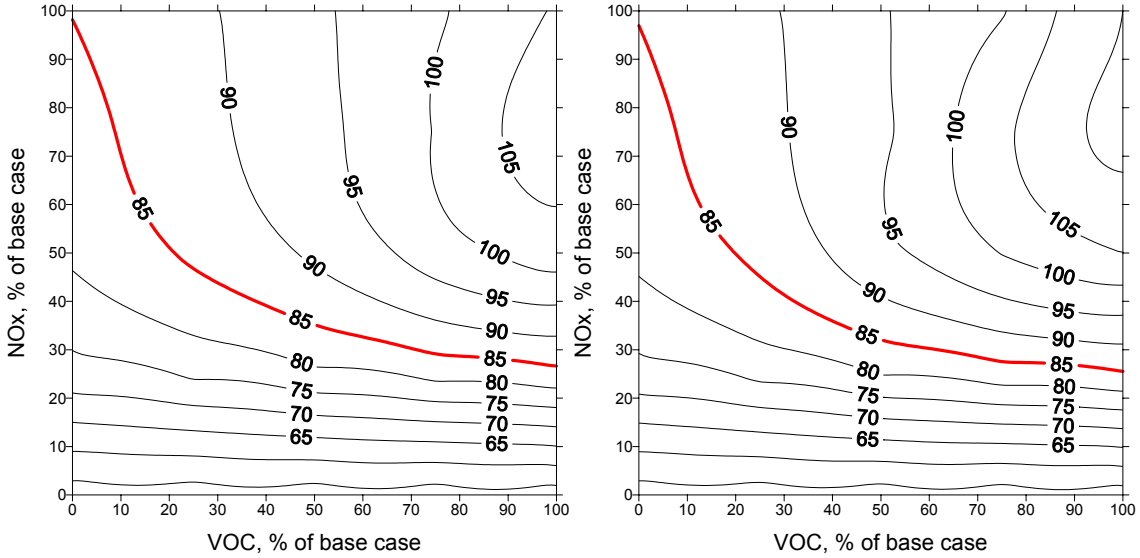

(c) 8-hour averaged ozone of basecase without Cl_2 (d) 8-hour averaged ozone of basecase with Cl_2

Figure D-5 Isopleth diagrams for 1-hour averaged domain-wide maximum ozone concentrations with various amount of NOx/VOCs reduction:(a) case without chlorine on August 29, (b) case with chlorine on August 29, Isopleth diagrams for 8-hour averaged domain-wide maximum ozone concentrations with various amount of NO_x/VOCs reduction:(c) case without chlorine on August 29, (d) case with chlorine on August 29

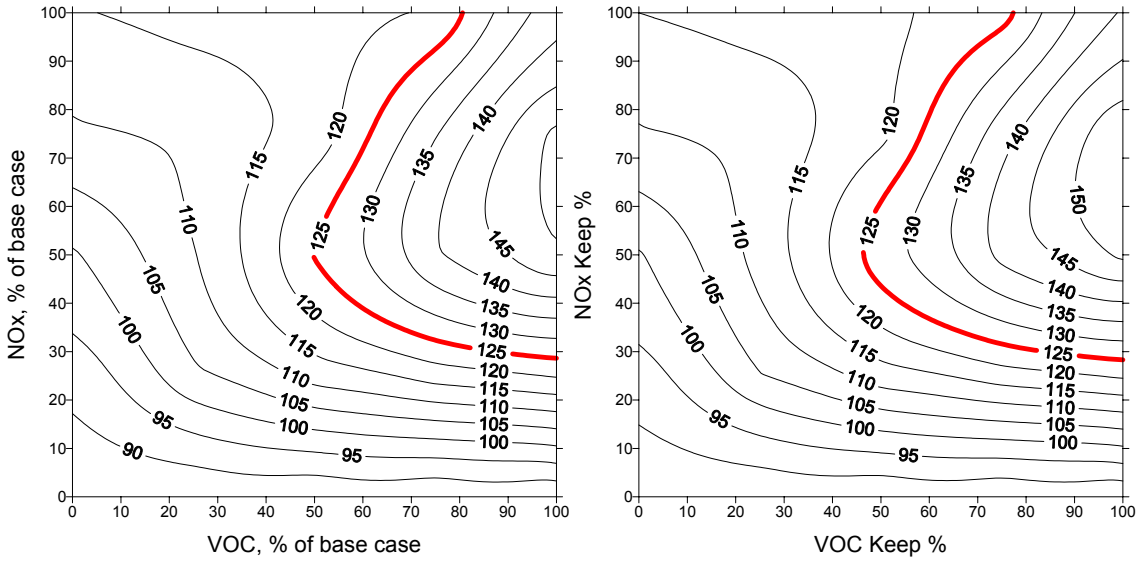

(a) 1-hour averaged ozone of basecase without Cl_2 (b) 1-hour averaged ozone of basecase with Cl_2

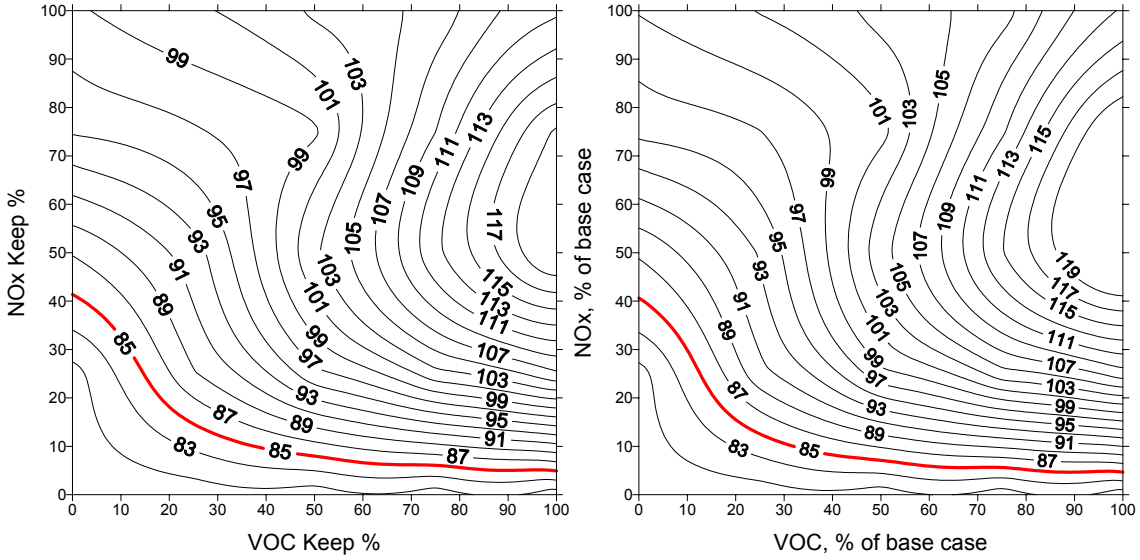

(c) 8-hour averaged ozone of basecase without Cl_2 (d) 8-hour averaged ozone of basecase with Cl_2

Figure D-6 Isopleth diagrams for 1-hour averaged domain-wide maximum ozone concentrations with various amount of NOx/VOCs reduction:(a) case without chlorine on August 30, (b) case with chlorine on August 30, Isopleth diagrams for 8-hour averaged domain-wide maximum ozone concentrations with various amount of NO_x/VOCs reduction:(c) case without chlorine on August 30, (d) case with chlorine on August 30

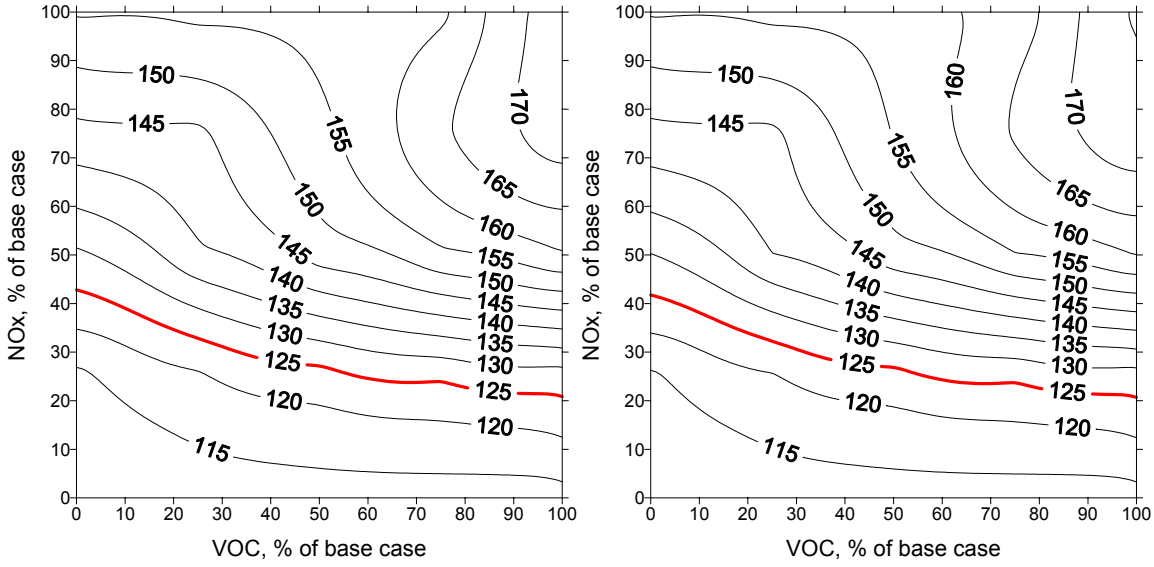

(a) 1-hour averaged ozone of basecase without Cl_2

(b) 1-hour averaged ozone of basecase with Cl_2

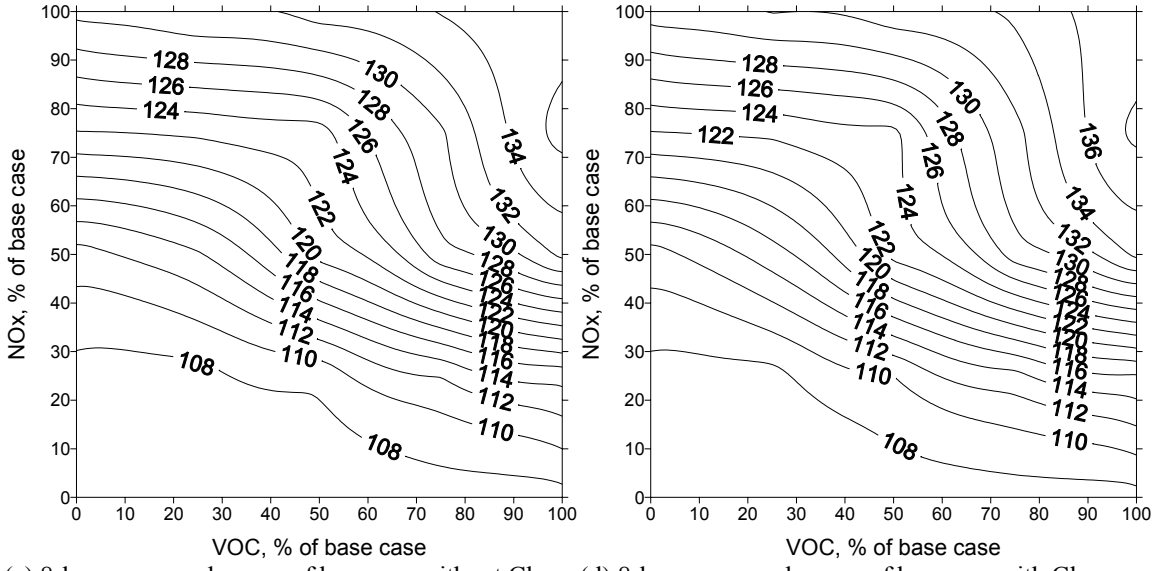

(c) 8-hour averaged ozone of basecase without Cl_2

(d) 8-hour averaged ozone of basecase with Cl_2

Figure D-7 Isopleth diagrams for 1-hour averaged domain-wide maximum ozone concentrations with various amount of NOx/VOCs reduction:(a) case without chlorine on August 31, (b) case with chlorine on August 31, Isopleth diagrams for 8-hour averaged domain-wide maximum ozone concentrations with various amount of NO_x/VOCs reduction:(c) case without chlorine on August 31, (d) case with chlorine on August 31

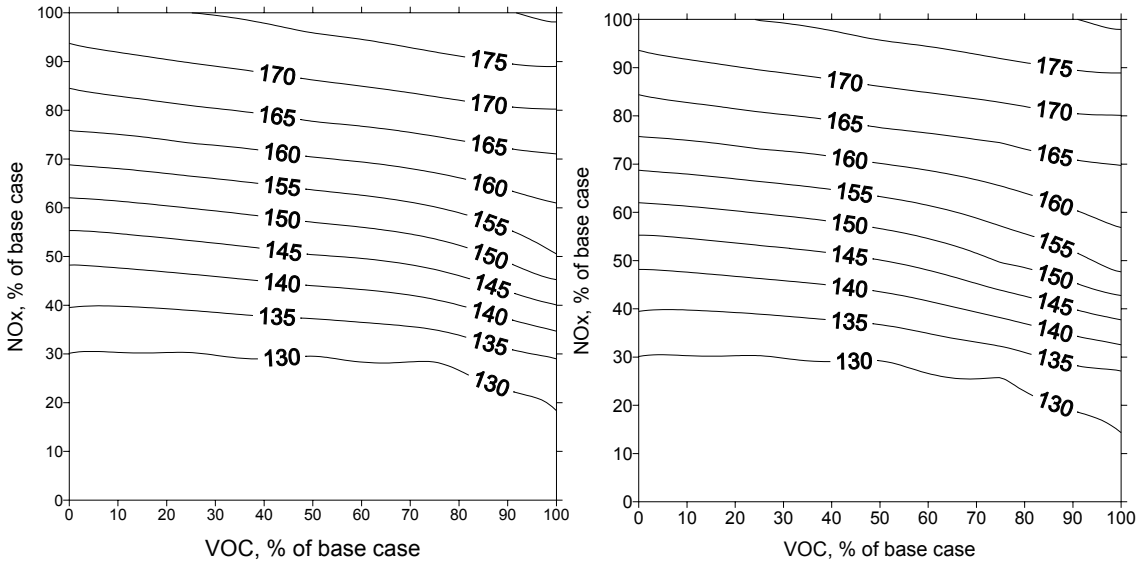

(a) 1-hour averaged ozone of basecase without Cl_2 (b) 1-hour averaged ozone of basecase with Cl_2

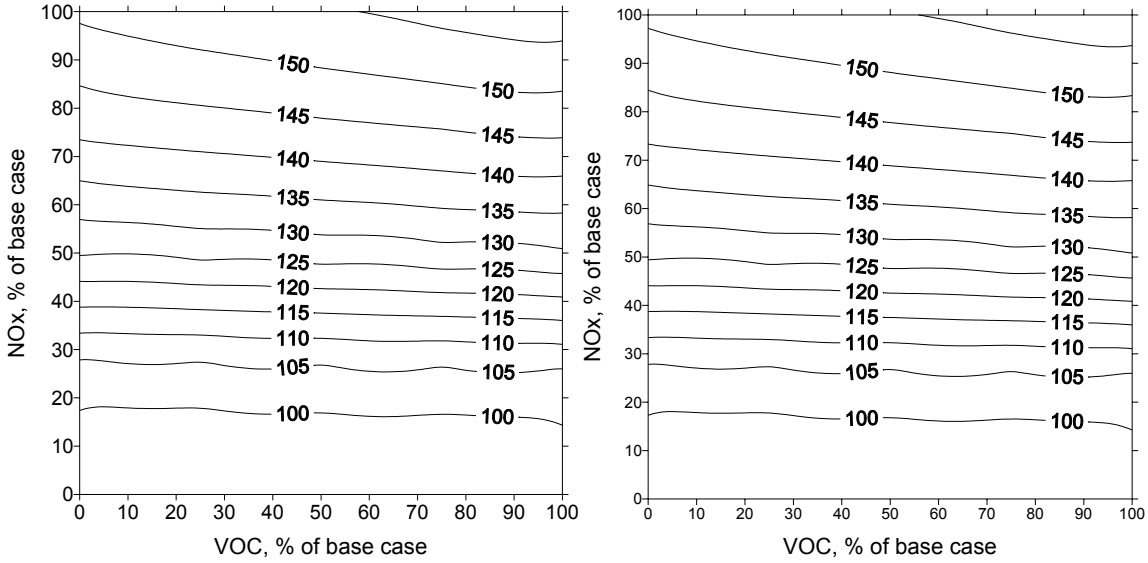

(c) 8-hour averaged ozone of basecase without Cl_2 (d) 8-hour averaged ozone of basecase with Cl_2

Figure D-8 Isopleth diagrams for 1-hour averaged domain-wide maximum ozone concentrations with various amount of NOx/VOCs reduction:(a) case without chlorine on September 1, (b) case with chlorine on September 1, Isopleth diagrams for 8-hour averaged domain-wide maximum ozone concentrations with various amount of NO_x/VOCs reduction:(c) case without chlorine on September 1, (d) case with chlorine on September 1

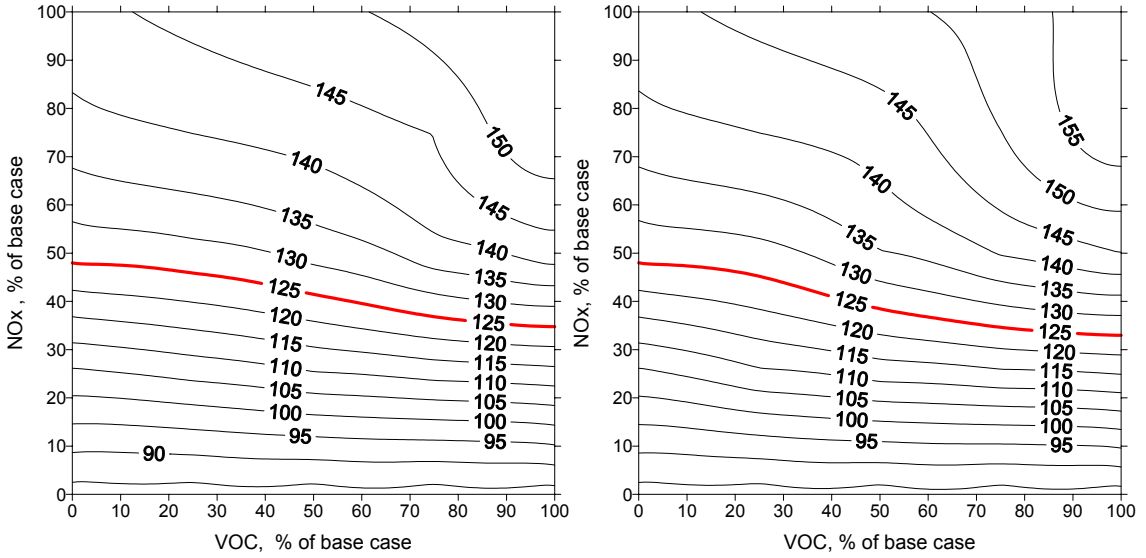

(a) 1-hour averaged ozone of basecase without Cl_2

(b) 1-hour averaged ozone of basecase with Cl_2

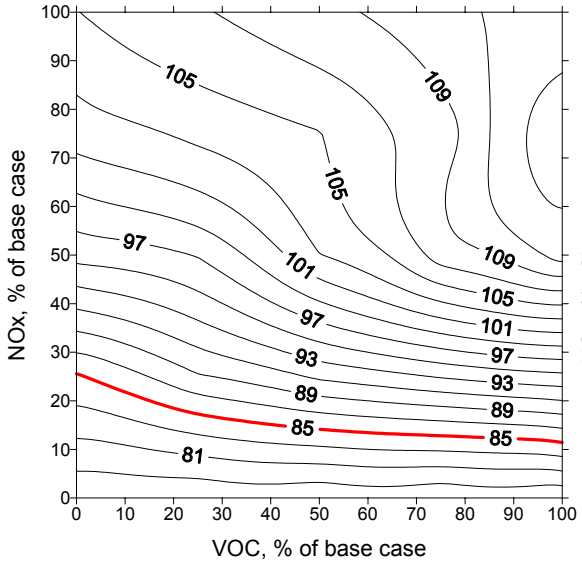

(c) 8-hour averaged ozone of basecase without Cl_2

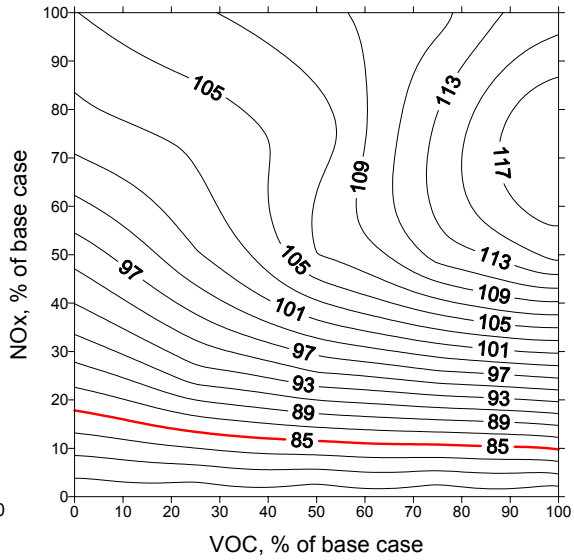

(d) 8-hour averaged ozone of basecase with Cl_2

Figure D-9 Isopleth diagrams for 1-hour averaged domain-wide maximum ozone concentrations with various amount of NOx/VOCs reduction:(a) case without chlorine on September 2, (b) case with chlorine on September 2, Isopleth diagrams for 8-hour averaged domain-wide maximum ozone concentrations with various amount of NO_x/VOCs reduction:(c) case without chlorine on September 2, (d) case with chlorine on September 2

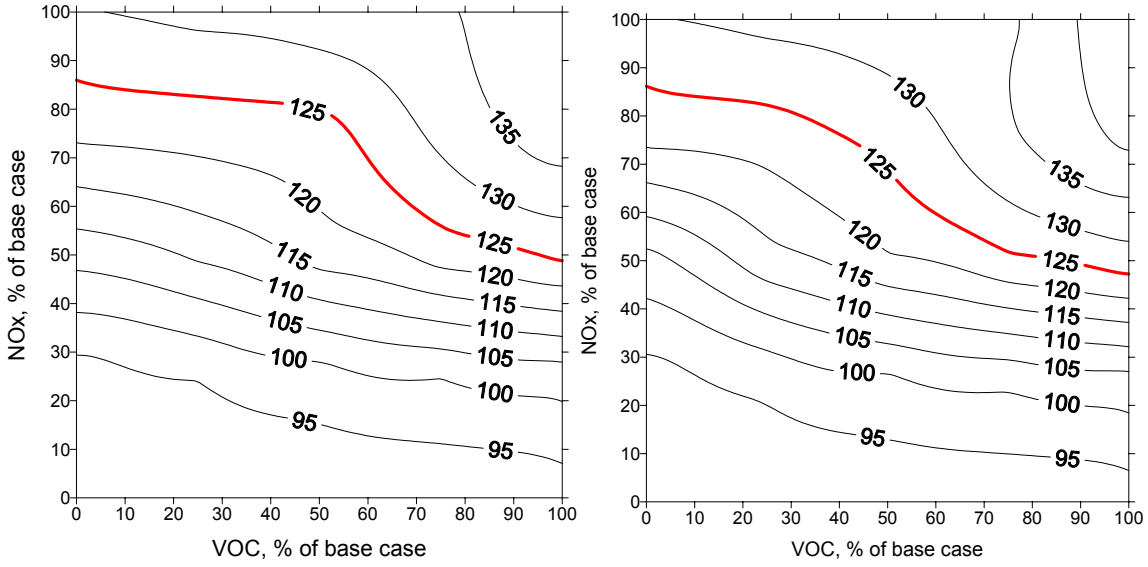

(a) 1-hour averaged ozone of basecase without Cl_2 (b) 1-hour averaged ozone of basecase with Cl_2

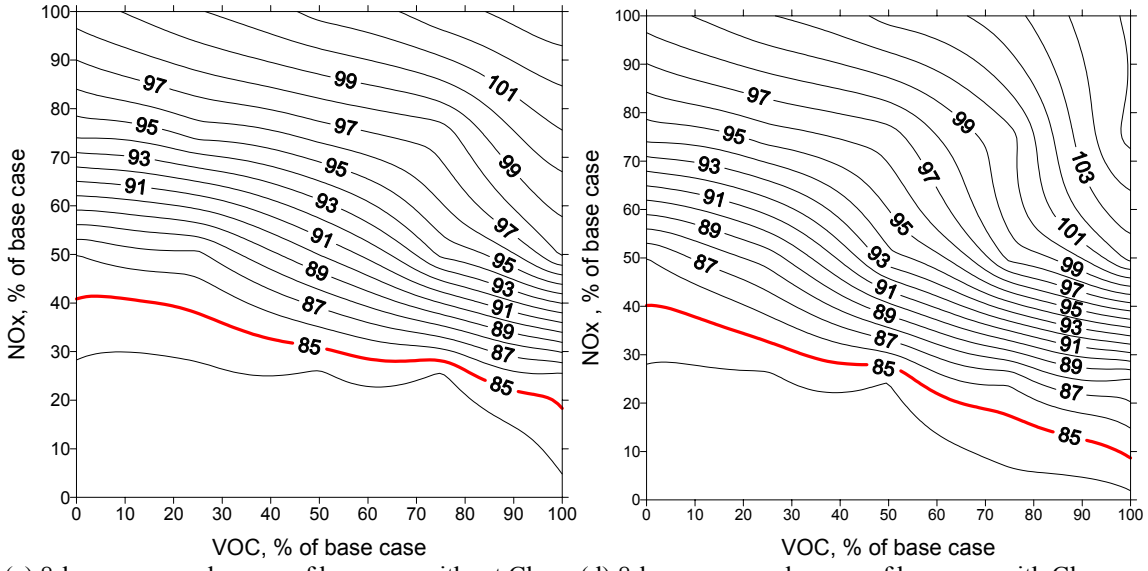

(c) 8-hour averaged ozone of basecase without Cl_2 (d) 8-hour averaged ozone of basecase with Cl_2

Figure D-10 Isopleth diagrams for 1-hour averaged domain-wide maximum ozone concentrations with various amount of NOx/VOCs reduction:(a) case without chlorine on September 3, (b) case with chlorine on September 3, Isopleth diagrams for 8-hour averaged domain-wide maximum ozone concentrations with various amount of NO_x/VOCs reduction:(c) case without chlorine on September 3, (d) case with chlorine on September 3

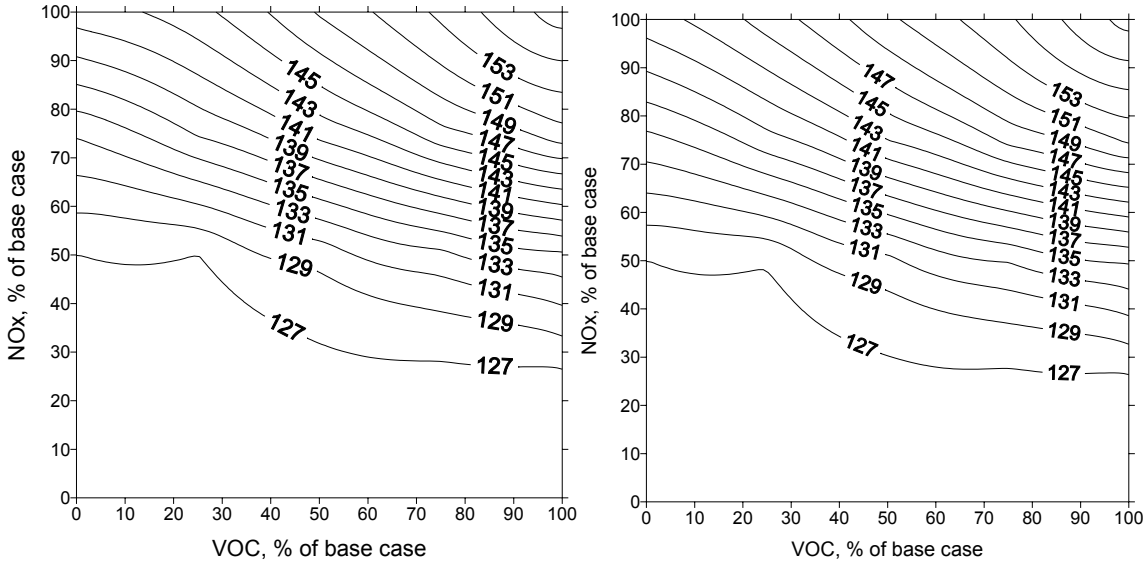

(a) 1-hour averaged ozone of basecase without Cl_2 (b) 1-hour averaged ozone of basecase with Cl_2

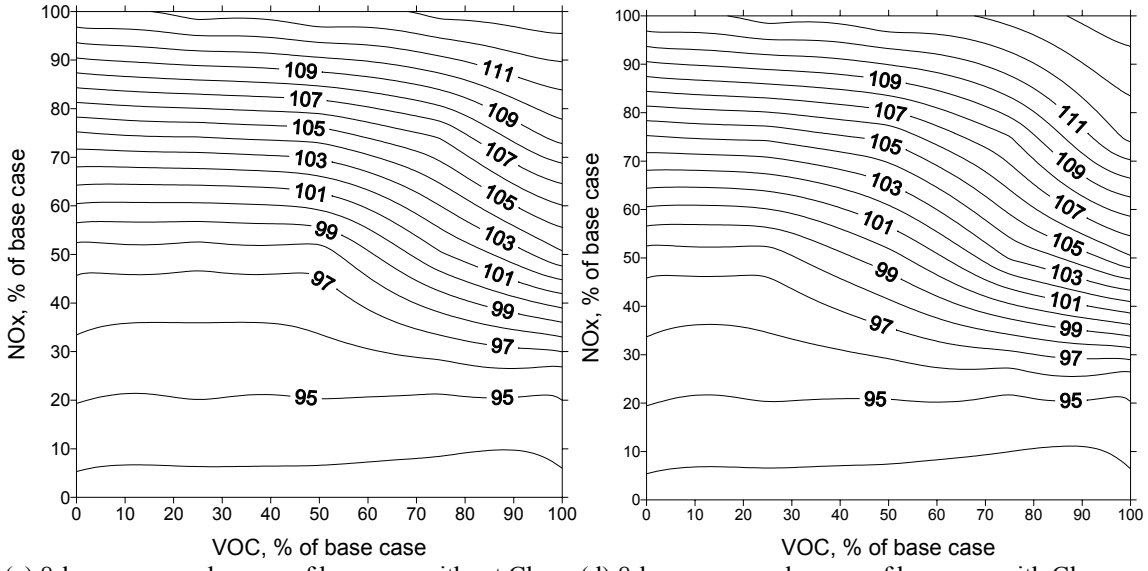

(c) 8-hour averaged ozone of basecase without Cl_2 (d) 8-hour averaged ozone of basecase with Cl_2

Figure D-11 Isopleth diagrams for 1-hour averaged domain-wide maximum ozone concentrations with various amount of NOx/VOCs reduction:(a) case without chlorine on September 4, (b) case with chlorine on September 4, Isopleth diagrams for 8-hour averaged domain-wide maximum ozone concentrations with various amount of NO_x/VOCs reduction:(c) case without chlorine on September 4, (d) case with chlorine on September 4

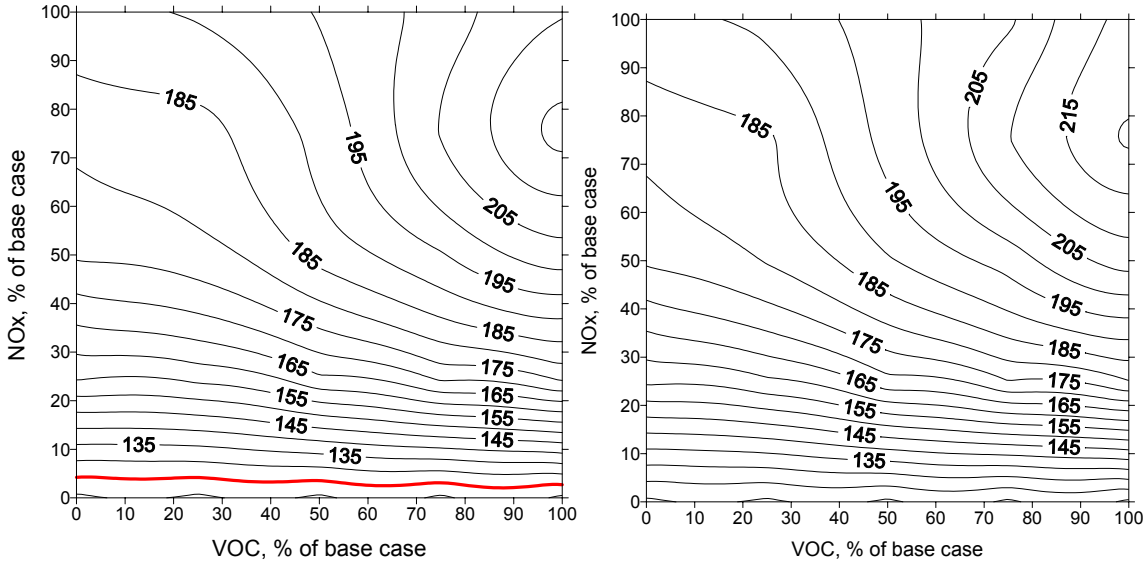

(a) 1-hour averaged ozone of basecase without Cl_2 (b) 1-hour averaged ozone of basecase with Cl_2

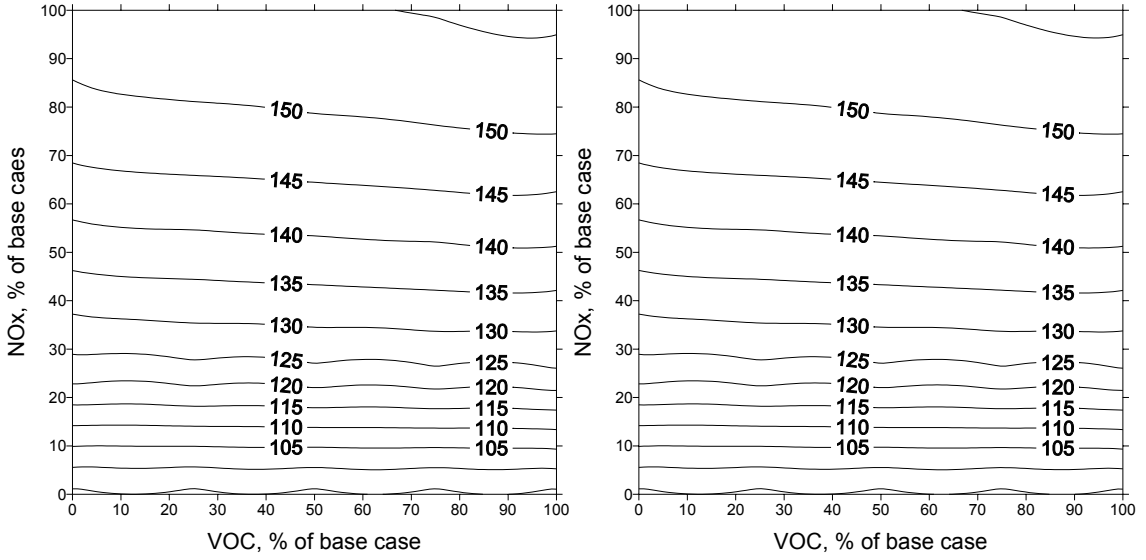

(c) 8-hour averaged ozone of basecase without Cl_2 (d) 8-hour averaged ozone of basecase with Cl_2

Figure D-12 Isopleth diagrams for 1-hour averaged domain-wide maximum ozone concentrations with various amount of NOx/VOCs reduction:(a) case without chlorine on September 5, (b) case with chlorine on September 5, Isopleth diagrams for 8-hour averaged domain-wide maximum ozone concentrations with various amount of NO_x/VOCs reduction:(c) case without chlorine on September 5, (d) case with chlorine on September 5

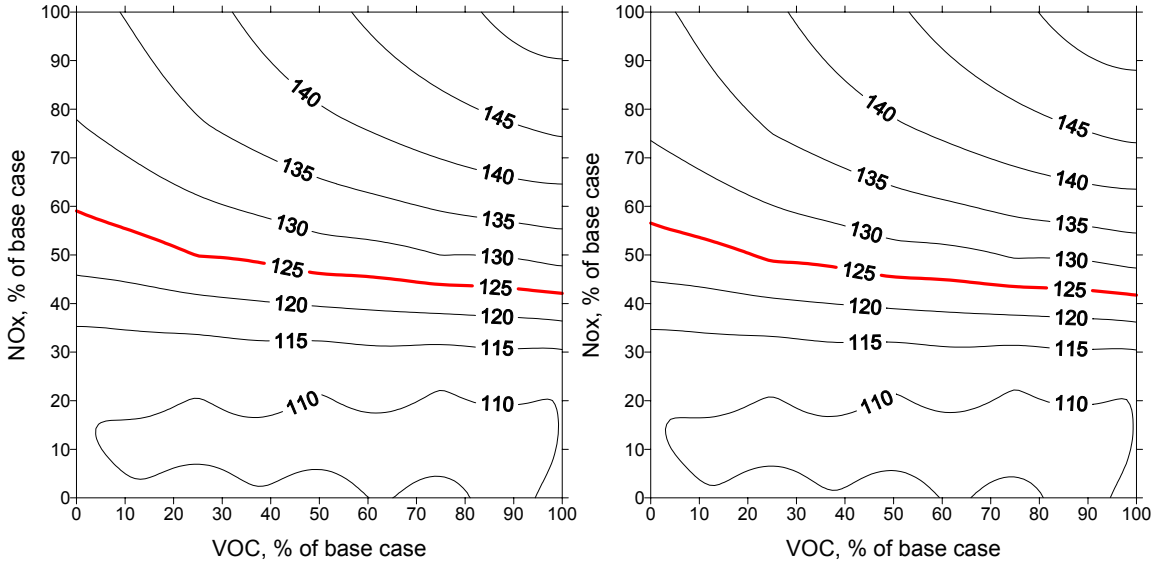

(a) 1-hour averaged ozone of basecase without Cl_2

(b) 1-hour averaged ozone of basecase with Cl_2

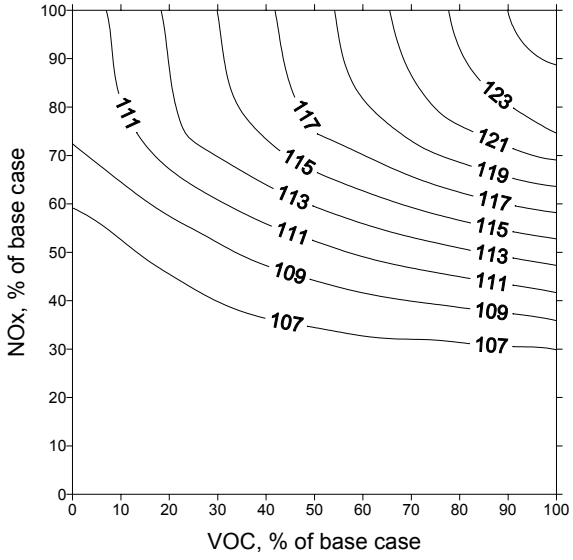

(c) 8-hour averaged ozone of basecase without Cl_2

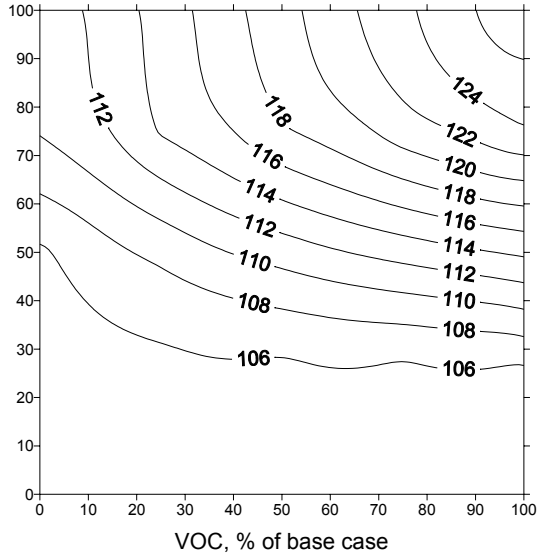

(d) 8-hour averaged ozone of basecase with Cl_2

Figure D-13 Isopleth diagrams for 1-hour averaged domain-wide maximum ozone concentrations with various amount of NOx/VOCs reduction:(a) case without chlorine on September 6, (b) case with chlorine on September 6, Isopleth diagrams for 8-hour averaged domain-wide maximum ozone concentrations with various amount of NO_x/VOCs reduction:(c) case without chlorine on September 6, (d) case with chlorine on September 6

Appendix E

Table E-1 Toxic Release Inventory (TRI) On-site Air Emissions Released (lbs/year) for facilities in all industries: Hydrochloric Acid (HCl) in Harris County, Texas

Figure E-1 Total particle chloride formation at 0600 and 0700 for entire episode

Table E-1 Toxic Release Inventory (TRI) On-site Air Emissions Released (lbs/year) for facilities in all industries: Hydrochloric Acid (HCl) in Harris County, Texas

	Facility	Address	City	**2000**	**2001**	**2002**	**2003**
1	ALBEMARLE CORP HOUSTON PLANT	2500 N S ST	PASADENA	29547	15565	11443	16758
2	CLEAN HARBORS DEER PARK LP	2027 BATTLEGROUND RD	DEER PARK	2160	1348	1423	1372
3	CROWN CENTRAL PETROLEUM CORP HOUSTON REFINERY	111 RED BLUFF RD	PASADENA	7008	7008	7008	7000
4	DEER PARK REFINING LTD PAR	5900 HWY 225	DEER PARK	0	44000	0	0
5	DOW CHEMICAL CO LA PORTE	550 BATTLEGROUND RD STE RESPONSIBLE CARE	LA PORTE	21	3785	2776	.
6	ENGELHARD PASADENA	10001CHEMICAL RD	PASADENA	15805	.	.	.
7	ETHYL CORP	1000 N S AVE	PASADENA	1912	500	1645	1707
8	EXXONMOBIL BAYTOWN CHEMICAL PLANT	5000 BAYWAY DR	BAYTOWN	254623	459715	446808	210939
9	EXXONMOBIL REFINING & SUPPLY BAYTOWN REFINERY	2800 DECKER DR	BAYTOWN	18984	21644	158000	154100
10	GALVANIZING SERVICES CO INC	7601 HARRISBURG	HOUSTON	1201	764	764	
11	K-T GALVANIZING CO	5105 E 3RD ST	KATY	823	914	1184	1123
12	KANEKA TEXAS CORP	6161 UNDERWOOD RD	PASADENA	2700	2700	2700	2700
13	LONGHORN GLASS	4202 FIDELITY ST	HOUSTON	.	.	33160	34364
14	LUBRIZOL CORP DEER PARK FACILITY	41 TIDAL RD	DEER PARK	30348	24223	26892	21623
15	MATHESON TRI-GAS INC	1920 WEST FAIRMONT PARKWAY	LA PORTE	755	255	755	755
16	MEMC PASADENA INC	3000 N S ST	PASADENA	750	750	1030	1075
17	MERCHANT METALS	4901 LANGLEY ROAD	HOUSTON	809	413	407	1029
18	OXY VINYLS L.P DEER PARK VCM PLANT	851 TIDAL RD	DEER PARK	5838	10125	10279	7371
19	OXY VINYLS LP LA PORTE VCM PLANT	2400 MILLER CUTOFF RD	LA PORTE	13003	12267	17674	18806
20	OXY VINYLS LP DEER PARK C/A	1000 TIDAL RD.	DEER PARK	2437	2535	36	36
21	PPG INDUSTRIES INC	1901 AVE H & 16TH ST	LA PORTE		250	250	12
22	RHODIA INC	8615 MANCHESTER ST	HOUSTON	121	247	402	298
23	RHODIA INC	3439 PARK ST	BAYTOWN	333	49	56	235
24	ROHM & HASS CO BAYPORT PLANT	13300 BAY AREA BLVD	LA PORTE	.	.	74	321
25	SOUTHWEST GALVANIZING INC	737 ALEEN ST	HOUSTON	373	296	104	163
26	UNITED GALVANIZING INC	6123 CUNNINGHAM RD	HOUSTON	12576	4171	5482	3700
27	VOPAK LOGISTICS SERVICES USA INC	2759 BATTLEGROUND RD	DEER PARK	.	.	10633	9168

Table E-1 (Cont'd) Toxic Release Inventory (TRI) On-site Air Emissions Released (lbs/year) for facilities in all industries: Hydrochloric Acid (HCl) in Harris County, TX

Facility	2000	2001	2002	2003
Total (pounds/year)	**402156**	**613552**	**741029**	**494697**
Total (metric tons/day)	**0.501**	**0.764**	**0.923**	**0.616**

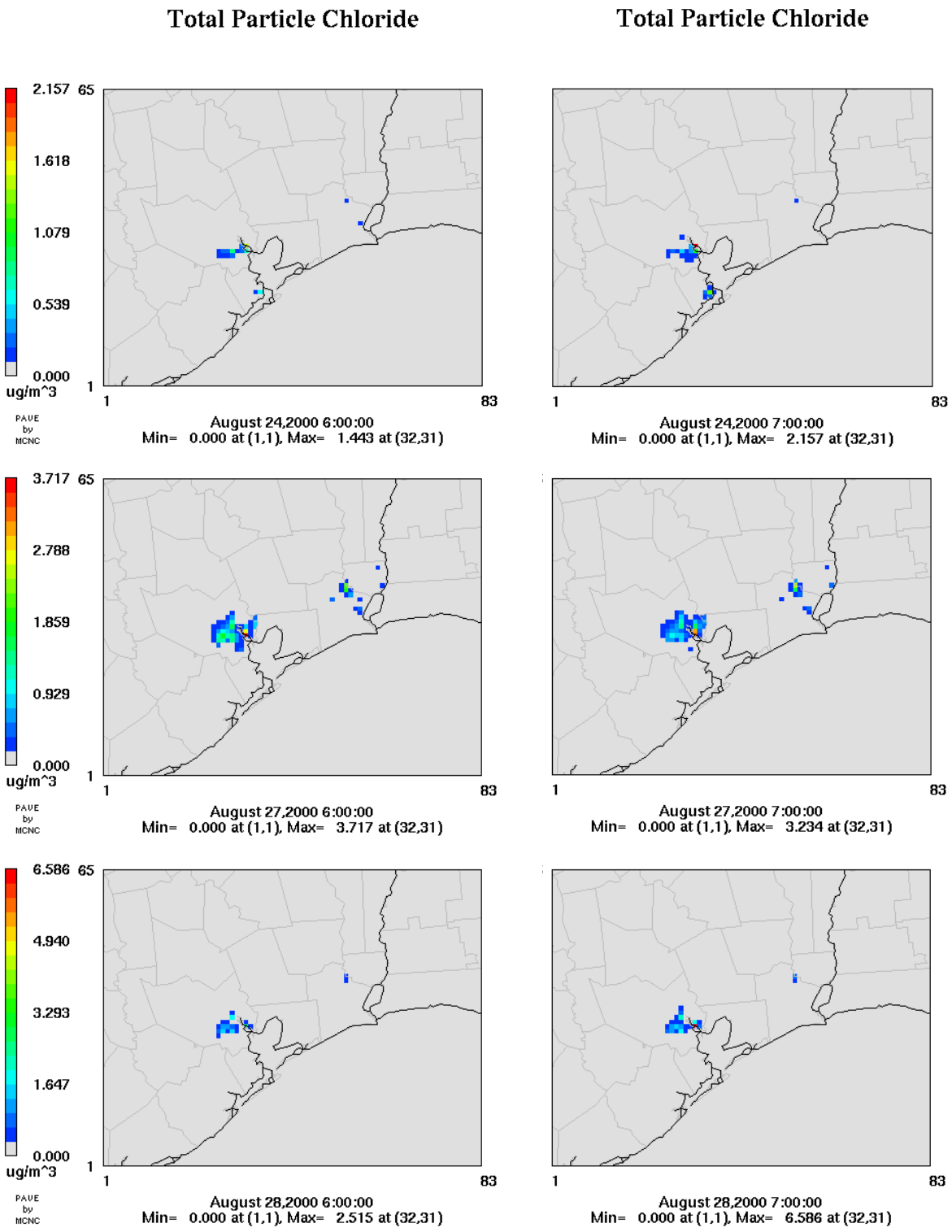

Figure E-1 Total particle chloride formation at 0600 and 0700 for entire episode

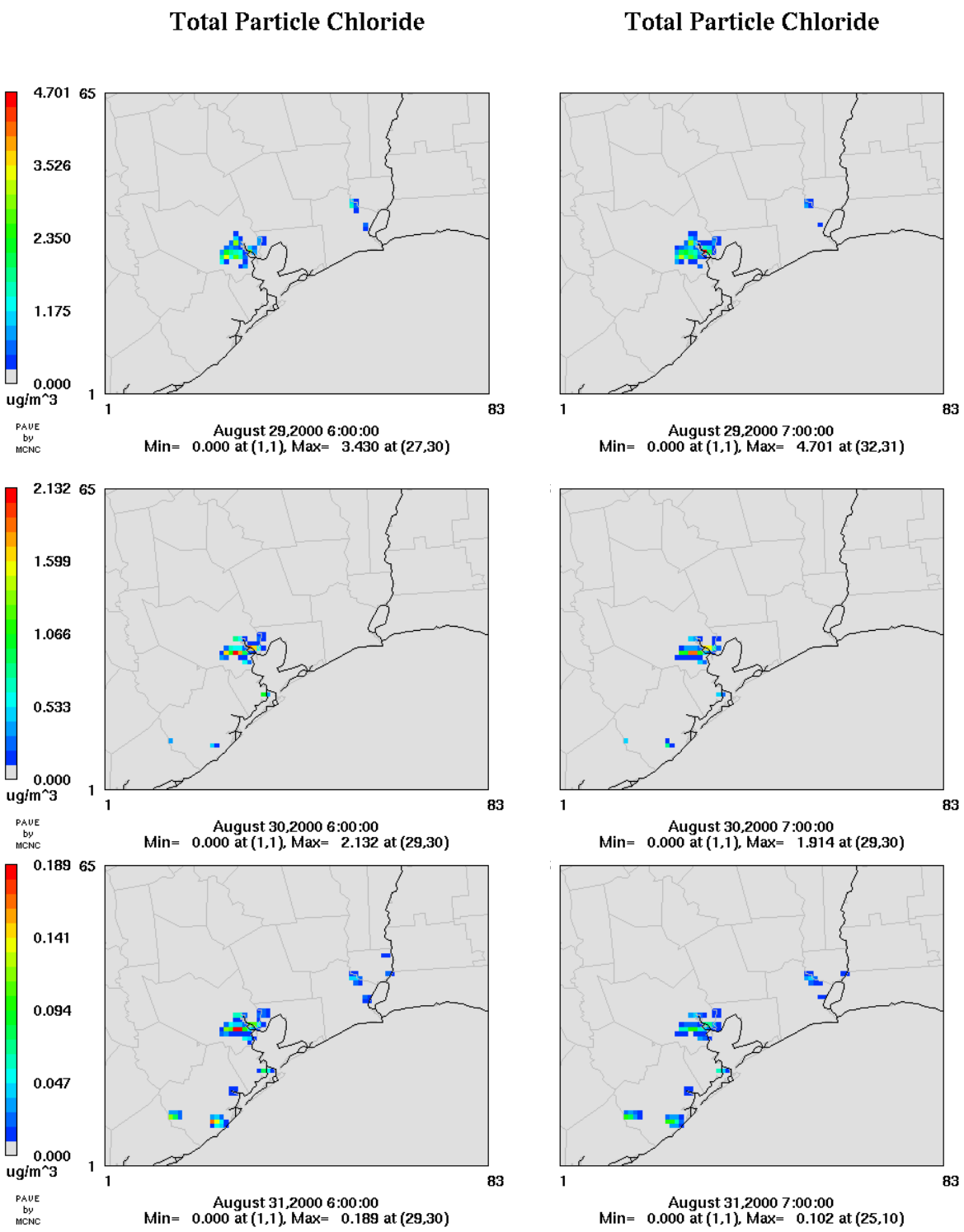

Figure E-1 (Cont'd) Total particle chloride formation at 0600 and 0700 for entire episode

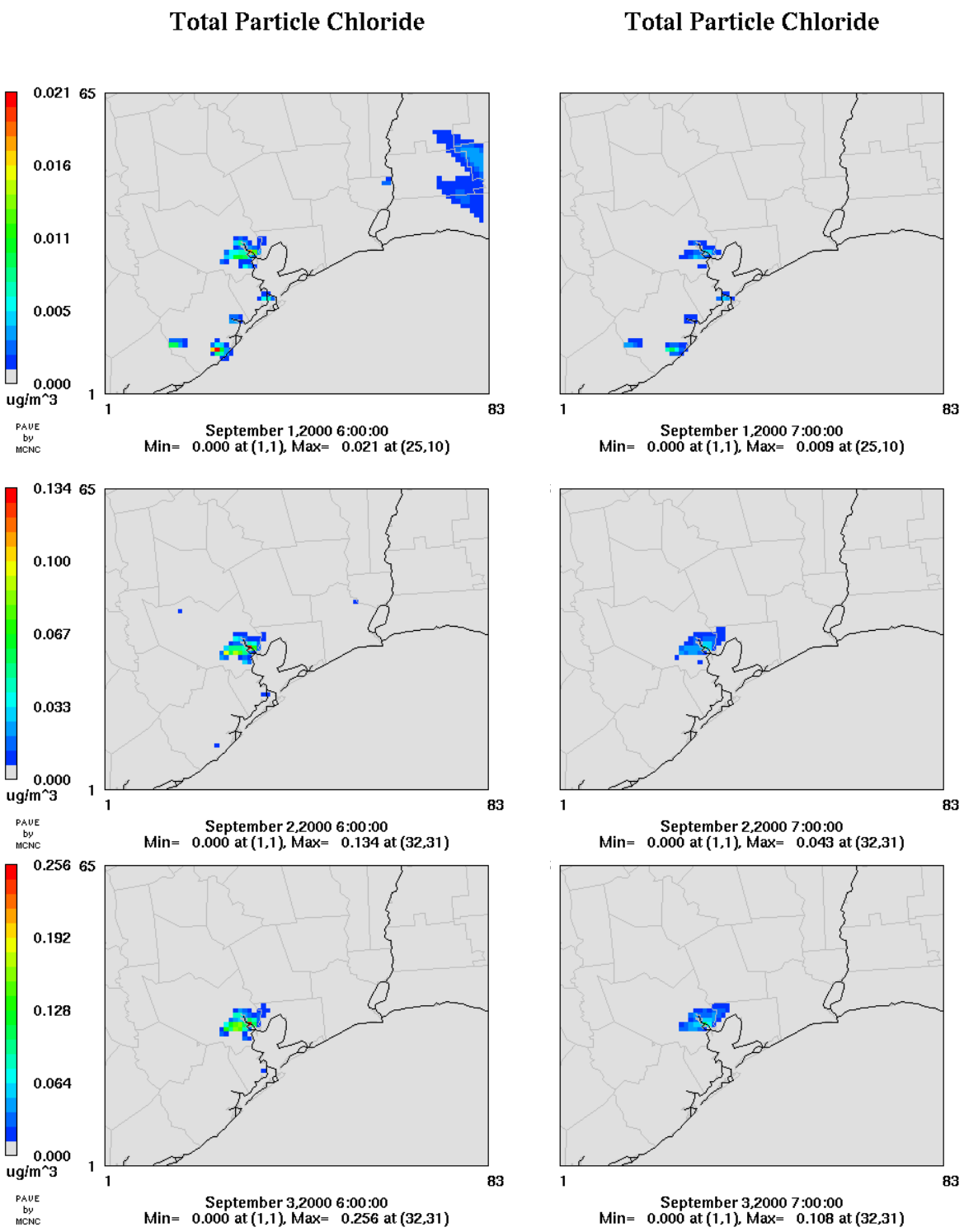

Figure E-1 (Cont'd) Total particle chloride formation at 0600 and 0700 for entire episode

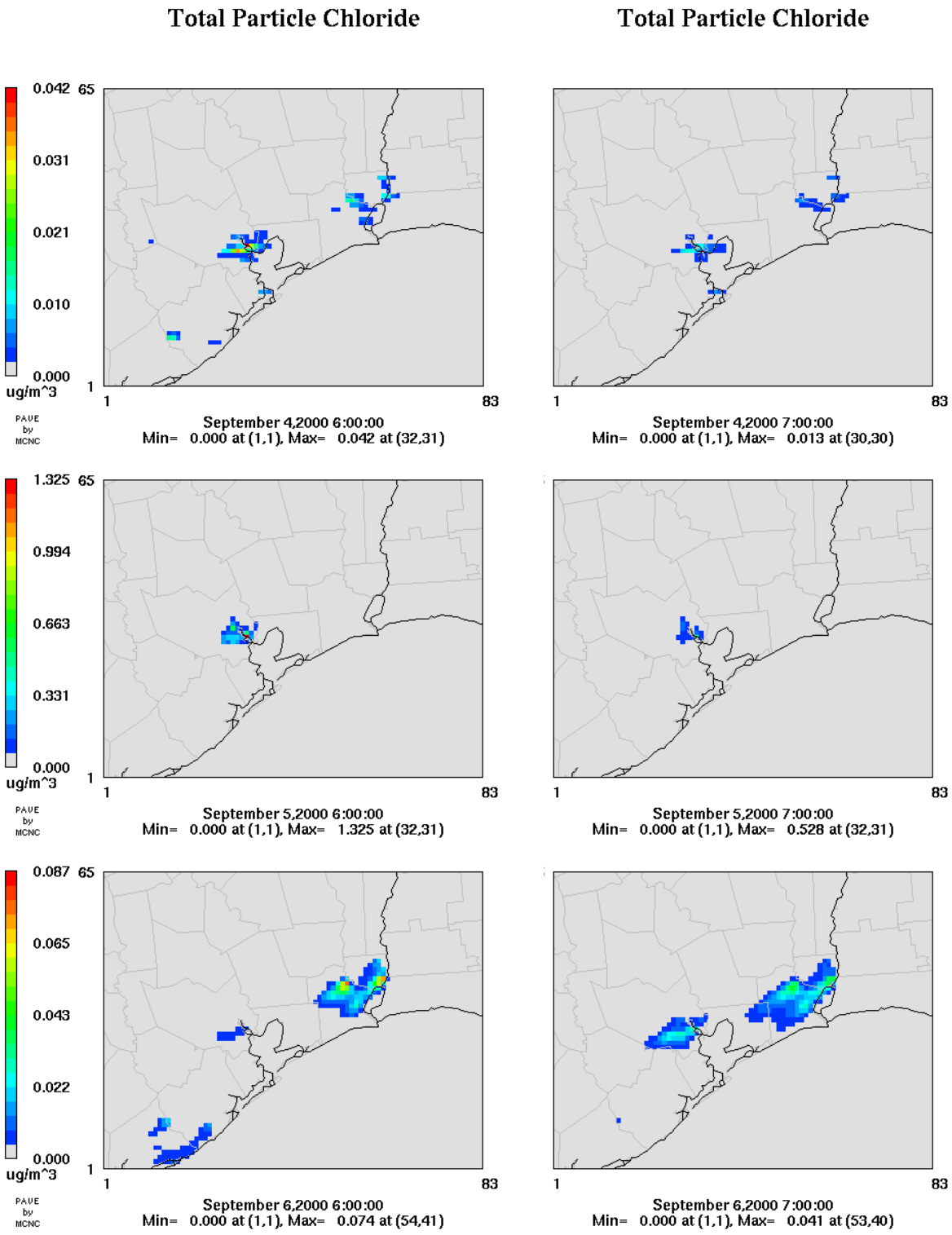

Figure E-1 (Cont'd) Total particle chloride formation at 0600 and 0700 for entire episode

Bibliography

Allen, D.T. and Price, J., 2002. Accelerated science evaluation: Atmospheric Chemistry. http://www.utexas.edu/research/ceer/texaqsarchive/accelerated.htm

Ayres, R.U., and Ayres, L.W., 1997. The Life Cycle of Chlorine, Part II, *Journal of Industrial Ecology* 1 (2), 65-89

Atkinson, R., Baulch, D.L., Cox, R.A., Hampson, R.F., Kerr, J.A., Rossi, M.J., and Troe, J., 1997. Evaluated kinetic, photochemical and heterogeneous data for atmospheric chemistry: supplement V, IUPAC subcommittee on gas kinetic data evaluation for atmospheric chemistry. *Journal of Physical and Chemical Reference Data* 26, 521-1011

Carter, W.P.L. 1996. Condensed atmospheric photooxidation mechanisms for isoprene. *Atmospheric Environment* 30, 4275-4290

Carter W.P.L., Pierce, J.A., Luo, D., and Malkina, I.L., 1995. Environmental chamber study of maximum incremental reactivities of volatile organic compounds, *Atmospheric Environment* 29 (18), 2499-2511

Carter W.P.L, 1997. Estimation of upper limit maximum incremental reactivities of VOCs, Statewide air pollution research center and college of engineering, Center for environmental research and technology, University of California Riverside, CA 92521.

Cantu, G., 2004. TCEQ Technical Analysis: Air Quality Modeling. By personal contact to gcantu@tceq.state.tx.us, Tel) 512.239.0326

Chang, S., 2002. Spatial and temporal impacts of chlorine chemistry on ozone formation in southeast Texas: Development of emission inventories for atomic chlorine precursors, Master's Thesis, University of Texas at Austin

Chang, S., Tanaka, P.L., McDonald-Buller, E.C., and Allen, D.T., 2001. Emission inventory for atomic chlorine precursors in southeast Texas, Report on Contract 9880077600-18 between the University of Texas and Texas Natural Resource Conservation Commission, Center for Energy and Environmental Resources, University of Texas, Austin, Texas

Chang, S., McDonald-Buller, E., Kimura, Y., Yarwood, G., Neece, J., Russell, M., Tanaka, P., and Allen, D., 2002. Sensitivity of urban ozone formation to chlorine emission estimates. *Atmospheric Environment* 26, 4991-5003

Carter, W.P.L, 1997. Estimation of Upper Limit Maximum Incremental Reactivities of VOCs, Documentation of William Carter's web page from University of California Riverside

Carter, W.P.L., Luo, D., and Malkina, I.L., 1997a. Investigation of the Atmospheric Reactions of Chloropicrin, *Atmospheric Environment* 31, 1425

Carter, W.P.L., Luo, D., and Malkina, I.L., 1997b. Investigation of the Atmospheric Ozone Formation Potential of Trichloroethylene, Draft Report to the Halogenated Solvents Industry Alliance, August 29

City of Houston, 2001. Letter, wastewater.controlcenter@cityofhouston.net,

Georgia Institute of Technology, 2005. ftp://ftp.al.noaa.gov/, login/user id: Houston, password: upd8data

Gery M.W., Whitten G.Z. and Killus J.P., 1988. Development and testing of the CBM-IV for urban and regional modeling. EPA-600/3-88-012, January

Greenlee, J., 2001. Acting Deputy Assistant Director, Water Production Branch, City of Houston, jim.greenlee@cityofhouston.net

ENVIRON International Corporation, 2002. Use's Guide: Comprehensive Air Quality Model with extensions, version 3.10, www.camx.com

ENVIRON International Corporation, 2004. Use's Guide: Comprehensive Air Quality Model with extensions, version 4.00, www.camx.com

Environmental Protection Agency, 'Water on Tap: What you need to know', 2005. http://www.epa.gov/safewater/wot/pdfs/book_waterontap_full.pdf

Environmental Protection Agency, National Ambient Air Quality Standards for Ozone; Final Rule, 2004. http://www.epa.gov/ttn/oarpg/naaqsfin

Holzwarth, G., Balmer, R.G., and Soni, L., 1984a. The fate of chlorine and chloramines in cooling towers. *Water Research* 18, 1421-1427.

Holzwarth, G., Balmer, R.G., and Soni, L., 1984b. The fate of chlorine in recirculating cooling towers. *Water Research* 18, 1429-1435

Jeffries H., T. Keating, and Z. Wang, 1997. "Integrated Process rate analysis of the effect of nitrogen oxides emission height on peak ozone concentration predicted by the urban airshed model." Department of Environmental Sciences and Engineering, School of Public Health, The University of North Carolina - Chapel Hill, http://airsite.unc.edu. Contract No. 5094-250-3069.

Khalil, M.A.K., Moore, R.M., Harper, D.B., Lobert, J.M., Erickson, D.J., Koropalov, V., Sturges, W.T., and Keene, W.C., 1999. Natural emissions of chlorine-containing gases: Reactive Chlorine Emissions Inventory, *Journal of Geophysical Research* 104 (D7), 8333-8346

Lawler, D., University of Texas at Austin, preliminary estimate of upper bound of potential volatilization of free chlorine in water and wastewater treatment, based on professional judgment, 2001.

Lobert, J.M., Keene, W.C., Logan, J.A., and Yevich, T., 1999. Global chlorine emissions from biomass burning: Reactive Chlorine Emissions Inventory. *Journal of Geophysical Research* 104 (D7), 8373-8389

MM5 Community model, 2004. http://www.mmm.ucar.edu/mm5/mm5-home.html.

NARSTO, NARSTO data set, 2005. http://eosweb.larc.nasa.gov/PRODOCS/narsto/table_narsto.html#houston

Pavlovic, R.T., 2005. *The impact of ammonia emissions on atmospheric particulate matter formation in Texas*, Master's thesis, University of Texas at Austin

Ragains, M.L. and Finlayson-Pitts, B.J., 1997. Kinetics and mechanism of the reaction of Cl atoms with 2-methyl-1,3-butadiene (isoprene) at 298K. *Journal of Physical Chemistry A* 101, 1509 –1517.

Riemer, D.D., 2001. Final Report to the Texas Natural Resource Conservation Commision: Confirming the presence and extent of oxidation by Cl in the Houston, Texas urban area using specific isoprene oxidation products as tracers, report, Univ. of Miami, Fla.

Russell, M., Allen, D.T., Collins, D.R., and Fraser, M.P., 2004. Daily, Seasonal, and Spatial Trends in $PM_{2.5}$ Mass and Composition in Southeast Texas, *Aerosol Science and Technology* 38 (S1), 14-26.

Tuazon, E.C., Atkinson, R., Aschmann, S.M., Goodman, M.A., and Winer, A.M., 1988. Atmospheric Reactions of Chloroethanes with the OH Radical, *Int. J. Chem. Kinet.* 20, 241

Riemer, D.D., 2001. Measurement of isoprene and Cl reaction products and other VOCs, Texaqs2000 study, UM/RSMAS/MAC, 4600 Rickenbacker Cswy., Miami, FL 33149; phone: 305-361-4630; fax (305) 361-4786; email: driemer@rsmas.miami.edu

Russell, M., Allen, D., Collins, D., and Fraser, M., 2004. Daily, Seasonal, and Spatial Trands in PM2.5 Mass and Composition in Southeast Texas. *Aerosol Science and Technology* 38 (S1), 14-26

Seinfield J. and S. Panids, 1998. *Atmospheric Chemistry and Physics.* John Wiley and Sons, Inc.

Song, J., Chang, S., Vizuete, W., Allen, D.T, Kimura, Y., Kembell-Cook, S., Yarwood, G., and McDonald-Buller, E.C. 2005. Comparisons of Modeled and Observed Isoprene Concentrations in Southeast Texas, submitted to *J. Air & Waste Managi. Assoc.*

Spicer, C.W., Chapman, E.G., Finlayson-Pitts, B.J., Plastridge, R.A., Hubbe, J.M., Fast, J. D., and Berkowitz, C.M., 1998. Unexpectedly high concentrations of molecular chlorine in coastal air. *Nature* 394, 353-356.

Stockwell, W.R., Geiger, H., and Becker, K.H., 2001. Estimation of incremental reactivities for multiple day scenarios: an application to ethane and dimethyoxymethane, *Atmospheric Environment* 35, 929-939

Tanaka, P.L., Reimer, D.D., Chang, S., Yarwood, G., McDonald-Buller, E.C., Apel, E.C., Orlando, J.J., Neece, J.D., Muyllins, C.B., and Allen, D.T., 2003. Direct evidence for chlorine enhanced urban ozone formation in Houston, Texas, *Atmospheric Environment* 37 (9-10), 1393-1400.

Tanaka, P.L., Allen. D.T., McDonald-Buller, E.C., Chang, S., Kimura, Y., Mullins, C.B., Yarwood, G., and Neece, J.D., 2002. Development of a chlorine mechanism for use in the carbon bond IV chemistry model. *Journal of Geophysical research* 108, ACH, (6-1) - (6-13)

Texas Air Quality Study (TexAQS), 2004. http://www.utexas.edu/research/ceer/texaqs

Texas Commission on Environmental Quality (TCEQ): State Implementation Plan (SIP), 2004a. http://www.tnrcc.state.tx.us/oprd/sips/index.html

Texas Commission on Environmental Quality (TCEQ): Proposed revisions to the State Implementation Plan (SIP) for the control of ozone air pollution: Houston/Galveston/Brazoria ozone nonattainment area, 2004b. http://www.tnrcc.state.tx.us/oprd/sips/june2004hgb_EDrec.html

Texas Commission on Environmental Quality (TCEQ): Houston/Galveston air quality science evaluation, 2004c. http://www.tnrcc.state.tx.us/air/aqp/airquality_photomod.html#ei4c

Texas Commission on Environmental Quality (TCEQ): Emission bank and trade, 2004d. http://www.tnrcc.state.tx.us/oprd/sips/capandtrade.html

Texas Commission on Environmental Quality (TCEQ), 2005a. http://www.tnrcc.state.tx.us/cgi-bin/monops/select_summary?region12.gif#map1

Texas Commission on Environmental Quality (TCEQ), 2005b. ftp://ftp.tceq.state.tx.us/pub/OEPAA/TAD/Modeling/HGMCR/CAMx/output/camx403.base5b.psito2n2/

Vizuete, W., Allen, D.T., Emery. C., Yarwood. G., and Jeffries. H., 2004. Evaluation of the July 31, 2000 ozone episode in the San Francisco bay area with the process analysis tool. Final Report Prepared for The Bay Area Air Quality Management District Modeling Advisory Committee, San Francisco, CA

Whitmey, R., 2001. Chief Engineer in Wastewater Operations in City of Houston. 713-641-9189, roger.whitney@cityofhouston.net

World Health Organization, 2005. Chemical Hazards, document is found online at: http://www.who.int/water_sanitation_health/bathing/recreaII-ch4.pdf

VITA

Sunghye Chang was born in Seoul, Republic of Korea on December 8, 1977, the daughter of Bong-Ou Chang and Soon-Ok Choi. After completing her work at Sacred Hear Girls' High School, Seoul, Republic of Korea, she entered the College of Engineering, Ewha Womans University, Seoul, Republic of Korea. She received the degree of Bachelor of Science and Engineering magna cum laude with distinction in Environmental Science and Engineering from Ewha Womans University in February 2000. In August 2000, she entered the Graduate School of The University of Texas at Austin on a competitive academic fellowship. She received the degree of Master of Science in Civil Engineering (Environmental Water Resources and Engineering) from the University of Texas at Austin. In May 2002, she continued her Ph.D studies at the Graduate School of The University of Texas at Austin.

Permanent address: 366-193, #301 Shin Dea Bang 2 Dong
Dong Jack-Gu
Seoul, 156-848
Republic of Korea

This dissertation was typed by the author.